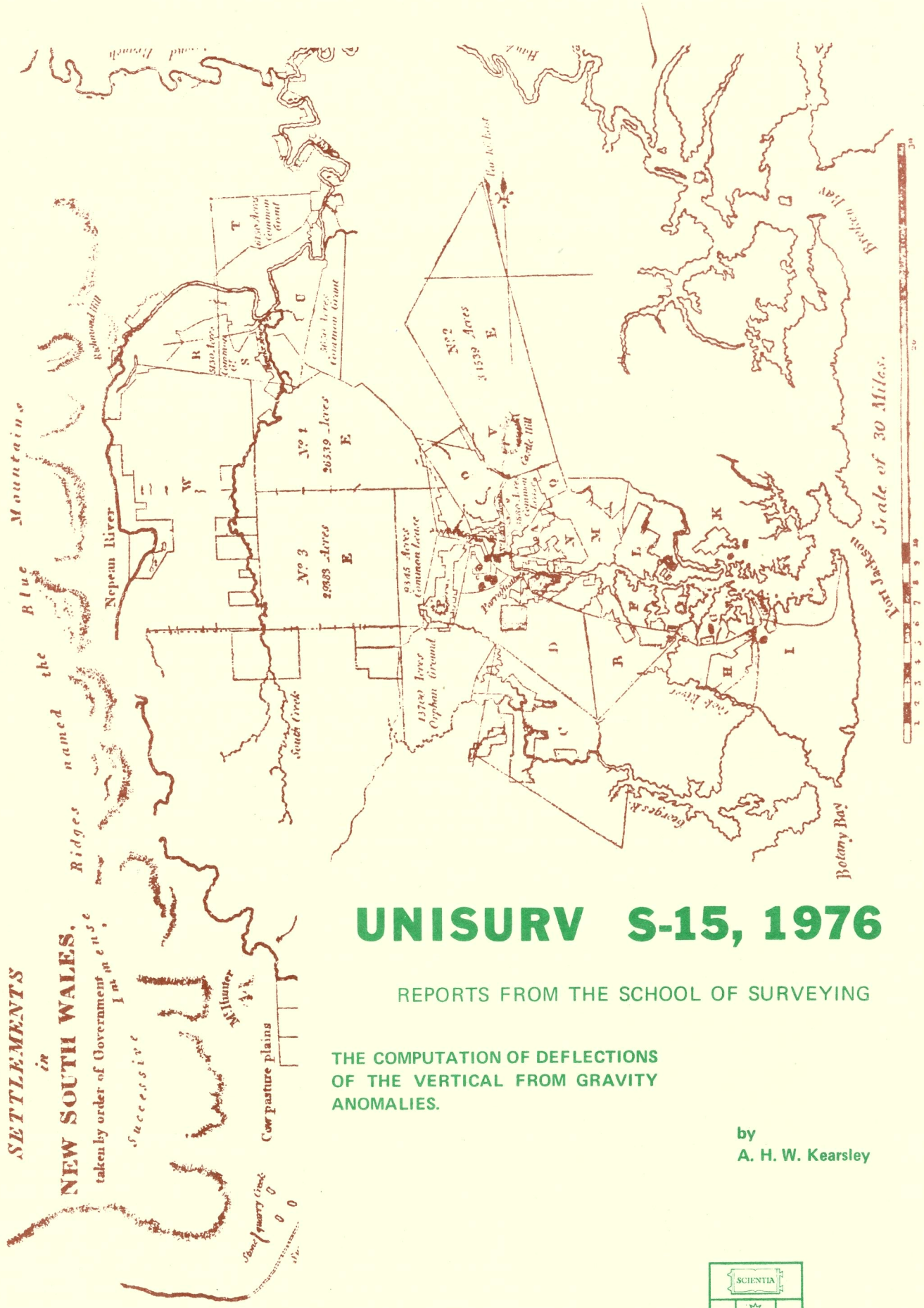

UNISURV S-15, 1976

REPORTS FROM THE SCHOOL OF SURVEYING

THE COMPUTATION OF DEFLECTIONS OF THE VERTICAL FROM GRAVITY ANOMALIES.

by
A. H. W. Kearsley

UNIVERSITY OF NEW SOUTH WALES
KENSINGTON. N.S.W. AUSTRALIA

UNISURV REPORT NO. S15, 1976

THE COMPUTATION OF DEFLECTIONS OF THE VERTICAL FROM GRAVITY ANOMALIES.

by

A.H.W. KEARSLEY

Received December, 1976

SCHOOL OF SURVEYING,
THE UNIVERSITY OF NEW SOUTH WALES,
P.O. BOX 1,
KENSINGTON, N.S.W., 2033, AUSTRALIA.

National Library of Australia
Card No. and ISBN
0 85839 023 X

ABSTRACT

The theory for the determination of the deflection of the vertical is explored using the concept of the telluroid in order to circumvent the theoretical shortcomings of the traditional approach brought about by the problem of the reduction of observed gravity to the geoid. Two main approaches investigated are the method developed by Molodensky using a surface-layer technique and the approach derived from the application of Green's Third Identity at the Earth's surface. The behaviour of these solutions under extreme topographic conditions is of particular interest. It is noted that the Molodensky solution breaks down when ground slopes near the computation point exceed 45°. The development from Green's Third Identity shows no such theoretical weakness and in its simplified form appears simpler to evaluate than Molodensky's correction term.

To test the various gravimetric methods evaluations of the deflections of deflections of the vertical were made at 12 stations in north-western NSW. The stations were chosen because a value for the deflection had already been found for them astro-geodetically and because they are situated in a variety of terrain types. This latter factor provides some control on the influence of the terrain effects on the evaluation, whilst the former allows some estimates of the precision and systematic errors of the gravimetric determination to be made. It was decided to concentrate attention on the region bounded by a radius of $1^{\circ}.5$ and to accept the values obtained from the 1970 geoid solution Australia for the region beyond this radius. Eventual incorporation of these values in the solution meant that the deflection value could then be obtained in an absolute sense.

Before any meaningful determination could be made it was necessary to supplement the existing gravity coverage with about 200 gravity stations. These were located so as to provide full representation of the gravity field in the critical region immediately surrounding the test stations, and to increase the general coverage where the density was considered inadequate. Computer routines were then developed to evaluate the deflection from the discrete gravity data. A modified Rice Rings approach was simulated on the computer, it being felt that this technique had the advantage of strength and flexibility over traditional computer techniques. Various methods were developed to provide extension of the gravity and height field from the discrete data. After testing it was found that the techniques used in topographic routines for the derivation of contours from spot heights proved most satisfactory for the purpose.

The results of the investigation show in general that the precision of the gravimetric determination is largely dependent upon the accurate assessment of the gravity field within a radius of $1^{\circ}.5$ of the computation point. For some of the test stations situated in the more mountainous terrain up to 90% of the signal comes from this region. For stations on the plains the improvement in the definition of the gravity field increases the precision from about $\pm 1''.5$ (the precision achieved before density of the gravity stations was increased) to about $\pm 0''.1$ to $\pm 0''.2$. The improvement for stations situated in the mountainous terrain is not as dramatic (0 $\{\pm 0''.5\}$), an indication of the terrain effects not yet unaccounted for. When the terrain corrections as calculated by the Molodensky approach are applied the precision of the deflections at these stations approaches that obtained at the stations only slightly affected by terrain. The evaluation of the terrain effect by the Green's Third Identity approach is found to be unsatisfactory in areas of rugged terrain. The correction term seems oversensitive to errors in the ground slope values. Some damping effect will have to be applied in future determinations if this approach is to be successful.

The high precision obtainable by the gravimetric determination can be achieved for a comparatively

low cost in countries which have medium scale topographic maps and reasonable gravity coverage. A cost-benefit analysis shows that the gravimetric method, when compared with the astro-geodetic approach, is capable of producing a higher precision in the deflection value for approximately one quarter the cost. It has the added advantage that the determination can be sited in areas likely to give more representative values of the tilt of the equipotential surfaces.

With doppler techniques having such an impact on methods of geodetic survey it is suggested that gravimetrically determined deflections used in conjunction with astronomically determined azimuths can be used to provide azimuth control in geodetic networks. The need for orienting local geodetic datums onto a geocentric ellipsoid is also increased with the advent of doppler. Here again comparisons of geocentrically-based deflections computed gravimetrically with astro-geodetic deflections determined with respect to a local ellipsoid can be used to find the values of the parameters needed for this orientation.

TABLE OF CONTENTS

TABLE OF CONTENTS

INDEX OF FIGURES

INDEX OF TABLES

'..... Mechanics is so distinguished from geometry in that what is perfectly accurate is called geometrical; what is less so is called mechanical. However, the errors are not in the art, but in the artificers. He that works with less accuracy is an imperfect mechanic."

Sir Isaac Newton in Preface to
'Mathematical Principles of Natural
Philosophy'

1. INTRODUCTION

1.1 Historical Perspective

The chain of activities involved in explaining a natural phenomonon in terms of a scientific "law" is often long and tortuous. It is hampered by imprecise or biased observations and poor modelling of the law involved. In the quotation above Newton perceives the division between the geometrical (the scientific law) and the mechanical (the observations), and seems to suggest that the fault lies with the practical side of the process. However it should be recognised that this process is an interactive one. The scientific law is based in the first instance on the examination of the observations. Failure in correspondence between new observations and the accepted law results in an alteration of this law.

The development of the science of geodesy gives a good illustration of this process. Newton (1686) had hypothesised the shape of the earth to be an oblate spheroid by at least 1666. This was at the time contradicted by the French whose measurements indicated the shape to be a prolate spheroid. It was not until 1736 that, under the auspices of the French Academy of Sciences, a series of expeditions measured meridional arcs near the equator and the North Pole and the resultant lengths indicated the Newtonian model to be correct. Even so, it has since been discovered that the arc measurement in Lapland was about 490 m too long. It is ironic to consider that, had the errors in measurement accumulated negatively, the deductions would have been reversed and conflict between theory and measurement remained. Not for the last time would errors in measurement help to verify a mathematical model.

Thus the difference existing between theory and observation, the geometrical and the mechanical, has been resolved and refined to the present day.

The field science of physical geodesy is much younger but has had a similar experience in its development. In 1849 G.G. Stokes laid down a mathematical basis in the form of Stokes' integral (STOKES, 1849). By postulating a mathematical figure of the earth which also held certain physical properties of mass and rotation he could compute the potential at the surface of this model. Comparisons of this theoretical value of gravity with a measured value produced an anomalous gravity field. Stokes' integral holds that the departure of the bounding equipotential surface of a spherical approximation of the Earth (the geoid) away from the theoretical surface can be determined if the gravity anomalies near the point being investigated are well known, and if the anomaly field for the rest of the world is fairly well represented. This theory was extended by F.A. Vening Meinesz (VENING MEINESZ 1928), whose formulae stated that, if the above conditions satisfied, then the tilt of the geoid with respect to the theoretical surface also be computed.

However, it was well into the middle of the 20th century before technology produced an instrument which enabled gravity to be measured easily, accurately and quickly. Prior to this gravity was measured more or less as in the time of Newton, that is by observing the period of a simple pendulum (NEWTON 1686, pp 288-294). This approach lacked accuracy and was very time-consuming and since the late 1930's, when the gravimeters were developed, gravity surveys over land surfaces of the Earth flourished. Two decades or so later the gravity field over the vast unsurveyed regions of the earth could be estimated by analysing the orbits of artificial satellites and by the mid-1960s numerical solutions to the Stokes and Vening Meinesz problems were being obtained to a limited degree of accuracy.

This improvement in gravity measuring techniques renewed interest in the gravimetric solutions to the geodetic boundary value problem. At first particular attention was directed toward the basic assumptions in the Stokes' solution which were known to be faulty. Strictly speaking the Stokes' (and thus the Vening Meinesz) integral cannot be used to find the shape of the Earth as

(i) gravity is measured at the surface of the Earth and not, as is assumed in the theoretical development, on the geoid; and

(ii) attracting matter lies outside the geoid

(BROVAR ET AL 1964, p 89). Various mathematical devices have been used in an attempt to overcome these problems. However these require a knowledge of the stratification of matter between the surface and the geoid and as this is a practical impossibility, the problem is not solved satisfactorily by these approaches.

In 1945 Molodensky (MOLODENSKII ET AL 1962, pp 76-81) proposed a simple but effective alternative approach which bypassed the above difficulty. He introduced a new theoretical surface which depended on the continuation of the normal gravity upward to the surface rather than the reduction of the measured gravity downward. At no stage therefore was a hypothesis of the nature of the sub-surface density distribution invoked. The separation between the theoretical surface (whose normal potential equalled that of the equivalent point on the Earth's surface) and the Earth's surface itself became known as the 'height anomaly'. It substituted for the geoid-ellipsoid separation in mapping what is called the 'quasi-geoid'.

The height anomaly is now firmly established in the geodetic world and a number of methods have been devised to solve for both it and its derivatives. One of the most interesting of these has been developed by BJERHAMMAR (1964). He postulated a sphere, internal to the surface, on which fictitious gravity anomalies were found such that, upon upward continuation of these anomalies, the actual gravitational field of the earth was generated. These fictitious anomalies were used in the generalised Stokes' integral to get the height anomalies at the surface.

The improvement in the observation of gravity has made the measurement of the second-order effects a practicality. PICK (1973) investigated the influence which these terms have on the geoidal parameters in a test area in the High Tatras of Czechoslovakia. By measuring the gravity gradient at 2 points per 1 km^2 in this region he found corrections of up to 0".4 to the deflections of the vertical from this source. Unfortunately the density and accuracy (±0.02 to ±0.05 mGal/m) requirements suggested for Pick's investigation could not be matched in the present study because of the lack of manpower and the relative unsophistication of the equipment. Obviously this effect is shown to be significant in areas of particularly rugged terrain, and should be taken into account for precise evaluations in such areas.

Recently many writers have reformulated the geodetic boundary value problem using comtemporary mathematical tools. For example, ARNOLD (1975), having recourse to some of the techniques of tensor analysis (eg. HOTINE 1969) has proved the important quality of uniqueness in the solution to the boundary value problem of physical geodesy. This quality has also been shown by NEDOMA (1973) using the principles of variational calculus, and by HÖRMANDER (1975, p 57) using functional analysis techniques (eg. MEISSL 1975). The conditions for uniqueness have been found in terms of classical potential theory (eg. BROVAT ET AL 1964, pp 164-167), but it is of interest to see its formulation in terms of the more powerful modern techniques mentioned above. However these formulations are of more theoretical than practical interest at this stage, and the present investigation will use the more classical approach in order to state the problems and to seek their solutions.

1.2 Explanation of the Problem

In descriptive terms, one can state that the geodetic problem being dealt with here is the definition or delineation of the earth's surface, either over some limited region or the entire globe. This is traditionally done by first approximating the surface by a methematical model (an ellipse of resolution), and then studying departures of the real surface from this model. As mentioned in the section above it is usual to introduce a third surface, namely the geoid, as an intermediate step as it is to this equipotential surface that measurements on the earth's surface can be related. By mapping the departures of the earth's topography from the geoid, and also the departures of the geoid from the ellpsoid one is able to fully define the surface of the earth, thus solving the geodetic problem.

In the older branch of geodesy, geometrical geodesy, one can find the *tilt* of the surface geop with respect to the adopted model (also known as the astro-geodetic deflection of the vertical) by comparing of the geodetic position of a point projected onto the model with the position of this point determined astronomically. The separation of the geoid from the ellipsoid (N) can not be found by this means, and it is usual to assume a value for the separation at the Fundamental Station or 'Origin' of the geodetic survey, and by astro-geodetic levelling through the network to compute relative values for N at the astro-geodetic stations. This should be contrasted with method of finding N in physical geodesy where, by applying Stokes' integral to the anomalous gravity field one can compute N directly. The solution of N by this method is described in general terms as a gravimetric solution.

The astro-geodetic deflection of the vertical in geometrical geodesy is therefore shown to be an important step in obtaining a value of N. It is obviously one of the basic parameters used in solving the geodetic problem. Since the deflection can also be computed directly in physical geodesy it forms a very important bridge between these two branches of geodesy.

This fact - that deflections can be found independently from both the astro-geodetic and gravimetric approaches - has a very important application in geodesy. Comparisons are used in 'astro-gravimetric levelling' to assist in the extension of the deflections throughout a subject area. (For a general description of this technique see MOLODENSKII ET AL 1962, pp 125-129); for more detailed applications, see BURSA 1965a; BURSA 1970; also HONKASALO 1974). Astro-geodetic deflections have traditionally been used to determine the model of best fit for particular continents or regions, using either straightforward averaging techniques (eg. BOMFORD 1967) or least squares surface fitting techniques (VANICEK AND MERRY 1973). By extending this approach and comparing gravimetrically computed deflections against astro-geodetic deflections at selected points through

a region or a continent it is possible to determine the orientation corrections to bring the locally adopted ellipsoid into coincidence with an absolute (geocentric) reference model (eg. MATHER 1970b; GROTEN 1974). In fact in all cases where 'natural' observations or their by-products are to be related to their geometrical equivalents the deflections of the vertical have an important role to play (MUELLER 1974, p 516).

Whereas the astro-geodetic approach is limited only by the accuracy of observation, the solutions obtained from both the Stokes and Vening-Meinesz formulae are subject to many more different kinds of uncertainties. In general it is fair to say that the limitations on the Vening-Meinesz solution are due, at least in part, to the paucity of gravity data in the vicinity of the computation point. This may not always be critical of course. For instance, if the anomalous gravity field in the immediate vicinity is featureless and can therefore be well represented by a few gravity stations, then the difficulty mentioned above no longer exists. In areas of rugged terrain the anomalous gravity field is bound to be disturbed and the number of points needed to properly describe the field will need to be greatly increased.

The aim of this work is to investigate the theory and practice of the computation of the deflections of the vertical from gravimetry as applied to a particular area of New South Wales, in order to assess the accuracy of this computation and to define the factors responsible for any remaining limitations of the method. Deflections at selected astro-geodetic stations in this test area will be computed gravimetrically. Because each of these stations has a position fixed both astronomically and geodetically, astro-geodetic deflections to observing accuracy can be determined and used as a means of providing absolute control on the stations. It is hoped that by looking at the discrepancies between the two types of deflections insight will be gained into gravimetric solutions of the deflections, and that the techniques of the computation of the deflection of the vertical and of their application in the solution to the geodetic boundary value problem will be enhanced.

1.3 Achievements to Date

It is instructive to review the results currently being achieved throughout the world for gravimetric determinations of the deflection. The number of cases where studies have been done to investigate exactly this problem are limited, and it will be necessary to review the literature on general geoid solutions of various continents or countries. It is also helpful to look at results achieved by astro-gravimetric techniques where, in order to interpolate deflections between control stations, comparisons of deflections found by both astro-geodetic (hereafter denoted as A/G) and gravimetric methods are used. This should provide a status report on the 'state of the art' in this field.

A good picture of the achievements in Australia can be found by reference to MATHER 1970a; MATHER 1970b; FRYER 1970; MATHER BARLOW AND FRYER 1971; and FRYER 1971 (wherein the results of the 1970 geoid solution of Australia are discussed). The fourth-mentioned reference gives a summary of the results of comparisons of gravimetric with astro-geodetic deflections after orientation parameters are applied to bring the regional ellipsoid onto the gravimetric ellipsoid. Comparisons at 38 stations, chosen because of their even spacing throughout Australia and because their inner zone gravity fields were well represented, showed the r.m.s. residuals ($M\{\sigma\}$) to be $\pm 1''.0$ for ξ and $\pm 1''.8$ for η. When the analysis is extended to include all 1084 stations included in the solution these values increase to $\pm 2''.0$ for ξ and $\pm 2''.6$ for η. An interesting breakdown of the frequency of the differences (A/G - gravimetric) is given in the form of a histogram, showing

normal distribution tendencies, but with large differences (> 4 arcsec) occurring at over 60 of the stations compared. As mentioned later in this investigation (section 8.2.1) the comparisons at the twelve test stations in the 1970 adjustment fell with the two extremes suggested above, showing a $M\{\sigma\}$ in ξ of $\simeq\pm2''.5$ and in η of $\simeq\pm1''.5$. This, as will be shown in section 8.2.1 is significantly improved by densification of the gravity and height data in the Inner Zone (ie. the area within 1° of the computation point) and it appears realistic to assume from this report that the $M\{\sigma\}$ generally obtainable under average conditions is of the order of 1.5 to 2.0 arcsec in both components. This is borne out by FRYER (1970, p 78) who used the value of 1.5 arcsec in the weighting of gravimetric deflections when computing an orientation of the Australian Geodetic Datum. It should also be remembered that the A/G deflections could have standard errors of the order of 0.3 to 0.6 arcsec themselves.

This figure also accords with that quoted by NAGY AND PAUL (1973), who comment that when using a constant value to represent a $\frac{1}{2}^{\circ}$ area the sensitivity of the resultant geoid would be dampened to the extent that local changes in the deflection of the order of 2 arcsecs would not be detected. In fact, a more recent study on the North American Datum comments that, if a constant anomaly is assumed over the area within a radius of 10 km from the computation point, and if terrain correction effects are not computed the expected $M\{\sigma\}$ of ξ and η in this continent is of the order of $2\frac{1}{2}$ arcsec (MATHER 1975, p 39).

Another recent study states that, when comparing the deflections of the vertical computed by A/G and gravimetric means at 235 stations throughout Finland, a 'quadratic mean of differences' ($\equiv M\{\sigma\}$) of ±0.7 arcsec were found (HONKASALO 1974). Using 21 stations with denser gravity cover gave the difference of ±0.35 arcsec. These figures are surprisingly good, particularly when the general gravity density used for the computation is considered; mean anomalies for 10 km x 10 km squares were computed and used. The good agreement must certainly be a reflection of the comparatively low topographic relief of that country.

Some very extensive and detailed studies have been carried out in Czechoslovakia by Bursa, among others. One of the purposes of the studies was to produce interpolated values of ξ, η at approximately 800 points on a 10' x 15' grid spacing by means of astro-gravimetric levelling. In the earlier studies, relative differences between astro-geodetic and gravimetric deflections ranged up to 1.1 arcsec in the mountainous regions to the east of the region (BURSA 1965a, p 7) whilst later studies which included the G_1 correction for topography improved the relative difference to the order of 0.6 arcsec (BURSA 1970, pp 19-21, especially p 20) in mountainous areas. Whilst these statements of accuracy are not, strictly speaking, in absolute terms (the computation for deflections from gravimetry were not taken beyond about 200 km, and there is no attempt to correct for differences of ellipsoid (IBID, p 2)) the results nevertheless indicate that the gravimetric deflections have been computed to quite a high degree of accuracy. As stated by BURSA (1968, p 9), the spacing of the gravity stations was 1 per 5 km^2, and this was further densified around the 37 astro stations used for control. This intensive coverage must be largely responsible for the very good average discrepancy for the relative differences of about 0.3 arcsec.

Unfortunately neither the report by HONKASALO nor those by BURSA referred to above give an estimate of the expected accuracy of the astro-geodetic deflections against which the gravimetric values are compared. A proper estimate of the accuracy of the gravimetric deflection should account for this factor (see section 8.2.4) so it is difficult to estimate what is to be stated as the actual accuracy of the gravimetric solutions from these two sources.

It can be tentatively concluded from this brief survey, however,that the precision of gravimetric

deflections is limited to the order of ±1.5 arcsec in areas where there is limited gravity information, whilst in fairly flat to undulating areas of good gravity cover this precision can be increased to that of astronomical position determination.

In mountainous areas, however, the best results are of the order of double this figure, indicating that the methods of computation of the terrain correction term are not sensitive enough to pick up all the topographic effects. It is hoped that in this study more light will be shed on the particular problems inherent in these difficult areas, so that some idea of optimum methods of solution may be obtained.

1.4 Outline of this Investigation

The astro-geodetic stations which were chosen for control for this study lie on the Narrabri and Manilla 1:250 000 map sheets, which cover a large area about 600 km north-west of Sydney and 300 km inland from the east coast of Australia (see figure 1 for locality). The stations themselves fall within the boundaries defined approximately by $-30^{\circ}07'$ to $-30^{\circ}52'$ in latitude and $149^{\circ}30'$ to $150^{\circ}45'$ in longitude. It is here that four sections of the national astro-geodetic levelling network meet, and so distributed through this area are 12 stations roughly 30 km apart (see figure 2).

There were a number of reasons for choosing this area. One was the abundance and distribution of control stations mentioned above, but it was chosen mainly because the computations for the 1970 geoid solution of Australia (see MATHER 1970a) had shown poor agreement between the gravimetric deflection and that defined astro-geodetically (see column 1, table 12). Also, because of the wide range of topographical types it provided to a certain extent some control on the degree of the terrain disturbance for purposes of testing terrain correction formulae.

The terrain varies from plains to the west, through undulating country with symmetrical and isolated hills to the east and south, and finally quite rugged and broken mountain ranges to the north. Three stations (Culgoora and Beelera to the west and Somerton South Base to the south east) are situated in areas of little or no relief about 700 to 1000 feet (200 to 300 m) above sea level. Willalla, Binalong, Goonbri, and Newry are in a second category, being on the tops of hills or ranges surrounded by flat to undulating country and Baldwin, Byar, Blue Mountain, Gulf Creek are set in more mountainous terrain. The last station, Kaputar is set on the top of a spectacular range of mountains nearly 5000 feet (1500 m) above sea level and is of particular interest in this study. Fortunately the area east of $150^{\circ}00'$ which contained the stations in this last category was well mapped at a scale of 1:31 680 (2 inches to a mile). The area west of $150^{\circ}00'$ was mapped at 1:100 000 which was considered quite adequate for the stations lying in this area. For details of the relief in the vicinity of the stations, see figures 10 to 21. Control stations for gravity were located at Narrabri and Tamworth, and these provided the terminal stations for the gravity traverses needed for the intensification of the gravity data. Details of the gravity coverage are found in section 4.1.

Having chosen the test stations suitable for the purposes of the investigation it is necessary to develop the theory which gives the deflection of the vertical from gravimetry and which defines the effect which the topography has on this parameter. The basic theory for these determinations is given in chapter 2, and this theory is developed for practical evaluation in chapter 3. The assembly of the data needed for the evaluation is described in chapter 4. Also in this chapter the data-handling techniques found to be most-suited to the task of the accurate determination of the deflection are outlined.

An important aspect in the evaluation process is the extension of the gravity field from discrete data points to a continuous field. This must accurately reflect the actual field around the computation point and in chapter 5 different methods of field extension are investigated. The technique chosen for the purpose of extension is an adaptation of a method used for contouring from discrete data. The evaluation is then performed at each of the test stations, and the results of the computation are presented in chapter 6. The terrain corrections which are evaluated using techniques similar to those used in the deflection determination are also presented in this chapter. Inherent in the computed values are errors due both to the errors in the data itself and to the approximations in the method of evaluation. The results of a theoretical analysis showing the effect which these errors have on the deflection values are presented in chapter 7.

The comparisons between the gravimetric values and the astro-geodetic values of the deflections of the vertical are presented in chapter 8. The comparisons are made before and after the terrain corrections have been applied so that some insight into the effectiveness of these corrections can be gained. Finally in chapter 9 the findings of the investigation are summarised and the applications of the gravimetrically determined deflection in the world of contemporary geodesy are explored.

1.5 Definitions and Notation

1.5.1 Notation

a	equatorial radius of ellipsoid of revolution
$C(r)$	covariance function (see equation 5.4)
$\underline{d}$	separation vector from point on surface to the associated point on the telluroid (see equation 2.29)
dm	point mass
ds	element of distance along surface of the ellipsoid
dS	element of surface area S
dS^1	dS projected onto the local horizontal plane
dz	element of orthometric elevation
$d\sigma$	element of surface area dS measured in steradians
$E\{x\}$, E_x	expected value, error of x
f	flattening of meridian ellipse
$f(\psi)$	Stokes' function (see equation 2.24)
$\underline{F}$	general term for force in vector analysis (see equation 2.12)
g	gravity observed on Earth's surface
g_1, g_2	1st and 2nd order terms in Moritz' recursive formula for terrain correction (see 3.5)
G	gravitational constant (see equation 2.11)
G'	terrain correction term developed by Pellinen (see equation 3.3)
G_o, G_1	parameters used to solve Molodensky's boundary value problem (equation 2.95)
h	ellipsoidal height of general point on Earth's surface
h_p	ellipsoidal height of P on Earth's surface
k	Molodensky's small parameter (equation 2.83)
k^1	Bouguer correction factor (see equation 3.4)
M	mass of the Earth (including atmosphere)
$M\{x\}$	global mean value of x
n	normal at a point
N	height of geoid above reference ellipsoid

$\underline{N}$	unit normal vector to the surface of the earth
$o\{X\}$	terms of the order of magnitude of X are neglected
r	distance between two points (eg. P and element of surface area)
r_o	r projected onto the surface of a sphere of radius R
R	mean radius of the Earth
$\overline{R}$	radius vector of transformed surface $\overline{S}$ (see equation 2.23)
R_o	radius vector of Bjerhammar sphere (see equation 2.105)
R_p	radius vector of P on the Earth's surface
S	surface of the Earth
T_p	disturbing potential at P (equation 2.17)
U	spheropotential (equation 2.3)
U_o	spheropotential on the reference ellipsoid
V	general term for potential
Vi)	(mass internal to S)
Ve)	contribution to total geopotential from(mass external to S) (equation 2.15)
Vr)	(rotational of the Earth)
W	geopotential of the Earth
W_o	potential of the geoid
x)	local rectangular Cartesian coordinate system, with z along the local normal n
y)	and xy defining the local horizon, x north and y east.
z)	
X)	
Y)	projection of distance r onto the xyz axes at Q' (see equation 2.35)
Z)	
$\frac{d[f(\psi)]}{d\psi}$	Vening Meinesz function (equation 2.27)
α	azimuth
α'	reverse azimuth
α_1	α
α_2	$90 - \alpha$
α_D	azimuth of dip of the telluroid
β	ground slope; subscripts $_1$ and $_2$ refer to components north and east
γ	normal gravity
γ_o	γ on the reference ellipsoid
γ_e	γ at the equator
Δg	gravity anomaly at the Earth's surface (see equation 2.5)
$\Delta g'$	predicted gravity anomaly
Δg^*	Δg continued downward to the Bjerhammar sphere (see equation 2.105)
Δg_c	Δg corrected for topography (see section 3.2.1)
Δg_t	contribution to Δg of the topography (see section 3.2.1)
$\Delta\xi$, $\Delta\eta$	difference in ξ, η of gravimetric value from the A/G value (see equation 8.1)
$\Delta\xi_t$	effect on ξ of topography (see equation 3.1)
ζ	height anomaly (see section 2.2.1)
ε	deflection if the vertical, positive of the outward vertical lies north, east of the normal (see equation 2.4)
ξ	component of ε in the north
η	component of ε in the east
ξ_1	ξ
ξ_2	η

ξ^1, η^1	corrections to ξ , η due to terrain effects (see equations 2.72, 2.73)
ρ	density of the gravitating body at the surface
σ	standard deviation or mean square error
τ	volume external to S
Φ	density of surface layer (see equation 2.76)
ϕ	latitude, positive north
λ	longitude, positive east
μ_x	mean value of x
χ	density parameter (see equation 2.84)
ψ	angular distance at the geocentre between two points (eg. computation point P and element of surface area of S)
ω	angular velocity of rotation of the Earth
$\underline{1}$)	(x)
$\underline{2}$)	unit vectors along the (y)axis of the local coordinate system
$\underline{3}$)	(z)
$\underline{\nabla}$	$\frac{\partial}{\partial x}\ \underline{1} + \frac{\partial}{\partial y}\ \underline{2} + \frac{\partial}{\partial z}\ \underline{3}$
∂	partial differential

Note: In some instances there is duplication of the above symbols. In these cases the meaning is clearly defined and unambiguous, and holds only for the section in which the duplicated symbol occurs.

1.5.2 Abbreviations

ACIC	- Aeronautical Chart and Information Center (now the Defence Mapping Agency Aerospace Centre), St. Louis, Mo.
AGD	- Australian Geodetic Datum
ANS	- Australian National Spheroid
A/G	- Astro-geodetic
BMR	- Bureau of Mineral Resources, Geology and Geophysics, Canberra, Australia.
IAG	- International Association of Geodesy
UNSW	- University of New South Wales
USC&GS	- United States Coast and Geodetic Survey

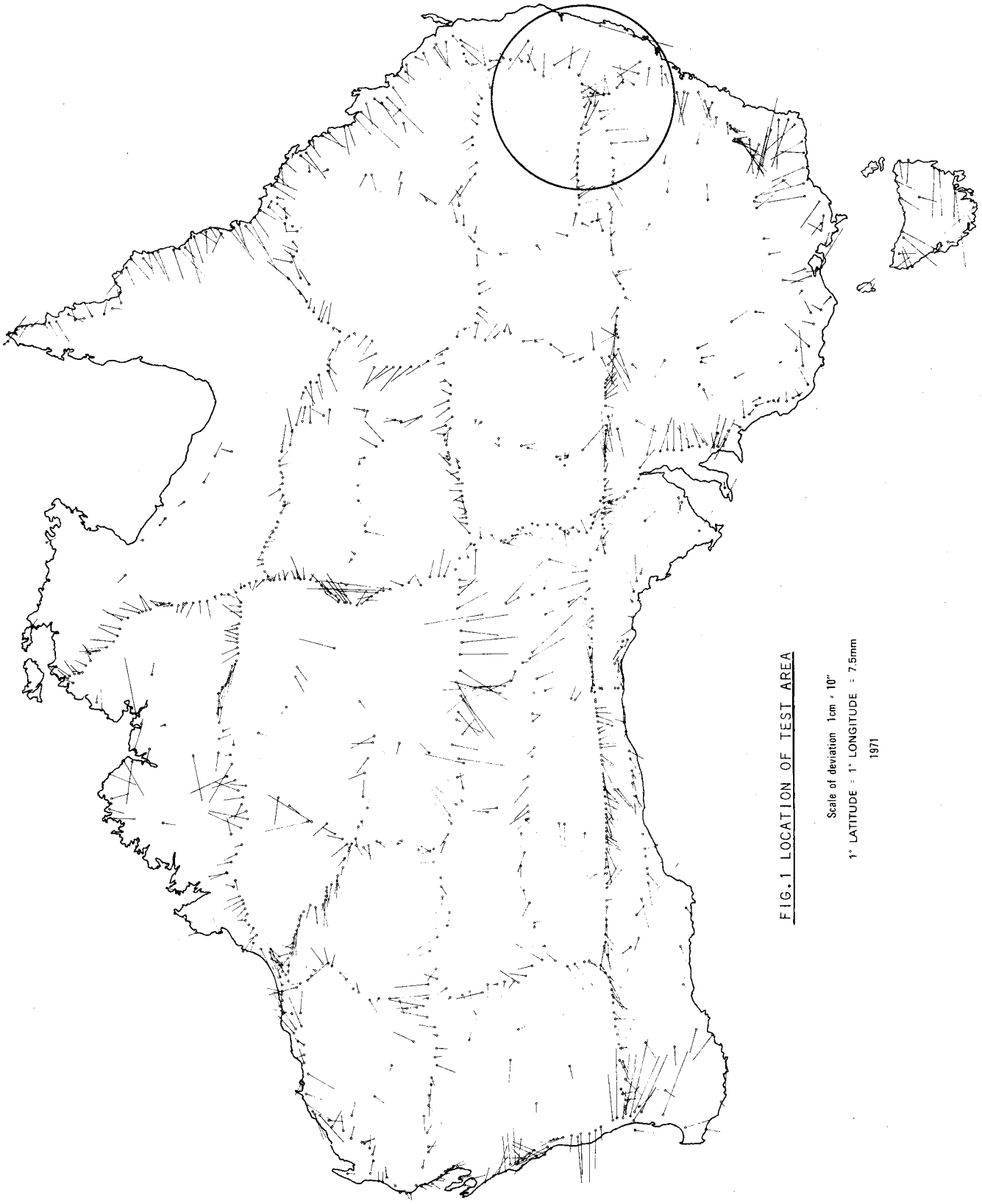

FIG.1 LOCATION OF TEST AREA

Scale of deviation 1cm = 10"

1° LATITUDE = 1° LONGITUDE = 7.5mm

1971

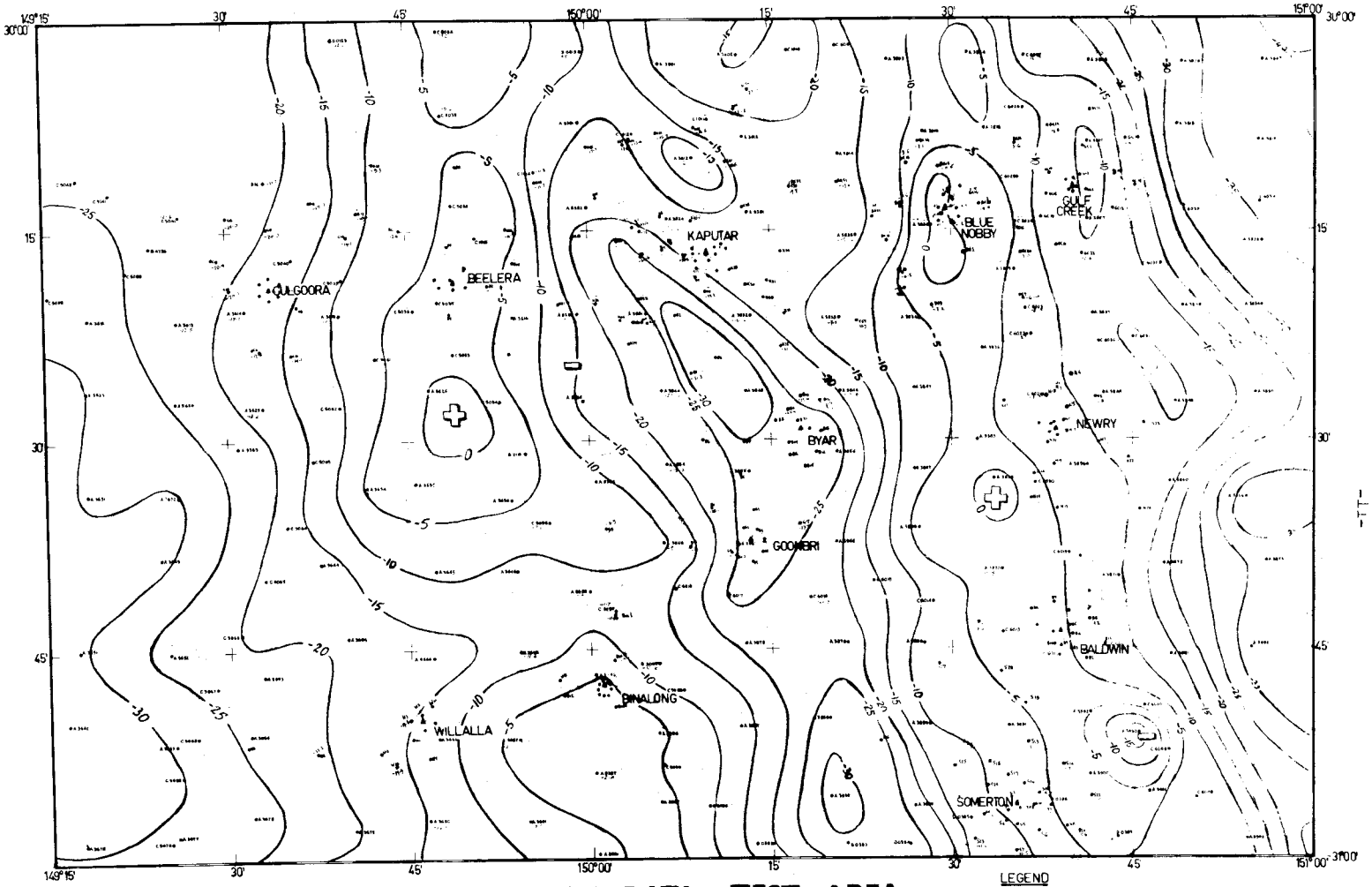

FIG: 2. **GRAVITY DATA - TEST AREA.**

LEGEND

- ▲ A/G (Computation) Station
- · Gravity Station
- ~ Bouguer Isogal

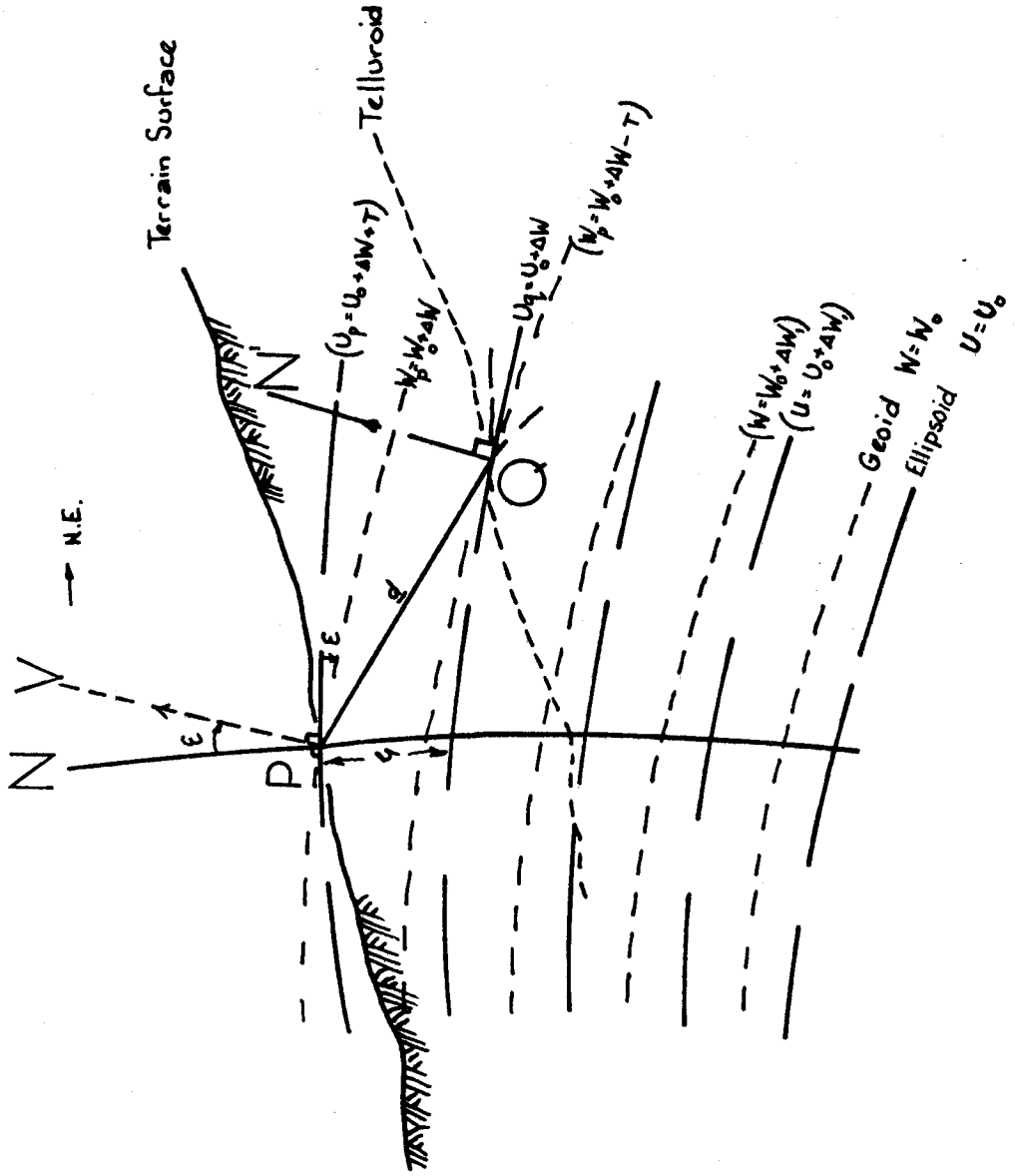

FIG. 3 EQUIPOTENTIAL SURFACES OF THE EARTH

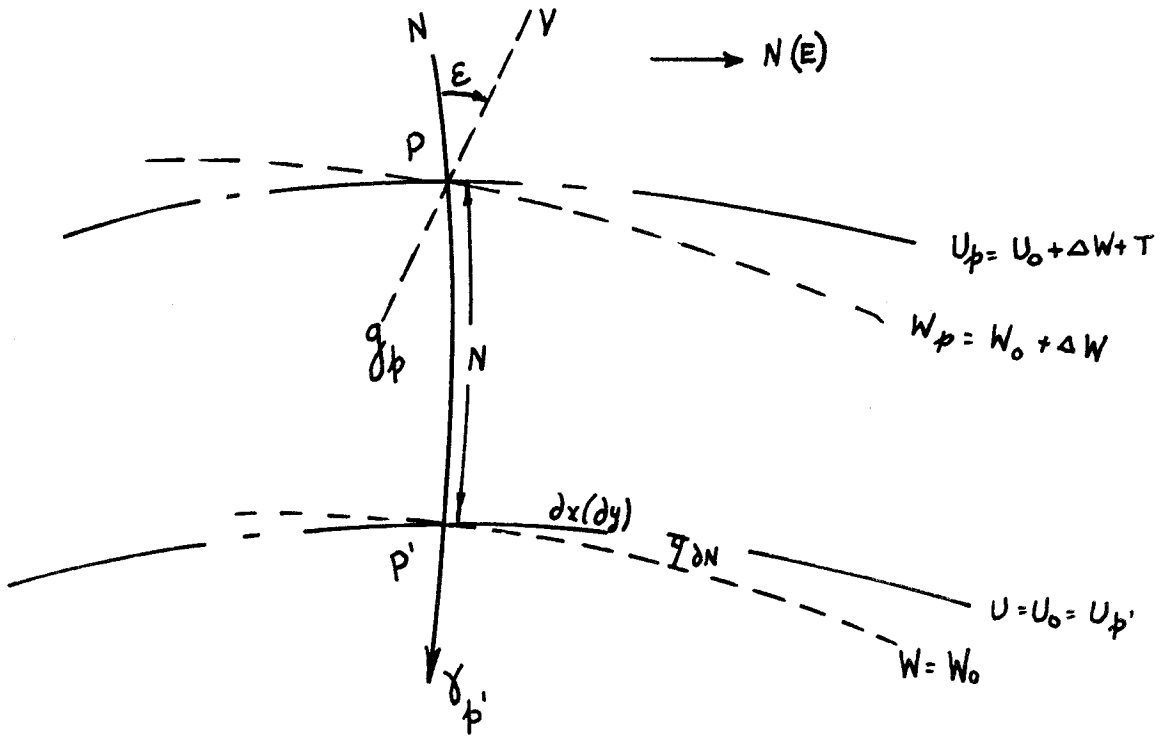

FIG. 4 RELATIONSHIPS OF GRAVITATIONAL FORCE

2. FUNDAMENTAL CONCEPTS AND RELATIONSHIPS

2.1 Introduction

In geometrical geodesy the mathematical figure of an ellipsoid of revolution is adopted as a convenient model on which to reduce and compute geodetic positions of points on the earth's surface. In a similar way, the physical geodesist adopts an ellipsoidal model with particular physical characteristics which fairly well represents these constants of the real earth. (For example, the International Ellipsoid was adopted by the International Association of Geodesy (IAG) in 1930 with the following constants: (see HEISKANEN & MORITZ 1967, p 79)

$$\begin{aligned} a &= 6\ 378\ 388\ \text{m} \\ f &= 1/297.000 \\ \gamma_e &= 978.049\ 000\ \text{Gal} \\ \omega &= 0.729\ 211\ 51 \times 10^{-4}\ \text{sec}^{-1} \end{aligned} \qquad (2.1).$$

All other parameters, such as potential and mass, can be computed from these fundamental constants. In particular, the International Gravity Formula based on the above ellipsoid is found to be

$$\gamma = \gamma_e(1 + 5.2884 \times 10^{-3} \sin^2 \phi - 5.9 \times 10^{-6} \sin^2 2\phi) \qquad (2.1a).$$

The advantage of having such an approximation in physical geodesy is that, whereas the potential of earth is very large ($W \simeq 6.3 \times 10^6$kGal metres), the differences between the potential of the earth and that of the model are relatively much smaller ($\simeq f^2 \times W$). This, as will be shown later in the development, allows linearization to be carried out in the solution of the problem to acceptable orders of accuracy, greatly simplifying the treatment.

(i) Equipotential Surfaces (see figure 3)

The geoid is the equipotential surface of the real earth at mean sea level said to have a potential of $W = W_o$. In conjunction with this specific surface is a family of 'geops' (geopotential surfaces)

$$W = \text{constant} \qquad (2.2).$$

The ellipsoid taken to model the earth is also an equipotential surface, having a potential $U = U_o$ ($=W_o$). Associated with this is a family of spherops, (spheropotential surfaces),

$$U = \text{constant} \qquad (2.3).$$

It is one of the tasks of physical geodesy to use the relationships between the equipotentials in each system to relate the position of a point on one surface to its position on the other surface.

The vertical distance between the geoid and the ellipsoid is known as the N, the geoid-ellipsoid separation. It will obviously be a function of the ellipsoid chosen to model the earth.

It should be remarked that the deflection of the vertical from the normal to the ellipsoid (ε) can be defined as the small change in N for a small change in distance along the surface of the ellipsoid

$$\text{i.e.} \quad \varepsilon = \frac{\partial N}{\partial s} \qquad (2.4)$$

This parameter as well as N must be evaluated if the point on the earth's surface is to be fully described in terms of the theoretical model.

(ii) Relationships between N, γ, T and g

The gravity at P (figure 4) is a vector of magnitude g directed along the vertical, whilst the normal gravity at the point P on the ellipsoid is magnitude γ directed along the normal through P. The difference is the gravity anomaly of magnitude

$$\Delta g = g_p - \gamma_{p'} \qquad (2.5),$$

the difference in direction between $\gamma_{p'}$ and g_p being the deflection of the vertical.

By inspection of figure 4 it can be seen that

$$U_p = U_{p'} + \left(\frac{\partial U}{\partial n}\right)_{p'} N \qquad (2.6).$$

Now by definition the differential of normal gravity along the normal is $-\gamma$, the force of gravity, hence (2.6) becomes

$$U_p = U_{p'} - \gamma N \qquad (2.7).$$

If we now define the disturbing potential (T) as the difference between the geopotential and spheropotential at a point P.

$$\text{i.e.} \qquad T_p = W_p - U_p \qquad (2.8)$$

(2.8) becomes

$$W_p = U_p + T_p = U_{p'} - \gamma N + T_p$$

But $W_p = U_{p'}$ and hence

$$T = \gamma N \qquad \text{or} \qquad N = T/\gamma \qquad (2.9).$$

This is Brun's formula and is important because it converts disturbing potential to the separation along the normal between the geop and the spherop of the same potential.

Following on from this, differentiating 2.7 with respect to z

$$\frac{\partial T}{\partial z} = \frac{\partial W}{\partial z} - \frac{\partial U}{\partial z}, \quad \text{where } z \text{ is measured along the normal } (\partial z \equiv \partial n).$$

By definition

$$\frac{\partial W}{\partial z} = -g_p + O\{f\Delta g\} \; ; \quad \frac{\partial U}{\partial z} = -\gamma_p$$

and thus

$$\gamma_p = \gamma_{p'} + \frac{\partial \gamma}{\partial z} N$$

So $$\frac{\partial T}{\partial z} = - g_p + (\gamma_{p'} + \frac{\partial \gamma}{\partial z} N)$$

or $$\frac{\partial T}{\partial z} = - \Delta g_p + \frac{\partial \gamma}{\partial z} \frac{T}{\gamma} \qquad (2.10).$$

This is also an important relationship, connecting the surface gravity anomaly to the disturbing potential. It has been called the "fundamental equation of physical geodesy" (HEISKANEN & MORITZ 1967, p 86).

(iii) Computation of the Disturbing Potential

Relating (2.9) back to (2.4), it is seen that in order to find the deflection of the vertical gravimetrically, it will be necessary to compute the disturbing potential T_p. The value of the normal gravity at $U_{p'}$ can be found, for example, on the International Gravity Formula in (2.1a), the approximate latitude of P' being easily determined. But to find U_p we apparently need to know N (see 2.7), the very quantity we are seeking.

We cannot evaluate the geopotential at P using the usual Newtonian relationships of gravitational force and potential. By definition, the potential at a point P distance r from attracting point mass dm is

$$V = G \frac{dm}{r}$$

where G, the gravitational constant is 6.672×10^{-14} m^3 g^{-1} s^{-2} (see MORITZ 1965a).

The total effect at the point from an infinite number of such point masses would be

$$V = G \iiint_V \frac{dm}{r} \qquad (2.11)$$

which requires knowledge of the mass distribution in the earth's interior. This is not known and even if it were, (2.11) would present difficulties in solution. To solve the problem it is necessary to use the theorems of potential theory and vector analysis developed last century by mathematicians such as Laplace, Gauss, Green and Stokes.

(iv) Green's Third Identity

Probably the greatest aid to solving the geodetic boundary value problem, i.e. evaluating N and its derivatives, comes from the Divergence theorem (which is also known as Ostrogradskii's theorem), and expressions which develop therefrom. These effectively express total potential resultant from a body in terms of the normal components of the potential over the whole surface of that body.

For example, this theorem states that

$$\iiint_V \underline{\nabla}.\underline{F} \, dV = \iint_S \underline{F}.\underline{N} \, dS \qquad (2.12)$$

where $\underline{\nabla}$, $\underline{F}$ & $\underline{N}$ are defined in Section 1.4 above.

KELLOGG expresses this descriptively as (KELLOGG 1929, p 39), ... "the integral of the divergence of a vector field over a region of space is equal to the integral of the surface of that region of

the component of the field in the outward directed normal to the surface."

The significance of this to gravimetric solutions in geodesy is that it enables one to use observed surface gravity in the place of unobservable earth's potential to solve the geodetic problem.

As shown in MORITZ 1965, pp 7-9, Green's Identities are derived from (2.12) by introducing the two functions $U = U(x, y, z)$ and $V = V(x, y, z)$.

If U becomes the function $1/r$, and V the potential defined in (2.11) above, it can be easily shown that

$$\iiint_\tau \frac{1}{r} \cdot \nabla^2 V \, d\tau = - p.V - \iint_s \left[\frac{1}{r} \underline{\nabla} \underline{N} V - V \underline{\nabla} \underline{N} \frac{1}{r}\right] dS \qquad (2.13)$$

where $p = 4\pi$ if P is (inside S
2π (on surface of S
0 (outside S

and τ is the volume exterior of surface S.
$\underline{N}$ is the outer normal of S.

(v) Laplace's Equation and Poisson's Equation

Another theorem of importance is Laplace's equation, which states that for an harmonic function (i.e. one which is continuous through space and approaches 0 as $1/r$), and the potential V fulfils this requirement outside the earth's surface S,

$$\nabla^2 V = \frac{\partial^2 V}{\partial x^2} + \frac{\partial^2 V}{\partial y^2} + \frac{\partial^2 V}{\partial z^2} = 0 \qquad (2.14).$$

However, it must be stressed that this only holds if there is no attracting matter outside S.

If the potential becomes discontinuous (eg. at the density discontinuity of the surface) then Poisson's equation holds at points occupied by matter

i.e. $$\nabla^2 V = - 4\pi G \rho$$

where G is the gravitational constant
and ρ is the density of the gravitating body at the surface.

(vi) Application to the Geoid

If the masses lying within surface S contribute amount V_i to the total potential W, and masses external to S contribute V_e and the potential due to the rotation of the earth is V_r, then

$$W = V_i + V_e + V_r \qquad (2.15).$$

Applying Green's Third Identity to V_i, V_e and V_r in turn, under circumstances where (2.14) holds it can be shown that the total earth's potential at P can be expressed as

$$W_p = 2V_{e_p} + 2V_{r_p} + \frac{\omega^2}{\pi}\iiint \frac{1}{r}\, d\tau - \frac{1}{2\pi}\iint\left(\frac{1}{r}\,\underline{\nabla}\,\underline{N}\,W - W\,\underline{\nabla}\,\underline{N}\,\frac{1}{r}\right) dS \qquad (2.16)$$

where W_p = total potential of the earth at P on the surface, and
ω = angular velocity of the earth about its rotational axis.

A similar expression in normal potential at P (U_p) is achieved if (2.16) is applied to the gravity model rather than actual earth. The assumptions which must be made about the model generating U are

(1) it has the same rotational characteristics as the earth;
(2) it has the same volume as the earth;
(3) it should have the potential $U_o = W_o$ at the reference surface.

This last assumption is difficult to achieve, since W_o is not really known. However $U_o = W_o$ is implied in subsequent development by making the zero and 1st order harmonic in the harmonic series, set up to represent the gravity anomaly surface, equal to zero.

By taking $W_p - U_p = T_p$ we find, by differencing (2.16) and its equivalent in U,

$$T_p = 2V_{e_p} - \frac{1}{2\pi}\iint\left[\frac{1}{r}\,\underline{\nabla}\,\underline{N}\,T - T\,\underline{\nabla}\,\underline{N}\,\frac{1}{r}\right] dS \qquad (2.17).$$

(vii) Evaluation of Disturbing Potential on the Geoid

(a) The geoid is, by definition, an equipotential surface. This allows a fairly simple evaluation of the first term in the kernel of (2.17). Any components of T along the surface of the geoid must be zero, i.e.

$$\frac{\partial T}{\partial x} = \frac{\partial T}{\partial y} = 0 \qquad (2.18)$$

and $$\underline{\nabla}\,\underline{N}\,T = \frac{\partial T}{\partial n} = \frac{\partial T}{\partial z}$$

From (2.10), $$\frac{\partial T}{\partial z} = -\Delta g_p + \frac{\partial \gamma}{\partial z}\,\frac{T}{\gamma}\,.$$

Using a spherical model of the earth (which will be correct to the order of the flattening 3×10^{-3}), we have

$$\gamma = \frac{GM}{R^2} \quad ; \text{ where } M \text{ is the mass of the earth.}$$

So $$\frac{\partial \gamma}{\partial z} \equiv \frac{\partial \gamma}{\partial R} = -2\,\frac{GM}{R^3}$$

or $$\frac{\partial \gamma}{\partial z} = -\frac{2\gamma}{R} + O\{f\} \qquad (2.19)$$

Thus $$\frac{\partial T}{\partial z} = -\Delta g_p - \frac{2\gamma}{R}\,\frac{T}{\gamma} \qquad (2.20).$$

(b) The second term is evaluated by assuming a spherical model for the earth, where R_p is the geocentric radial distance to P, R is this same distance to the general point Q, and ψ the angle at the geocentre subtended by PQ.

Thus $$r^2 = R_p^2 + R^2 - 2R_p R\cos\psi$$

and $$\underline{\nabla}\,\underline{N}\,\frac{1}{r} \equiv \frac{\partial}{\partial R}\,\frac{1}{r} = -\frac{1}{2Rr} \qquad (2.21).$$

(c) Substituting (2.20) and (2.21) into (2.17), we get

$$T_p = \frac{1}{2\pi}\iint \left[\frac{1}{r}\left(\Delta g + \frac{2\gamma}{R}\,\frac{T}{\gamma}\right) + T\left(-\frac{1}{2Rr}\right)\right] dS$$

$$= \frac{1}{2\pi}\iint \left[\frac{1}{r}\left(\Delta g + \frac{3}{2}\,\frac{T}{R}\right)\right] dS$$

or $$T_p = \frac{1}{4\pi}\iint \frac{1}{r}\left(2\Delta g + \frac{3T}{R}\right) dS \qquad (2.22).$$

The solution of this expression will not be developed here, as it has no direct interest in the investigation as such. A full treatment can be found in (eg. HEISKANEN & MORITZ 1967, p. 92ff). It can be shown that

$$T_p = \frac{R}{4\pi}\iint f(\psi)\ \Delta g\ d\sigma$$

and $$N_p = \frac{R}{4\pi\gamma}\iint f(\psi)\ \Delta g\ d\sigma \qquad (2.23)$$

where $$f(\psi) = 1 + \operatorname{cosec}\tfrac{1}{2}\psi - 6\sin\tfrac{1}{2}\psi - 5\cos\psi -$$

$$- 3\cos\psi\ \ln\{\sin\tfrac{1}{2}\psi\,(1 + \sin\tfrac{1}{2}\psi)\} \qquad (2.24)$$

is known as Stokes' function and ψ is the angular distance from P to the element of surface area,

Δg is the gravity anomaly at $d\sigma$, and
$d\sigma$ is the element of surface area in steradians.

The assumptions and approximations made to date are as follows:

A. With respect to the Model

(i) The adopted ellipsoid has the same mass and centre of mass as the earth;
(ii) it has the same surface potential as the geoid;
(iii) there is no mass outside the surface;
(iv) it has the same rotational potential as the earth.

The adoption of these characteristics allows us to solve the otherwise insoluble (2.16). By differencing the W in (2.16) with the U resulting from the model (2.16) is in effect made linear, as is shown in (2.17).

B. With respect to the Geoid

The main assumption is that there is no matter outside the geoid's surface. This is a faulty assumption and if left unresolved must only produce approximations to the geoid. One device which is used is to correct the surface gravity anomaly for the amount of attracting material between the geoid and the surface i.e. use the Bouguer anomaly in Stokes' formula (2.23). This will produce a value for N which will differ from the true geoid-ellipsoid separation (as the model is obviously still not a true reflection of reality) and the indirect effect of this correction should be considered. In some cases isostatic reductions have been considered. (MORITZ 1965, p 27), or a

surface layer introduced onto the geoid in order to account for the mass exterior to it. However, a number of writers since Stokes have produced solutions which circumvent the problem presented here completely.

(viii) Computation of the Deflection of the Vertical

The angle between the vertical and the normal through a point P on the geoid is defined as the deflection of the vertical. Usage and convenience have created the convention of resolving ε into two components:

ξ along the meridian and
η along the prime vertical at P, where

ξ is considered +ve if the vertical is north of the normal and
η is considered +ve if the vertical is east of the normal.

By considering figure 4 we see that

$$\xi = -\frac{\partial N}{\partial x} \quad ; \quad \eta = -\frac{\partial N}{\partial y} \tag{2.25}$$

where N is defined in (2.23).

Now

$$\partial x = -R\ \partial\psi\ \sec\alpha$$
$$\partial y = -R\ \partial\psi\ \operatorname{cosec}\alpha$$

where α = azimuth of $\partial\psi$ from P.

Since

$$\xi = -\frac{\partial N}{\partial\psi}\frac{\partial\psi}{\partial x} \quad \text{and} \quad \eta = -\frac{\partial N}{\partial\psi}\frac{\partial\psi}{\partial y}$$

and $$\frac{\partial\psi}{\partial x} = -\frac{\cos\alpha}{R} \quad ; \quad \frac{\partial\psi}{\partial y} = -\frac{\sin\alpha}{R}$$

therefore $$\xi_i = \frac{1}{4\pi\gamma}\iint \Delta g\ \frac{\partial f(\psi)}{\partial\psi}\cos\alpha_i\ d\sigma \quad ; \quad i = 1, 2 \tag{2.26}$$

where $\xi_1 = \xi \qquad \xi_2 = \eta$

and $\alpha_1 = \alpha \qquad \alpha_2 = 90 - \alpha$

Differentiating Stokes' function (2.24) with respect to ψ gives

$$\frac{\partial f(\psi)}{\partial\psi} = -\tfrac{1}{2}\operatorname{cosec}^2\tfrac{1}{2}\psi\cos\tfrac{1}{2}\psi + 5\sin\psi - 3\cos\tfrac{1}{2}\psi + 3\sin\psi\ \ln[\sin\tfrac{1}{2}\psi\ (1+\sin\tfrac{1}{2}\psi)\ ] -$$
$$- \frac{3\cos\psi\ \frac{1}{2}\left[\cos\tfrac{1}{2}\psi + 2\sin\tfrac{1}{2}\psi\cos\tfrac{1}{2}\psi\right]}{\sin\tfrac{1}{2}\psi\ (1+\sin\tfrac{1}{2}\psi)} \tag{2.27}.$$

Equations (2.26) are known as the Vening Meinesz formulae for deflection of the vertical.

The comments on the assumptions inherent in the Stokes' integral made at the end of the previous section apply also to the Vening Meinesz formulae.

In the next sections methods adopted to circumvent the short-comings in the Stokes & Vening-Meinesz formulae will be outlined and developed.

2.2 Contemporary Solutions

2.2.1 The Telluroid

In 1960 Molodensky published a solution which by-passed the need to reduce information to the geoid. To appreciate his approach, and methods associated with it, it is necessary to explain new concepts on which this method depends.

The surface of the earth (S) is referred to a second surface known as the telluroid. This was initially defined by HIRVONEN (1960, p 39) as the locus of points whose positions were given by the geodetic ϕ and λ of the surface point P and whose spheropotential was equal to the geopotential at the point P. (see figure 3). This is the intersection of the normal through P with the spherod $U = W_P$. Definition in this way is inconclusive and a modification was suggested by DE GRAAFF-HUNTER (1960, p 193). In his system the 'Terroid' became the locus of associated points defined by the astronomically determined values of ϕ_A and λ_A for P on the spherop $U = W_P$ (see point Q, fig. 3),

i.e. $$\phi_Q = \phi_{P_A} \quad , \quad \lambda_Q = \lambda_{P_A} \quad , \quad U_Q = U_0 + (W_P - W_0) \qquad (2.28).$$

In terms of location and derivation this change makes little difference, but it did provide a more absolute definition of the position of the reference surface (hereafter called the 'telluroid') as its planimetric location was no longer dependent on the ellipsoid chosen for the geodetic model. It can be seen that the telluroid is a reflection of the terrain but displaced from it by the vector $\underline{d}$, where this is defined as

$$\underline{d} = R\,\xi\,\underline{1} + R\,\eta\,\underline{2} + \zeta\,\underline{3} \qquad (2.29)$$

where $\underline{1}$, $\underline{2}$ and $\underline{3}$ are defined in section 1.4.

The normal to the spherop through Q (N' in figure 3) will have the same spatial orientation as the vertical through P. The x and y axes, which together with N'(z) will define a rectangular coordinate system at Q, will point north and east respectively. (See MORITZ 1965, pp 13, 14; MATHER 1968a, pp 34 and 42).

As can be seen from figure 3 , ζ is the distance measured along the vertical between geop W_P and spherop U_q . ξ and η are the components of the deflection of the vertical at the surface, ie. of the angle between PV and PN(ε). Thus it can be seen that the task presented by this more recent postulation of the problem is to evaluate ζ . The development in 2.1(ii) can be repeated for ζ, with ζ substituting for N, and with P, P' now becoming the surface point and associated telluroid point respectively (ie. P and Q in figure 3). PICK(1973, pp 174-175) shows this development and extends it to include second-order effects. A summary of this is given below. The disturbing potential ($T_p = W_p - U_p$) is differentiated in the direction of normal gravity, γ , to give

$$\frac{\partial T_p}{\partial z} = \frac{\partial W_p}{\partial z} - \frac{\partial U_p}{\partial z}$$

or $$-g_p = \frac{\partial T_p}{\partial z} - \gamma_p \qquad \text{(assuming } -g_p \cos\varepsilon = -g_p \text{ for small } \varepsilon\text{)}.$$

$\frac{\partial T_p}{\partial z}$, γ_p are expanded by a Taylor's expansion to give

$$\frac{\partial T_p}{\partial z} = \frac{\partial T_q}{\partial z} + \frac{\partial^2 T_q}{\partial z^2}\,\zeta + \ldots$$

and

$$\gamma_p = \gamma_q + \frac{\partial \gamma_q}{\partial z}\,\zeta + \tfrac{1}{2}\,\frac{\partial^2 \gamma_q}{\partial z^2}\,\zeta^2 + \ldots$$

Thus

$$-g_p + \gamma_q = \frac{\partial T_q}{\partial z} + \frac{\partial^2 T_q}{\partial z^2} - \frac{\partial \gamma_q}{\partial z} - \frac{\partial^2 \gamma_q}{\partial z^2}\,\frac{\zeta}{2} \ldots$$

which on expansion, gives

$$-\Delta g = \frac{\partial T_q}{\partial z} - \frac{T_p}{\gamma_q}\,\frac{\partial \gamma_q}{\partial z} - \frac{T_p}{\partial q}\,\frac{\partial^2 T_q}{\partial z^2} \quad .$$

Comparison with equation (2.10) show that a second-order term $\frac{T_p}{\gamma_q}\,\frac{\partial^2 T_q}{\partial z^2}$ has been applied to this original expression. The effects of this correction on the evaluation of ξ and η are referred to later (see section 8.4.2).

As ζ is analogous to N in (2.26) and indeed substitutes for it when mapping a surface known as the quasi-geoid on the reference ellipsoid (see HEISKANEN & MORITZ 1967, p 293 and MOLODENSKII ET AL 1962, p 76), it must obviously be evaluated as a first step to determining the ξ and η at the surface.

2.2.2 The Deflection at the Surface

The deflection of the vertical at P can now be defined as the angle produced by the small change in the separation between U_p and W_q $(d\zeta)$ for an increment in the distance along the surface Wp (ds). The two components at the surface in the meridian and the prime vertical are therefore

$$\xi = -\frac{d\zeta}{ds_\phi} \quad ; \quad \eta = -\frac{d\zeta}{ds_\lambda} \tag{2.30}$$

The variable ζ is calculated at the telluroid, hence it is necessary to account for the fact that the reference surface is no longer a level surface, as it was in the case of the geoid.

Using the axis system as defined in (2.2.1) above, and remembering that ζ itself is a function of ϕ, λ (or x, y), we get

$$\left(\frac{d\zeta}{dx}\right)_{U=W_p} = \left(\frac{\partial \zeta}{\partial x}\right)_{Tell} + \frac{\partial \zeta}{\partial z}\,\frac{\partial z}{\partial x} \quad .$$

Now $\frac{\partial z}{\partial x} = \tan \beta_1$; where β_1 is the slope of the telluroid in the northerly direction

and

$$\frac{\partial \zeta}{\partial z} = \frac{\partial}{\partial z}\left(\frac{T}{\gamma}\right) = -\frac{1}{\gamma}\left(-\frac{\partial T}{\partial z} + \frac{1}{\gamma}\,\frac{\partial \gamma}{\partial z}\,T\right) = -\frac{\Delta g}{\gamma} \tag{2.30a}$$

by equation 2.10

It follows that

$$\xi = -\frac{d\zeta}{dx} = -\left(\frac{\partial\zeta}{\partial x}\right)_{Tell} + \frac{\Delta g}{\gamma}\tan\beta_1 \qquad (2.31).$$

Similarly,

$$\eta = -\frac{d\zeta}{dy} = -\left(\frac{\partial\zeta}{\partial y}\right)_{Tell} + \frac{\Delta g}{\gamma}\tan\beta_2 \qquad (2.32)$$

where β_2 is the slope of the telluroid in the easterly direction.

2.2.3 Evaluation of ζ and ξ , η

There are two main ways of evaluating ζ , ξ and η in the telluroid-earth's surface system, and a review of these will be stated here. The first approach was developed by Molodensky (as reported in MOLODENSKII ET AL 1962, pp 118-124) who devised a method which expresses the anomalous potential T as the potential of a surface layer on the telluroid. The mathematical derivation is outlined in section 2.4 However the solution which evolves contains two parts; a 'first-order' contribution which is merely the standard Stokesian (or Vening Meinesz) solution for the non-regularised geoid; and a second order term which is a correction for the fact that the telluroid departs from a level surface, and is therefore a function of height and gravity differences.

The second approach has been mentioned by BROVAR (BROVAR ET AL 1964, pp 154-157) and MORITZ (1965 pp 16018) but has not achieved wide acceptance as a method of solution. It applies the linearised form of Green's Third Identity (2.17), to the telluroid, ie. tries to evaluate term by term the quantities which eventuate from this application. Its full development is shown in section 2.3, and it will be seen that its solution again consists of two components, a Stokesian term and a correction for the departure of the topographic surface from a level surface.

Both of these methods of correction are evaluated and used in the computation of deflections in the test area. The results of these computations and interpretations are given in chapter 8.

2.2.4 Bjerhammar's Sphere

In 1964 BJERHAMMAR (1964) introduced a completely different approach to the solution of the boundary value problem. He postulated the model of a sphere on which fictitious gravity anomalies (Δg^*) would be located such that, upon upward continuation of these anomalies, the actual gravitational field on the earth's surface (Δg) was generated. The task of finding the values of Δg^* contains certain problems of a philosophical nature (eg. the difficulty of downward continuation through a non-continuous medium from the surface) but once the concept is accepted, the boundary value problem is solved on the surface of the Bjerhammar sphere using spherical formulae. A further discussion of this method is given in section 2.5.

2.3 Direct Evaluation of Green's Third Identity

2.3.1 Introduction

The approach which is developed below is substantially that given in (MATHER 1970a) although it can also be found to a lesser stage of development in (MORITZ 1965). Brovar's treatment (BROVAR ET AL 1964, pp 154-157) whilst starting from the same premise develops along different lines.

The general idea is to evaluate the linearised form of Green's Third Identity at the earth's surface and then apply this to deflections at the surface. To do this it is necessary to consider in detail the expression (2.17), particularly relating it to the present test region.

Thus,

$$T_p = \frac{1}{2\pi} \iint \left(T \, \underline{\nabla} \, \underline{N} \, \frac{1}{r} - \frac{1}{r} \, \underline{\nabla} \, \underline{N} \, T \right) dS \qquad \text{from (2.17)}$$

where r is the distance from dS to the computation point P

dS is the element of surface area on the earth

T is the disturbing potential (in the integral, this refers to the T at dS ; T_p is T at P)

$\underline{N}$ is the unit normal vector to dS.

The disturbing potential at P is given by

$$T_p = (W_o - U_o) + \gamma \, \zeta$$

as can be seen directly from figure 3.

For convenience we will assume $W_o = U_o$ throughout. This condition is effectively forced by ignoring zero-degree harmonics in the Stokes' solution and since it is in the nature of a datum shift, will not in any case have an effect on ξ or η.

The vertical gradient of the disturbing potential is therefore

$$\frac{\partial T}{\partial z} = - \left(\Delta g + \left| \frac{\partial \gamma}{\partial z} \right| \zeta \right) \qquad \text{from (2.10).}$$

Note that in the following development the letter Q will be used to denote the general point on the earth's surface and Q' will be the equivalent point on the telluroid. P will be reserved specifically for the point at which the computation takes place, and P' its corresponding point on the telluroid.

2.3.2 Unit Normal Vector $\underline{N}$

To evaluate (2.17) we must first find the unit normal vector at each point of the telluroid's surface in terms of known or measurable parameters. (The definition of the telluroid has been given above (section 2.2.1) as the locus of points Q' which have the same astronomical latitude and longitude as the surface points Q and with normal potential $U_q = U_o + \Delta W$, using the revised notation).

At each discrete point Q' a local cartesian coordinate system (x, y, z) is adopted, such that z lies along the normal to the spherop at Q', with the $x\,y$ plane tangential to the spherop at Q', x oriented to the north and y eastward.

We define α_D as the azimuth of the 'dip' of the telluroid at T (the dip being the line of greatest slope in a plane). This closely approximates the dip of the ground surface at Q, the slope of which is taken to be β .

If the ground slope is positive to the north and east, the direction cosines of the telluroid normal can be seen from figure 5 to be

$$- \sin\beta \cos(\pi + \alpha_D) \; , \; - \sin\beta \sin(\pi + \alpha_D) \; , \; \cos\beta \qquad (2.33).$$

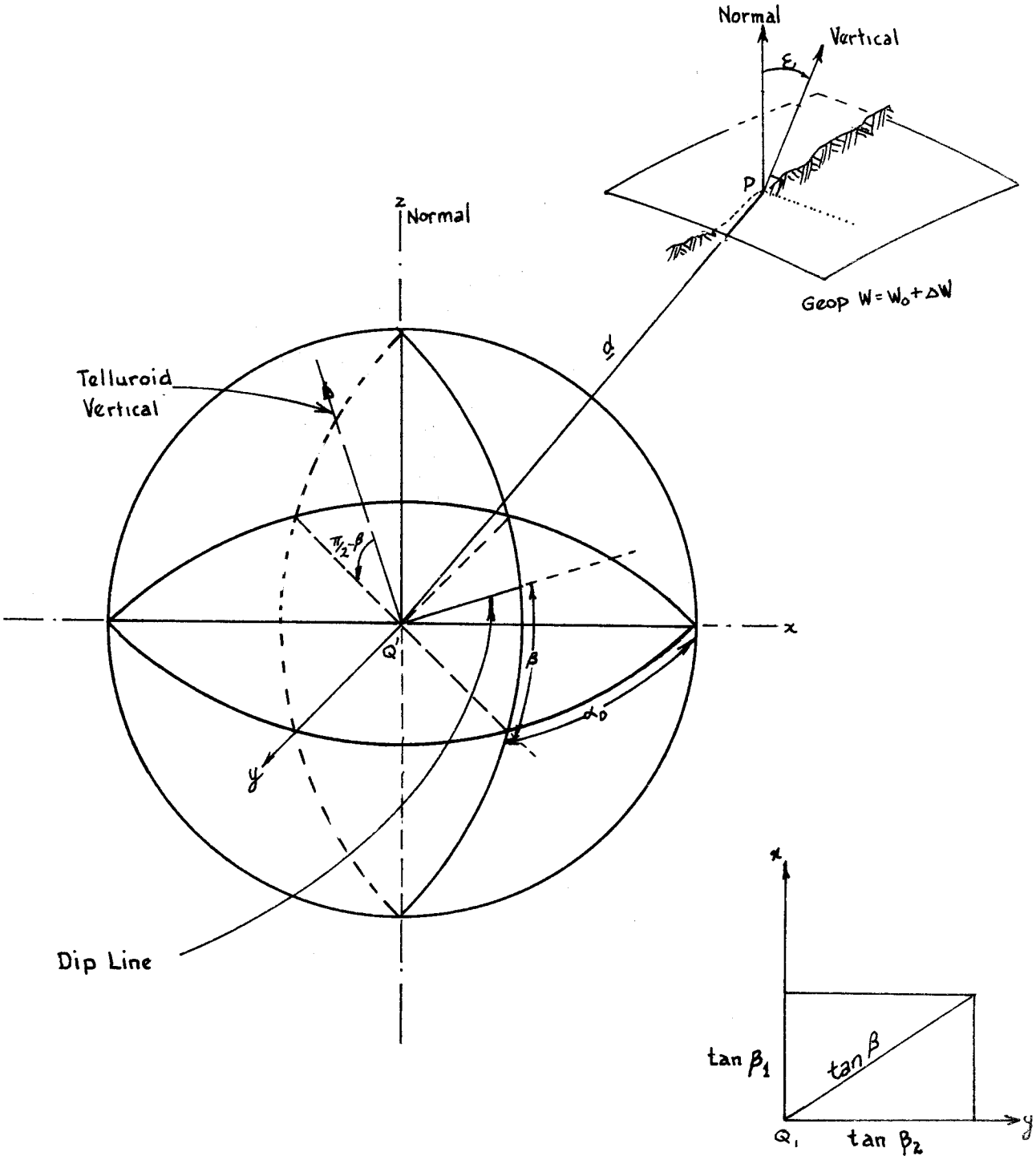

FIG.5 TOPOGRAPHICAL GRADIENTS IN THE LOCAL CARTESIAN FRAME ON THE TELLUROID

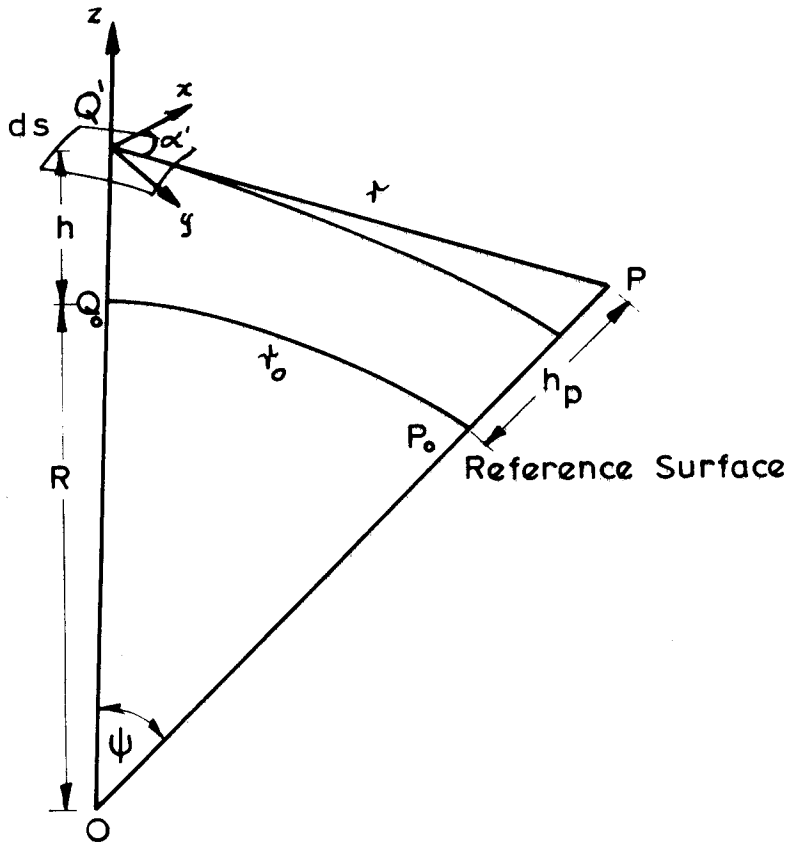

Fig. 6

The topographical effect for a spherical approximation of the earth.

Taking β_1, β_2 to be the ground (and telluroid) slopes to the north and east respectively, then

$$\tan \beta_1 = \tan \beta \cos \alpha_D \quad (2.33a) \qquad \text{and} \qquad \tan \beta_2 = \tan \beta \sin \alpha_D \quad (2.33b).$$

Thus we can also express the unit normal vector purely in terms of the terrain slope by substituting for $\cos \alpha_D$, $\sin \alpha_D$ to get

$$\underline{N} = - \cos \beta \tan \beta_1 \underline{1} - \cos \beta \tan \beta_2 \underline{2} + \cos \beta \, \underline{3} \qquad (2.34).$$

(i) Term $\underline{\nabla} \, \underline{N} \, \frac{1}{r}$

The distance r is measured from the element of area dS to the computation point P',

$$r^2 = X^2 + Y^2 + Z^2$$

where X, Y, Z are the projection of r onto the x, y, z axes at Q', respectively.

Now $$\nabla \frac{1}{r} = - \frac{1}{r^3} (X \, \underline{1} + Y \, \underline{2} + Z \, \underline{3}) \qquad (2.35).$$

So compounding this with $\underline{N}$ from (2.34) above, we get

$$\underline{\nabla} \, \underline{N} \frac{1}{r} = \frac{1}{r} (\cos \beta \tan \beta_1 X + \cos \beta \tan \beta_2 Y - \cos \beta \, Z) \qquad (2.36).$$

Q' rather than Q is used here as the surface point because it can be fixed spatially by means of the definition in section 2.2.1. In other words, because the telluroid can be exactly defined and yet so closely resembles the ground surface, all development relates to the telluroid.

(ii) Term $\underline{\nabla} \, \underline{N} \, T$

In a similar fashion, remembering $\frac{\partial T}{\partial x} = \gamma \frac{\partial \zeta}{x}$ and $\xi = \frac{\partial \zeta}{\partial x}$

$$\underline{\nabla} \, \underline{N} \, T = \cos \beta (\gamma [\xi \tan \beta + \eta \tan \beta] + \frac{\partial T}{\partial z}) \qquad (2.37)$$

(iii) Combining to find T_p

Substituting (2.36) and (2.37) into (2.17) we get

$$T_p = \frac{1}{2\pi} \iint [\frac{\cos \beta \, T}{r^3} (X \tan \beta_1 + Y \tan \beta_2 - Z) -$$

$$\frac{\cos \beta}{r} \{ \gamma (\xi \tan \beta_1 + \eta \tan \beta_2) + \frac{\partial T}{\partial z} \}] \, dS.$$

Collecting terms,

$$T_p = 1 \iint \frac{\cos \beta}{r} [(- \frac{\partial T}{\partial z} - T \frac{Z}{r^2}) +$$

$$+ T (\frac{X}{r^2} \tan \beta_1 + \frac{Y}{r^2} \tan \beta_2) - \gamma \xi \tan \beta_1 - \gamma \eta \tan \beta_2] \, dS \qquad (2.38).$$

The term $\cos\beta\, dS$ can be thought of as the plane elemental area on the telluroid dS projected on to the associated spherop, as the slope of telluroid is β, $dS \cos\beta$ can be replaced by horizontal elemental area dS'. This can in turn be expressed in terms of the solid angle subtended at the earth's centre by dS (or dS'). Taking R as mean earth radius, and h as the general expression for the normal height of dS, we get that

$$\cos\beta\, dS = (R + h)^2\, d\sigma \tag{2.39}$$

where $d\sigma$ is in steradians.

2.3.3 Evaluation of Spatial Elements

(i) r

r is the general distance in space between P' and Q'. It is convenient to express this in terms of the distance projected onto the reference surface by $P'Q'$ and the radial displacements of P' and Q' from this surface.

From figure 6,

$$r_o = 2R \sin\tfrac{1}{2}\psi \tag{2.40}$$

using a sphere as the mathematical model.

Now if h, hp are the normal heights of Q' and P' respectively, we get by the cos rule

$$r^2 = (R + h)^2 + (R + h_p)^2 - 2\,(R + h)(R + h_p)\cos\psi$$

where ψ is the angle subtended by r_o at the earth's centre.

Expanding this,

$$r^2 = r_o^2 + (h - h_p)^2 + 2\,h\,R\sin^2\tfrac{1}{2}\psi + 2\,h_p\,R\sin^2\tfrac{1}{2}\psi + 2\,h\,h_p\sin^2\tfrac{1}{2}\psi$$

or

$$r^2 = r_o^2\left[\,1 + \frac{(h-h_p)^2}{r_o^2} + \ldots\,\right], \tag{2.41}$$

as it can be easily shown that the last three terms can be ignored as contributing insignificantly to the value of r.

Also

$$\frac{1}{r} = \frac{1}{r_o}\left[\,1 - \tfrac{1}{2}\left(\frac{h-h_p}{r_o}\right)^2 + \ldots\,\right] \tag{2.42}$$

for $\left|(h-h_p)/r_o\right| < 1$

Because of the sensitivity of the deflection computation to the gravity field in the immediate vicinity of the computation point, it is important to evaluate accurately the spatial elements when $r \to 0$. Ignoring the height dependent terms altogether will lead to large errors in the estimation of r for small r. In the extreme case in the test region this could introduce up to a 40% error, although in flat regions its contribution is negligible.

(ii) $\frac{Z}{r^3}$

As Z was defined as the component of r along the z axis at Q' it can be seen from figure 6 that

$$-Z = (R + h_p) \cos \psi - (R + h),$$

thus

$$-\frac{Z}{r^3} = \frac{(R + h_p) \cos \psi - (R + h)}{r_o^3 \left[1 + \left(\frac{h - h_p}{r_o}\right)^2\right]^{3/2}}$$

$$= \frac{h_p - h - r_o^2/2R}{r^3} \qquad (2.43).$$

If $(h - h_p)/r_o < 1$ and ψ is small $(< 1.5^o)$, it follows from (2.42) that

$$-\frac{Z}{r^3} = \frac{h_p - h - r_o^2/2R}{r_o^3} \left[1 - \frac{3}{2}\left(\frac{h - h_p}{r_o}\right)^2 \ldots\right] \qquad (2.44)$$

which reduces to

$$= -\frac{1}{2Rr_o} + \frac{h_p - h}{r_o^3} + 0\{\frac{fZ}{r_o^3}\}$$

if $|(h - h_p)/r_o| \not> 5 \times 10^{-2}$.

The problem posed by terrain slopes of $> 45^o$ (i.e. $|(h - h_p)/r_o| > 1$) forces use of the form expressed in (2.43), to avoid the divergent series which is otherwise introduced if (2.44) is adopted.

(iii) Terms in $\frac{X}{r^3}$, $\frac{Y}{r^3}$

From figure 6,

$$X = (R + h_p) \sin \psi \cos \alpha' \qquad (2.45)$$

where $\alpha' = \alpha \pm \pi$.

So, if $|(h - h_p)/r_o| < 1$

$$\frac{X}{r^3} = \frac{X}{r_o^3}\left[1 + \frac{h - h_p}{r_o}^2 + 0\{\frac{h - h_p}{r_o}^4\}\right] \qquad (2.46).$$

Using the analogous expressions for Y, by routine substitution it is shown that

$$\frac{X}{r^3} \tan \beta_1 + \frac{Y}{r^3} \tan \beta_2 = (R + h_p) \sin \psi \ (\cos \alpha' \tan \beta_1 + \sin \alpha' \tan \beta_2).$$
$$\cdot \left[1 - \frac{3}{2} \frac{h - h_p}{r_o}^2 + 0\{\frac{h - h_p}{r_o}^4\}\right] \qquad (2.47).$$

If the computation point is located in a steep mountainous area, the assumption for $(h - h_p)/r_o$ may break down and it will then be necessary to evaluate r in its undeveloped form (2.41).

MATHER (1970a, p 22) shows it is possible to interpret the term $\cos\alpha' \tan\beta_1 + \sin\alpha' \tan\beta_2$ as $\frac{dh}{dr_o}$, hence (2.47) becomes

$$\frac{X}{r^3} \tan\beta_1 + \frac{Y}{r^3} \tan\beta_2 = \frac{(R + h_p) \sin\psi}{r_o^3} \frac{dh}{dr_o} \left[1 - \frac{3}{2} \left(\frac{h - h_p}{r_o} \right)^2 \right] \qquad (2.48).$$

(iv) Collecting Terms (i) - (iii)

Substituting (2.48), (2.44) and (2.42) into (2.38), and applying Bruns formula gives

$$\zeta_p = \frac{1}{2\pi\gamma} \iint \left[-\frac{\partial T}{\partial z} \frac{1}{r_o} \left\{ 1 - \tfrac{1}{2} \left(\frac{h - h_p}{r_o} \right)^2 \right\} + T \left(-\frac{1}{2Rr_o} + \frac{h_p - h}{r_o^3} \right) + T \frac{(R + h_p) \sin\psi}{r_o^3} \frac{dh}{dr_o} \left\{ 1 - \frac{3}{2} \left(\frac{h - h_p}{r_o} \right)^2 \right\} - \frac{\gamma}{r} (\zeta \tan\beta_1 + \eta \tan\beta_2) \right] dS' \qquad (2.49).$$

It is interesting to observe that the last term is not expressed in the approximate form $r = f(r_o, h, h_p)$. It will be shown later that this is the most significant term in the correction terms, and it is noteworthy that it has not yet been affected by the instability of the expanded form of r as $\beta \to 45^o$.

The expression (2.49) can be reorganised for convenience to take the form

$$\zeta_p = \frac{1}{2\pi\gamma} \iint (I_1 + I_2 + I_3) \, dS'$$

where

$$I_1 = \frac{1}{r_o} \left(-\frac{\partial T}{\partial z} - \frac{T}{2R} \right) \qquad (2.50)$$

$$I_2 = \frac{T R \sin\psi}{r_o^3} \frac{dh}{dr_o} - \frac{\gamma}{r} (\zeta \tan\beta_1 + \eta \tan\beta_2) \qquad (2.51)$$

and

$$I_3 = \frac{(h_p - h)}{r_o^3} T + \frac{3}{4Rr_o} \left(\frac{h - h_p}{r_o} \right)^2 T - \frac{3R \sin\psi}{2r_o^3} \frac{dh}{dr} \left(\frac{h-h}{r_o} \right)^2 T - \tfrac{1}{2} r_o I_1 \left(\frac{h - h_p}{r_o} \right)^2 + O\left\{ \left(\frac{h - h_p}{r_o} \right)^4 \right\} \qquad (2.52).$$

I_1 is seen to be equivalent to the kernel of Stokes' integral (see equation (2.22) and the development leading up to this). This term will therefore give the Stokesian contribution to ζ_p, i.e.

$$N_p = \frac{1}{2\pi\gamma} \iint I_1 \, dS' \qquad (2.53).$$

The second term takes into account the slope of the telluroid at all points Q', and can be considered

to be a correction for the fact that the subject surface is no longer level, viz.

$$\zeta' = \frac{1}{2\pi\gamma} \iint I_2 \, dS'.$$

The remaining terms in I_3 are corrections for the departure of the subject surface from the spherop through P'. They will be insignificant except in cases of small r. Also, according to the development in 3.3 this term will also be diminished because $T \to T_p$ as $r_o \to 0$. Thus only the first term, being the most significant term, will be included in I_2.

Hence
$$\zeta_p = N_p + \zeta_p' \tag{2.54}$$

where
$$N_p = \frac{R^2}{2\pi\gamma} \iint I_1 \, d\sigma \tag{2.55}$$

$$\zeta_p' = \frac{R^2}{2\pi\gamma} \iint \left[\left(\frac{R \sin\psi}{r_o^3} \frac{dh}{dr_o} + \frac{h_p - h}{r_o^3} \right) T - \frac{\gamma}{r} (\xi \tan\beta_1 + \eta \tan\beta_2) \right] d\sigma \tag{2.56}.$$

(v) r not approximated

The advantage of expanding $r = f(r_o, h, h_p)$ is that it permits the splitting of the resultant expression for ζ (2.49) into a Stokesian term and terrain corrections to this term.

If r is not expanded, (2.49) becomes

$$\zeta_p = \frac{R^2}{2\pi\gamma} \iint - \left[\frac{\partial T}{\partial z} \frac{1}{r} - T \frac{(h_p - h - r^2/2R)}{r^3} + \right.$$

$$\left. + T \left\{ \frac{(R + h_p) \sin\psi}{r^2} \frac{dh}{dr} - \frac{1}{r} (\gamma \xi \tan\beta_1 + \gamma \eta \tan\beta_2) \right\} \right] dS' \tag{2.57}.$$

For evaluation it is necessary to express $\frac{\partial T}{\partial z}$ in terms of the gravity anomaly Δg in a manner similar to the development in (iv) above. This can be accomplished by an iterative procedure developed by MATHER (1973 , pp 30-34).

(vi) Comments

Confirmation of the major elements of the expression derived in equation (2.57) can be seen from the "Arnold" type solutions, as summarised in (MORITZ 1966, pp 71-74; 91-92). Starting from a simple gradient formula, viz.

$$T = \frac{R}{4\pi} \iint \left[\Delta g - \frac{\partial \Delta g}{\partial h} (h - h_p) \right] f(\psi) \, d\sigma \tag{2.58}$$

a solution is achieved, making some 'planar' approximations in the process, whereby the correction to the disturbing height is expressed as

$$\partial\zeta = - \frac{R^2}{2\pi\gamma} \iint \frac{1}{r_o} (\xi \tan\beta_1 + \eta \tan\beta_2) \, d\sigma +$$

$$+ \frac{R^2}{2\pi\gamma} \iint \frac{h - h_p}{r_o^2} \gamma (\xi \cos\alpha + \eta \sin\alpha) \, d\sigma .$$

Remembering that $\frac{dh}{dr_o} = (\cos\alpha' \tan\beta_1 + \sin\alpha' \tan\beta_2)$

and approximating $R \sin \psi \simeq r_o$ for small ψ then (2.56) becomes, after rearranging terms

$$\zeta' = \frac{R^2}{2\pi\gamma} \iint \left[\frac{N}{r_o^2} (\cos \alpha' \tan \beta_1 + \sin \alpha' \tan \beta_2) + \frac{h_p - h}{r_o^3} \right] d\sigma$$

$$- \frac{R^2}{2\pi\gamma} \iint \frac{\gamma}{r} \left(\xi \tan \beta_1 + \eta \tan \beta_2 \right) d\sigma \, .$$

The difference between the less significant terms are due to the basic difference in the derivational approach (ie. by use of upward continuation of the anomaly from sphere to ground instead of the evaluation of $\underline{\nabla} \underline{N} \frac{1}{r}$ on the telluroid).

2.3.4 The Evaluation of ξ , η

Recalling (2.31) and (2.32), we see that

$$\xi = - \frac{d\zeta}{dx} = - \left(\frac{\partial \zeta}{\partial x} \right)_{Tell} + \frac{\Delta g}{\gamma} \tan \beta_1 \qquad \text{from (2.31)}$$

$$\eta = - \frac{d\zeta}{dy} = - \left(\frac{\partial \zeta}{\partial y} \right)_{Tell} + \frac{\Delta g}{\gamma} \tan \beta_2 \qquad \text{from (2.32)}$$

with the sign convention as shown in section 2.3.2.

Now ζ, as evaluated in (2.54) to (2.56), is seen to be a function of ψ, α and z, all of which are variables related to the x and y above.

Using the fact that

$$- \left(\frac{\partial \zeta}{\partial x} \right) = - \frac{1}{R} \frac{\partial \zeta}{\partial \phi} \tag{2.59}$$

$$- \left(\frac{\partial \zeta}{\partial y} \right) = - \frac{1}{R \cos \phi} \frac{\partial \zeta}{\partial \lambda} \tag{2.60}$$

we can express the ξ and η in the following manner

$$- \left(\frac{\partial \zeta}{\partial x} \right)_{Tell} = - \frac{1}{R} \left[\frac{\partial \zeta}{\partial \psi} \frac{\partial \psi}{\partial \phi} + \frac{\partial \zeta}{\partial \alpha} \frac{\partial \alpha}{\partial \phi} \right] - \frac{\partial \zeta}{\partial z} \frac{\partial z}{\partial x} \tag{2.61}$$

$$- \left(\frac{\partial \zeta}{\partial y} \right)_{Tell} = - \frac{1}{R \cos \phi} \left[\frac{\partial \zeta}{\partial \psi} \frac{\partial \psi}{\partial \lambda} + \frac{\partial \zeta}{\partial \alpha} \frac{\partial \alpha}{\partial \lambda} \right] - \frac{\partial \zeta}{\partial z} \frac{\partial z}{\partial y} \tag{2.62}.$$

This, when substituted into (2.31) and (2.32) produces

$$\xi_{U=W_p} = - \frac{1}{R} \left[\frac{\partial \zeta}{\partial \psi} \frac{\partial \psi}{\partial \phi} + \frac{\partial \zeta}{\partial \alpha} \frac{\partial \alpha}{\partial \phi} \right] \tag{2.63}$$

$$\eta_{U=W_p} = - \frac{1}{R \cos \phi} \left[\frac{\partial \zeta}{\partial \psi} \frac{\partial \psi}{\partial \lambda} + \frac{\partial \zeta}{\partial \alpha} \frac{\partial \alpha}{\partial \lambda} \right] \tag{2.64}$$

as the last term in (2.61, (2.62) cancels.

That part of the expression (2.49) which is denoted as the Stokesian contribution will, on differentiation according to the above, produce the Vening Meinesz integrals (2.26a) and (2.26b). We must now try to evaluate the correction terms to see how departures from the level surface $U = Wp$ affect the deflection at the surface.

Remembering that

$$r_o = R\psi$$

in the vicinity of the computation point, and that therefore

$$\frac{\partial}{\partial\psi}\frac{1}{r_o} = -r_o^2 R = -\frac{1}{R\psi^2}$$

$$\frac{\partial}{\partial\psi}\frac{1}{r_o^3} = -3r^{-4}R = -\frac{3}{R^3\psi^4} \quad ,$$

then

$$\frac{\partial}{\partial\psi}\frac{T}{r_o^3}\left(r_o\frac{dh}{dr_o} + h_p - h\right) = \frac{RT}{r_o^3}\left\{-2\frac{dh}{dr_o} - \frac{3}{r}(h_p - h)\right\} \tag{2.65}$$

$$\frac{\partial}{\partial\alpha}\left\{\frac{T}{r_o^2}\frac{dh}{dr} + \frac{h_p - h}{r_o}\right\} = \frac{T}{r_o^2}(-\sin\alpha'\tan\beta_1 + \cos\alpha'\tan\beta_2) \tag{2.66}$$

$$\frac{\partial}{\partial\bar{\psi}}\left[\frac{\gamma}{r}(\xi\tan\beta_1 + \eta\tan\beta_2)\right] = \frac{1}{\bar{\psi}^2}(\xi\tan\beta_1 + \eta\tan\beta_2) \tag{2.67}$$

where $\bar{\psi}$ is the angular distance subtended by r at the geocentre.

Also by reference to figures 7(a) to 7(c) it can be shown from triangles PLP_1, PLQ and PMP_2, PQM

$$\frac{\partial\psi}{\partial\phi} = -\cos\alpha \tag{2.68}$$

$$\frac{\partial\alpha'}{\partial\phi} = \frac{\sin\alpha}{\sin\psi} \tag{2.69}$$

$$\frac{\partial\psi}{\partial\lambda} = -\sin\alpha\cos\phi \tag{2.70}$$

and

$$\frac{\partial\alpha'}{\partial\lambda} = -\frac{\cos\phi\cos\alpha}{\sin\psi} \tag{2.71}.$$

Substituting (2.65) to (2.71) into (2.63), (2.64) produces the corrections to the deflections for the terrain effects, viz.

$$\xi' = \frac{1}{2\pi}\iint\left[\frac{\cos\alpha}{\bar{\psi}^2}(\xi\tan\beta_1 + \eta\tan\beta_2) - \frac{N}{R\psi^3}\left\{\left(2\frac{dh}{dr_o} + 3\frac{h_p - h}{r_o}\right)\cos\alpha + \sin\alpha\frac{\partial}{\partial\alpha}\frac{dh}{dr_o}\right\}\right]d\sigma \tag{2.72}$$

$$\eta' = \frac{1}{2\pi}\iint\left[\frac{\sin\alpha}{\bar{\psi}^2}(\xi\tan\beta_1 + \eta\tan\beta_2) - \frac{N}{R\psi^3}\left\{\left(2\frac{dh}{dr_o} + 3\frac{h_p - h}{r_o}\right)\sin\alpha - \cos\alpha\frac{\partial}{\partial\alpha}\frac{dh}{dr_o}\right\}\right]d\sigma \tag{2.73}$$

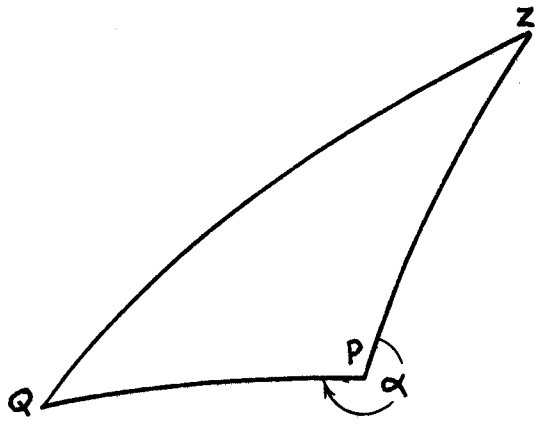

FIG.7(a)

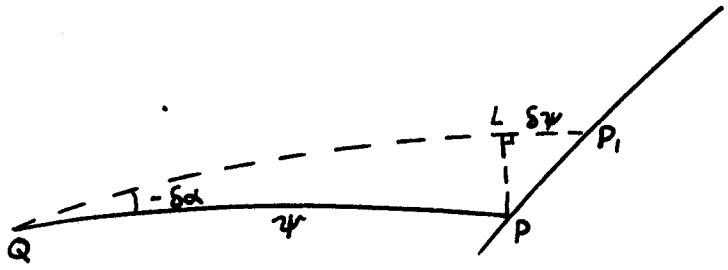

FIG.7(b)

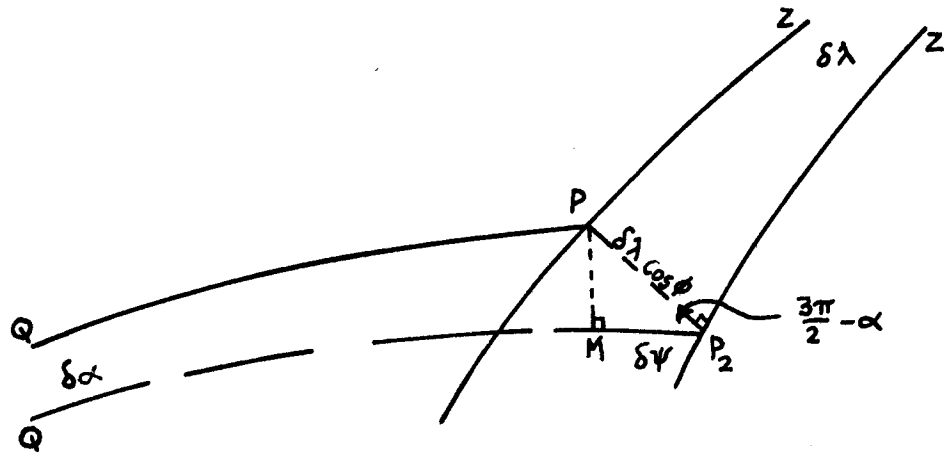

FIG.7(c)

FIG.7 DIFFERENTIAL RELATIONSHIPS BETWEEN THE COMPUTATION POINT AND Q

with $\frac{dh}{dr_o}$, $\frac{d}{d\alpha}\frac{dh}{dr_o}$ defined in (2.50), (2.66) respectively, and $\overline{\psi}$ is defined in (2.67).

In mountainous regions close to the computation point it is critical that $\overline{\psi}$ be computed in full and not approximated by ψ . As explained in 2.3.3(i) large errors will result if ψ is used, and this will be particularly detrimental in the computation of the deflection which is so sensitive to errors in this immediate vicinity.

Further comments with respect to the modification of expressions (2.72) and (2.73) can be found in section 3.2.3.

2.4 Molodensky's Solution by Surface Layer Techniques

2.4.1 Introduction

The theory was first developed by Molodensky in 1945 and can be found in (MOLODENSKII ET AL 1962, pp 78-81, pp 118-124). The derivation, with slight variations, can also be found in (BROVAR ET AL 1964, pp 157-163, pp 167-171 and HEISKANEN AND MORITZ 1967, pp 300-307, pp 312-315). The outline given here will follow the derivation given by Molodensky.

Molodensky's solution is founded on the idea expressed in Chasle's theorem, that the potential of a body can be expresses in terms of an attracting layer on the surface of that body. This is extended so that the disturbing potential of the earth is expressed in terms of a surface layer, the component of normal potential being computed on the telluroid.

Thus

$$T_p = \iint \frac{\Phi}{r} \, dS \tag{2.76}$$

where Φ is related to the density of the surface layer on S which is producing the disturbing potential T_p at P and r is the distance between the computation point P and the element of surface area dS.

The outward derivative along the normal can be than expressed by

$$\underline{\nabla}\,\underline{N}\,T_p = -2\pi\Phi\cos\beta + \iint \Phi\,\underline{\nabla}\,\underline{N}\,\frac{1}{r}\,dS \tag{2.77}$$

(see HEISKANEN AND MORITZ 1967, p 6 and p 301) where all symbols retain their meanings as defined in section 1.4, and used throughout chapter 2. The first term on the right is due to the discontinuity of the derivative at the surface.

We now substitute this into the boundary condition (2.10) to find

$$2\pi\Phi\cos\beta - \iint \underline{\nabla}\,\underline{N}\,\frac{\Phi}{r}\,dS + \frac{1}{\gamma}\iint \frac{\partial\gamma}{\partial z}\,\frac{1}{r}\,dS = \Delta g \tag{2.78}.$$

As already derived in (2.20)

$$\frac{1}{\gamma}\frac{\partial\gamma}{\partial z} = -\frac{2}{R} \tag{2.79}$$

Also, since $r^2 = R_p^2 + R_q^2 - 2R_pR_q\cos\psi$

using a spherical model of the earth, we find

$$\underline{\nabla}\,\underline{N}\,\frac{1}{r} = \frac{\partial}{\partial r}\,\frac{1}{r} = -\frac{R_p - R_q\cos\psi}{r^3} + o\{f\}$$

$$= -\frac{1}{2R_p r} + \frac{R_q^2 - R_p^2}{2R_p r^3}\,, \quad r \neq 0 \tag{2.80}.$$

Substituting (2.79) and (2.80) into (2.78), we get

$$2\pi\Phi\cos\beta = \Delta g + \frac{3}{2R_p}\iint\frac{\Phi}{r}\,dS + \frac{1}{2R_p}\iint\frac{R_q^2 - R_p^2}{r^3}\,\Phi\,dS \tag{2.81}$$

which, when terms are gathered, becomes what Molodensky terms the Fundamental Equation, viz.

$$2\pi\Phi\cos\beta - \iint\left(\frac{3}{2R_p r} + \frac{R_q^2 - R_p^2}{2R_p r}\right)\Phi\,dS = \Delta g \tag{2.82}.$$

The problem now is to solve this linear integral equation in Φ obtain T from (3.1), thence ζ and ξ, η in the usual way.

2.4.2 Solution of the Fundamental Equation

The general solution of (2.82) involves the introduction of a small parameter relating the radius vector of the surface to that of a spherical model, expanding the expression in terms of this small parameter and then the matching of powers of the parameter to achieve a series of equalities.

The physical surface of the earth S is related to an intermediate surface $\overline{S}$ (see figure 8) such that

$$\overline{R} = R + k\,(R_p - R) = R + k\,h_p \tag{2.83}$$

where $\overline{R}$ = radius vector of the general transformed surface $\overline{S}$
R_p = radius vector of the point on the surface S at P
R = radius of the spherical model
k = a constant coefficient, $0 < k < 1$.

Also, the fundamental equation (2.82) is amended by introducing the function χ such that

$$\chi = \frac{R_p^2}{R^2}\,\Phi\sec\beta \tag{2.84}$$

and remembering $\quad d\sigma = \dfrac{dS\cos\beta}{R^2}$

then (2.82) becomes

$$2\pi\chi\cos^2\beta = \frac{R_p^2}{R^2}\,\Delta g + \frac{3}{2}\,R_p\iint\frac{\chi}{r}\,d\sigma + \tfrac{1}{2}R_p\iint\frac{R_q - R_p}{r^3}\,\chi\,d\sigma \tag{2.85}.$$

A similar expression can be written for analogous terms on the transformed surface,

$$2\pi\overline{\chi}\cos^2\overline{\beta} = \frac{\overline{R}_p^2}{R^2}\,\Delta g + \frac{3}{2}\,\overline{R}_p\iint\frac{\overline{\chi}}{\overline{r}}\,d\sigma + \tfrac{1}{2}\overline{R}_p\iint\frac{\overline{R}_q - \overline{R}_p}{\overline{r}^3}\,\overline{\chi}\,d\sigma \tag{2.86}$$

where a new disturbing potential $\overline{T}$ can be expressed in terms of the new density $\overline{\chi}$

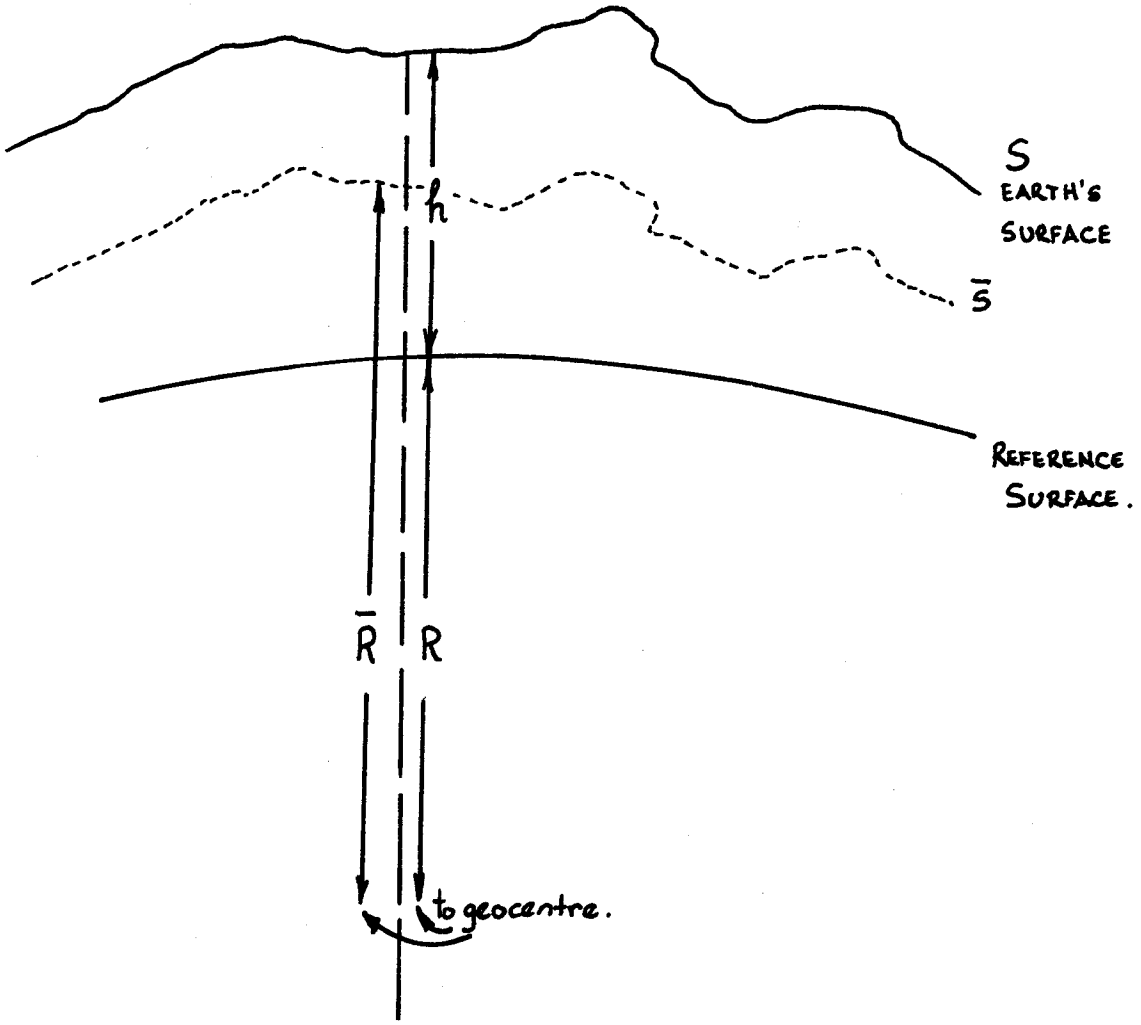

FIG.8 MODEL FOR MOLODENSKY'S SOLUTION.

$$\overline{T} = R^2 \iint \frac{\overline{\chi}}{\overline{r}} \, d\sigma \tag{2.87}$$

and

$\overline{r}$ = distance between elemental area $d\overline{S}$ with radius vector $\overline{R}_q = R + k\, h_q$ and the fixed point on $\overline{S}$ with radius vector $\overline{R}_p = R + k\, h_p$

$\overline{\beta}$ = angle between the normal to $\overline{S}$ and the radius vector $\overline{R}$ at the computation point.

The quantities $\overline{T}$ and $\overline{\chi}$ are functions of k and can be explicitly expressed as a power series in k, viz

$$\overline{\chi} = \sum_{n=0}^{\infty} \chi_n k^n = \chi_o + \chi_1 k + \chi_2 k^2 \ldots \tag{2.88}$$

$$T = \sum_{n=0}^{\infty} T_n k^n \tag{2.89}$$

whilst $\overline{r}$ and $\overline{\beta}$ can be expressed as

$$r = [r_o^2 + k^2 (h - h_p)^2]^{\frac{1}{2}} + 0\{\tfrac{hr}{R}\} \tag{2.90}$$

$$\tan \overline{\beta} = k \tan \beta \tag{2.91}.$$

So if $\beta < 45^o$ we find for all k between 0 and 1 the convergent series

$$\cos^2 \overline{\beta} = (1 + k^2 \tan^2 \beta)^{-1} = 1 - k^2 \tan^2\beta + k^4 \tan^4 \beta - \ldots \tag{2.92}.$$

Expanding the left and right hand sides of (2.86) in terms of (2.88) to (2.92) and dropping the subscript q for the general point, we get

$$2\pi(\chi_o + \chi_1 k + \chi_2 k^2 + \ldots)(1 - k^2 \tan^2 \beta + k^4 \tan^4 \beta \ldots) =$$

$$= \Delta g + \frac{3}{2} R \iint \frac{1}{r_o} (\chi_o + k\chi_1 + k^2 \chi_2 \ldots)\{1 - \tfrac{1}{2} k^2 (h-h_p)^2 + 3 k^4 (h-h_p)^4 \ldots\} \, d\sigma$$

$$+ R^2 \iint \frac{1}{r_o^2} (\chi_o + k\chi_1 + k^2 \chi_2 \ldots)(h-h_p)k \{1 - \frac{3}{2} k^2 (h-h_p)^2 + \ldots\} \, d\sigma \tag{2.93}.$$

By matching coefficients of k^n, we find a general expression for each value of n, viz:

$$2\pi \chi_n - \frac{3}{2} R \iint \frac{\chi_n}{r_o} \, d\sigma = G_n \tag{2.94}$$

where

$$G_o = g - \gamma = \Delta g$$

$$G_1 = R^2 \iint \frac{h-h_p}{r_o^3} \chi_o \, d\sigma \tag{2.95}$$

$$G_2 = R^2 \iint \frac{h-h_p}{r_o^3} \chi_1 \, d\sigma - 3R \iint \frac{(h-h_p)^2}{r_o^3} \chi_o \, d\sigma + 2\pi \chi_o \tan^2 \beta$$

and so on.

The problem now is to solve for surface density χ_n and then by applying (2.87) we can compute T (and ζ, ξ and η).

Let us concentrate on the solution of (2.94) for $n = 0$. From this

$$2\pi\chi_o = \frac{3}{2} R \iint \frac{\chi_o}{r_o} d\sigma + G_o \qquad (2.96).$$

Also, from the expanded form of (2.87)

$$T_o = R^2 \iint \frac{\chi_o}{r_o} d\sigma \qquad (2.97)$$

or

$$\frac{3T}{2R} = \frac{3R}{2} \iint \frac{\chi_o}{r_o} d\sigma .$$

Hence we can write (2.96) as

$$2\pi\chi_o = \frac{3T_o}{2R} + G_o \qquad (2.98).$$

But T_o, considered to be the first approximation for T on the sphere, is given by Stokes' integral (2.23) as

$$T_o = \frac{R}{4\pi} \iint G_o \, f(\psi) \, d\sigma \qquad (2.99).$$

So (2.98) may be expressed as

$$2\pi\chi_o = \frac{3}{2R} \left\{ \frac{R}{4\pi} \iint G_o \, f(\psi) \, d\sigma \right\} + \Delta g \qquad (2.100).$$

Now, substituting (2.99) into (2.98) we obtain

$$\frac{3}{8\pi} \iint G_o \, f(\psi) \, d\sigma + \Delta g = \frac{3T_o}{2R} + \Delta g \qquad (2.101)$$

or

$$T_o = \frac{R}{4\pi} \iint G_o \, f(\psi) \, d\sigma .$$

In like manner, by operating on (2.94) for $n = 1$, we find

$$T_1 = \frac{R}{4\pi} \iint G_1 \, f(\psi) \, d\sigma .$$

Since $T = T_o + T_1 + \ldots$ at the earth's surface where $k = 1$, we can say $\zeta = \zeta_o + \zeta_1 + \ldots$

thus

$$\zeta = \frac{R}{4\pi\gamma} \iint G_o \, f(\psi) \, d\sigma + \frac{R}{4\gamma} \iint G_1 \, f(\psi) \, d\sigma + \ldots \qquad (2.102),$$

where G_o, G_1 are defined in (2.95), χ_o being expressed as a function of T_o and G_o in (2.98).

This expression (2.102) can be interpreted as providing a solution for ζ in a series of approximations, where the first approximation is provided by Stokes' integral ($\equiv N$) and the remaining terms are corrections to this due to the irregularities of the earth's surface. For this reason, the terms in G_1 and higher are often referred to as terrain corrections to the basic Stokesian solution. The greatest correction will come from the G_1 term, which accounts for the departure of the earth's surface from a level surface. The slope of the terrain is corrected for in the second and higher order terms.

Some general comments should be made on this approach. The solution requires (in theory) the G_1 integration to be taken over the earth's surface. In practice (see section 4.3.2), it is only required to compute G_1 out to a distance of about 40 km from the (G_1) computation point. Nevertheless,

in common with (2.57), it contains the term $\frac{\Delta h}{r}$ and therefore suffers from the same shortcomings as were mentioned in section 2.3.3(iii) for this term. The problem is likely to be worse for G_1 because, whereas in (2.57) the weakness only made its presence felt in the vicinity of the computation point for G_1 it is critical throughout the region for which it is computed.

That is, there is no guarantee of stability if terrain slopes in the immediate vicinity are greater than 45^o. If the slopes exceed 45^o anywhere within the computational limit of G_1 then, in theory at least, the G_1 term again becomes unstable. This situation will lead to a general instability of the solution depending on the extent of the topography thus tilted, and on the nearness of the topography to the computation point.

According to (2.95) and (2.98),

$$G_1 = \frac{R^2}{2\pi} \iint \frac{h - h_p}{r_o^3} \left(\Delta g + \frac{3}{2R} T_o\right) d\sigma .$$

MORITZ (HEISKANEN AND MORITZ 1967, pp 307-312) proves that this can be split into two parts, G_{11} and G_{12}, where

$$G_{11} = - h \frac{\partial \Delta g}{\partial h}$$

is the free-air reduction, so that this part of the G_1 term in (2.102) produces the height anomaly at sea level, the ζ_{12} resulting from G_{12} is in effect

$$\zeta_{12} = - \frac{\Delta g}{\gamma} h$$

which on addition reduces the sea level ζ upward to the ground level, and that

$$G_1 = \frac{R^2}{2\pi} \iint \frac{h - h_p}{r_o^3} \Delta g \, d\sigma + O\{\frac{h}{R}\} .$$

Other developments of this terrain correction term are discussed in section 3.1.

2.4.3 Deflections of the Vertical

As in section 2.3.7, the expressions (2.31) and (2.32) are applied to ζ to get ξ and η.

Thus, it follows directly that

$$\xi = \frac{1}{4\pi\gamma} \iint (\Delta g + G_1) \frac{df(\psi)}{d\psi} \cos\alpha \, d\sigma - \frac{\Delta g}{\gamma} \tan\beta_1 \qquad (2.103)$$

$$\eta = \frac{1}{4\pi\gamma} \iint (\Delta g + G_1) \frac{df(\psi)}{d\psi} \sin\alpha \, d\sigma - \frac{\Delta g}{\gamma} \tan\beta_2 \qquad (2.104)$$

where $\frac{df(\psi)}{d\psi}$ = Vening Meinesz function defined in (2.27).

As MORITZ shows, (HEISKANEN AND MORITZ 1967, p 314) this can be further developed by again splitting the G_1 term into the two components G_{11} and G_{12} mentioned in the preceding section.

Thus the G_1 contribution to ξ (ξ') can be expressed as

$$\xi' = - \frac{1}{4\pi\gamma} \iint \frac{\partial \Delta g}{\partial h} h \frac{df(\psi)}{d\psi} \cos\alpha \, d\sigma - \frac{\partial \zeta_{12}}{R\partial\phi}$$

$$= -\frac{1}{4\pi\gamma}\iint \frac{\partial\Delta g}{\partial h}\, h\, \frac{df(\psi)}{d\psi}\, \cos\alpha\, d\sigma + \frac{1}{R\gamma}\,\frac{\partial}{\partial\phi}(h\,\Delta g) + 0\,\{\frac{\partial\gamma}{\partial\phi}\}$$

$$= -\frac{1}{4\pi\gamma}\iint \frac{\partial\Delta g}{\partial h}\, h\, \frac{df(\psi)}{d\psi}\, \cos\alpha\, d\sigma + \frac{\Delta g}{\gamma}\tan\beta_1 + \frac{h}{\gamma}\,\frac{\partial\Delta g}{R\partial\phi} \qquad (2.105).$$

It can be seen that the term containing the ground slope will cancel when (2.105) is substituted into (2.103), producing

$$\xi' = -\frac{1}{4\pi\gamma}\iint \frac{\partial\Delta g}{\partial h}\, h\, \frac{df(\psi)}{d\psi}\, \cos\alpha\, d\sigma + \frac{h}{\gamma}\,\frac{\partial\Delta g}{\partial\phi} \qquad (2.106).$$

This forms has the practical advantage that the potentially large term $\frac{\Delta g}{\gamma}\tan\beta_1$ is now compensated before enumeration of the terms takes place. Unremoved the term is evaluated twice by two different methods and unlikely to compensate exactly in the evaluation, especially in steep mountain regions.

The expression can be further modified by using a device suggested by Pellinen (see also section 3.2.1(b)) wherein the equipotential through the point P, instead of the mean sea level, is made the 'datum' for heights.

The last term in (2.106) now drops out (again removing a source of error in the computation), and when the correction term ζ' is combined with the first approximation from the Vening Meinesz formulae this gives

$$\begin{Bmatrix}\xi\\ \eta\end{Bmatrix} = \frac{1}{4\pi\gamma}\iint [\Delta g - \partial\Delta g\,(h - h_p)]\begin{Bmatrix}\cos\alpha\\ \sin\alpha\end{Bmatrix} d\sigma \qquad (2.107)$$

the development for η being analogous to that for ξ.

2.5 Bjerhammar's Discrete Point Solution

In the solutions to the boundary value problem given above in sections 2.3 and 2.4, the assumption is made that the gravity is known at all points on the earth's surface. In reality we know gravity at discrete points only, and to evaluate these solutions some interpolation or prediction of the field is necessary.

BJERHAMMAR (1964) redefined the geodetic problem in terms of the known gravity points in the following way: "A finite number of gravity stations are known on an irregular surface, and it is required to find a solution such that the boundary values for the gravity data are satisfied in all given points."

The surface gravity (Δg) is thought to be generated by a set of fictitious gravity anomalies Δg^* on a reference sphere at mean sea level. The problem then is to find the g^* on the sphere which, by upward continuation from the sphere to the surface, will produce the measured quantities Δg on this surface (see figure 9).

The theory is developed in full by BJERHAMMAR (1969), and will only be outlined here. The basic relationship is developed from Poissons' integral for harmonic functions which when applied to $R\Delta g$, $R_o\Delta g^*$ produces

$$\Delta g = \frac{R^2 - R_o^2}{4\pi R}\iint \frac{\Delta g^*}{r^3}\, dS \qquad (2.108)$$

where Δg, Δg^* are defined above

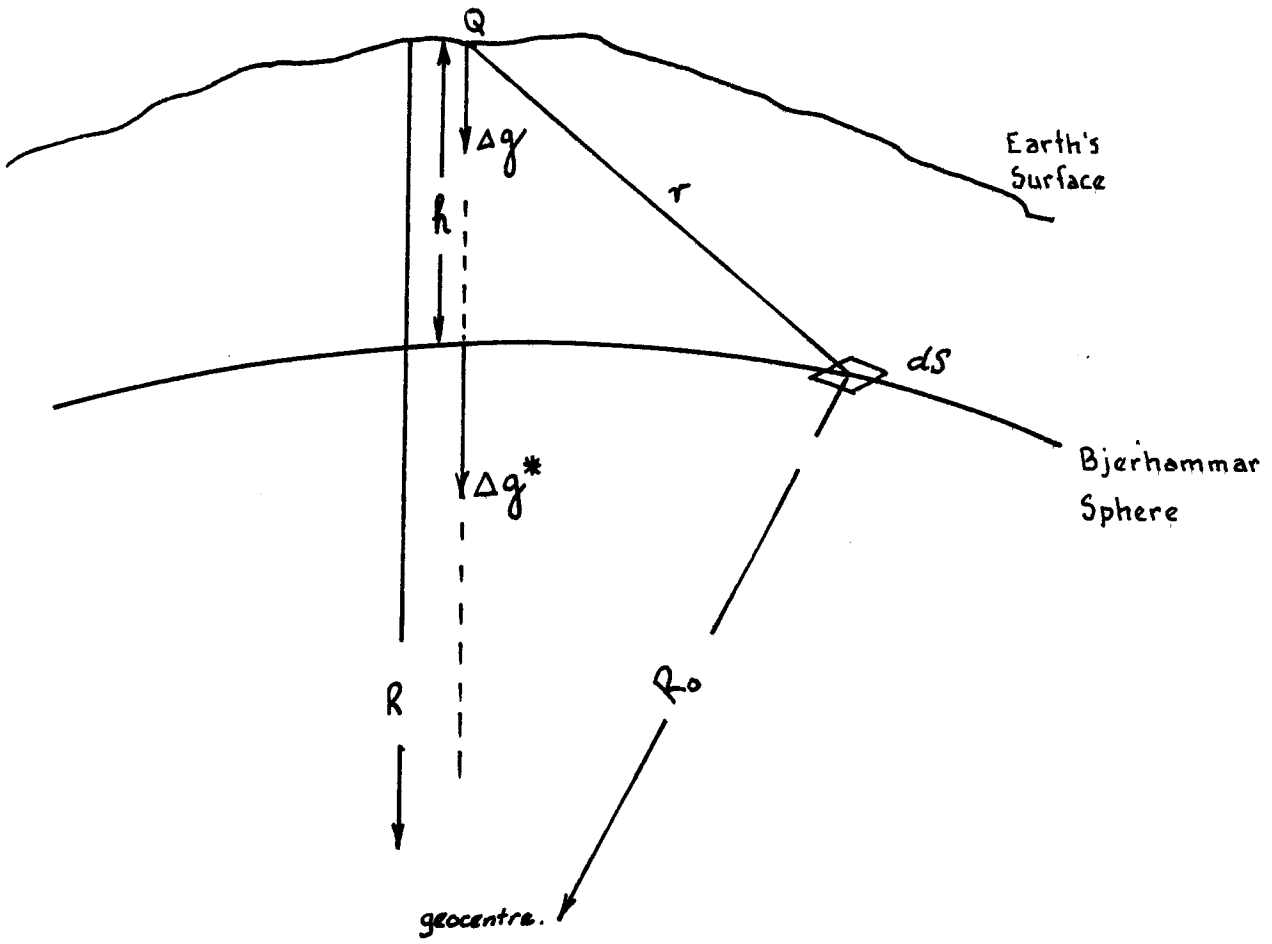

FIG.9 THE BJERHAMMAR SPHERE.

R is radius vector of the computation point Q

R_o is the radius of the Bjerhammar sphere

r is the distance from Q to elemental area dS.

The solution for this, as shown in (BJERHAMMAR 1969, p 179), is

$$\Delta g_q^* = \frac{R^2}{R_o^2}\left[\Delta g_q + \frac{R^2 - R_o^2}{4\pi R}\iint \frac{\Delta g_q^* - \Delta g^*}{r^3}\right] dS \qquad (2.109).$$

The numerical solution can be found in a number of ways (BJERHAMMAR 1973, pp 481-486). One approach is to use successive approximations (HEISKANEN AND MORITZ 1967, p 318), where Δg_q and Δg are used initially as the best estimates of Δg_q^* and Δg^* on the right hand side, to achieve a second estimate of Δg_q^*. (This procedure can continue until the change in Δg_q^* becomes insignificant). As a first approximation, $(R^2 - R_o^2)/2R \simeq h$, and thus

$$\Delta g_q^* = \Delta g_q + \frac{h}{2\pi}\iint \frac{\Delta g_q - \Delta g}{r^3}\, dS \qquad (2.110).$$

Alternately observation equations can be set up from (2.108) for each point Q which will give a set of linear equations, viz.

$$\Delta G_i = \Delta g_i - \frac{R_i^2 - R_o^2}{4\pi R_i}\iint \Delta g^*\, dS\,, \qquad i = 1 \text{ to } n \qquad (2.111).$$

A least squares solution can now be used and values of Δg^* are then chosen to give minimum sum of the squares of ΔG_i in the classical manner.

Once the values for Δg^* have been computed, a solution to the boundary value problem can be carried out by substitution of Δg^* into the generalised Stokes' integral, to obtain at the surface

$$T_q' = \frac{1}{4\pi R}\iint \Delta g^*\, f(R,\psi)\, d\sigma \qquad (2.112)$$

where $f(R,\psi) = \frac{2R_o}{r} + \frac{R_o}{r} - \frac{3R_o}{R^2} - \frac{R_o^2}{R^2}\cos\psi\left(5 + 3\ln\frac{R - R_o\cos\psi + r}{2R}\right).$

This expression leads, on substitution of the surface radius vector for R and application of Brun's theorem (equation 2.9), to a height anomaly which is equivalent to that in equation (2.56). In other words, equation 2.112 will result in the surface-telluroid separation when applied to the Earth's surface.

The formulae for the deflections of the vertical at the surface can be found in the usual way (see equation 2.25), gives

$$\xi_i = \frac{t}{4\pi\gamma}\iint \Delta g^*\frac{\partial f(R,\psi)}{\partial\psi}\cos\alpha_i\, d\sigma \qquad i = 1,\ 2 \qquad (2.113)$$

where

$$\xi_1 = \xi\,, \qquad \xi_2 = \eta$$

$$\alpha_1 = \alpha\,, \qquad \alpha_2 = 90 - \alpha$$

$$t = \frac{R_o}{R}\,,$$

and

$$\frac{\partial f(R,\psi)}{\partial \psi} = -t^2 \sin\psi\left(\frac{2}{D^3} + \frac{6}{D} - 8 - 3\,\frac{1-t\cos\psi-D}{D\sin^2\psi} - 3\,\ell n\,\frac{1-t\cos\psi+D}{2}\right)$$

where $D = \frac{r}{R}$

(see HEISKANEN AND MORITZ 1967, p 235; BJERHAMMAR 1969, p 183).

This approach has been questioned by a number of writers (eg. see BJERHAMMAR 1973, p 475), a major misgiving being that it is not possible to downwards continue an harmonic function through material likely to contain discontinuities (see MOLODENSKII ET AL 1962, p 120). BJERHAMMAR (1968, p 178), in answer to this, points out that the purpose is not to create a sphere with some direct physical meaning, but rather to use the sphere as an intermediate step in the recreation of the potential field which exists at the Earth's surface and beyond. The fact that the analytical continuation does not reflect the actual field inside the Earth is not considered to be a problem as this is not in any case the subject of the determination.

However, although this method is called the "discrete-point approach', implicit in the computation is the assumption that the Δg is representative of a square or block on the Earth's surface (BJERHAMMAR 1969, p 175). This infers an interpolation or prediction from the original data prior to computation. Because of the deterioration of downward continuation (2.110) in mountainous terrain, it is necessary to limit the minimum value which r can take. BJERHAMMAR (1969, p 194) mentions a block size of 10 km x 10 km as a feasible area which will provide a convergent solution on iteration. As will be shown later (eg. sections 7.3.1, 7.3.2) the assumption that a gravity anomaly can adequately represent such a large area will break down in mountainous terrain. If this assumption is maintained in the immediate vicinity of the deflection computation point it will smooth all the short wave length signal in this critical region, and place severe limitations on the accuracy which could be expected from this method (see also section 6.2.2).

For $\psi > 20$ km this will no longer be a problem and there is no doubt that the method could be used effectively for middle to outer zone computations for ξ and η. Also, because the N computation is not as sensitive for $\psi \to 0$ it would be a suitable method for the evaluation of this parameter.

This approach has now been accepted as an important contribution to the solution of the boundary value problem, though not widely used. Reference will be made below (section 3.4) to a study which does use this method for computing ξ and η. This investigation compares a number of different ways of evaluating these parameters and it is interesting to see how this method compares in both accuracy and computing effort with the more generally used methods.

3. MODIFICATION TO THE ORIGINAL EXPRESSIONS

3.1 Introduction

The solution to the boundary value problem in purely theoretical terms was given in Chapter 2. This chapter deals with the various developments which have taken place from these original expressions in order to simplify or stabilise them, or simply to assist in evaluation. From this it is desired to find the most suitable expressions for the present test.

A number of authors have reviewed the developments of the basic expressions. Of these probably the most exhaustive work has been done by MORITZ (1966, 1968a, 1968b, 1969) who has done valuable work in the comparative analysis, as well as the physical interpretation and the modification, of the various approaches. PELLINEN (1968) has also given us a summary of some of the methods which have developed from MOLODENSKY'S AND BJERHAMMAR'S approach. More general summaries can also be found in (EMRICK 1973, pp 21-39) and (KEARSLEY 1973).

3.2 Modifications of Molodensky's Expression

Of the three different approaches outlined in Chapter 2, the method which has received the lion's share of attention is the Surface Layer Technique developed by Molodensky. Many writers have investigated ways of improving or simplifying the original statement (2.102), in particular PELLINEN (1962, 1964 and 1968), MORITZ (1966, 1968a and BROVAR 1964). Others have carried out tests on models, computing deflections by means of (2.102) to the first and in some cases higher order corrections (eg. G_1 , G_2) and compared the result with a value derived by theoretical analysis of the postulated model. For examples, see YEREMEEV in (MOLODENSKII ET AL 1962, pp 217-230), YEREMEEV (1970), VELKOBORSKY (1970), PICK (1970) and PICK AND JAKUBCOVA (1973). The second last study tests a modified version of Molodensky's method on a model with side slopes up to 50°, with some success although the convergence of the solution was very slow. The result of these computations proved the approach capable of producing accurate results is of the order of 0.1 to 0.2 arcsec (these being the differences achieved when corrected deflections and compared with theoretically derived values), and this certainly helps to show that the approach is feasible. However the conditions of the test are idealised and one can never expect them to be reproduced in a real-life situation.

3.2.1 Modifications by Pellinen

(a) In 1962, Pellinen suggested an approach which aims at removing the effect of the topography from the general solution and independently evaluating the effect the 'removed' topography will have on the deflection. This method as originally developed is given in (PELLINEN 1962) and is also outlined in (MORITZ 1969, pp 27-30).

The free-air anomaly at the surface is adjusted to account for the contribution made to this anomaly by the topography above a stated reference surface.

i.e. $$\Delta g_c = \Delta g - \Delta g_T$$

where Δg_c is the anomaly corrected for topography
Δg is the free-air anomaly at the surface
and Δg_T is the contribution to Δg of the topography.

Δg_c is substituted for Δg in the equations (2.102 to 2.104) to find the parameters defining the

anomalous field at the reference surface. Thus, to a first order approximation, we find

$$\xi_j = \frac{1}{4\pi\gamma} \iint [\Delta g_c + G_{1c}] \frac{df(\psi)}{d\psi} \cos\alpha_j \, d\sigma + \Delta\xi_{jT} \qquad (3.1)$$

where

$$\Delta\xi_{jT} = -\frac{G\rho R^3}{\gamma} \iint \frac{h-h_p}{r_o^3} \sin\psi \cos\alpha_j \, d\sigma \, , \quad j = 1, 2 \, ;$$

G = the gravitational constant

G_{1c} = G_1 with Δg_c substituted for Δg, and

$\xi_1 = \xi \quad \xi_2 = \eta \quad ; \quad \alpha_1 = \alpha \quad \alpha_2 = 90 - \alpha$.

As mentioned by Moritz, an advantage in this approach is that the Δg_c values will be smaller and smoother than the Δg values in the original expression (8). However, G_{1c} may attain large values being in essence the Bouguer anomaly, as might the corrections $\Delta\xi_{jT}$. This state of affairs (ie. large effects being compensated by large corrections) should be avoided if at all possible because of the increase in the size of the errors likely to result. Also, (3.1) presents quite a large computational task which seems unnecessarily onerous.

(b) A device to decrease the magnitudes of G_{1c} and the corrections to ξ , η has been suggested by PELLINEN (1962, p 346) and is also described in (MORITZ 1969, pp 30-33).

A spherical surface, concentric with the original reference surface at sea level and passing through the computation point P, is held to have a surface layer of density ρh which produces an anomalous potential field. The gravity anomaly resulting from this surface layer will have a compensating influence on the mass of the topography removed in the aforementioned approach. If the anomaly accumulating in this way (which is shown to be the Faye anomaly; the free-air anomaly plus the terrain correction only) is now used in place of Δg_c in the earlier expression (3.1), and due consideration given to the correction term which results, it is found that (MORITZ 1969, p 31)

$$\xi_j = \frac{1}{4\pi\gamma} \iint (\Delta g + C) \frac{d\, f(\psi)}{d\psi} \cos\alpha_j \, d\sigma$$

$$+ \sum_{n=1}^{\infty} \frac{1}{4\pi\gamma} \iint \bar{g}_n \frac{d\, f(\psi)}{d\psi} \cos\alpha \, d\sigma + \delta\xi_j \qquad \ldots j = 1, 2$$

where $\Delta g + C$ is the Fay anomaly.

$\bar{g}_n$ are the correction terms computed using the Bouguer anomalies and

$$\delta\xi_j = \frac{G\rho R^3}{\gamma} \iint \frac{h - h_p}{r_o^2} \left(\frac{1}{r_o} - \frac{1}{r_1}\right) \sin\psi \cos\alpha_j \, d\sigma$$

$$C = G\rho R^2 \iint \left(\frac{1}{r_o} - \frac{1}{r_1}\right) d\sigma \qquad (3.2).$$

By using this device the gravity anomalies and the correction term $\delta\xi_j$ are both reduced in size. Also, as with the first approach, the uncertainty of the density of the sub-surface is overcome because it is compensated when the correction term is added. The adoption of the reference surface passing through the computation point (as in the second approach) should also improve the convergence of the higher order terms, and improve the accuracy of the first order approximation.

(c) A very important development is given by PELLINEN (1964). Here he adopts a correction term G' which is equivalent in function to the G_1 of Molodensky, where

$$G' = \frac{R^2}{2\pi} \iint \frac{(h-h_p)\ (\Delta g-\Delta g_p)}{r^3}\ d\sigma + O\{f\} \qquad (3.3).$$

This will help to stabilise the solution because the term containing Δg is now referred to the gravity anomaly at the point of computation.

A development from (3.3) (IBID, p 330) makes use of the general assumption

$$\Delta g = \Delta g'' + k' h$$

$\Delta g''$ being the Bouguer anomaly and k' is the Bouguer correction factor.

(3.3) then becomes

$$G' = \frac{k'R^2}{2\pi} \iint \frac{(h-h_p)^2}{r^3}\ d\sigma \qquad (3.4).$$

Some writers (eg. MATHER 1975, p22) have expressed doubt as to the validity of this latter expression, particularly if the summation is carried out over extensive areas. In this situation the assumption that the Bouguer anomaly, and perhaps also that k' is constant throughout the region is weak and likely to lead to systematic errors in the value of G'. (See EMRICK 1973, p 106 for comments on the use of (3.3) as opposed to (3.4)).

(d) MORITZ (1968b) has shown the equivalence between equation (3.4) and the expression for the terrain correction to the deflection derived from the "Arnold-type" expression (equation 2.58) using the assumptions in (c) above. Hence, indirectly, one can see the connection between the G' term in equation (3.3) and the correction term from Green's third identity (equations 2.72 and 2.73).

3.2.2 Moritz' Developments

Another type of approach used in solving Molodensky's expression employs mathematical devices in order to simplify them. In this respect it is worth mentioning a method developed by MORITZ (1969, 1971) who uses analytical continuation of the gravity anomaly from surface to sea level and thus achieves a solution by means of successive approximations. While some doubts about the validity of this approach (ie. continuation below the surface of the attracting body) are expressed, it is felt to be justified by the equivalence gained with matched terms of the modified Molodensky approach. In this way, MORITZ (1969, pp 35-37) derives to second-order accuracy

$$\xi = \frac{1}{4\pi\gamma} \iint (\Delta g + g_1 + g_2) \frac{d\ f(\psi)}{d\ \psi} \cos \alpha_j\ d\sigma$$

where

$$g_1 = -(h-h_p)\ L_1\ (\Delta g)$$

$$g_2 = -\tfrac{1}{2}(h-h_p)^2\ L_1\ \{L_1\ (\Delta g)\} - (h-h_p)\ L_1\ (g_1)$$

with

$$L_1(f) = \frac{R^2}{2\pi} \iint \frac{f-f_p}{r_o^3}\ d\sigma \qquad (3.5)$$

Moritz claims that, though for all practical purposes this is identical with Molodensky's original expressions, it is an easier statement to evaluate. A big advantage from the computing viewpoint is that successive terms of the series are evaluated recursively, although it is probable that the 2nd order is as high an order as is needed for most cases. Nevertheless their expressions do appear simpler to evaluate than those in (2.95), although care must be taken to ensure the terms converge

significantly. To assist in this, as Moritz states, it is possible to substitute the Faye anomaly for the free-air anomaly in (3.5) and apply the corrections as per (3.2). Now the g_1 and g_2 terms being computed from the Bouguer anomalies will be smaller and this should aid convergence.

3.3 Modification of Green's Identity Approach

i) The expressions for ξ' , η' in (2.57), (2.58) are modified by introducing a datum shift of the geoid into the system, relating the height of the geoid at the points Q to this height at P. This will not affect the tilt of the equipotential surface; as already mentioned in section 2.3.1 the effect of $W_o - U_o$ can be ignored as it has no influence on deflections.

The terms in $\frac{N}{R\psi^3}$ $(N \equiv N_q)$ in equations (2.72) and (2.73) are therefore amended to $\frac{N_q - N_p}{R\psi^3}$, helping to dampen the oversensitivity of this term in the practical evaluation in areas of large N (eg. 30 m). This device also greatly assists the convergence of the affected part of the expressions as the points Q approach P thus helping to bring about a situation which is known should exist i.e. that the correction term should approach zero as $\psi \to 0$.

ii) An expression for ζ_p in terms of, as opposed to $r = r(r_o , h , h_p)$ has been developed by Mather (see MATHER 1973, pp 34-36, pp 102-105, pp 117-120). The aim is to develop an expression such as the one in (2.57) which contains the Stokesian solution as a first approximation and the remainder as the correction for topography. As can be appreciated from (2.46) the series expansion for $\frac{\Delta h}{r^3}$ becomes a diverging one when ground slopes in the vicinity of P exceed 45^o. As the nature of all the stations used for testing is for the computation to be located on the tops of the hills, with plateaus to a lesser or greater extent surrounding them (see figure 28 for analysis of innermost zone heights) it was safely assumed that the approximation for was adequate.

It should be pointed out that no approximation exists when the slopes of the surrounding topography are taken into account. These enter the expression directly as the tan of the slope and are thus fully accounted for. In fact, the problem under discussion will only have an effect in the unusual situation when the deflection is being computed on, or on the edge of, extremely steep topography of considerable extent.

3.4 Practical Evaluation of the Modified Correction Term

a) In an investigation completed recently, EMRICK (1973) compared the deflections at two points $(+38^o50 , -105^o00$ and $+38^o50'37''.5 , -105^o02'37''.5)$ in the region of Pike's Peak, U.S.A. He also evaluated the various correction terms resulting from the expressions discussed in section 3.1 above.

Terrain corrected anomalies were found on a 5' grid throughout a $3^o \times 3^o$ area centred on the two computation points, the free-air anomalies being predicted by means of a covariance function (see section 5.3), and terrain information taken from the 1:24 000 map sheets for the area. The deflections were evaluated only to a distance of 1.5^o from the computation station and so cannot be regarded as having any absolute significance. Nevertheless, the results do certainly give insight into the relative merits of the different approaches of determining the effect of the terrain in a fairly mountainous region.

The main correction terms tested were as follows: the G' derived by Pellinen in (3.3); Pellinen's terrain correction term $\Delta\xi_{jT}$ in (3.1); Moritz's recursive formula, described in (3.5) to order 3;

and Bjerhammar's iterative expression (2.111) modified by Moritz (1966, pp 60-61) to become

$$\Delta g^{*1} = \Delta g$$

$$\Delta g^{*(i+1)} = \Delta g - \Delta h \frac{R^2}{2\pi} \iint \frac{\Delta g^{*(i)} - \Delta g_q^{*(i)}}{r_o^3} d\sigma \qquad (3.6)$$

In this test, 6 iterations were used. Δg^{*6} is then substituted for Δg in the Vening Meinesz formulae to produce ξ, η.

Emrick also computed by hand the Hayford terrain correction using the Hayford zone systems at two of the grid points to provide checks on the computations.

The results of the deflection computations at two stations are tabulated in (*IBID*, p 97) and are interesting to consider. Out to a distance of 1.25 minutes ($\simeq$ 2.25 km) there is little difference between the methods, and in fact the contribution of the correction terms are quite small, the largest computing at 0.1 arcsec in ξ and 0.2 arcsec in η, with a range in computed values of the order of 0.1 arcsec in both components. The area from 1!25 to 10' (2.25 km to 18 km) showed about a 0!!4 correction for the terrain in ξ and 0!!2 in η, with a range in the correction computed using different approaches of 0!!25 in ξ and η. The contribution coming from terrain corrections between 10' and $1^{\circ}5$ was small, of the order of 0!!05 on average.

The point to be noticed is that there is little improvement achieved by calculating the relatively long process of the iterative or recursive procedures, (3.5) and (3.6) compared with the simpler Pellinen correction shown in (3.3),particularly in the close zones of the computation. Emrick summaries his results (*IBID*, p 99) as follows "Assuming the iterative solution to give the best results for the data sample used, the results of the computations show that a maximum error of 1!!08 may occur by neglecting all correction terms as of 0!!53 by using only linear correction terms."

In his conclusions (*IBID*, pp 106-109), Emrick recommends the use of the linear correction term in less rugged terrain, as the iterative solution makes large demands on a computer and the refinement gained is only felt in mountainous regions.

(b) BURSA (1969), in his investigation of the terrain effects on deflections in Czechoslovakia, used the Pellinen correction described in (3.2). This resulted in some improvements in the relative accuracies of the gravimetric deflections (*IBID*, p 56). In view of the similarity of this approach with the simpler terrain correction expression (3.3), and the suitability of this expression to programming, it was decided to compute this G' correction term at all gravity stations in the test region and include it in the computation of deflections computed in this region.

(c) DIMITRIJEVICH (1972) computed the correction term (3.4) in order to find the effect the G' terms have on the gravimetrically determined deflections at 23 stations spread through the U.S.A. The reasons given for choosing this form (*IBID*, p 3)were "It is a very simple solution, requiring only that the terrain corrected free-air gravity anomaly ($\Delta g + G'$) be used in place of the free-air gravity anomaly (Δg).

Using the assumption that the free-air gravity anomalies are linearly correlated with elevation, Moritz has shown that this solution is equivalent to several other linear solutions which have been developed...."

This latter comment, whilst borne out by Emrick's results is nevertheless based on an assumption

introduced to simplify the Pellinen correction (3.2). Since (3.2) is quite simple to evaluate on the computer in any case, and also has the advantage of ease of application mentioned first by Dimitryevich, it was preferred to use the form of Pellinen correction which was free from the assumption of linear correlation. This would then circumvent any breakdown in the assumption which, according to recent studies in North America by MATHER (1975, p 22) was found to happen over distances in excess of 50 km.

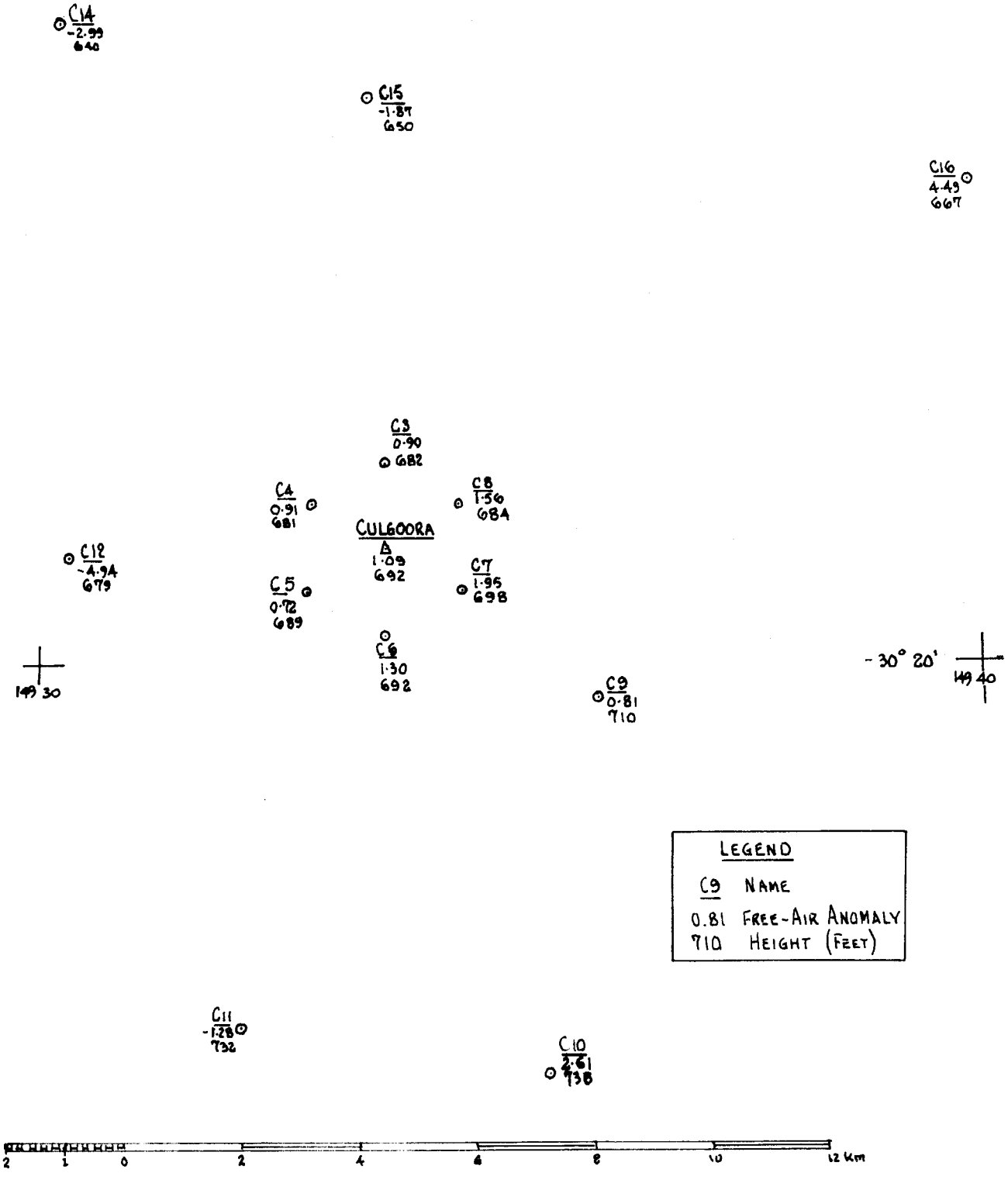

FIG. 10 CULGOORA

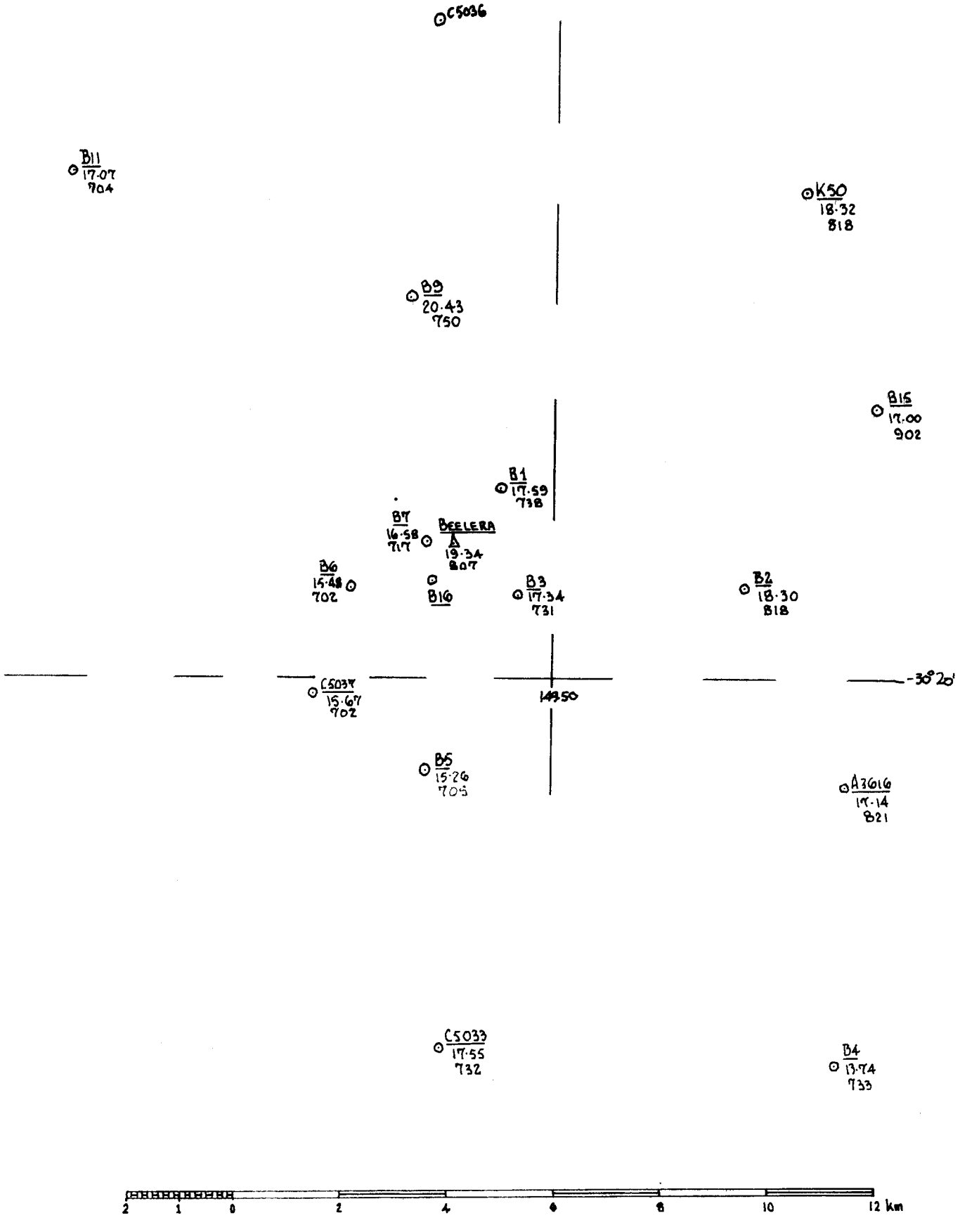

FIG. 11 BEELERA

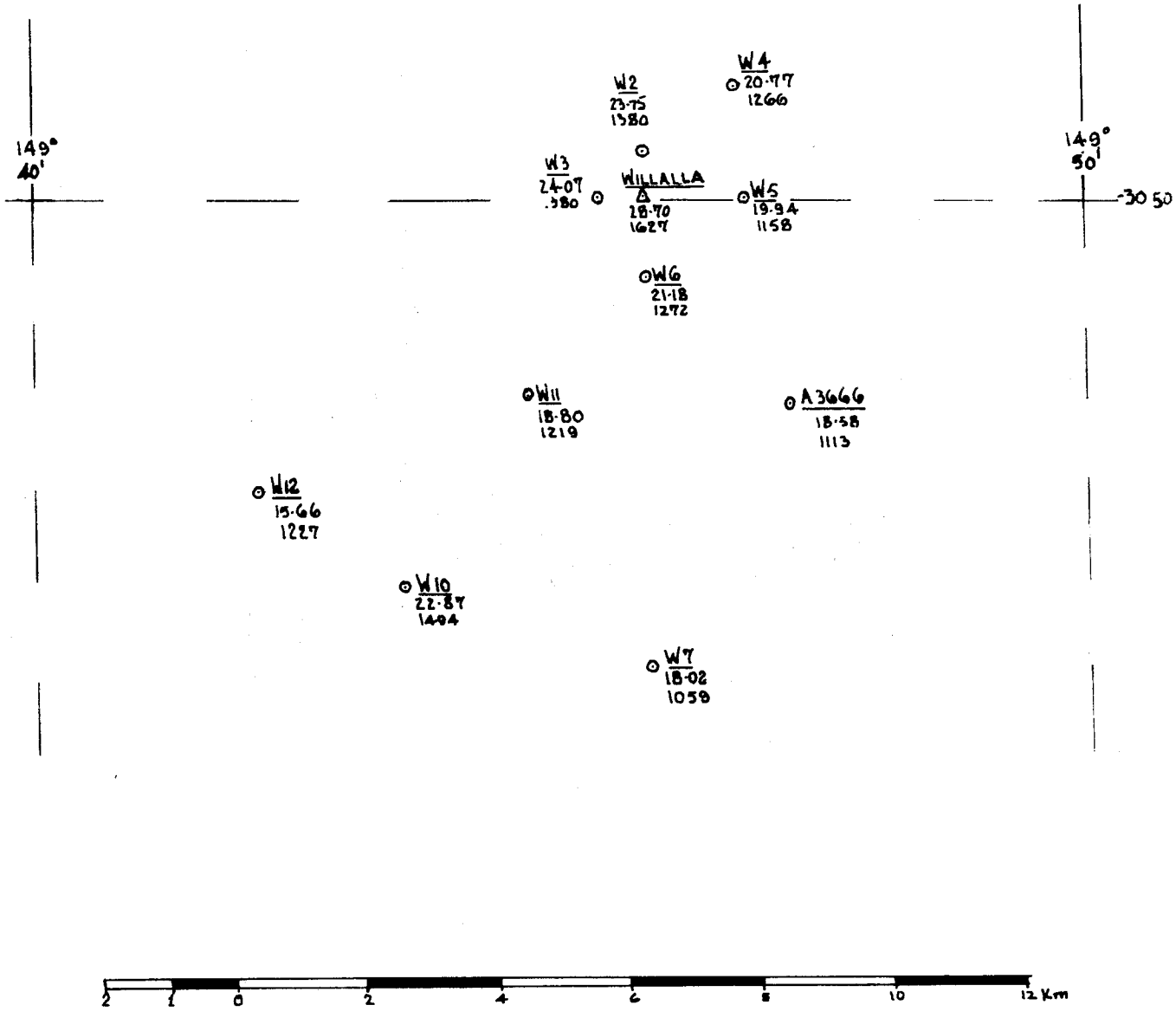

FIG. 12 WILLALLA

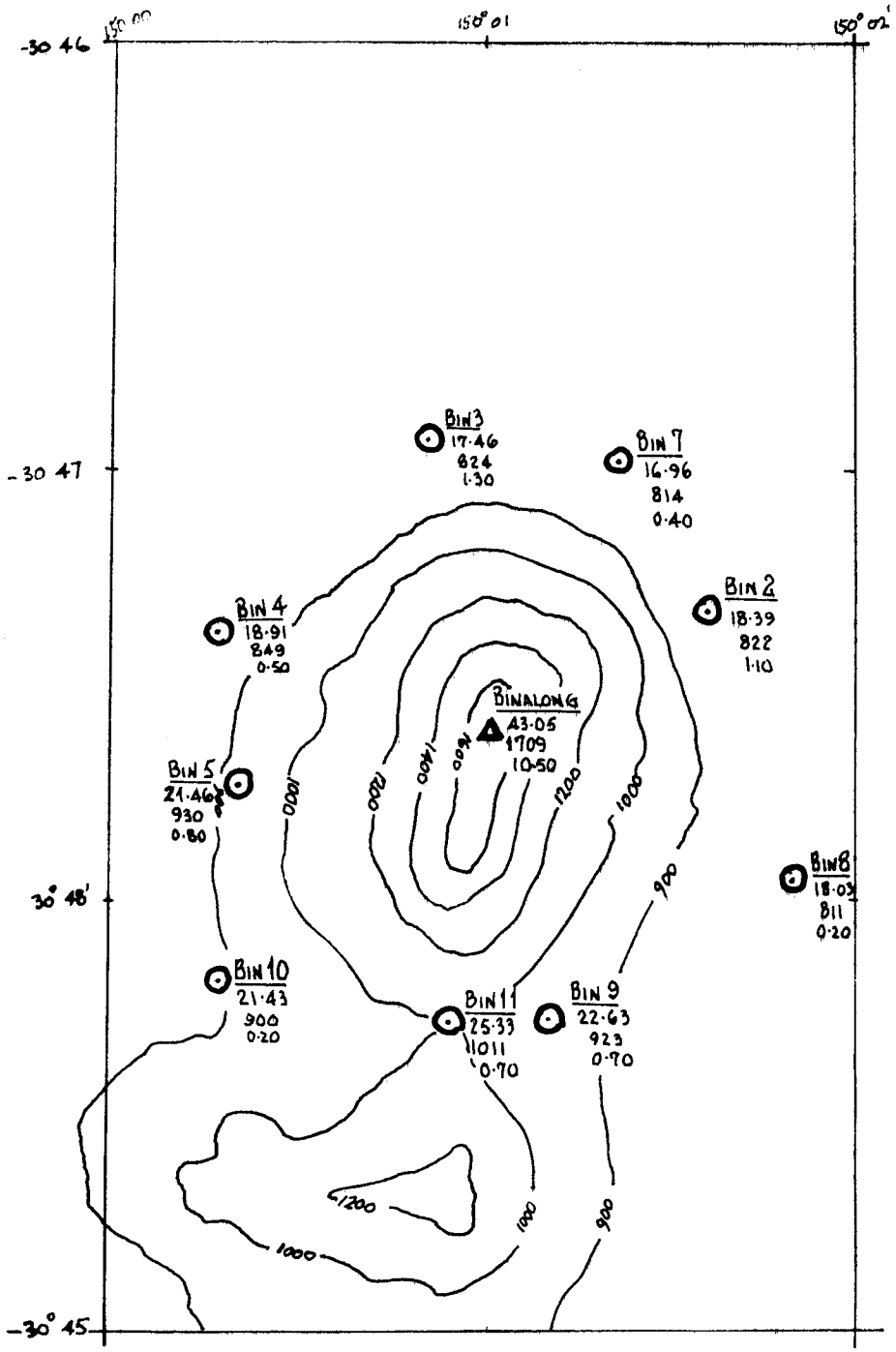

FIG.13 BINALONG

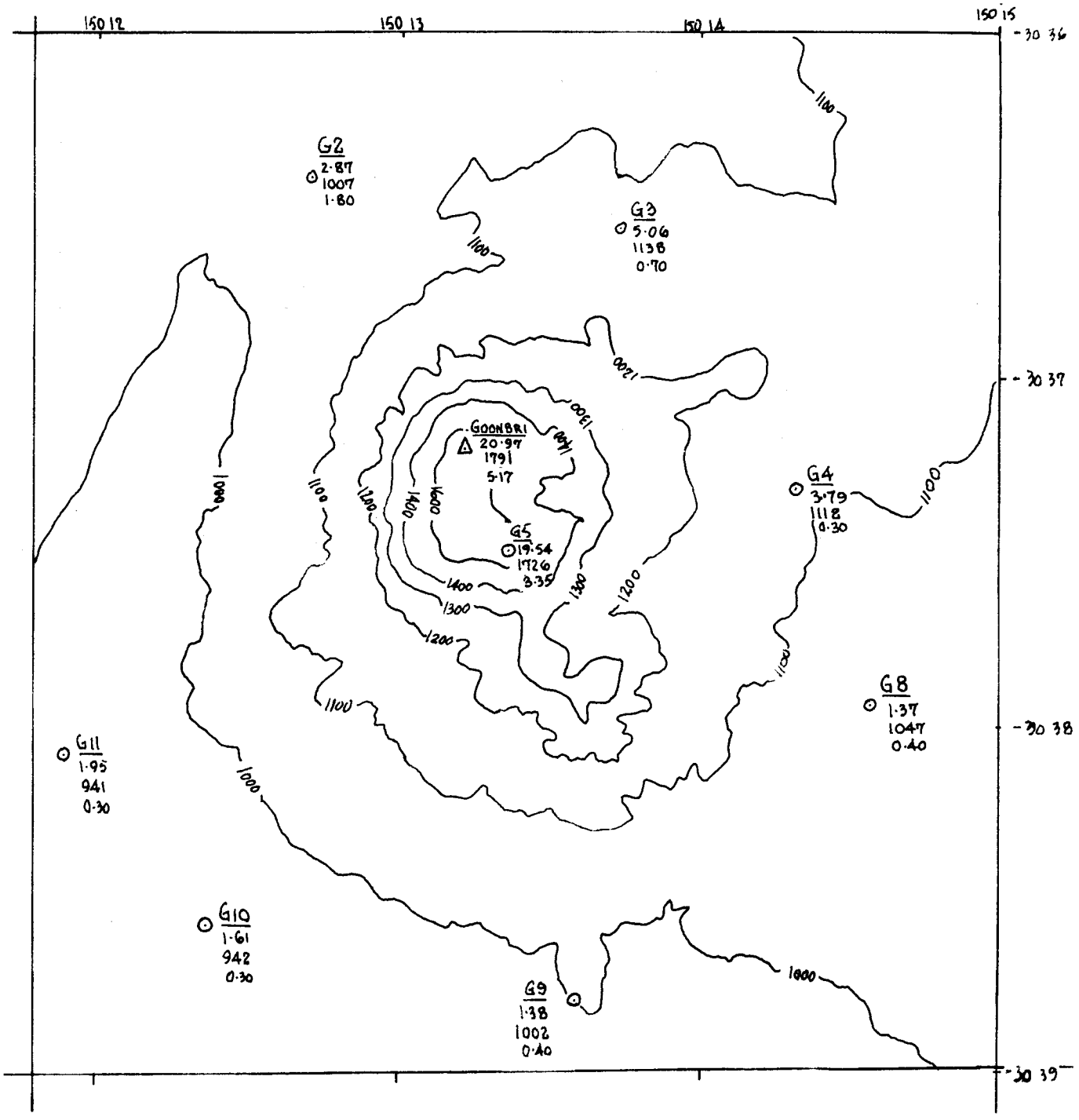

FIG.14 GOONBRI

LEGEND

G9 NAME
1·38 FREE-AIR ANOMALY
1002 HEIGHT (FEET)
0·40 G'

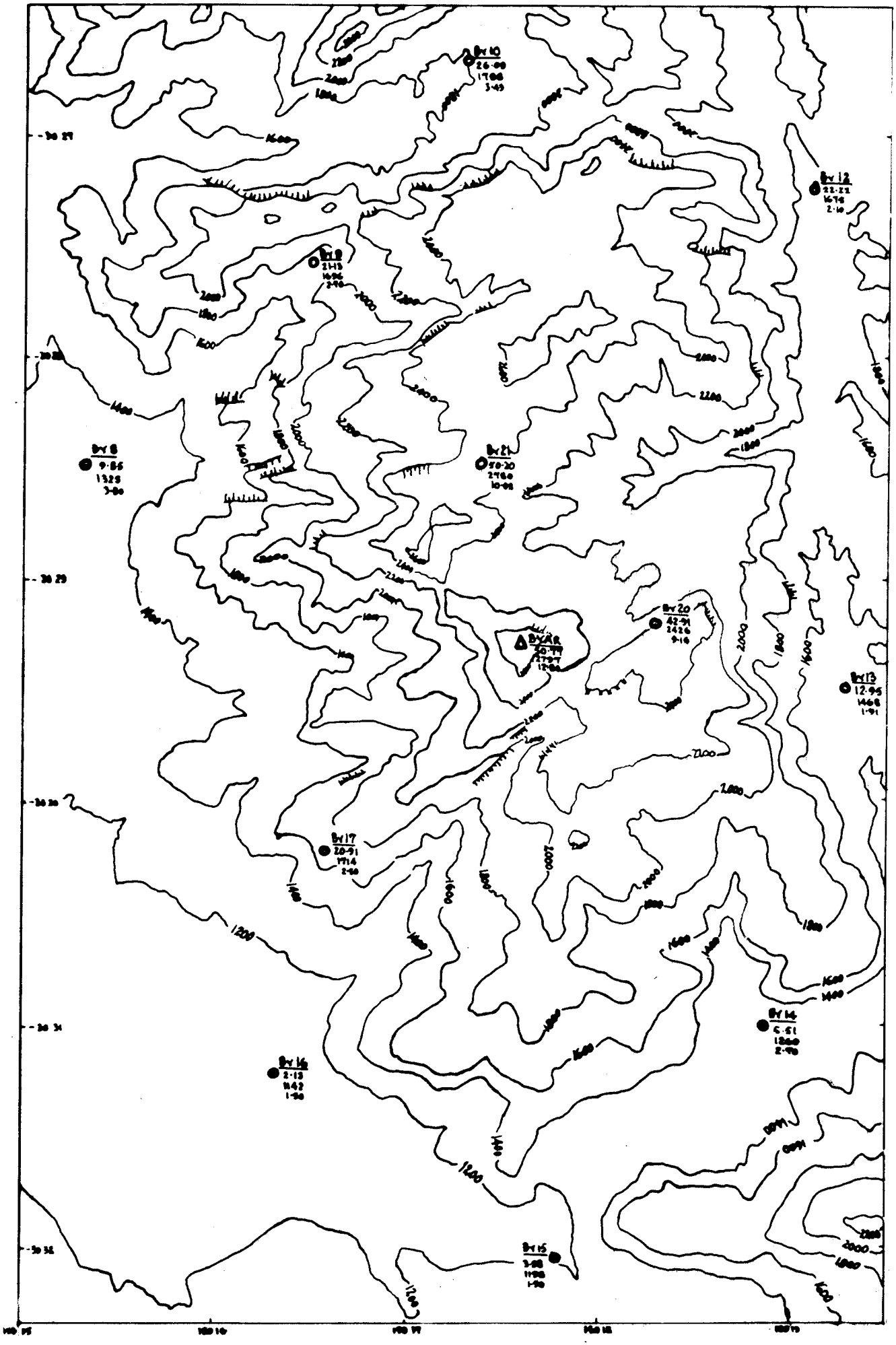
Byr 10
26-09
1706
3-45
Byr 12
22-22
1678
2-16
Byr 9
21-15
1696
2-96
Byr 8
9-85
1325
3-86
Byr 21
20-20
2960
10-98
Byr 20
42-91
2426
9-16
BYAR
20-77
2797
12-86
Byr 13
12-95
1468
1-91
Byr 17
20-91
1714
2-50
Byr 14
6-61
1860
2-98
Byr 16
2-13
1642
1-96
Byr 15
3-88
1998
1-98

FIG. 15 - BYAR

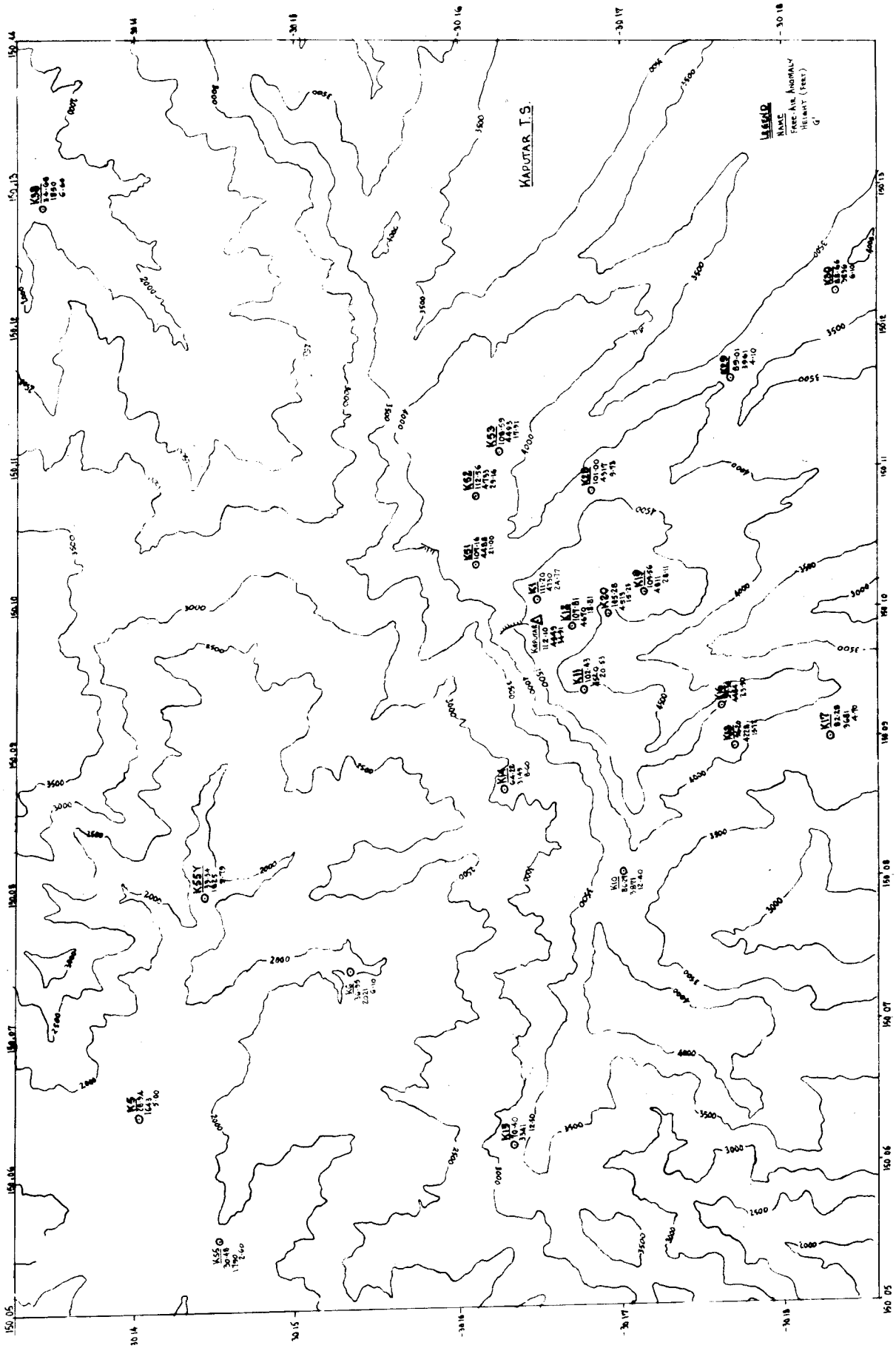

FIG. 16 - KAPUTAR

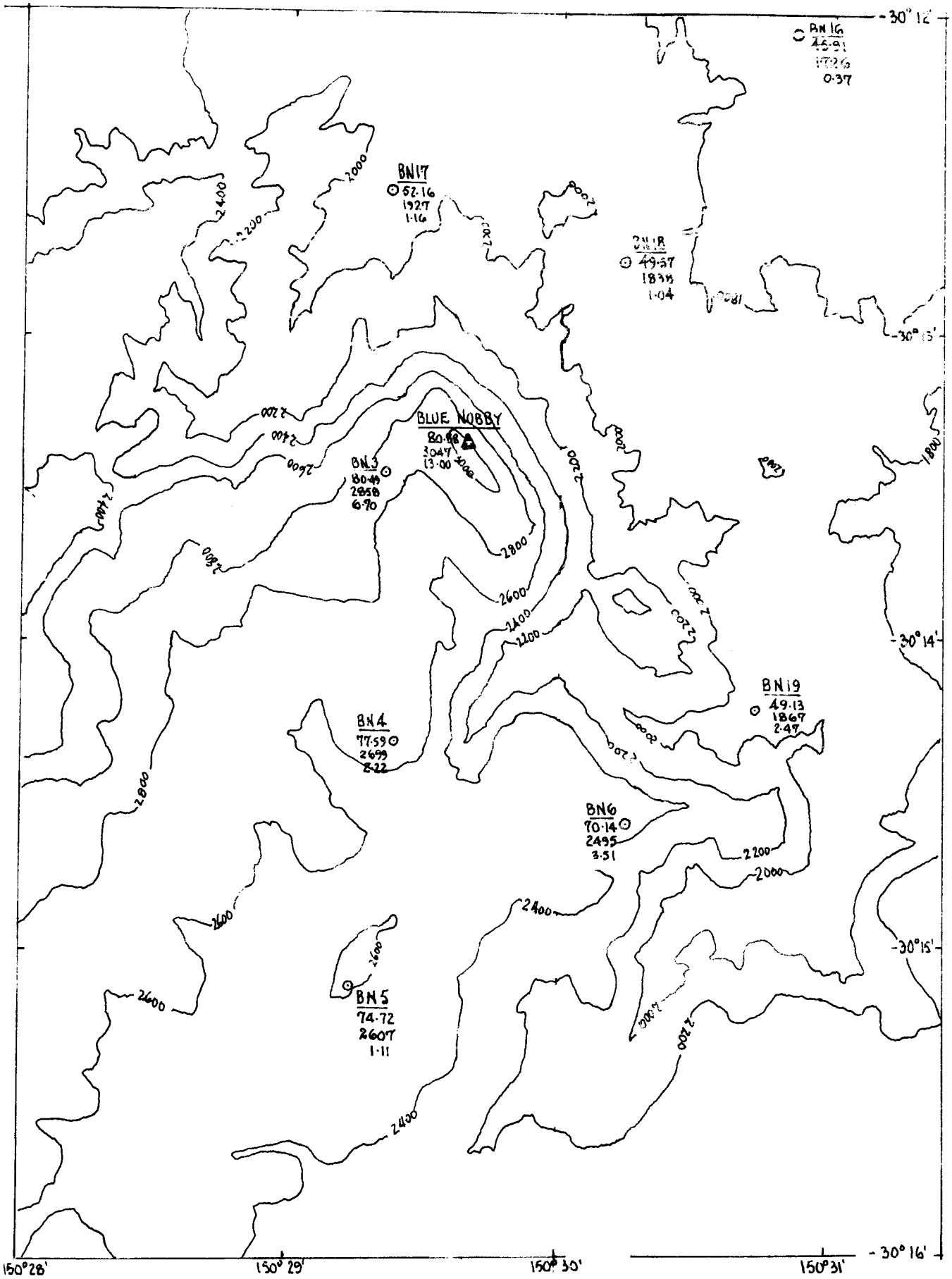

FIG. 17 BLUE NOBBY

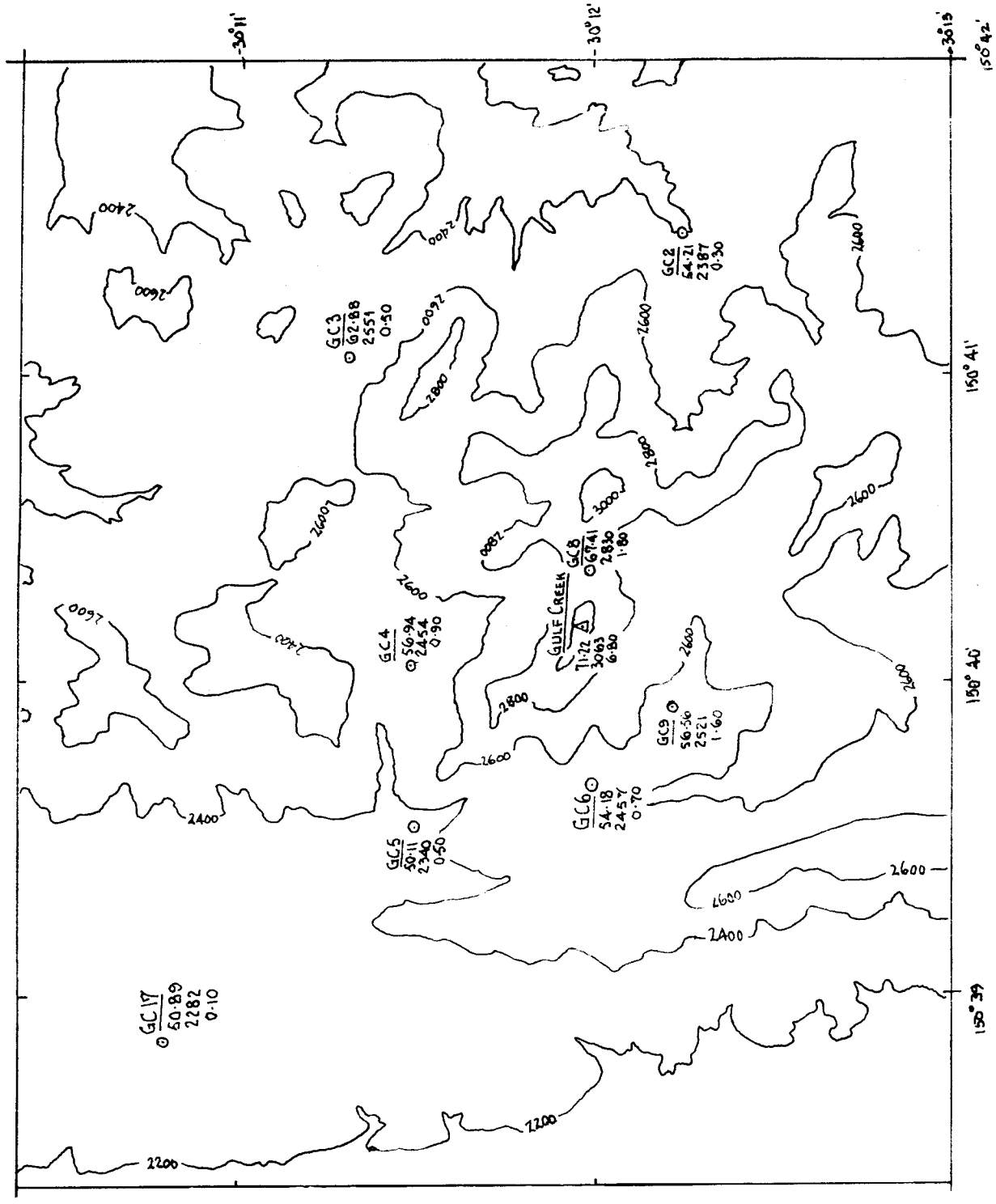

FIG.18 GULF CREEK

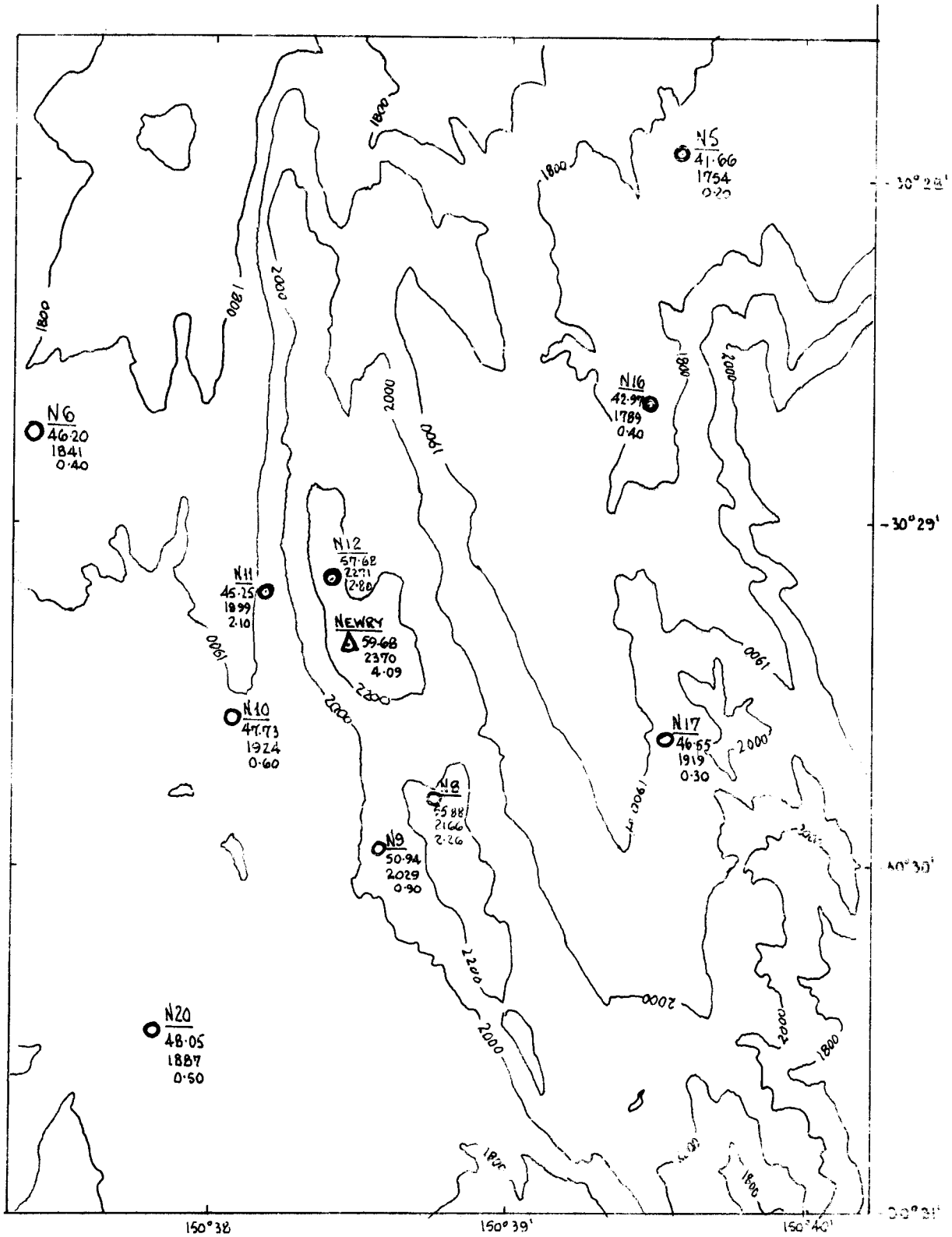
N6
46·20
1841
0·40
N5
41·66
1754
0·20
N16
42·97
1789
0·40
N11
45·25
1999
2·10
N12
57·68
2271
2·80
NEWRY
59·68
2370
4·09
N10
47·73
1924
0·60
N17
46·55
1919
0·30
N8
55·88
2166
2·26
N9
50·94
2029
0·90
N20
48·05
1887
0·50
1800
2000
2200
30° 29'
30° 30'
150° 38
150° 39'
150° 40'

FIG.19 NEWRY

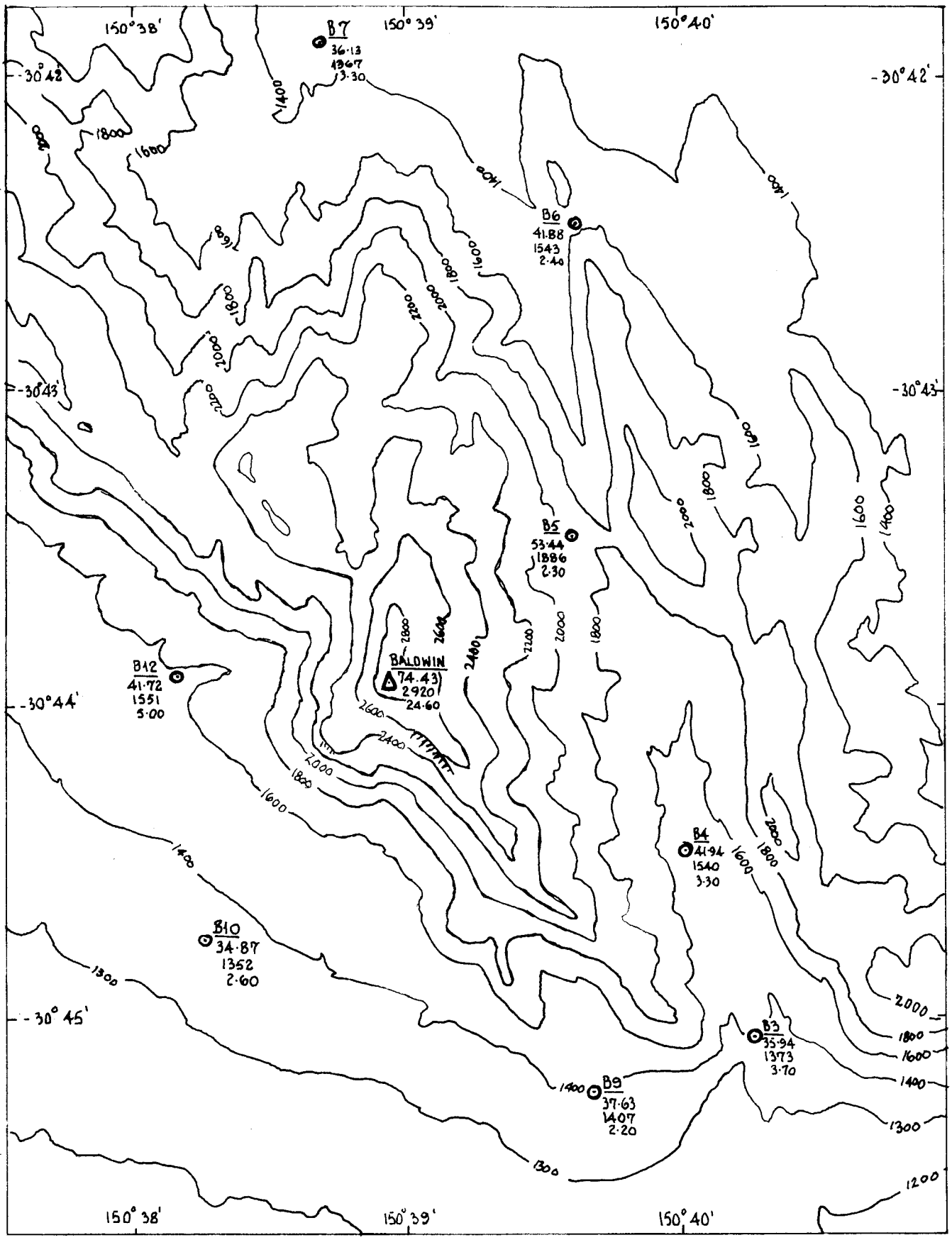

FIG. 20 BALDWIN

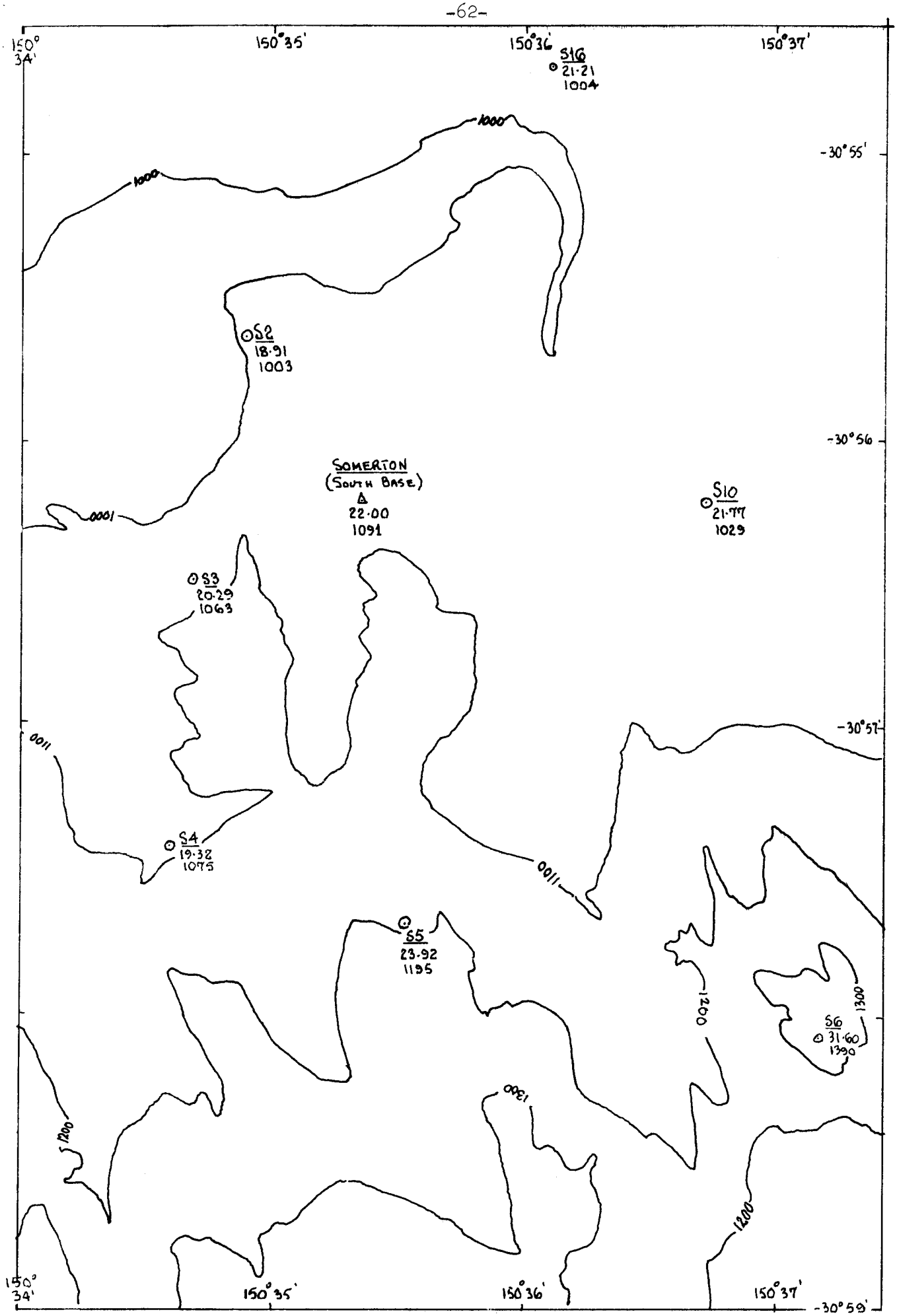

FIG. 21 SOMERTON

4. PRACTICAL EVALUATION

4.1 Assembly of Data

4.1.1 Gravity Data

The Australian continent has been systematically surveyed for gravity anomaly maps by the Australian Government's Bureau of Mineral Resources, Geology and Geophysics (hereafter referred to as the BMR). The gravity surveys for these are based on a gravity control network established throughout Australia known as the Isogal network, so called because the routes followed by the gravimeters between successive control stations were along the isogals, ie. the small circles of latitude. Roughly 230 Isogal stations (gravity control stations) have been established throughout Australia, and two of these were used as datums for densification surveys undertaken in the region, Narrabri 6491-1108 and Tamworth 6491-9109. (See MATHER, BARLOW AND FRYER 1971, pp 6-10 for more details of the Isogal network).

The density of gravity stations in the test area existing at the start of the project varied from about 1 station per 20 km^2 in the flat areas to the west to 1 station per 16 km^2 in the mountainous regions to the east. The bulk of this work was done using helicopters for transport with a pattern of loops with common junction points established to provide a link between adjoining loops. Gravity measurements were taken with Worden gravimeters (or instruments capable of similar accuracy), whilst height was fixed barometrically. (See BARLOW 1967 and MATHER, BARLOW AND FRYER 1971, pp 6-10 for more details of the techniques used in survey.) The accuracy stated for the resultant anomalies is <1 mGal, and certainly provides a good background of gravity information for the purposes of this study.

The density of the gravity stations in the vicinity of the computation point which is required for precise determinations of the deflection of the vertical is obviously a function of the wave length of the gravity field itself and this will generally be much higher in rugged areas than on the plains. Some writers have expressed opinions on this topic and they are quoted below.

PELLINEN (1968, p 352) has claimed a need for "1 point every 0.5 km to 1 km within several kilometres of the control station."

Mather has decided on "a $0^{o}.05$ ($\simeq$ 5 km) grid within 50 km of the control point, with a $0^{o}.01$ ($\simeq$ 1 km) grid within 10 km of the point when evaluating using a computer" (MATHER, BARLOW AND FRYER 1971, p 27). Bursa in his investigations used a very dense network of 1 gravity station per 5 km^2 , and this was further densified around the computation point (BURSA 1968, p6). Brovar (BROVAR ET AL 1964, p 290) in an optimisation for a gravity survey around a deflection point shows a need for 1 point within 2 km of the computation point P, 6 points within 8 km of P measured with a σ of ±0.9 mGal, a further 7 points within the next region out to 21 km with a σ of ±1.3 mGal and another 8 points out to 48 km measured to ±1.9 mGal.

These estimates of densities are higher than the existing gravity station pattern in the test area, particularly in the immediate vicinity of the computation point. It was therefore necessary to intensify the gravity data before a proper investigation could take place. To this end five field trips, each of five to ten days duration, were made to the test region. The two prime tasks were to (i) define the gravity field in the vicinity of each of the twelve computation stations to an order of accuracy thought to be sufficiently accurate for the purpose of the investigation (estimated at 0.3 mGal) and (ii) to fill in the gaps of the existing gravity survey.

The pattern of close gravity stations for the stations are shown in figures 10 to 21 . The survey of Willalla was never satisfactorily completed for a variety of logistical reasons. The detailed aim of the survey was to (i) determine gravity at the A/G station itself then (ii) encircle it with a network of 6 to 8 gravity stations at about a 0.5 to 1 km radius, and with similar pattern of gravity stations 5 to 10 km radius from the A/G station.

It was not always possible to fulfil these specifications as at times the terrain made access difficult. Often it was not possible to get the line of sight conditions desired particularly for the closer ring of gravity stations (see below for methods used to fix height and position of these stations).

(a) Gravity Measurement

A Worden gravimeter (W 140) on loan from the Bureau of Mineral Resources was used for gravity determination on four of the field trips. Worden gravimeter A.G. No. 2 belonging to the School of Geophysics at the University of NSW was employed on the fifth.

The main gravity traverse would start and finish at an Isogal Station located at Narrabri (6491-1108) or Tamworth (6491-9109) and extended over a period of 3 to 4 days. In some cases when gravity closure exceeded expectations this main gravity traverse was broken into smaller traverses, using as terminal data the gravity values at the base station established at the camp. This value was determined from the series of short runs between the Isogal station and the base station. In all cases misclosures were adjusted proportionately with respect to elapsed time through the traverse (see table 2 for summary of traverse misclosures).

Drift checks were also made each morning and evening at base camp, as the rigorous field method usually adopted for this was not feasible (eg. DOBRIN 1960, pp 220-223). Access to some gravity stations took more than half a day's walk in rugged terrain and revisiting these stations would have enormously increased time requirements for the job. Figures 22a to 22e illustrate these drifts and encourage the device of using the shorter traverses on a day to day basis because of apparent irregularities.

Calibration runs were done before or after each field trip on the calibration line Fuller's Bridge (6091.0105) to Wahroonga (6091.0305) in Sydney or by carrying gravity from Wahroonga to the local Isogal Station en route to the test area, which provided a check calibration (although not as precise because of the period of elapsed time and the necessity to reset the gravimeter at Muswellbrook). See table 2 for calibration details. Because of field methods adopted it is expected the standard errors of gravity measurement to be of the order of ±0.3 mGal. Check determinations at stations measured on different traverses confirm this estimate.

(b) Height and Position Determination

The method of survey used to fix the gravity stations depended on the location and accessibility of the station. EDM radiations or subtense methods were used for points close to the computation point.

These were estimated to give a precision in height (σ_h) of $\simeq$ ±0.01 m and ±0.3 m respectively. For more distant stations barometric levelling was used to fix heights and positions were scaled off medium scale maps (1:31 680). The precision for the height of these stations is estimated as ±1 m, care being taken to limit the distance between field and base station. This estimate is

Trip No.	Traverse No.	Starting		Finishing		Misclose (mGal)	Elapsed Time (hrs)	Gravimeter
		Station	Time	Station	Time			
1	1	Kaputar Base	2/0815	Kaputar Base	3/0800	1.6	24	Worden W140(BMR)
	2	"	3/0800	"	3/2030	0.0	12½	
	3	"	4/0800	"	4/1705	-0.5	9	
	4	N'Bri IsoGal	5/0930	N'Bri IsoGal	8/0910	-0.3	96	
2	1	Gunnedah Base	2/605	Gunnedah Base	2/2020	-0.1	12	"
	2	"	3/0810	"	3/1905	-0.1	11	
	3	"	4/0745	"	4/1920	-0.3	12	
	4	"	5/0845	"	5/1755	-0.8	9	
	5	"	6/0905	N'Bri IsoGal	6/1720	-1.4	8	
3	1	N'Bri IsoGal	1/1630	N'Bri IsoGal	2/1920	+0.2	27	"
	2	"	2/1920	"	3/1745	-0.1	22	
	3	"	3/1745	"	4/2030	-1.1	27	
4	1	Barraba Base	2/0600	Barraba Base	2/1945	0.2	14	"
	2	"	3/0625	"	3/2130	-0.7	15	
	3	"	4/0815	Tamworth IsoGal	4/1500	-0.6	7	
	4	Tamworth IsoGal	4/1500	"	8/1940	+1.3	100	
5	1	Tamworth IsoGal	1/1700	Tamworth IsoGal	3/1830	+0.4	49	Worden A G 2(UNSW)
	2	"	3/1830	Narrabri IsoGal	6/0800	-0.4	62	
	3	Narrabri IsoGal	6/0800	Tamworth IsoGal	7/1055	-0.7	27	

NOTE: (i) Narrabri IsoGal is IsoGal Station No. 6491-1108 located near Narrabri Post Office

(ii) Tamworth IsoGal is IsoGal Station No. 6491-9109 located at Tamworth Air Port

TABLE 1 SUMMARY OF GRAVITY TRAVERSE MISCLOSES

Trip/Gravimeter	1/W140	2/W140	2/W140	2/W140	3/W140	3/W140	4/W140	4/W140	5/AG2
Date	21.5.71	13.6.71	13.6.71	30.6.71	7.12.71	12.12.71	13.5.72	20.5.72	6.2.74
IsoGal Stn/Reading	W'Gah 1357.5	F'Bridge 1192.2	W'Gah 1250.3	W'Gah 2195.3	W'Gah 2159.2	W'Gah 2130.7	W'Gah 2287.5	W'Gah 1898.8	W'Gah 1326.1
Muswellbrook C.P.	20.7			858.7	822.7	794.6	892.6	561.4	
Dial Units/Time Interval	4½hrs 1336.8	N/A	N/A	5 hrs 1336.6	4 hrs 1336.5	4 hrs 1336.1	4 hrs 1336.1	4 hrs 1337.4	N/A N/A
Muswellbrook Reset	1806.9			2252.5	2283.0	2271.5	2227.2	2220.4	
IsoGal Stn/Reading	N'Bri 283.6	W'Gah 584.7	F'Bdg 1858.7	N'Bri 738.2	N'Bri 759.6	744.7	2½hrs 820.5	2½hrs 815.1	F'Bdg 1945.6
Dial Units/Time Interval	4 hr 1523.3	607.5	608.4	24hrs 1514.3	5 hrs 1523.4	6 hrs 1526/8	T'Wth 1406.7	1405.3	619.5
Total Measured Intervals	8½hrs 2860.1	¾ hr 607.5	½ hr 608.4	29hrs 2850.9	9 hrs 2859.9	10hrs 2862.9	6½hrs 2742.8	6½hrs 2742.7	½ hr 619.5
Fixed Difference(mGal)	291.85	61.99	61.99	291.85	291.85	291.85	279.87	279.87	61.99
Calibration(Dial Units/ mGal)	0.102 04	0.102 04	0.101 88	0.102 37	0.102 05	0.101 94	0.102 04	0.102 04	0.100 06

Legend of IsoGal Stations

W'Gah	Wahroongah	6091.0305
N'Bri	Narrabri	6491.1108
T'Wth	Tamworth	6491.9109
F'Bridge	Fullers Bridge	6091.0105

Calibration	By Me		Quoted
W140	0.10205	±.000 07	0.102 0
A2	0.10006	-	0.100 3

TABLE 2 CALIBRATED CHECKS, WORDEN GRAVIMETERS W140 (BMR) AND AG2(UNSW)

FIG.22 DRIFT CHECKS-NARRABRI MANILLA GRAVITY SURVEYS.

TRIP 1:14.5.71 TO 19.5.71 GRAVIMETER:WORDEN W140

BASE: MT.KAPUTAR CAMPING AREA.

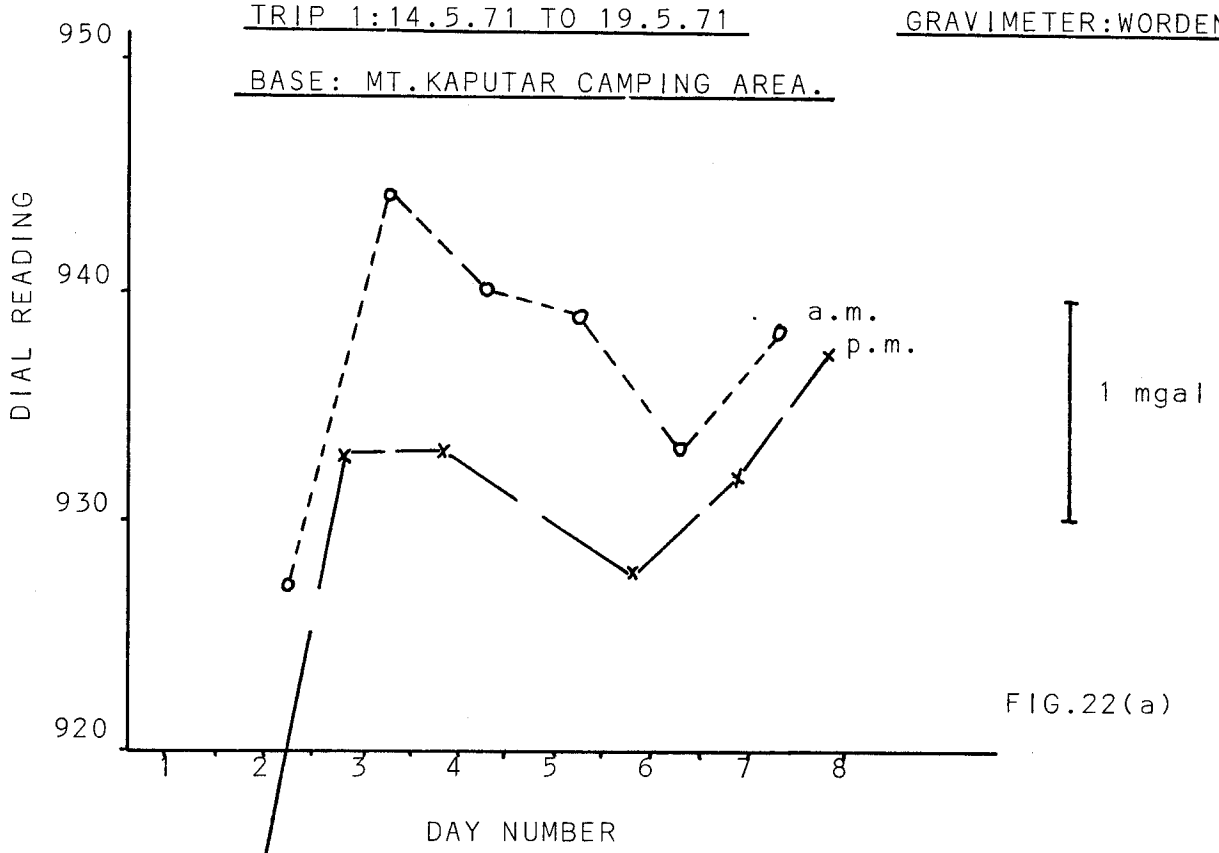

FIG.22(a)

TRIP 2:29.6.71 TO 5.7.71 GRAVIMETER:WORDEN W140

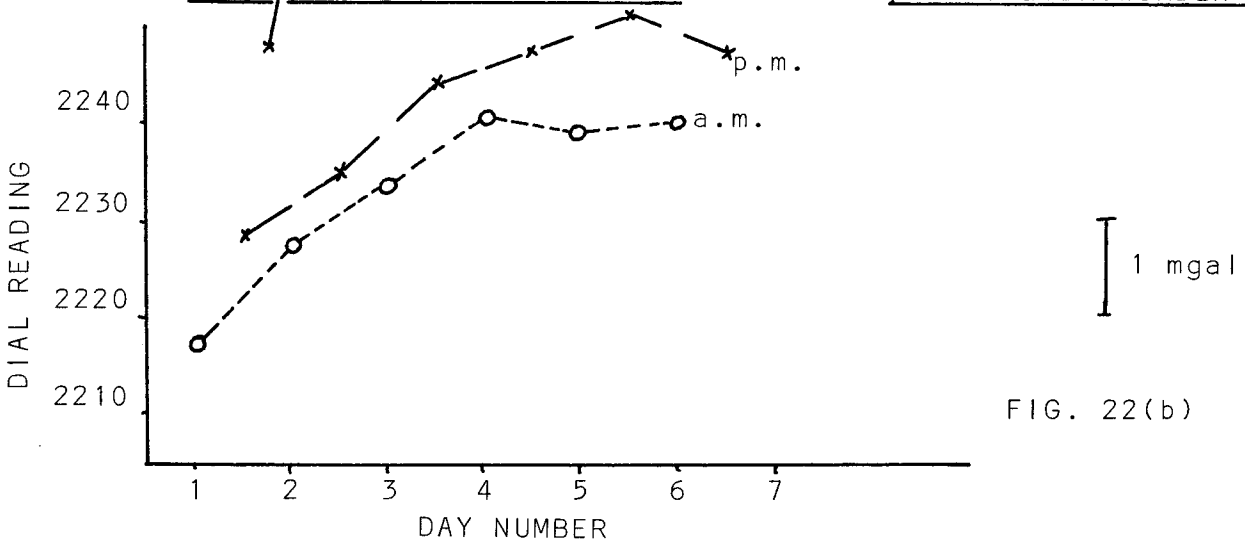

FIG. 22(b)

TRIP 3: 7.12.71 TO 12.12.71 GRAVIMETER:WORDEN W140

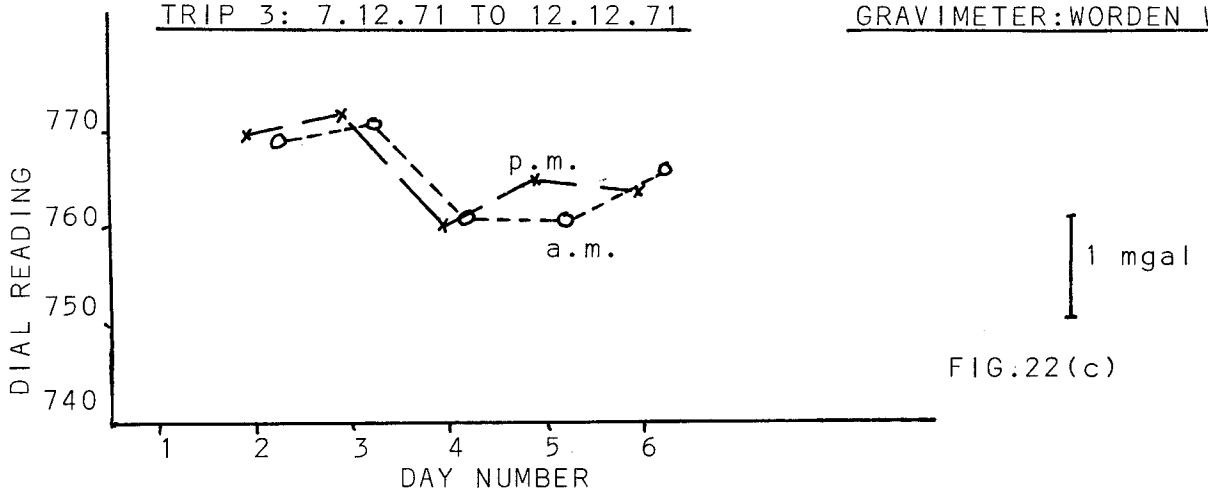

FIG.22(c)

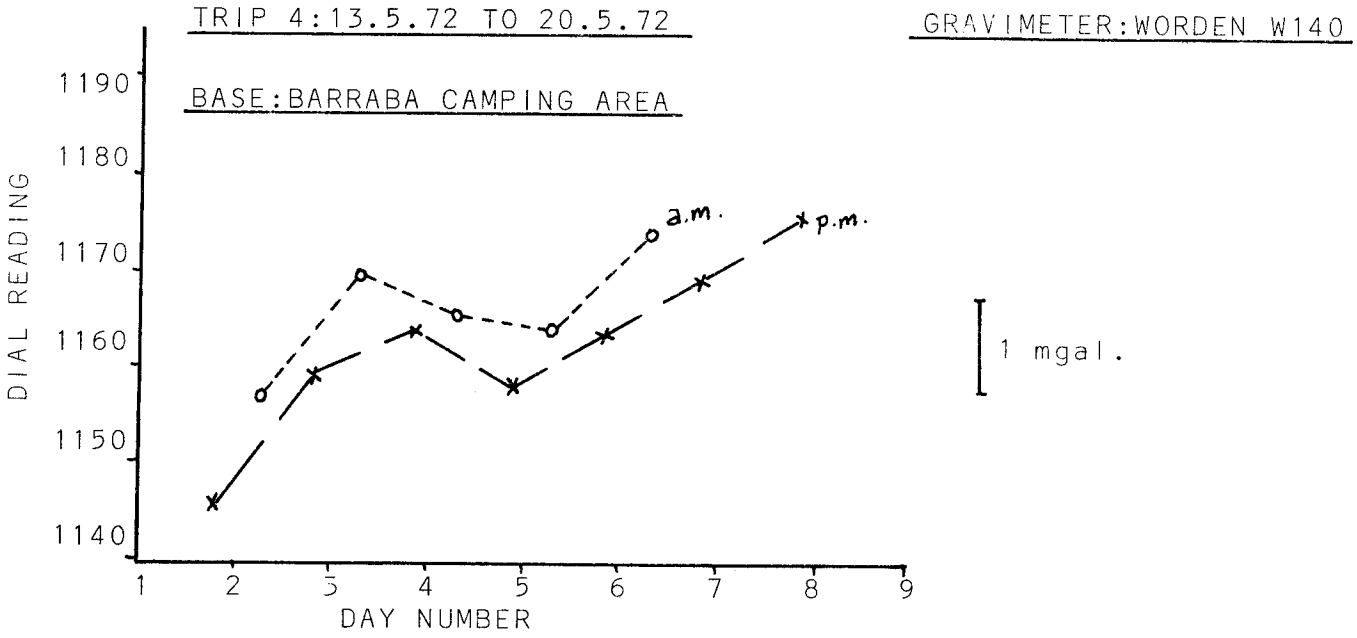

FIG.22d

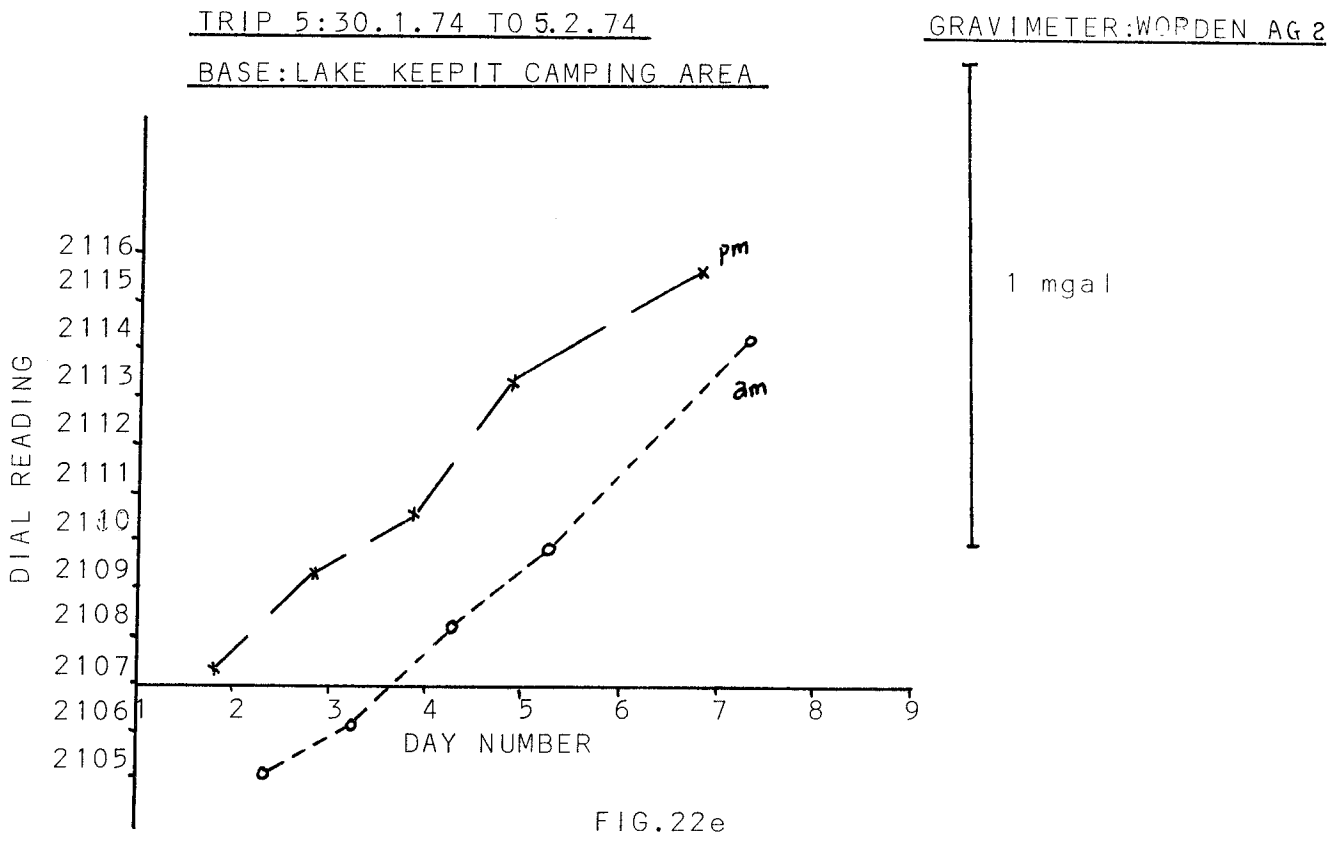

FIG.22e

supported by check determinations (eg. simple trig heighting) and comparisons with heights interpolated from contours.

The positions of the gravity stations are not critical and need only be known to ±20 m in each direction. This could be achieved by scaling off medium scale maps, although for radiated stations the position was computed directly to a much higher precision.

(c) Collation and Storage of Gravity Data

The field measurements were punched onto data cards and processed to produce a file containing the latitude, longitude (expressed in decimal degrees to the fourth place), height in feet and free-air gravity anomaly. This file was combined with the BMR gravity data organised in the same fashion in the region bounded by $-28^{\circ}.5$ to $-32^{\circ}.00$ in latitude and $+148^{\circ}.5$ to $+152^{\circ}.0$ in longitude. Together they created a file of 1550 points which was called GRAVBNK, and which was ordered according to longitude to assist in computer searching operations. Each station file was subsequently expanded when the G' values for each of the gravity stations within certain limits of the A/G stations were computed. The reason and methods for this will be described in detail in section 4.4.

4.1.2 Auxiliary Height Points

As was shown in Chapters 2 and 3 the full solution takes into account terms which are topography dependent. The gravity stations alone do not give an adequate description of the terrain. Quite apart from their spacing, which is far greater in rugged areas than the wave length of the main trends of the topography, they are likely to systematically underestimate the terrain heights, as most ground based (cf. helicopter borne) surveys are limited to areas accessible by 4-wheel drive vehicles. For these reasons it was felt essential to augment the gravity data with extra height data from the maps.

The aim of this "height bank" was to give a faithful picture of the terrain. The general trends were recorded by taking heights at 3' x 1½' grid intersections (6 x 3 km) grid intersection, with any notable differences from this (eg. large uplifts or deep valleys) also being digitised. As was found in the earlier computations it was necessary to further intensify the height field in the vicinity of the computation points. Otherwise the computational technique employed tended to over-smoothen the topography in this critical area.

The height file, which was initially called HTBIN, consisted of roughly 1200 points defined in latitude, longitude and height, and was organised as a function of longitude to assist computer searching.

4.1.3 Geoidal Information

The solution derived from Green's Third Identity requires geoidal information ξ, η & N as well as terrain parameters h and β. The values of N were obtained from the 1970 geoid solution for Australia by Mather (see MATHER 1970a; MATHER 1970b).

(a) N

This was calculated on the Australian Geodetic Datum (AGD) for each A/G station as well as for a

number of interpolation stations to the north and west of the region (see fig. 23). Subsequently N was transformed to the International Ellipsoid to conform with the datum adopted throughout the gravimetric computations.

(b) ξ , η

The values of ξ , η computed in the 1970 geoid solution mentioned above were likely to have large errors of short wavelength owing to the relative lack of gravity data in the innermost region of computation. So the usual method of taking the first approximations of ξ , η computed in this solution from the Vening Meinesz formulae was not used for the purposes of this exercise, mainly because it was felt that the A/G deflections would be less likely to introduce uncertainties into the evaluation.

Diagrams of the geoidal parameters can be found in figures 23 to 25 . The final input data consisted of latitude, longitude, N, ξ and η for each of the A/G stations and for interpolated stations needed to provide information beyond the limits of the area described by the A/G stations. In all 17 stations were used to describe the geoid throughout the region. See section 6.4 for details of methods used to compute geoidal parameters at discrete points in the solution of the correction terms.

4.2 Computational Methods

4.2.1 The Traditional Approach

The method originally postulated to compute the deflection of the vertical was a purely graphical approach (STOKES 1849, p 170), deriving deflections from geoid elevations. The Vening Meinesz integral enables us to evaluate deflections analytically, using the gravity anomalies themselves as data. The computational approach used in this evaluation will be discussed here as they will have an important bearing on the techniques developed in this investigation.

In 1947 SOLLINS (q.v.) published tables to be used in the computation of deflections. Recognising the fact that the Vening Meinesz integral was a continuous summation over the whole earth's surface, and that the kernel of the integral did not solve as a closed analytic function, he used the standard technique of breaking the surface up into small discrete areas. The contribution from each area to the deflection was then computed and accumulated through the whole surface to find the sum total value for ξ and η .

The tables of Sollins (*IBID*, pp 286-300) give values of $\frac{df(\psi)}{d\psi} \sin\psi$, and $\int \frac{df(\psi)}{d\psi} \sin\psi \, d\psi$ starting from a value of ψ equivalent to 10 m and incrementing by 10 m out to 5560 m. With such small steps it was felt that almost any type of areal subdivision could be used for the evaluation of the Vening Meinesz expression.

We shall look briefly at the approach taken by Sollins to prepare these tables.

Sollins expressed the Vening Meinesz integral thus

$$\xi_i = \frac{1}{2\pi\gamma} \iint \Delta g \, \frac{df(\psi)}{d\psi} \sin\psi \cos\alpha_i \, d\psi \, d\alpha \; ; \qquad i = 1, 2 \qquad (4.1), \; [\text{from } (2.26)]$$

where

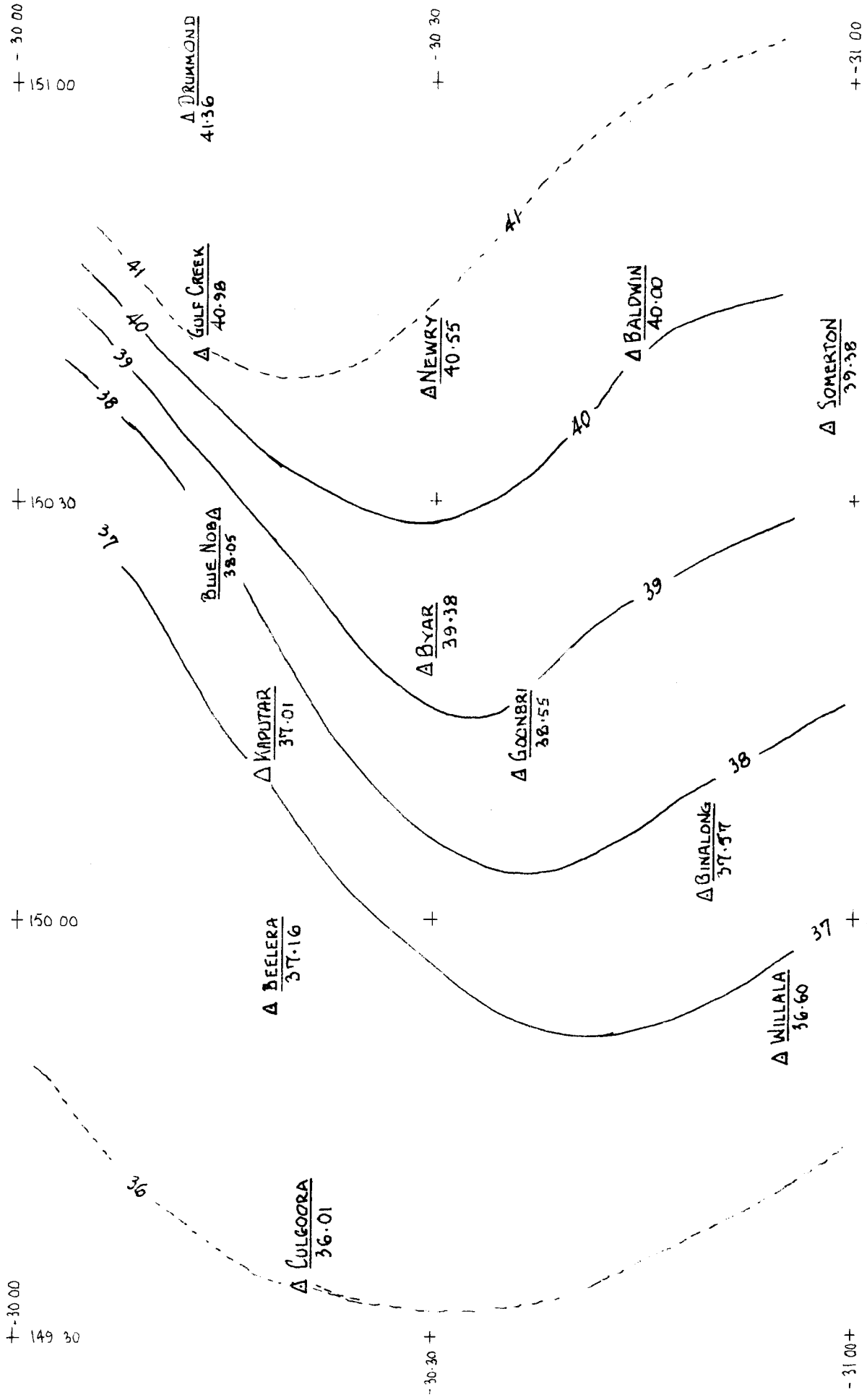

FIG.23 GEOID-ELLIPSOID SEPARATIONS IN THE TEST AREA

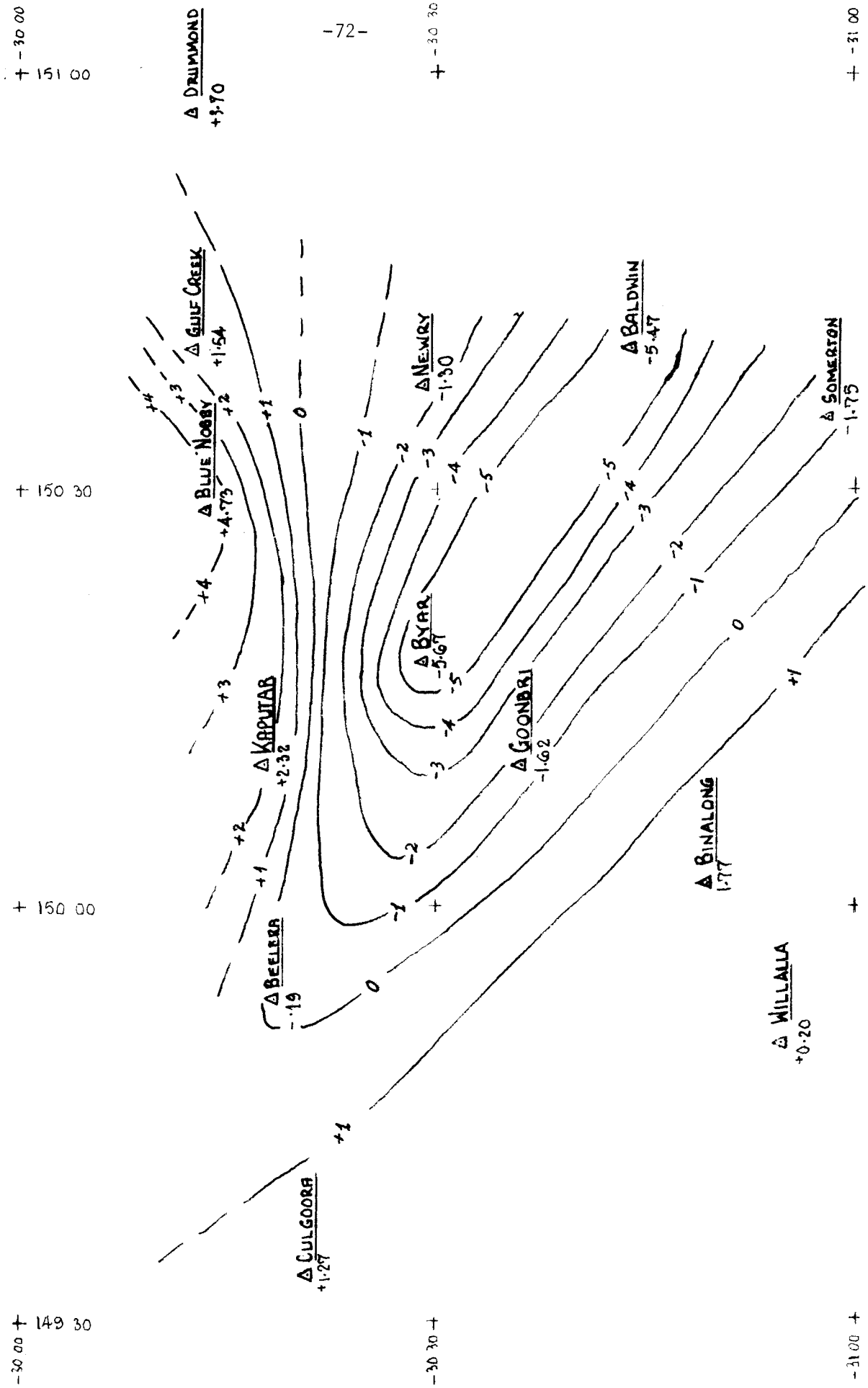

FIG.24 ξ A/G ON A.G.D. CORRECTED ONTO GEOCENTRE

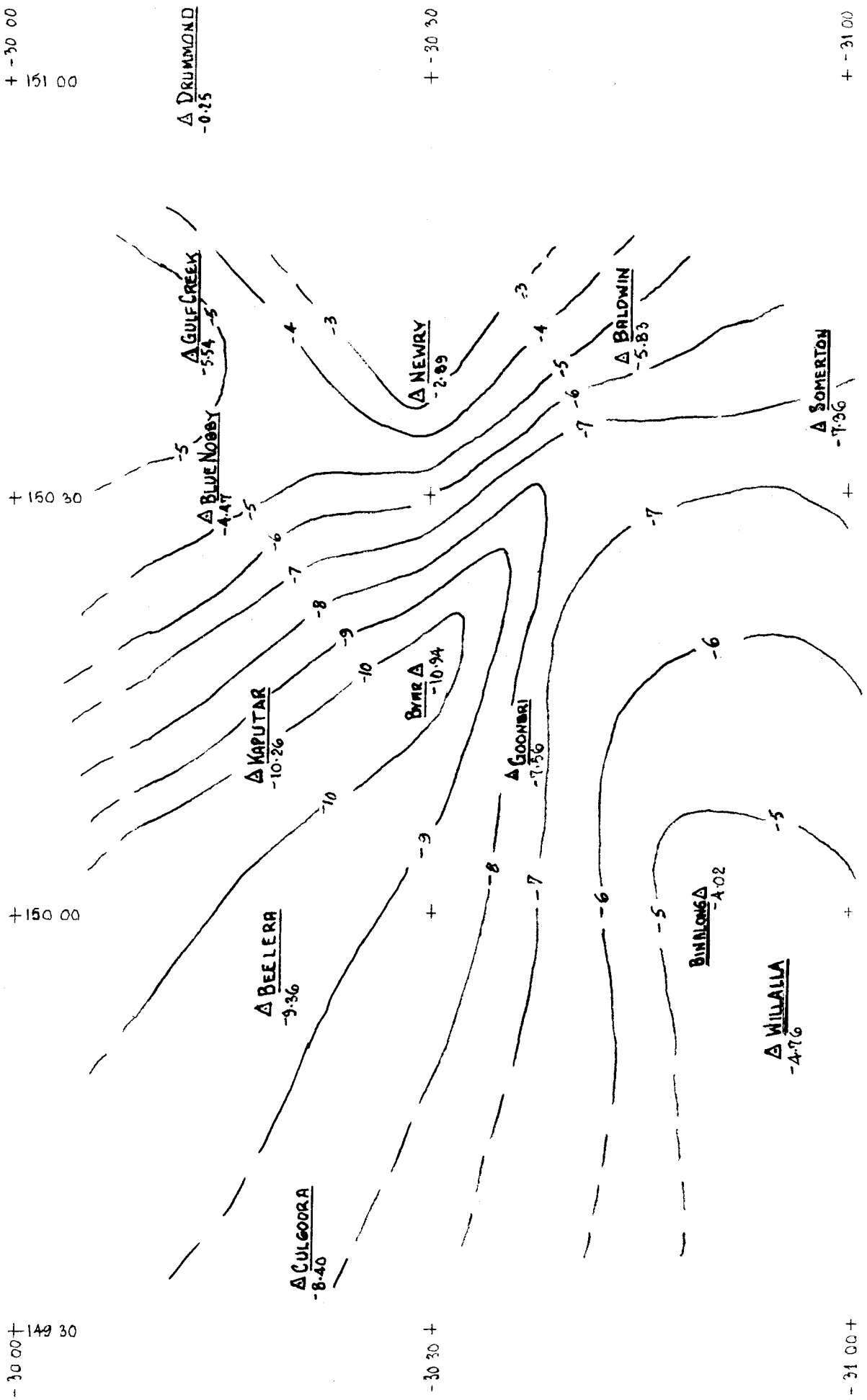

FIG.25 η A/G ON A.G.D. CORRECTED ONTO GEOCENTRE

$$\sin\psi \; d\psi \; d\alpha \;=\; d\sigma$$

$$\xi_1 \;=\; \xi \quad , \xi_2 \;=\; \eta$$

$$\alpha_1 \;=\; \alpha \qquad \alpha_2 \;=\; 90 - \alpha$$

and the Vening Meinesz function as

$$\frac{df(\psi)}{d\psi} \;=\; \tfrac{1}{2}\left[-\frac{\cos\frac{1}{2}\psi}{2\sin^2\frac{1}{2}\psi} - 3\cos\tfrac{1}{2}\psi + 5\sin\psi + 3\sin\psi \;\ln(\sin\tfrac{1}{2}\psi + \sin^2\tfrac{1}{2}\psi) - \right.$$

$$\left. - \frac{3}{2}\left(\frac{1+2\sin\frac{1}{2}\psi}{1+\sin\frac{1}{2}\psi}\right)\cot\tfrac{1}{2}\psi \;\cos\psi \;\right] \qquad (4.2) \quad [\text{cf}(2.27)]$$

The series expansion of $\frac{df(\psi)}{d\psi} \sin\psi$, $\int \frac{df(\psi)}{d\psi}\sin\psi \, d\psi$ will be seen to be

$$\frac{df(\psi)}{d\psi}\sin\psi \;=\; -\frac{1}{\psi} - \frac{3}{2} - \frac{49}{24}\;\psi + \ldots \qquad (4.3)$$

$$\int \frac{df(\psi)}{d\psi}\;\sin\psi \, d\psi \;=\; -\ln\psi - \frac{3}{2}\psi - \frac{49}{48}\;\psi^2 + \ldots \qquad (4.4)$$

which, upon substitution for ψ is the basis for Sollins tables.

Rice used the Sollins' tables to develop his well-known ring pattern for computation of deflections of the vertical (RICE 1952). They can also be derived in the following manner. If we accept a constant apex angle $(d\alpha)$ it is possible to use (4.3) to develop a series of radii which, for a given mean gravity anomaly for the area $d\psi \;\sin\psi\, d\alpha$ will give a constant radial deflection of the vertical at the computation point. Rice's Rings (as the concentric circles thus generated are known) give a radial deflection of 0.001 arcsec for a 1 mGal anomaly, and a 10° step between successive radii .

So the values of ψ could be found from (4.3) in this way.

If we restate (2.26) as

$$\xi''_i \;=\; C_1 \iint \Delta g \,\frac{df(\psi)}{d\psi}\;\sin\psi\cos\alpha_i \;\; d\psi \quad d\alpha \quad ; \quad i = 1, 2 \qquad (4.5)$$

where $C_1 \;=\; \frac{\text{cosec } 1''}{2\pi\gamma}\; d\alpha \qquad (4.6)$

Then for $d\alpha \;=\; 10^{\circ}$,

$$\overline{\gamma} \;\simeq\; 979770$$

$$C_1 \;=\; 0.005\;858\,.$$

We can now impose the condition that an increment in ψ give a deflection of 0.001 arcsec for a 1 mGal anomaly i.e.

$$C_1\left[-\ln\;\psi_j - \frac{3}{2}\;\psi_j - \frac{49}{48}\;\psi_j^2\;\right] \;=\; C_1\left[-\ln\psi_i - \frac{3}{2}\;\psi_i - \frac{49}{48}\;\psi_i^2\right] \;- 0.001 \qquad (4.7)$$

where $j = i + 1$

The first approximation of ψ_j (ψ_j') is found by

$$\ln \psi_j' = \ln \psi_i + \frac{0.001}{C_1}$$

or

$$\psi_j' = \ln^{-1} (\ln \psi_i + \frac{0.001}{C_1}) \qquad (4.8)$$

This expression could be substituted back into (4.6) and a more exact value for ψ_j found. However, with modern computing technology it is easier to evaluate the first approximation of ψ_j, substitute the value itself into the smaller terms in ψ_j and re-evaluate $\ln \psi_j$ in this new circumstance.

Thus a series of rings intersected by radii with 10^o apex angles are generated from a minimum radius of (in Rice's case, *IBID*, p 288) 100 m to a maximum of 1094.3 km in 56 steps. Each 'compartment' has an area which will contribute 0.001 arcsec to the radial deflection of the vertical at the computation point for a mean anomaly of 1 mGal.

The rings are used in a way which is directly comparable to the computation of the terrain correction using Hayford zones. Plotted on a transparent sheet, they are overlayed on gravimetric and hypsometric maps with the centre of the circles on the point of computation. The mean gravity anomaly and height for each compartment is then extracted and combined to get the compartmental mean free-air anomaly. The resultant deflection is then split into its two components and these accumulated through the entire template of rings.

A similar technique was developed in Russia, as reported in (MOLODENSKII ET AL 1962, pp 168-171). These templates computed the influence of 1 mGal producing a radial deflection which varied in four stages depending on the distance of the compartment from the computation point starting from 0".005 for an initial radius of 5 km to 0".000 371 for very distant zones (2000 km). The apex angle was not kept fixed at 10^o, but was also varied in the stepping process. The aim of this presumably was to introduce a certain correspondence between the compartment size and the density of data usually available at various distances away from the computation point. Certainly, as is shown in section 6.3, the original Rice Rings subdivision is too fine for the density of the data being used and some re-organisation of the rings pattern can improve the efficiency of computation by this method.

Whether modified or not, the Rice Rings approach possesses a certain strength in solution coupled with flexibility of application which is not easily obtained in the grid pattern approach usually adopted for computer solutions. This will be discussed more fully in section 4.3 after the approaches to computer solutions have been reviewed. Nonetheless, the ease in application of the Rice Rings approach can be appreciated when one considers computations with incomplete data, or even error analyses using this method. For an error analysis one simply substitutes the error in the gravity anomaly for the gravity anomaly itself and then finds the resultant error in the deflection. If the gravity field is augmented after a first approximation is computed, one can compute the radial deflection resulting from the new data and accumulate the result with the earlier value. But probably the most valuable aspect from the point of view of maintaining accuracy in computation is that the changing sizes of the compartments gives one insight into the density requirements of data for the maintenance of accuracy in solution. In this respect it could be compared with optimising techniques in survey networks which ensure that survey methods are employed to produce values satisfying the accuracy requirements of the task.

4.2.2 Contemporary Methods of Computation

The contemporary approach to evaluation is greatly influenced by the coming of electronic computers, now the *sine qua non* of calculation and data handling tools. This has led to the evolution of new techniques for data manipulation and storage in order to increase the efficiency of computations. It has also led to the re-formulation of the solutions to suit the methods of data handling dictated by computer techniques.

The earliest attempts at solving geophysical problems on the digital computer were in the late 1950s. For example, BOTT (1959) reports on a method of evaluating gravimetric terrain corrections out to Hayford Zone E using a combination of graphical and computer approaches. This was not a direct simulation of the Hayford Zone system on the computer, however.Mean height and gravity values were found and stored for squares resulting from a grid placed over the area around the computation point. The correction was then evaluated for each square in turn and accumulated through the area. In other words, there was a trend away from the system which eased the computational load in the manual evaluation and towards methods which enhanced the data handling aspects of the computation. Even so, the use of the grid pattern meant that some processing of the data had to occur before it could be presented in this form.

This approach established itself in the geophysical world. In 1962, KANE (q.v.) published a paper describing techniques for the computation of the terrain correction done completely on the digital computer. Data was again stored in matrix form, and the paper underlines the problem associated with storing data in a grid system, particularly as the calculations approach the central point. The general inflexibility of this approach is such that, if too large a size is adopted as the basic unit for terrain representation, it is too coarse to reflect the actual situation. If on the other hand too small a square size is taken, the amount of computer storage is increased greatly, and as a result so also is the time of computation of the terrain correction. The end result is a compromise; square sizes are varied according to distance from the computation point and in general their magnitudes and made comparable with the compartment sizes of the Hayford Zones.

This again shows the need for some pre-processing of data before a computation can be carried out.

In 1962 CAMPBELL (q.v.) investigated the computation contribution of the central area to the deflection of the vertical using 'square storage areas'. In this development the element of surface area in the Vening Meinesz formulae $d\sigma$ is expressed in terms of the parallels and meridians defining the square, viz:

$$d\sigma = \cos\phi \; d\phi \; d\lambda \qquad (4.9)$$

The system of successive subdivision of the grid pattern was as follows. Firstly the given area is subdivided into a 9 x 9 grid, giving 81 squares, from which the innermost (3 x 4) 9 squares are further subdivided to give 81 squares. This process is repeated until a sufficiently small 3 x 3 pattern of squares are obtained at the centre to assume constant gradient of the anomalous gravity field. Because of the nature of the subdivision a simple algorithm for evaluation can be derived. Tests on theoretical and actual fields compared well with the Rice Rings solution.

Campbell concludes that the Rice method gives good results for minimum effort, but that for a completely automated procedure on an electronic computer the 'square method' approach is best.

Among the first to employ computers in the solution of the geodetic problem was Fischer from the US Army Map Service and the concept of storing data in a grid pattern was employed by her (FISCHER 1966a; FISCHER 1966b). This was due not only to reasons of storage but also because deflections were being

computed at the grid intersections themselves in order to facilitate interpolation of A/G deflections. Each computation point (P) is surrounded by a set of belts. The first belt (B_1) consists of four rectangles (a x b) having a common vertex at P. The second belt (B_2) consists of 12 rectangles, B_3 of 20 rectangles and so on. With a subdivisional technique analogous to that mentioned by Campbell above, a simple algorithm can be derived and the Vening Meinesz integral evaluated. Again there is a need for organising the data before the computation can take place.

There are a few real shortcomings in the grid approach which will be mentioned here. The first relates to the wavelength of the gravity data or height data which must be faithfully reflected in the nearest zones for deflection computations if precision is not to be lost. There seems little doubt that the storage of gravity anomaly means of 5^o, 1^o, 0.5^o or even 0.1^o squares for general geoidal computations is the most convenient and efficient approach to take (COLOMBO 1976) but to carry this approach right up to the computation point itself, as is needed in deflection computations, creates difficulties on the detailed analysis of results. It is useless simply to continue subdividing existing square sizes in the hope that this will increase the sensitivity of the computation. It is, of course, necessary to actually evaluate the mean value of these smaller squares by observation, and this is what is done in most cases. For example, EMRICK (1973, pp 75-82) adopting the Fischer idea of subbelts, found the mean terrain heights of the innermost 7'.5 squares from the 1:24 000 topographical map series, and the gravity anomalies were interpolated from the United States Coast and Geodetic Survey (USC and GS) Bouguer anomaly map of the area.

A second and important shortcoming is of a practical nature. It is pure coincidence if the computation point sits on a grid intersection formed by one of the subdivisional techniques. In fact both Fischer and Emrick computed deflections at the intersections of grid lines, and then used an interpolation method to find the deflection at the actual A/G station for which the comparison was needed. This must certainly introduce errors in areas of disturbed gravity as the model for interpolation could never properly reflect the short wavelength signals of the immediate gravity field to which the deflection is so sensitive.

The third point relates to the strength of the function in the kernel of the Vening Meinesz integral which is used for the grid system. The form of the elemental area used in the grid approach is given in equation 4.9 and is compounded with the Vening Meinesz function (4.2) to evaluate the integral. It can be seen on inspection that the kernel approaches infinity for $\psi \to 0$ as a function of $\mathrm{cosec}^2 \frac{1}{2}\psi$. On the other hand, if the polar coordinate form is used (equation 4.1) the Vening Meinesz function is multiplied by $\sin\psi$ $(= 2 \sin\frac{1}{2}\psi \cos\frac{1}{2}\psi)$ and the kernels approach to infinity for $\psi \to 0$ is a function of $\mathrm{cosec}\frac{1}{2}\psi$. This significantly strengthens the function as errors in Δg now have the coefficient $\mathrm{cosec}\frac{1}{2}\psi$ instead of $\mathrm{cosec}^2\frac{1}{2}\psi$. For a detailed investigation such an improvement must be considered significant.

There is no doubt that for general geoid solutions the efficiency of the programming system is greatly assisted if the data is stored in a grid pattern. This has generated research into such areas as the storage and retrieval aspects of data (eg. BUCK AND TANNER 1972) and also into the optimum grid to be adopted for gravimetric solutions. In this regard, for example, PAUL 1973 has devised a scheme which attempts to maintain equal surface areas for the square sizes used for the storage of data, in order to overcome problems of inequalities of sample sizes posed by a straight geographical grid.

At this stage the subdivisional approach adopted by MATHER (1969, p 501; 1970a, pp 83, 84) for the 1970 geoid solution of Australia will be described as this will form the basis for the 'outer' zone computations in this present investigation. A consistent set of $0.1^o \times 0.1^o$, $\frac{1}{2}^o \times \frac{1}{2}^o$, and $5^o \times 5^o$ area means were obtained from a combination of satellite data and surface gravimetry.

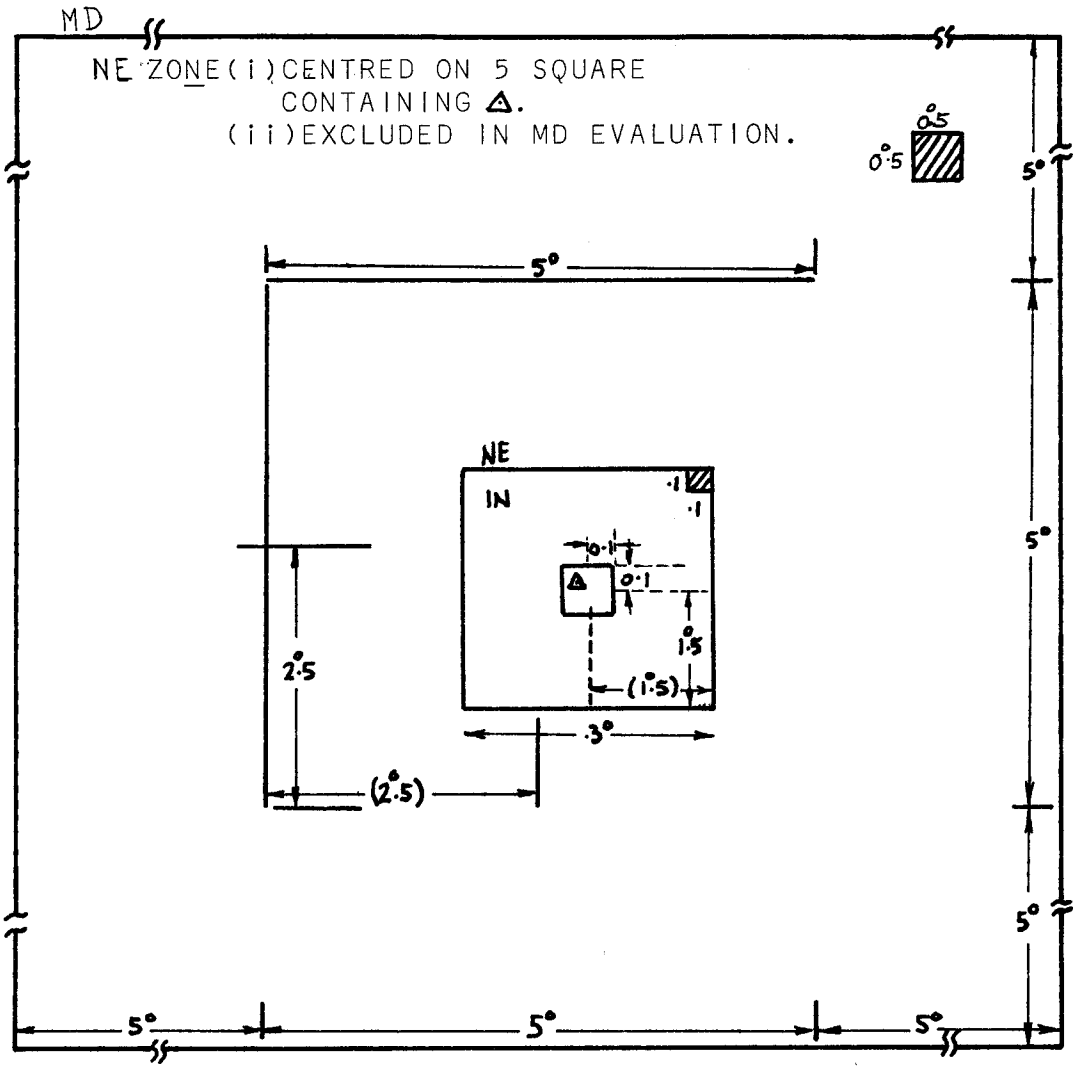

FIG.26(a) INNER ZONE STRUCTURE.

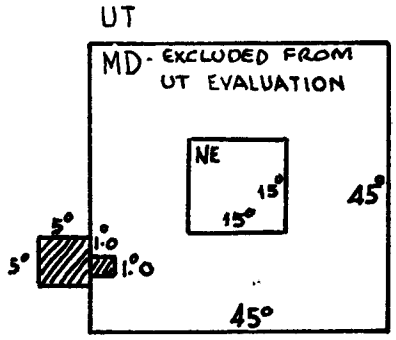

FIG.26(b) OUTER ZONE STRUCTURE.

NOTE: ▨ INDICATES SQUARE MEAN ANOMALY USED IN EVALUATION.

FIG.26 SUBDIVISIONAL APPROACH USED IN 1970 GEOID SOLUTION OF AUSTRALIA.

The computation was performed in discrete stages, as illustrated in figure 26. The four 0.1^{o} squares containing the computation point (P) forms the basic starting point for the pattern of squares which develops. The 3.0^{o} square centred on the 1^{o} square containing P using 0.1^{o} means taken from surface gravimetry is the next unit of computation.

Then the 15^{o} square centred on the 5^{o} square containing P is computed using 0.5^{o} square means, and omitting the area already computed in IN. This is the Near (NE) zone computation. The Mid (MD) zone is the $45^{o} \times 45^{o}$ zone centred on (and omitting in computation) NE, and is computed using 1^{o} means. Beyond this (UT) 5^{o} means are used.

Because of the relatively long wave length nature of the contribution to ξ , η of the NE to UT zones, and since there had been no significant change to this data, it was decided to accept the 1970 computations for contributions to ξ , η from these zones for each of the 12 test stations. The results of this computation are presented in section 6.2.3. The present investigation concentrated on the crucial inner zone of computation and its contribution to the deflections (ie. $0 < \psi < 1.5^{o}$).

4.3 Techniques adopted for Solutions

4.3.1 Computation of the Deflection

Because of the bulk and intricacy of the computational work involved in the investigation, not only in the computation of ξ and η but also the evaluation of G' and the other terrain correction terms resulting from the solution by Green's Third Identity, it was necessary to set up a computing system on the CYBER 70 (model 72) at the University of New South Wales. This system had to provide the maximum in accuracy, flexibility and detailed analysis. The shortcomings of the 'traditional' approach explained in section 4.2.1 can be summarised as (i) the need to preprocess the data, forcing some smoothing into the data which may interfere with its faithful reflection of the real situation; (ii) the asymmetry of the grid representing the terrain/gravity model with respect to the position of the computation point.

On the other hand, the Rice Ring approach contains some attractive features, such as

(i) the relative strength of the kernel of the Vening Meinesz integrals when expressed in the polar form;

(ii) the fact that the asymmetry now rests in the transition between the outer-most ring and the inner boundary of the NE computation: at this distance ($\psi \simeq 1.5^{o}$), the asymmetry is no longer critical;

(iii) an increase in the flexibility of the approach, particularly if the rings are computer generated. It is much simpler to refine or coarsen subdivisions (compartment sizes) as density of data demands;

(iv) there is no preprocessing of data, ie. analysis is carried out on the data in its raw state. This is important as it allows for a detailed analysis to be undertaken on discrete parts of the solution directly from the actual data.

There is some precedent for using a Rice Rings approach in a computer solution for deflection

computations: DIMITRIJEVICH (1972, p 4) states "The contribution of the gravity anomalies in the innermost zone . . . is computed using the circle ring method of Rice, using the ACIC computer program CIRC.", although no further details are given. Referring back to equations (4.7) and (4.8) one can see how simple it is to generate rings with 10^{o} apex angles giving a 0".001 radial deflection for a 1 mGal anomaly. To a first approximation

$$\psi_j' = \ln^{-1} (\ln \psi_i + \frac{0.001}{c_1}) \qquad \text{from} \qquad (4.8)$$

where $j = i + 1$

A simple substitution for the 0".001 of a more suitable radial contribution per compartment (say 0".005) generates a new set of rings for use (for example) in a less disturbed area.

The subroutine developed for use in this investigation (see flow chart for RICERNG, appendix A) simply computes the coordinates of the mid compartment points and nominates the starting and finishing radius of the set of rings called. Experiment showed it was usually sufficient to start at 100 m, and generates compartments giving a 0".002 deflection out to a distance of 130 km (see table 3 for details). Experience also taught that it was possible to combine adjacent compartments (and effectively change the apex angle by a whole number of 10^{o} units), particularly in the rings nearest the computation. This greatly speeded up computation without significant loss of accuracy.

Using the new data from GRAVBNK it is possible to compute the mean anomaly for each compartment or combination thereof. The deflection resulting from this can then be split into its two components and added into accumulators for ξ and η.

The main problem posed in this approach is how to extend the gravity field from the discrete gravity stations in order to get the best estimate of Δg for each compartment. This problem will be looked at in Chapter 5.

4.3.2 Computation of G'

In theory it is necessary to find the correction term G' at every point on the earth's surface (or at least at every point within the range of the computation point which will significantly affect the solution). In this respect it is analogous to the Δg itself, and thus techniques for prediction and extension of the Δg field can also be applied to the G' field. For this reason it was considered best to compute G' at every point at which gravity had been measured (rather than on some arbitrary grid) and, because of the fairly long wave length of the field, it was considered feasible to apply the same extension techniques to the G' field as were applied to the Δg field (see chapter 5).

The fact that the data was maintained in its unprocessed state meant that, for the computation of G' at any one point, it was again possible to use some system of rings. It is possible, of course, to find the contribution to the G' for each compartment of the Rice Rings pattern which could be generated around the G' computation point. However these rings have no real relationship to the parameter being evaluated, and it was decided to develop a new set of rings (called for convenience KSRINGS) which would properly reflect the sensitivity of the computation.

The aim, therefore, was to derive a function giving equal contributions of G' per compartment to G' at point P, for a stated difference in height and gravity anomaly.

Ring No.	RADIUS (m)			ψ_M (Radians)
	Inner	Outer	Mean	
2	100.0	140.8	120.4	0.000 022
3	140.8	198.3	169.6	0.000 031
4	198.3	279.3	238.3	0.000 044
5	279.3	393.4	336.3	0.000 062
6	393.4	554.0	473.7	0.000 087
7	554.0	780.1	667.0	0.000 123
8	780.1	1 098.6	939.4	0.000 173
9	1 098.6	1 547.0	1 322.8	0.000 243
10	1 547.0	2 178.4	1 862.7	0.000 342
11	2 178.4	3 067.3	2 622.8	0.000 482
12	3 067.3	4 318.5	3 692.9	0.000 678
13	4 318.5	6 079.3	5 198.9	0.000 955
14	6 079.3	8 556.7	7 318.0	0.001 344
15	8 556.7	12 040.7	10 298.7	0.001 891
16	12 040.7	16 937.6	14 489.2	0.002 660
17	16 937.6	23 814.9	20 376.3	0.003 740
18	23 814.9	33 462.1	28 638.5	0.005 255
19	33 462.1	46 973.0	40 217.5	0.007 377
20	46 973.0	65 851.9	56 412.5	0.010 342
21	65 851.9	92 146.2	78 999.1	0.014 471
22	92 146.2	128 600.9	110 373.6	0.020 196

TABLE 3: RICE RINGS FOR 0".002 RADIAL DEFLECTION

for 1 mGal per compartment with 10" apex angle

HAMMER ZONES

Ring No.	G' Contribution	Inner Radius	Outer Radius	No. of Compartments	Hammer Zone	Zone Details		No. of Compartments
						Radius Inner	Range Outer	
2	7.5×10^{-5}	100	137	6	D	53	170	6
3	"	137	217	6	E	170	390	8
4	"	217	526	6	F	390	890	8
5	1.5×10^{-5}	526	734	9	G	890	1 530	12
6	"	734	1 218	9	H	1 530	2 615	12
7	"	1 218	3 556	9	I	2 615	4 469	12
8	4×10^{-6}	3 556	7 287	9	J	4 469	6 653	16
9	1×10^{-6}	7 287	9 878	12	K	6 653	9 900	16
10	"	9 878	15 330	12	L	9 900	14 740	16
11	"	15 330	34 210	12	M	14 740	21 944	16

All distances are in metres.

TABLE 4 KSRINGS

Difference in height of 100 m and Difference in gravity anomaly of 1 mGal gives contribution to G^1 at subject point as listed.

Consider the expression

$$C = \frac{R^2}{2\pi} \int_{\alpha_1}^{\alpha_2} \int_{\psi_1}^{\psi_2} \frac{d\sigma}{r_o^3} \qquad (4.10)$$

where $r_o = 2R \sin\frac{1}{2}\psi$

$d\sigma = \sin\psi \, d\psi \, d\alpha$

So (4.10) becomes

$$C = \frac{R^2}{2\pi} \int_{\alpha_1}^{\alpha_2} \int_{\psi_1}^{\psi_2} \frac{\sin\psi \; d\psi \; d\alpha}{8 R^3 \sin^3\frac{1}{2}\psi}$$

$$= \frac{1}{16\pi R} \int_{\alpha_1}^{\alpha_2} \int_{\psi_1}^{\psi_2} \frac{2 \sin\frac{1}{2}\psi \cos\frac{1}{2}\psi}{\sin^3\frac{1}{2}\psi} \; d\psi \; d\alpha$$

$$= \frac{\alpha_2 - \alpha_1}{16\pi R} \int_{\psi_1}^{\psi_2} \frac{\cos\frac{1}{2}\psi}{\sin^2\frac{1}{2}\psi} \; d\psi$$

$$\therefore \quad C = \frac{\alpha_2 - \alpha_1}{8\pi R} \left(\frac{1}{\sin\frac{1}{2}\psi_1} - \frac{1}{\sin\frac{1}{2}\psi_2} \right)$$

But $r_o = 2R \sin\frac{1}{2}\psi$

$$\therefore \quad C = \frac{\alpha_2 - \alpha_1}{4\pi} \left(\frac{1}{r_{01}} - \frac{1}{r_{02}} \right) .$$

To generate compartments with 10^o apex angles which give equal contributions to G' at the computation point of (say) .001 mGal for a height difference of (say) 100 m and gravity anomaly difference of 1 mGal, we know from equation 3.3 that

$$C = G'_j - G'_i = \frac{R^2}{2\pi} \iint \frac{(h-h_p)\,(\Delta g - \Delta g_p)}{r_o^3} \, d\sigma \qquad (j = i + 1)$$

$$= \frac{\alpha_2 - \alpha_1}{4\pi} \left(\frac{1}{r_{oi}} - \frac{1}{r_{oj}} \right) \delta h \; \delta\Delta g$$

or $$0.001 = \frac{10\pi}{180} \; \frac{1}{4\pi} \left(\frac{1}{r_{oi}} - \frac{1}{r_{oj}} \right) \quad (100x1)$$

If we take r_{01} as minimum radius, then

$$0.001 = \frac{100}{18x4} \left(\frac{1}{r_{01}} - \frac{1}{r_{02}} \right)$$

and $$r_{02} = 1 \,/\, \left[\frac{1}{r_{01}} - \frac{0.001}{2.7778x10^{-2}} \right]$$

or

$$r_{02} = 1 \,/\, \left[\frac{1}{r_{01}} - 0.036 \right] \qquad (4.11).$$

It becomes obvious that r_{01} cannot exceed 27.8 m (the inverse of 0.036) which indicates the figure chosen as the contribution per compartment is unrealistic. Moreover it shows that from time to time the right-hand side of (4.11) becomes negative and it is necessary to choose a fresh value of C to overcome this problem.

After some practical experimentation, and by comparing resultant sets of ring radii with the Hammer Zones (see DOBRIN 1960, pp 231-234) it was decided to choose the following set of C values: $7.5x10^{-5}$, $1.5x10^{-5}$, $4x10^{-6}$, $1x10^{-6}$, $2x10^{-7}$. This generates the set of rings shown in table 4 .

It is interesting to note that beyond about 35 km the value of C must be very small in order to generate a ring of any meaningful size. As a result $\delta\Delta g$ and δh must attain large values to contribute significantly to G'. This emphasises the point that beyond about 40 km the contribution to G' is extremely small. This point is supported in practice by a number of investigations, including HAGIWARA (1973, pp 305-311; 1974, pp 446-448), who computed G' out to 20 km in the rugged Tanzawa Mountain region of Japan, and BURSA (1965b, p 145) who estimates a limit of 50 to 80 km on this computation. In the actual G' computations in Czechoslovakia, BURSA (1969, p 10) comments that it is sufficient to restrict the computation to within about 43 km of the computation point.

A real advantage in using this ring technique is that it adapts easily to the system developed to compute the deflections.

A flow chart of the subroutine to compute G' is shown in appendix B, and the way in which it is used to compute G' at every gravity station within $1^{\circ}.5$ of any of the subject A/G test stations using discrete data is shown by way of flow chart in appendix C . The results of the computations evaluating the effect of the G' term on the deflection are shown in section 6.4.1.

4.3.3 Computation of Ground Slopes

The correction terms (2.72, 2.73) resulting from an evaluation of Green's Third Identity contains parameters for the ground slopes β_1 and β_2 . This term does not lend itself to the kind of development carried out above, and so it was decided to estimate the slope for a compartment or set of compartments of Rice Rings by computing the maximum slope and its azimuth from the three points from GRAVBNK and HTBIN which form the closest circumscribing triangle. This suits the method used to interpolate gravity anomalies and heights of midcompartment points, and a small subroutine GRSLP was developed (see appendix D). The expression used to compute these basic parameters is derived below.

Let the vertices of the corners of the circumscribing triangle of Q be 1, 2 & 3 (where 1 happens to be the point closest to Q, 2 the 2nd closest point). The slopes of the sides 1-2 and 1-3 (β_{1-2} , β_{1-3}) can be easily found, as can the azimuths α_{1-2} , α_{1-3} (see figure 27).

Projecting 1 - 2 and 1 - 3 onto a sphere, centre at 1, zenith Z we can construct great circles Z 1 1', Z 2 2' where 1' and 2' is the intersection of Z1 and Z2 with the horizontal plane through 1.

Now, following the development given in (MAUGHAN 1975, pp 88-89), we see the problem is to calculate the shortest distance from the pole (Z) to the great circle passing through 2 and 3. This will be the distance ZX, where X is the intersection of the great circle 2-3 and the polar great circle perpendicular to that great circle.

Hence, by applying Napier's Analogies to spherical triangle 3ZX

$$\cos (3ZX) = \tan ZX \tan \beta_{13}$$

Also, in spherical triangle 2ZX

$$\cos (2ZX) = \tan ZX \tan \beta_{12}$$

Dividing the second equation by the first gives

$$\frac{\cos\ (2ZX)}{\cos\ (3ZX)} = \frac{\tan\ \beta_{12}}{\tan\ \beta_{13}}$$

But $2ZX = \alpha_{12} - \alpha_{13} + 3ZX = \Delta\alpha + 3ZX$

Substituting and expanding

$$\frac{\cos\ \Delta\alpha\ \cos(3ZX) - \sin\ \Delta\alpha\ \sin(3ZX)}{\cos(3ZX)} = \frac{\tan\ \beta_{12}}{\tan\ \beta_{13}}$$

or
$$\tan(3ZX) = \frac{\cos\ \Delta\alpha - \tan\beta_{12}/\tan\beta_{13}}{\sin\ \Delta\alpha} \qquad (4.12)$$

$3ZX$ can now be evaluated and we can see that

$$\alpha_{1X} = \alpha_{13} - 3ZX \qquad (4.13)$$

where α_{1X} is the azimuth of the line of greatest slope in the plane 123.

Substitution of the angle $3ZX$ back into the first expression above gives

$$ZX = \tan^{-1}\ [\ \tan\ \beta_{13}/\cos(3ZX)] \qquad (4.14)$$

where the greatest slope β is given by

$$\beta = 90 - ZX \qquad (4.15)$$

Given the azimuth and slope for the line of maximum slope we can find, from (2.33a) and (2.33b), the values of the ground slope in the meridian and prime vertical directions β_1 and β_2 .

All other parameters in the correction term under consideration are not functions of the surface topography and must be found by some interpolation process. The computing system developed for the evaluation of this expression, along with the results of the computations, can be found in section 6.4.2.

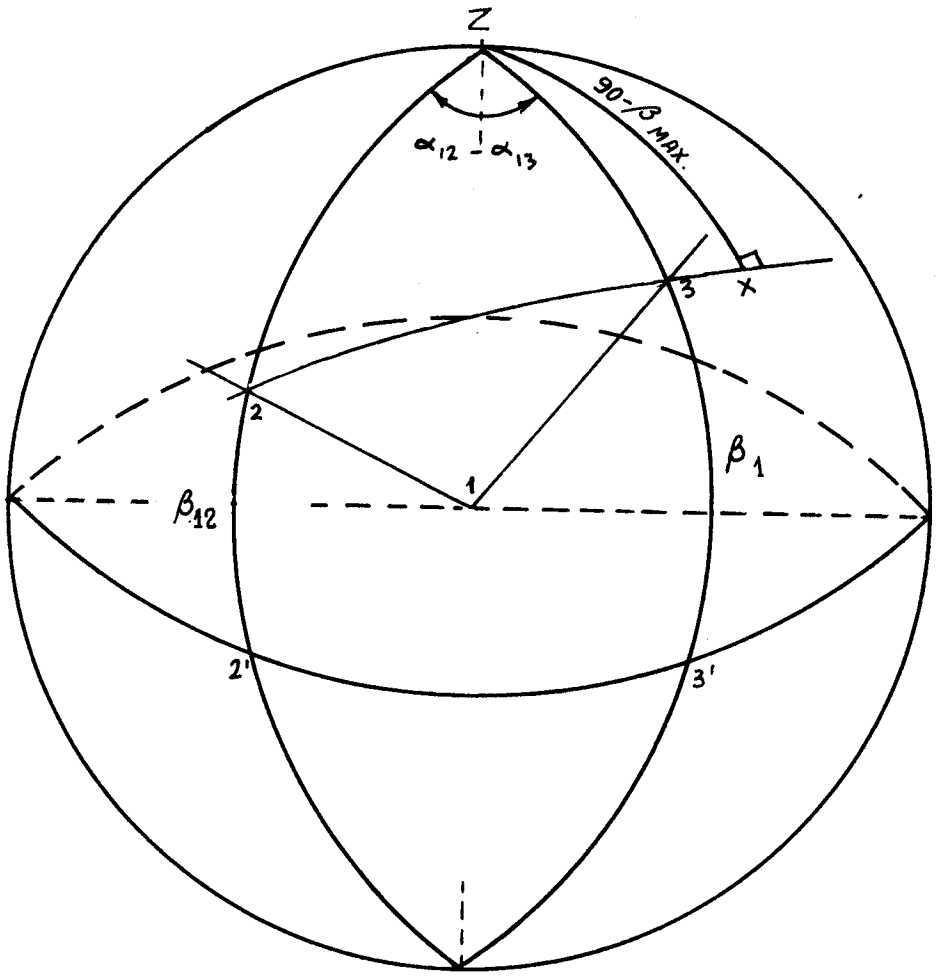

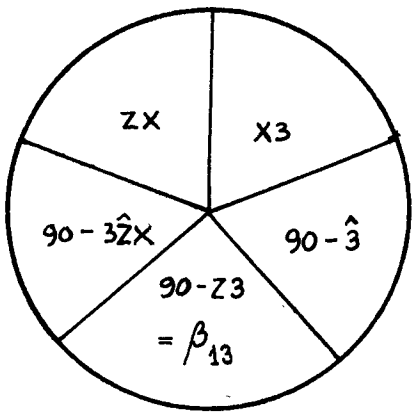

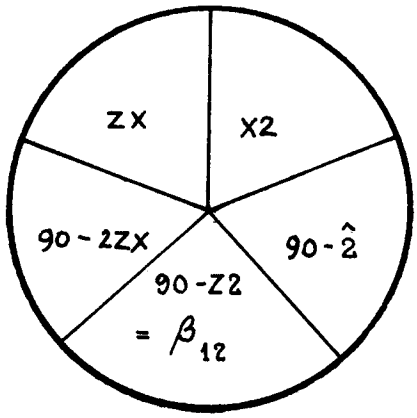

FIG.27 COMPUTATION OF MAXIMUM GROUND SLOPE

5. PREDICTION AND EXTENSION OF THE GRAVITY FIELD

5.1 Introduction

One of the chief tasks which must be undertaken before attempting a solution of the geodetic boundary value problem, although it in itself is an issue quite independent of this problem, is the extension of the gravity field beyond the discrete points of observation. The Stokes or Vening Meinesz formulae assume a surface summation over a continuous field, and thus an important step in the course of their solution is the presentation of the field in a continuous form. (This is what is effectively done to gravity data when it is processed and sorted into the grid patterns described in section 4.2).

The aim of this chapter is to review the techniques which have been used to extend the gravity field from its discrete form to a continuous one, particularly with a view to its suitability to a ring type solution on computers. Since some form of the ring system is used for the evaluation of the G' and ξ' , η' terms, as well as for ξ , η , the method of gravity extension will obviously have direct influence on all facets of the computation.

This problem is barely recognised as such in a manual computation of (say) deflections by the Rice Rings. There the ring pattern is overlayed on the anomaly or topographic map, and mean values of gravity or height abstracted by eye.

One might not appreciate the number of complex decisions being made in this process, and indeed, it is difficult to see the complexity of the problem until the steps are written up in a logical sequence for programming purposes. Admittedly, on maps provided with isogal lines or contours the data has already been converted from a discrete to a continuous field. Nevertheless, even when working from discrete data, the mind can intuitively carry out a number of logical steps in an interpolative process which, when programmed, show themselves as answers to problems which are both intricate and complex.

Because of the volume of data analysis to be carried out for these computations it was decided that manual computation would be prohibitive except for checking purposes. A method which supplied the most accurate means of field extension by computer was therefore sought.

It should be mentioned that in all prediction it was felt essential to use the two elements of the free-air anomaly, the Bouguer anomaly and the height in two separate phases of the prediction process. This technique has long been accepted practice (eg. RAPP 1964, p 143) as it separates the relatively long wave length Bouguer anomaly field from the higher frequency of the topography. The height information can be intensified separately in critical regions by abstracting heights from medium scale topographic maps.

The question of how best to find the mean anomaly of a compartment is another point which must be considered at this stage. Various schemes can be devised, such as taking the mean of the four corners of the compartment or using some other selection of points through the compartment as a representative sample of the field therein. Again this task is fairly readily resolved by eye using template overlays on charts as trends and dominant features can be easily detected and assimilated. In an automated process this would require detailed sampling, which for the present task is prohibitive. It was decided after testing that prediction of the mid-compartment point was adequate for the purpose. In cases where this gave unrealistically high contributions to the element currently being evaluated the compartment was broken into more discrete units, and the contribution for each unit accumulated into the total. This again shows the advantage of computing

with the versatile ring system using the raw data.

Tests of this approach under the more extreme conditions encountered gave quite reasonable results when compared with hand computations by ring overlays on maps. The results of these comparisons will be referred to when consideration is given to error propagation in chapter 7. For the purpose of this chapter it will be assumed that the mid-compartment value represents the compartment itself, and so the problem is how best to predict anomalies and heights at discrete points.

5.2 Surface Fitting

5.2.1 Second Order Three Dimensional Functions

This technique was suggested by KIRKPATRICK (1975) and appeared attractive because the surface undulates and in that respect has a similar form to Bouguer anomaly surface and to the terrain.

Say a function f_i is known at n points, $(\equiv \Delta g_i , h_i)$ whose positions are defined on a plane by the cartesian coordinates $x_i , y_i , i = 1 \ldots n$.

Let $$\delta g_i = f_i - f_1 ,$$

$$X_i = x_i - x_1$$

and assume that the general relationship

$$\delta f_i = aX_i + bY_i + cX_i^2 + dX_i Y_i + e Y_i^2 \qquad (i = 2, n) \qquad (5.1)$$

represents the surface.

The coefficients a to e can be solved uniquely if 6 points are known (producing 5 simultaneous equations). The position of the prediction point (Q) is then applied to (5.1), and f for this point deduced.

For the best results, the point 1 should be the closest point to Q, and the 6 known points chosen so that they surround Q (ie. to obviate extrapolation).

The above approach was extended slightly to seven known points and the solutions for the coefficients done by least squares using matrix algebra.

The observation equations can be expressed as

$$\begin{vmatrix} F_1 \\ F_2 \\ \cdot \\ \cdot \\ F_n \end{vmatrix} = \begin{vmatrix} a & b & c & d & e \end{vmatrix} \begin{vmatrix} X_1 & Y_1 & X_1^2 & X_1Y_1 & Y_1^2 \\ X_2 & Y_2 & .. & . & Y_2^2 \\ \cdot & & & & \\ \cdot & & & & \\ X_n & Y_n & \ldots & & Y_n^2 \end{vmatrix}$$

or more briefly as

$$F = A X$$

The solution is given by

$$A = (X^T X)^{-1} X^T F \qquad (5.2)$$

A program POLYFIT (see appendix E) was developed which was capable of searching through data for seven points and having solved (5.2) resubstituted the matrix A back into (5.1) to find the gravity anomaly and height for Q. The seven points had a particular configuration whereby the three closest points to Q were found irrespective of their location with respect to Q and then four more points, one in each quadrant defined by the axis system at Q, were chosen. The closest station was denoted point 1 in expression (5.1).

POLYFIT was tested using generated data and found to work well. However, when applied to real data it was found that the amplitudes of the surface resulting from the 2nd order terms produced highly irregular results. Fairly severe weighting systems were introduced (the inverse of the squared distance between Q and the i^{th} point) but this had little impact on the result. The number of points involved in the surface fit was progressively increased to about 14 points, at which stage the effect of the higher order terms was dampened.

However, the real advantage in an approach like this is its relative simplicity in searching through the data for the points needed for the analysis. The first three points are chosen only on distance, the next four according to quadrant and distance; but at no stage does the actual geometric configuration described by the chosen points have to be tested or limited in any form.

5.2.2 Least Squares Plane Fitting

Almost in reaction to the over-amplification of the undulations of the real surface which was produced by the above technique it was decided to try fitting a plane to the 7 points chosen for that technique. This meant a very simple modification to 5.1, viz. the deletion of all terms in X and Y of second order. This results in the expression

$$\delta f_i = a X_i + b Y_i \qquad (i = 1, 7)$$

where a, b are solve by way of (5.2).

This technique, whilst giving favourable results in the flatter regions of sparse data, was insensitive in regions of high anomaly or topographic disturbance. Weighting according to the inverse of the distance, and even the square of the distance, from Q had little effect. The net result was that in the vicinity of the computation point, where the location of the mid-compartment point changed very little with respect to the 7 points chosen for the purpose of prediction, there was practically no change in the predicted value when one moved from compartment to compartment.

Obviously, if prediction in rugged areas was to be made using some surface fitting technique, one had to find the happy medium between the least squares plane fit just described and the oversensitive least squares polynomial fit outlined in section 5.2.1.

5.2.3 Simple Plane Fitting

Prediction of gravity in a field described by discrete points has much in common with the inter-

polation of contours from spot heights. The data in both cases is a field of discrete points fixed in three dimensions. In the former case, the problem is to find the function $z = z(x,y)$ in the region $x_1 \leq x \leq x_2$, $y_1 \leq y \leq y_2$, whereas in the contouring situation it is the determination of the x & y coordinates of a point (or series of points) whose z has been nominated. Many mapping organisations have automated the process of drawing contours in an area defined by discrete points, and valuable insights can be gained from consideration of some of the techniques they adopt.

The simplest geometrical figure which can be used for an interpolative process is a plane. The method used in a topographic package of computer programs and the NSW Department of Lands is to form a network of adjoining and plane triangles through the area using the planimetric coordinates of all points in the field, such that no one triangle overlaps another. The contour lines are then found by linear interpolation of the heights along the sides of successive triangles.

This is a system which uses smoothing only in the interpolating process, ie. the figures themselves are fitted uniquely to the raw data. This concept had attractive features, for if the 'spot heights' or gravity anomalies are properly chosen then a series of planar interpolations are completely adequate for the representation of the field.

Consideration must be given to the fields on which interpolation is to be performed. Firstly consider the gravity anomaly field, which is fairly smooth even in areas of rugged terrain. One of the factors influencing the location of gravity stations was the definition of likely changes in grade (such as around the base of a mountain). Secondly, consider how the height field is described. This was defined partly by the gravity stations, but augmented by spot heights read from maps. These were not necessarily on a strict grid pattern but, with the rules of linear interpolation in mind, radical changes in the grade of the topography were also recorded. It was felt that the simple plane fit to this data should be tested as a means of extending the gravity field.

For a number of reasons it was decided not to set up a bank of triangles as is done for contouring. It must be appreciated that in the contouring problem the interpolation is only a first step - the next step is to describe the contour line itself and for this purpose the triangles are again useful. By contrast, in prediction, once the triangle has been formed the information required from it can be computed and stored in an accumulator. There is also the problem of having to reform the triangles in any area which may have additional data included at any stage of the computation. For these and other 'logistical' reasons it was decided to form the triangles as required at any particular stage of a computation.

The next question is which triangle is the most suitable for the purposes of prediction. The answer is obvious. The most accurate interpolation will occur if it is performed between the points which are closest to the subject point. For this reason it was necessary to find the smallest triangle which circumscribed the point in question.

The subroutine which performed this operation (SORT3) is described by means of flow chart in appendix F , but the approach adopted will be briefly outlined here (where the point to be predicted is denoted as Q). The first step searches through the data file to find the point closest to Q (1), and then the second closest point (2), such that the angle $Q12 \neq 100^{\circ}$ (this is to try and ensure that the resultant triangle is fairly well conditioned). The search is then performed on the data file to find the next closest point which, with the first two points, circumscribes Q. The algorithm to find this was suggested by TEOH (1975), and simply tests the sines of the angles 1Q2, 2Q3, and 3Q1 to ensure that they are all of the same sign.

The expression used in the interpolation can be found in(HEISKANEN AND MORITZ 1967, p 265) and is as follows

$$Z = \frac{(x_2 - x)(y_3 - y_2) - (y_2 - y)(x_3 - x_2)}{(x_2 - x_1)(y_3 - y_2) - (y_2 - y_1)(x_3 - x_2)} Z_1$$

$$+ \frac{(x_3 - x)(y_1 - y_3) - (y_3 - y)(x_1 - x_3)}{(x_3 - x_2)(y_1 - y_3) - (y_3 - y_2)(x_1 - x_3)} Z_2$$

$$+ \frac{(x_1 - x)(y_2 - y_1) - (y_1 - y)(x_2 - x_1)}{(x_1 - x_3)(y_2 - y_1) - (y_1 - y_3)(x_2 - x_1)} Z_3 \qquad (5.3)$$

where x, y, z are the coordinates of the prediction point and $x_i\ y_i\ z_i$ are the coordinates of the i^{th} point, $i = 1 \rightarrow 3$.

The prediction of the free-air anomaly is done in a number of steps. First the Bouguer anomaly is predicted by SORT3 using the GRAVBNK as the data file. The prediction of the height has two phases, remembering that HTBIN only augments GRAVBNK in the description of the terrain and is not meant to represent it in its own right. The smallest circumscribing triangle in HTBIN is found by SORT3, and these 3 points combined with the 3 points from GRAVBNK to form a small file of 6 close points. The SORT3 search is then performed on these 6 points to find the best possible triangle of height points from the two data files. The predicted height is then combined with the predicted Bouguer anomaly to find the free-air anomaly for the point.

This system showed itself to be sensitive to the changes in terrain, particularly in the immediate vicinity of the computation point. Comparative results between computer and hand computations are given in section 7.2.2. It was also very simple to compute ground slopes by the method described in section 4.3.3.

5.2.4 Surface of Minimum Curvature

The problem encountered when using the second order surface (section 5.2.1) prompted the thought that a system of surfaces should have some kind of constraint placed on the curvature in order to restrain the enormous departures of the generated surfaces from reality. The use of adjoining planes will obviously underrate the curvature of the terrain. The question is how to find a satisfactory compromise.

A system for contouring has been developed in the Bureau of Mineral Resources by BRIGGS (1974) in which the system of plane surfaces has been replaced by fitting a third-order spline in two dimensions to the data. The differential equation used in the solution "describes the displacement of a thin sheet under the influence of point forces. The boundary conditions are not only at the ends of the boundary, but within the region of interest. The solution is forced to take up the value of the observation at the point of observation" (*IBID*, p 39). Having determined the parameters of the cubic spline z values are found on a grid pattern to assist the ensuing contouring process. It is, of course, possible to find the z of any nominated point within the region of observation, and thus to apply this scheme to the prediction of free-air anomalies.

This technique contains many attractive features, but a difficulty still remains of amending the surface should it be necessary to add points to the height data file. It was felt that, for the purpose of this investigation, it was essential to maintain flexibility in case of possible up-grading of the surface. It could be used in discrete sections as was the plane fitting method.

For this at least 7 points would be required in the vicinity of the prediction point, and the solution of the parameters, being iterative, would be quite expensive timewise when carried right through the complete range of points to be predicted.

5.2.5 Solids of Revolution

A method of simulating parts of the Earth's surface by the surface of revolution which most closely resembled it was suggested by PICK ET AL (1962). One of a selection of surfaces was used to represent one zone in the Hayford system of rings, and the terrain correction for this zone computed using this surface rather than the usual practice of assuming a horizontal plane at the average height of the terrain.

The surfaces suggested as possibilities were as follows:

(i) a conical surface with its axis horizontal and the apex on the z axis passing through the computation point Q. This is represented by the expression

$$z = h + r \tan \beta$$

where h is the height of the apex above Q measured along the z axis through Q
r is the radius of the sector body being considered
β is the slope of the side of the cone on the edge of the sector.

(ii) a rotational paraboloid, where the upper surface of the sector is limited by part of a rotational paraboloid produced by the rotation of a paraboloid $Z = kr^2 + h$ about the z axis through Q (the notation being defined above).

(iii) an hyperbolic paraboloid, where the upper surface of the sector is limited by the rotation of a parabola

$$r = kz^2 + q$$

about the z axis, and q is the radial distance from Q to the intersection of the surface with the horizon.

(iv) an oblique plane, where the upper side of the sector is limited by an oblique plane represented by

$$i = \arctan (I \cos \alpha_D)$$

where i is the inclination of an arbitrary line lying in the oblique plane

α_D the azimuth of the dip of the plane, and
I the dip of the plane.

This last surface has already been effectively treated in sections 5.2.2 and 5.2.3. The other three surfaces have some similarities with the second order surface in section 5.2.1 and must suffer the same shortcomings, such as the inflexibility of the shape imposed to take any large discrepancies in topography into account. It must be noted that each zone is represented by one of these surfaces and experience of geomorphological shapes makes one sceptical of the

suitability of representing such large areas by such regular and distinctive shapes. Also the axis of the surface generated is always through the computation point, and it is doubtful that the terrain will always be so organised and that this will be a realistic simulation. Obviously this could be overcome by relocating the axis in the most suitable place to best simulate the terrain, but this will then introduce problems in the calculation of the terrain correction. Further, the computer time needed to search through the terrain models to find which best fits the data for each particular zone in the computation would be prohibitive in this study.

An appreciation of the problems which may come from this approach when dealing with irregular and broken terrain reinforces the opinion that the terrain is best simulated by a series of planes which can be varied in number according to the nature of the topography and the sensitivity of the computation to that part of the topography.

5.3 Statistical Methods

5.3.1 Introduction

A method of extending the gravity field which is based on the statistical characteristics of that field has received a great deal of attention in physical geodesy. In this technique, known as covariance analysis, the gravity field is analysed to define what is known as the covariance function for the field. This function is then applied to the known field to predice the gravity in the unknown region of the field. This approach has more recently been extended for use in predicting all parameters of the geoid solution (eg. N, ε), the general solution being known as Collocation. In this study it is the prediction of the gravity anomalies which is of most interest.

The technique has been used mainly to extend the gravity data for large (eg. $5^{o} \times 5^{o}$) square means in the largely unmapped ocean areas of the Earth and for the study of the effect of errors in distant gravity fields on the geoid solutions at particular points. This emphasis is obvious when one considers the earlier literature on this subject, reviews of which can be found in (RAPP 1964, pp 2-5), and the paper by Rapp in (ORLIN 1966, pp 49-52).

For example KAULA (1957), in an investigation to find the expected errors in gravimetrically determined geoid heights and deflections, used estimates for the accuracies of the mean gravity of 1^{o}, 5^{o} and 10^{o} squares which were based on covariance functions derived for central United States and Central Europe. Two years later, KAULA (1959) used a more extensive analysis of the Earth's gravity field, and predicted the mean free-air anomalies for $10^{o} \times 10^{o}$ squares throughout the world from available $1^{o} \times 1^{o}$ mean anomalies.

The most extensive report on prediction by covariance methods is that produced by RAPP in 1964 (q.v.). This study, based on the theory of least squares prediction developed by MORITZ (eg. see HEISKANEN AND MORITZ 1967, chapter 7) uses covariance techniques to predict point anomalies, as well as 5' and 30' mean square anomalies in two well-defined areas of the USA. This was a much finer subdivision of the gravity field than any of the earlier studies mentioned above and provided empirical comparisons of results which enabled some external estimates of accuracies as well as giving an appreciation of the most suitable techniques for the method. It was found, for example, that the best prediction of point anomalies was made by using the ten closest known points to the prediction point, and an increase in the number of points used in the prediction gave no significant increase in accuracy (*IBID*, p 141). The mean square error for the prediction of point Bouguer anomalies in this way, in a field which had a range of 41 mGal,

was quoted as ±3 mGal (*IBID*, p 105). The investigation also concluded that the prediction of height (for the free-air reduction) in this way was unsatisfactory (*IBID*, p 104).

As mentioned earlier, covariance functions have been used mainly to predict 1^{o} (or larger) square mean anomalies for global geoid solutions. However EMRICK (1974, p 43) used a degree 10 polynomial representing the covariance function in the area being investigated to generate gravity date on a 5' and 37'.5 grid in his recent study on deflection computations. The method is well suited to predicting data on a grid pattern and as this was the form in which many investigators organise their data it fits easily into a computing system being designed for geoid solutions. However, there are some shortcomings in the accuracy of prediction which, in the critical inner zone of the gravity field could introduce uncertainties into deflection computations which may not be tolerable.

5.3.2 Analysis of the Theory

A complete development of the theory is given in HEISKANEN AND MORITZ (1967, pp 249-286) and will be outlined here so that an analysis of the basic assumptions can be undertaken. Particular emphasis will be placed on the suitability of the method for the prediction of the local field in the vicinity of the computation point.

Motitz describes the underlying philosophy as follows (*IBID*, p 253):

"The covariance characterizes the *statistical correlation* of the gravity anomalies Δg and Δg_x, which is their tendency to have about the same size and sign. If the covariance is zero, then the anomalies Δg and Δg_x are uncorrelated, in other words, the size and sign of Δg has no influence on the size and sign of Δg_x.

If we consider the covariance as a function of r = PQ, then we get the *covariance function* C(r), whereby

$$C(r) = M\{\Delta g \ \Delta g_x\} \tag{5.4}$$

For r = 0, we have

$$C(0) = M\{\Delta g^2\} = \text{var}\{\Delta g\} \tag{5.5}$$

Here the $M\{\Delta g\} = 0$, which, if not the case in the first instance can be enforced by centering the gravity anomalies.

One can immediately see a similarity between this approach and the theory of errors, where the Δg above is analogous to the residuals or random errors in observations. Two very important properties of the anomalous gravity field are inferred from the above expressions:-

(i) The field is isotropic (ie. the covariance function is a function of distance only and not also of direction) as inferred from (5.4).

(ii) The field is homogeneous (ie. the covariance function is independent of the location of the field being analysed).

The accuracy of the covariance function, and hence of its ability to predict accurately, will depend

on how well the anomalous gravity field is described by these two statements. Unfortunately, the basis for the whole of the development rests on a qualitative statement (that the closer a point is to a given point the more likely is its Δg to be similar to the Δg of that given point) and it is a great 'leap' to then infer the two properties of the field which then form the starting point of the mathematical development. In particular, the condition of isotropy does not really reflect the nature of many local gravity fields, where ridges of high and low values are extensive and correlation between Δg values is quite definitely a function of direction as well as separation. The condition thus imposed will surely weaken the accuracy of the predicted points and in fact may introduce a systematic error into extensive parts of the local field which will in turn adversely affect the accuracy of the deflection computation.

The importance of the basic assumptions becomes clearer when the method of prediction is shown in detail.

Denoting the predicted value of the gravity anomaly at Q by $\Delta g'_q$ the gravity anomaly at the known points i (i = 1, n) as Δg_i and the coefficient related to the correlation between $\Delta g'_q$ and Δg_i as α_{qi} then

$$\Delta g'_q = \sum_i \alpha_i \Delta g_i \qquad (i = 1, n) \tag{5.6}$$

To find the most probable value for α_{qi} the standard least squares approach is adopted, viz.,

$$\varepsilon_q = \Delta g_q - \Delta g'_q = \Delta g_q - \Sigma \alpha_i \Delta g$$

where ε here refers to the error in the prediction of q.

Squaring $\quad \varepsilon^2 = (\Delta g_q - \Sigma \alpha_{qi} \Delta g_i)(\Delta g - \Sigma \alpha_{qj} \Delta g_j)$

$$= \Delta g_q^2 - 2 \sum_i \alpha_{qi} \Delta g_q \Delta g_i + \sum_i \sum_j \alpha_{qi} \alpha_{qj} \Delta g_i \Delta g_j \qquad (i=1,n;\ j=1,n)$$

Averaging this for all points Q over the area being considered,

$$m_q^2 = M\{\varepsilon_q^2\} = M\{\Delta g_q^2\} - 2 \sum_i \alpha_{qi} M\{\Delta g_q \Delta g_i\} + \Sigma \Sigma \alpha_{qi} \alpha_{qj} M\{\Delta g_i \Delta g_j\}$$

Now, $M\{\Delta g_q^2\}$ and $M\{\Delta g_i \Delta g_j\}$ are not known (if they were then there would be no need for the prediction, ie. all Δg_q would already be known) and their values are estimated from an analysis of the known field by means of (5.4) and (5.5).

Hence $\quad M\{\Delta g_q^2\} = C_o \quad , \qquad M\{\Delta g_q \Delta g_i\} = C(r_{qi}) = C_{qi}$

and (5.5) becomes

$$m^2q = C_o - 2 \Sigma \alpha_i C_{qi} + \sum_i \sum_j \alpha_{qi} \alpha_{qj} C_{ij} \tag{5.7}.$$

(C being the covariance matrix) m_q^2 is minimised, giving

$$\alpha_{qi} = \sum_{i=1}^{n} C_{ij}^{-1} C_{qi} \tag{5.8}$$

It can be seen from this development that the conditions of isotropy and homogeneity are assumed *a priori*. If the field is not well represented by these descriptions then these conditions are forced (by way of 5.8) onto the predicted field, the covariance coefficients C_{ij} and C_{qi} taking

up the mean values for the entire field analysed. This again may not be an accurate description of the true position in the area of prediction.

In fact for local prediction it is preferable to avoid the smoothing effect of regional covariances, and perhaps even to avoid as many of the *a priori* assumptions as possible about the field.

Suppose, for example, the four points lay at the corners of a square and it was desired to find the best possible coefficients for this particular field, ie. to find the α's which gave the least sum of squares in the errors of the prediction.

The observation equations will be

$$\varepsilon_1 = \Delta g_1 - (\alpha_{12}\ \Delta g_2 + \alpha_{13}\ \Delta g_3 + \alpha_{14}\ \Delta g_4)$$

$$\varepsilon_2 = \Delta g_2 - (\alpha_{21}\ \Delta g_1 + \alpha_{23}\ \Delta g_3 + \alpha_{24}\ \Delta g_4)$$

$$\varepsilon_3 = \Delta g_3 - (\alpha_{31}\ \Delta g_1 + \alpha_{32}\ \Delta g_3 + \alpha_{34}\ \Delta g_4)$$

$$\varepsilon_4 = \Delta g_4 - (\alpha_{41}\ \Delta g_1 + \alpha_{42}\ \Delta g\ + \alpha_{43}\ \Delta g_3)$$

where the only unknowns will be the coefficients α_{ij}. This array cannot be solved (6 unknowns, 4 equations), so some assumptions will have to be made *vis-a-vis* the local field

eg. (i) Assume the coefficients to be similar for a similar direction

ie. $\alpha_{12} = \alpha_{34} = \alpha'$ $\qquad$ $\alpha_{14} = \alpha_{23} = \alpha''$

$\alpha_{24} = \alpha'''$ $\qquad$ $\alpha_{13} = \alpha'^{V}$

This assumption is likely to be a fair representation in a smooth field, and will give a unique solution for all α. If the grid is extended a least squares value for α' to α'^{V} can be found which will be superior only if the anomalous field still exhibits the same characteristics over the extended grid. Other α's can be found for the longer sides of the enlarged grid and a local 'covariance' function found for the field.

(ii) Extend the assumptions that a relationship is set up between the α', α'' and the α''', α'^{V} coefficients

eg. $$\alpha''' = \alpha'^{V} = (\alpha'^{2} + \alpha''^{2})^{\frac{1}{2}}$$

This makes the number of unknowns 2, and so a least squares solution would have to be performed on the original 4 equations. This assumption may still not be an unfaithful reflection of the true position, particularly if the field exhibits symmetry.

(iii) It is of interest to note the effect of the basic assumptions for the covariance analysis. This assumes $\alpha' = \alpha''$, and that $\alpha''' = \alpha'^{V}$, which values are found by analysis of Δg's outside the immediate area of prediction. In fact the more data included in the analysis the less likely it will be that the analysis reflects the fine details of the local field.

Perhaps the most striking feature of the above development when compared with the standard approach is that the Δg's are treated more as observations than as errors. This difference is also stressed when one compares the approaches to the error analysis of the predicted quantities.

The accepted method of error analysis (HEISKANEN AND MORITZ 1967, pp 269-270) is to substitute the α's found in (5.8) into (5.7), ie.

$$m_q^2 = C_o - 2 \sum_i \sum_j C_{ij}^{-1} C_{qi} C_{qj} + \sum_i \sum_k \sum_j \sum_l C_{ij}^{-1} C_{qi} C_{kl}^{-1} C_{jl}$$

which on multiplication becomes

$$m_q^2 = C_o - \left| C_{q1}\ C_{q2} \ldots C_{qn} \right| \left| \begin{matrix} C_{11} & C_{12} \ldots & C_{1n} \\ C_{21} & C_{22} \ldots & C_{2n} \\ . & & . \\ . & & . \\ C_{n1} & C_{n2} \ldots & C_{nn} \end{matrix} \right|^{-1} \left| \begin{matrix} C_{q1} \\ C_{q2} \\ . \\ . \\ C_{qn} \end{matrix} \right|$$

m_q^2 is the mean square error of the predicted value $\Delta g_q'$.

This in my opinion is far too idealised an analysis to provide any proper assessment of the expected error in Δg_q. It is based on the assumption that the elements of the covariance function C_{ij} are error-free, which must be questioned. In fact, an estimate of these errors can be easily determined by a simple analysis of the data which is processed to develop the covariance function (see section 5.3.3)

Returning to the original statement (5.6) then

$$\Delta g_q' = \sum_i \alpha_i \Delta g_i \qquad (i = 1, n)$$

then

$$Q_{\Delta g_q} = \sum_i \alpha_i Q_{\Delta g_i} + \sum_i \Delta g_i Q_{\alpha i}$$

and

$$\sigma^2_{\Delta g_q} = \sum_i \sum_j \sigma_{\Delta g_i} \sigma_{\Delta g_j} \alpha_i \alpha_j + \sum_i \sum_j \sigma_{\alpha_i} \sigma_{\alpha_j} \Delta g_i \Delta g_j +$$

$$+ 2 \sum_i \sum_j \sigma_{\alpha i} \sigma_{\Delta g_j} \alpha_i \Delta g_j$$

where σ_{α_i} is found by analysis of the field for C_i and $\sigma_{\Delta g_i}$ is found by analysing the observational techniques used in finding Δg.

This should give a more realistic appraisal of the error in the predicted anomaly based on the errors in the given data and on the technique adopted to go from that given data to the predicted value.

It should be emphasised that the technique of prediction from covariance functions is being appraised here as a tool for field extension in very limited regions, especially in the critical region in the immediate vicinity of the computation point. The fear expressed is that the covariance function derived by the analysis of (say) a $1^o \times 1^o$ data set will not reflect the short wave length signal of the field where the typical separations are of the order of 2 to 5 km. This will be detrimental to the accuracy of the ξ and η computed therefrom. See also section 5.5 for further comment.

5.3.3 Statistical Analysis of the Test Region

It was decided to carry out a simple covariance analysis in the test region to gauge the applicability of this theory to a local region. To this end the program COVFN was developed (see appendix G)

As has already been mentioned above (section 5.3.1) the most convenient distribution of data for this analysis is on a grid pattern. This would need some interpolation or prediction as a first step to come from the points of observation onto the grid, and this would obviously defeat the purpose of the exercise. It was decided therefore to use the raw data, and to organise the cross-producted data into 'cells' using distance between the data points as the argument. These arguments are fairly arbitrarily chosen (see tables 5a to 5b), but should nevertheless give some idea of the behaviour of the covariance function in this very limited and specific test area.

It was also decided that the field should be subdivided on the basis of topography. The field in the undulating to mountainous areas was analysed separately from the field in the flatter country of the test region and 'prediction' of the gravity anomaly of selected points done by applying the relevant covariance coefficients to the seven closest points. This is not the optimum of ten suggested by Rapp, but is certainly of that order. Nor, as is commonly practised (eg. HEISKANEN AND MORITZ 1967, p 255) is a function fitted to the covariance elements and the covariance value for a particular separation extracted from this function. Rather the covariance for the separation for each of the 7 selected points is taken directly from the relevant table. In fact, the 'prediction' is not really a serious attempt to use this technique, as the erratic nature of the 'covariance' values and the standard errors of the cells make this an unrealistic proposition for prediction. The main purpose of the analysis is to discover how the gravity fields behave and how their behaviour varies from region to region.

As can be seen by reference to the tables, neither covariance pattern follows the shape of the idealised covariance function (eg. see HIRVONEN 1962) for the smaller separations, although the trend toward this shape is evident as distance between points increases. The standard deviations of the covariances are large, particularly for the smaller distances and this must be due in part to the relatively small samples in these cells. However this fact underlines the danger of applying the mean covariances for the short distances likely to be encountered in the critical region near the deflection point. (In fact the standard error quoted for the predicted Δg_q does not include the errors in the covariance values used in prediction. It is found by simple analysis of the seven different values predicted for this point. Inclusion of the errors in the covariance coefficients will only deteriorate this expected accuracy further).

One can also see a marked difference between the two covariance patterns, underlining the danger in using the covariance function derived for one local region of a particular topographical type for prediction in a different terrain. The analysis in the mountain region suggests that there is no correlation between anomalies at 30 km whilst for the flat area this condition is reached at (apparently) about 50 km. This implies that the high frequency signal from the terrain dominates the signal in the first case while in the second the influence of topography is absent and the broader regional trend dominates the field.

As a tentative conclusion it does appear that for limited data and for short distances the conditions of isotropy and homogeneity are absent and the use of this technique for prediction under these conditions is not considered justifiable.

Terrain: Flat

Limits of Region Analysed -30° To -31° ; 149° to 150°

No. included in analysis is 149; Mean Anomaly -17.67

Co = 111.45

Cell No.	Dist (m) to	Dist (m)	Mean Cvfn	Sigma	Popn
1	0	2000	81.92	23.2	37
2	2000	4000	94.13	12.4	60
3	4000	6000	109.15	13.3	71
4	6000	8000	83.46	23.3	93
5	8000	10000	89.94	7.4	151
6	10000	12000	91.04	7.2	152
7	12000	14000	67.97	5.2	174
8	14000	16000	77.95	6.3	148
9	16000	18000	68.12	7.4	223
10	18000	20000	57.61	.7	187
11	20000	22000	32.25	1.9	194
12	22000	24000	53.50	3.8	204
13	24000	26000	44.30	2.3	234
14	26000	28000	41.18	2.7	273
15	28000	30000	17.99	6.0	270
16	30000	32000	20.24	.5	261
17	32000	34000	25.81	1.6	255
18	34000	36000	30.17	.4	261
19	36000	38000	15.20	.6	288
20	38000	40000	11.18	2.8	255

Predicted Value of Q ($\phi_Q = 30^{\circ}.5$, $\lambda_Q = 149^{\circ}.5$) -48.69 Standard Error ±25.48 mGal

cf. -22.9 from map.

TABLE 5A ANALYSIS OF COVARIANCE FUNCTION

Terrain: Undulating to Mountainous

Limits of Region Analysed $-30^{\circ}.1$ to $-30^{\circ}.9$; $150^{\circ}.1$ to $150^{\circ}.9$

No. included in Analysis is 238; Mean Anomaly -13.23

Co = 83.21

Cell No.	Dist (m) to	Dist (m)	Mean Cvfn	Sigma	Popn
1	0	2000	85.97	21.2	138
2	2000	4000	91.14	5.7	263
3	4000	6000	75.52	3.1	334
4	6000	8000	64.98	2.8	364
5	8000	10000	60.79	3.0	400
6	10000	12000	66.27	1.1	400
7	12000	14000	72.10	3.6	400
8	14000	16000	61.07	1.3	400
9	16000	18000	59.58	.7	400
10	18000	20000	51.41	.4	400
11	20000	22000	45.69	.5	400
12	22000	24000	35.29	3.1	400
13	24000	26000	34.13	.7	400
14	26000	28000	30.14	1.2	400
15	28000	30000	9.60	1.3	400
16	30000	32000	-5.81	.8	400
17	32000	34000	-24.42	4.0	400
18	34000	36000	-36.65	3.0	400
19	36000	38000	-51.05	8.5	400
20	38000	40000	-23.01	3.1	400

Predicted Value of Q ($\phi_Q = -30^{\circ}.5$, $\lambda_Q = 150^{\circ}.5$) -3.47 Standard Error ±0.95 mGal

cf. -4.9 from map

TABLE 5B ANALYSIS OF COVARIANCE FUNCTION

5.3.4 Comments

It must be concluded that the covariance approach to prediction is unsuited in local areas such as the test area wherein the density of discrete observations is relatively high and wavelengths of small amplitudes which are reflected in the data are also expected to be reproduced in the predicted information. The analysis of a large region in order to predict point anomalies introduces a smoothing effect to a far greater extent than is tolerable. In fact from the limited data samples it is questionable whether the assumptions on which the theory is based do in fact hold at the level of local predictions. This thought is echoed by other writers concerned with much larger regions than are involved here. For instance, GAPOSHKIN (1973, pp 197-208) used covariance analysis techniques to obtain $5^{o} \times 5^{o}$ means from $1^{o} \times 1^{o}$ mean gravity anomalies. Separate covariance functions were found for the ocean and continental regions, assuming isotropy. He found (*IBID*, p 208) "the differences between the covariances are significant, and one must conclude that gravity is not stationary (homogeneous). Any estimation procedure that assumes stationarity (homogeneity) must be carefully examined."

Similarly, in a statistical analysis of the anomalous gravity field of Czechoslovakia, VYSKOCIL (1970) analysed the covariance function for Δg means of 10' x 15' blocks, and concluded "the theoretical assumption of the homogeneity and isotropy of fields Δg_p and h_p is basically only forced and in reality it will probably not always be satisfied."

The amendments to the approach, suggested in section 5.3.2, which concentrates on analysis in the locality of the point of prediction, becomes more complicated if the points are not regularly spaced. The fact that the test data is not spaced in this fashion and that this solution will apparently tend towards a simple plane fit in any case, obviated the need to experiment any further with this approach. This observation, ie. the tendency of the solution to a plane, is supported by a theoretical analysis done by MORITZ (1975b, p 3-11), who shows that if a continuous covariance function is used to predict a point from three circumscribing points close by, then this prediction is equivalent to the unique plane fit described in section 5.2.3. This is because, for small distances, the covariance function can be approximated linearly, and the 'prediction' function becomes a simple linear ratio.

The approximation will deteriorate if more than the minimum number of points is involved and an adjustment is then required to achieve the 'most probable' value. Conditions of isotropy must then be invoked with the consequent deterioration in the faithfulness of the model to reality. Also the prediction once more becomes dependent on the particular covariance function adopted for the field. Obviously it is preferable that the area in which the prediction is to take place should also provide the data for the covariance analysis. For example the covariance function resulting from analysis of the combination of the fields used in the above tests would differ from each of the individual functions. If this combined function were used it would deteriorate the resultant prediction in both of the component fields. It is necessary to ensure that only that data which is representative of the area of prediction is included in the analysis. See also section 5.3.3 for further comments on this matter.

5.4 Series Fitting

The gravity field has been described using terms such as 'wave length' and 'amplitude' and it is therefore not unnatural to employ trigonometric series to define it mathematically and to help in the extension process.

In an extension of the gravity field in South Australia (expressed in terms of ½, 1 and 2 degree square means), MATHER used a two-dimensional trigonometrical series (see MATHER 1967, p 9 and MATHER 1968a, pp 183-197). This was expressed in the following way

$$\Delta g' = \sum_{i=0}^{a} A_i \cos \{ \pi(\phi - \phi_o)\, i \} + \sum_{i=a+1}^{2a} A_i \sin \{ \pi(\phi - \phi_o)(i - a) \}$$

$$+ \sum_{i=2a+1}^{3a} A_i \cos \{ \pi(\lambda - \lambda_o)(i-2a) \}$$

$$+ \sum_{i=3a+1}^{4a} A_i \sin \{ \pi(\lambda - \lambda_o)(i-3a) \}$$

where ϕ_o , λ_o are the coordinates of the SW corner of a $2^o \times 2^o$ area

ϕ , λ are the coordinates of the $0.1^o \times 0.1^o$ square corner which is represented by the gravity anomaly $\Delta g(\phi, \lambda)$ and $\Delta g'$ is predicted gravity anomaly at point ϕ_q , λ_q. $4a$ is the number of known gravity stations in the area.

The coefficients A_i are determined by setting up an observation equation for each known point in the area of prediction

$$r_j = \Delta g_j - \sum_{i=1}^{4a} A_i \; f_i(\phi, \lambda)$$

where r_j is the residual of the jth gravity station which will form an array (in matrix form)

$$FA - G = R$$

For a least squares determination of the coefficients A

$$\tfrac{1}{2} R^T W R = \text{minimum} \qquad (W \text{ being the matrix of weight coefficients})$$

and $$A = (F^T W F)^{-1} F^T W G$$

This technique was used to extend the anomaly field into unsurveyed $2^o \times 2^o$ areas of South Australia, the differences between predicted and observed values at 154 known stations being normally distributed with a standard error of ±7 mGal. This must be due, at least in part, to the sparseness of the data used in the prediction and to the fact that methods of spectral analysis are not reliable when applied in the general case to irregularly spaced data.

5.5 Conclusions

The field is well represented with density ranging from 1 point per 1 km^2 near computation stations to about 1 point per 20 km^2 in areas 50 to 100 km from the computation station. It was found that techniques which are used to predict mean gravity anomalies for large blocks are not suited to the present task. The least squares techniques discussed in 5.2.1 and 5.2.2 above also proved unsatisfactory by placing unrealistic constraints upon the modelling for the gravity field.

The task in hand is much more comparable to problems confronted when contouring from discrete data. As a result the techniques used by mapping agencies involved in automatic contouring were adopted with certain refinements to suit the peculiarities of the task. As a general rule, plane fitting techniques were used, with unique planes being used to describe terrain when the three data points

straddled the compartment whose mid-compartment point was being sought, and least squares plane fitting on 7 properly selected points when the compartment size exceeded the closest three circumscribing points.

In the next chapter it will be shown how the prediction technique adopted becomes an integral part of the system used to evaluate ξ , η and their various corrections.

6. COMPUTATION OF DEFLECTION AND CORRECTION TERMS

6.1 Introduction

Techniques for computing deflections and of handling data for this computation were discussed in chapter 4. It was decided, for the reasons given in section 4.4, to use a ring pattern for all inner zone computations. Because it is so adaptable a similar approach was used to compute the correction terms. Methods of extending the anomalous gravity field were investigated in chapter 5. The technique chosen as most suitable for the computational approach and data organisation was that of interpolation from simple triangles formed about the prediction point. In this chapter a description is given of how the system is operated, and of its combination with other phases of the gravimetric computation to achieve a total gravimetric solution at each station.

The scheme for computation of the deflection was as follows. An innermost zone, for radii (r) in the range $0 \leq r \leq r_o$ was chosen such that conditions listed in section 6.2.1 were effectively fulfilled. The inner zone was then computed for the region $r_o \leq r \leq 130$ km using a basic Rice Rings approach, with refinements explained in section 6.2.2. The zones beyond 1.5^o of the computation point had already been evaluated in the 1970 geoid solution by MATHER (1970a). The system adopted for this solution is explained in section 6.2.3 and the results extracted. The transition from the outermost Rice Ring is considered also and its effect evaluated. Thus the full Vening Meinesz solution is presented for each station in section 6.2.

The final section deals with the computation of the G' term using the KSRINGS approach. The results of some examples of the computation are presented and compared with hand computed values.

6.2 Evaluation of the Vening Meinesz Formulae

6.2.1 The Innermost Zone

Because of the insolubility of the Vening Meinesz formulae as the computation nears the computation point ($\psi \to 0$) it is necessary to define a small zone about this point wherein the anomalous field can be assumed planar, allowing for a relatively simple geometrical evaluation of the contribution of this zone. The theory for this evaluation is developed in (SOLLINS 1947, p 282). In this development if x and y are north and east respectively the Δg is expressed as

$$\Delta g = \Delta g_p + x \left(\frac{\delta \Delta g}{\delta x}\right)_o + y \left(\frac{\delta \Delta g}{\delta y}\right)_o$$

$$= \Delta g + r_o \cos \alpha \left(\frac{\delta \Delta g}{\delta x}\right)_o + r_o \sin \alpha \left(\frac{\delta \Delta g}{\delta y}\right)_o \qquad (6.1)$$

which is obviously based on an assumption that Δg varies linearly within the region $0 \to r_o$ (hence the use of the terms $\left(\frac{\delta \Delta g}{\delta x}\right)_o$, $\left(\frac{\delta \Delta g}{\delta y}\right)_o$).

Now equation (4.3) expressed

$$\frac{df(\psi)}{d\psi} \sin \psi = -\frac{1}{\psi} - \frac{3}{2} - \frac{49}{24} \psi + \ldots \qquad \text{from (4.3)}$$

By substituting $\frac{r_o}{R}$ for ψ and $\frac{dr_o}{R} = d\psi$

$$\frac{df(\psi)}{d\psi} \sin\psi \, d\psi = -\left(\frac{1}{r_o} + \frac{3}{2R}\right) dr_o \qquad (6.2)$$

Substituting (6.2) in the Vening Meinesz equations (2.26)

$$\xi_i = \frac{1}{2\pi\gamma} \int_0^{r_o} \int_0^{2\pi} \left[\Delta g + r_o \cos\alpha \left(\frac{\delta\Delta g}{\delta x}\right)_o + r_o \sin\alpha_i \left(\frac{\delta\Delta g}{\delta y}\right)_o\right].$$

$$.\cos\alpha_i \left[\frac{1}{r_o} + \frac{3}{2R}\right] d\alpha \, dr \qquad i = 1, 2$$

which gives upon integration,

$$\xi'' = [0.105\, r_o + 0\,\{r_o^2 \times 10^{-8}\}] \left(\frac{\delta\Delta g}{\delta x}\right)_o \qquad (6.3a),$$

and

$$\eta'' = [0.105\, r_o + 0\,\{r_o^2 \times 10^{-8}\}] \left(\frac{\delta\Delta g}{\delta y}\right)_o \qquad (6.3b)$$

assuming mean values for γ and R.

The values chosen for r_o in various solutions vary greatly, and must be largely determined by the nature of the anomalous gravity field near the computation point. For example, Rice adopted values which ranged from 279 m to 4320 m, depending on the intensity of the survey in this innermost region (RICE 1952, pp 289-290). In a comparative study carried out by Szabo in 1962 (q.v.) r_o was chosen as 4320 m again (this value is the outer limit of zone 21 of the original Rice Rings pattern). MATHER (1970a, p 94) used 3 km as the outer radius of the innermost zone for computation at 38 stations, the bulk of which were located on small hills on extensive plains.

Bursa recognising this problem in the "central zone" (BURSA 1967), investigated methods of improving the solution which is based on the planar assumption in the region 200 m to 5 km, and instead fitted various polynomials or quadrature expressions to the field in this zone. The solutions were achieved using "(i) mechanical quadrature formulae of the highest algebraic degree of accuracy, introducing a weight function $p(r) = r^{-1}$ and (ii) the Gauss mechanical quadrature formula and interpolation polynomials in an analogical form" (IBID, p 14). These methods were tested on models consisting of high mountain massifs, and on two real terrain models, with the result that each of the methods tested gave the same theoretical accuracy (IBID, p 32). The Gauss quadrature formulae were also tested for the innermost region (0 to 1 km) for three test models and compared with the gradient method (6.3a and 6.3b) and the theoretical value. The gradient method suffered by comparison, giving results which were up to 1"0 in error. This must be largely due to the inaccuracy of the planar assumption inherent in the gradient solution, whereas higher order surfaces are 'fitted' in the quadratures approach.

A number of the computation stations in the present test are located in regions of rugged terrain (see figures 10 to 21) and it would be unsafe to assume planar conditions out to 1 km. Because of the ability of the computing system to start the inner zone computations at any nominated value, and because of the simplicity of (6.3a) and (6.3b), it was decided to limit the value of r_o to 100 m wherein it was considered safe to assume planar variations of the anomaly field.

The actual contribution for the innermost zone was computed using the method suggested by RICE (1952, p. 290) whereby a mean gradient for this innermost circle was evaluated by establishing a grid of spacing $0.707\, r_o$. The mean gradient in the prime directions were found by giving a weight of 2 to 1 in favour of the line through the computation point as compared with the two flanking gradients in each case.

Figure 28. INNERMOST ANOMALIES AND HEIGHTS

1620 + 45.4	1700 + 47.6	1640 + 45.9	1575 + 16.2	1600 + 16.8	1625 + 17.5
1640 + 45.9	1709 + 47.9	1620 + 45.4 ↑	1640 + 17.9	1790 + 21.0	1775 + 21.6
		71 m			
1660 + 46.5	1680 + 47.1	1600 + 44.8 ↓	1725 + 20.3	1775 + 21.5	1760 + 21.1
a. BINALONG			b. GOONBRI		
2675 + 48.2	2680 + 47.5	2670 + 47.5	4800 + 108.4	4650 + 104.4	4625 + 104.0
2725 + 49.8	2797 + 50.8	2690 + 48.9	4800 + 108.2	4949 + 112.1	4775 + 109.4
2675 + 48.1	2725 + 49.5	2675 + 48.1	4850 + 109.8	4900 + 110.9	4825 + 112.3
c. BYAR			d. KAPUTAR		
3010 + 81.1	2975 + 77.8	2875 + 74.4	2975 + 68.7	2950 + 68.5	2950 + 69.4
3020 + 80.7	3047 + 80.9	2975 + 79.2	3000 + 69.5	3063 + 71.2	3025 + 71.0
3000 + 80.8	3030 + 80.8	3025 + 80.5	2900 + 66.7	2960 + 69.1	2975 + 70.2
e. BLUE NOBBY			f. GULF CREEK		
2275 + 57.1	2330 + 59.0	2325 + 58.6	2900 + 71.8	2800 + 71.2	2830 + 72.5
2250 + 54.7	2371 + 59.7	2345 + 58.7	2800 + 71.1	2920 + 74.4	2750 + 70.1
2200 + 53.0	2300 + 56.5	2320 + 58.7	2800 + 71.3	2825 + 72.0	2750 + 69.9
g. NEWRY			h. BALDWIN		

Legend : Height (feet) + Free-Air Anomaly (mGal)

The height values were scaled off the medium scale maps (1:31 680) and the Bouguer anomalies from the detailed gravimetric survey of the stations. Details of these innermost values can be found in figures 28a to 28h , and results of the computation tabulated in row 6, table 6.

As can be seen from these results the contribution of this innermost zone can be most significant in terms of the order of accuracy being sought (± 0".3). It was for this reason that the computation was carried out manually despite the fact that it could be easily programmed and inserted into the system for computing the deflection. Heights for the eight cardinal points were in fact included into HTBIN to assist in the height prediction of the mid-compartment points of the close inner zone rings.

The error analysis for this zone, along with comments of a practical nature, can be found in section 7.3.1.

6.2.2 Computations of the Inner Zone

As investigated in chapter 4, and concluded in section 4.4.1 it was decided to compute the inner zone of the deflection computation (100 m $\leq \psi \leq$ 130 km) by means of Rice Rings, suitably modified to suit both the solution by computer and the density of data. The modifications were as follows.

(a) The contribution of each compartment was changed from the 0".001 radial deflection for a 1 mGal anomaly suggested by Rice to 0".002 deflection for the same anomaly. This halved the number of rings and significantly reduced the memory requirements of the programme without loss of accuracy in the evaluation. The rings progressed from 100 m to 130 km in 21 steps (see, table 3 and section 4.3.1).

(b) A multiple of 10° which was also a real fraction of 360° (eg. 90, 60, 40, 30 or 20) was used for the apex angle instead of the usual 10° throughout the computation. This was necessary in order to optimise the efficiency of the evaluation. For the nearest rings in particular there was little to be gained by computing each basic compartment as the data used for a number of the compartments (say n) would be the same. Hence the sum of these compartments would give the same result as the contribution of the middle compartment times 'n'. This assisted in cutting the time by 1/6 to 1/4 without significant loss of accuracy.

(c) The starting position of the compartment count was staggered between adjoining rings. This was to ensure that all available data was used in prediction.

All data likely to be needed for the inner zone computation (eg. out to $\psi = 1^{\circ}.5$) was read from GRAVBNK (see section 4.1.1) into a local file for speedier processing. This placed certain constraints on the programme as memory requirements ($\simeq$ 100 K bytes) now approached the limit for efficient operation on the CYBER 70 (Model 72) at UNSW.

The general flow of the computation can be seen in Appendix H, where a flow chart for CONTRL2 is presented. CONTRL is the generic name given to the programmes developed to manipulate data and sub-routines in the computation of deflections, G' or other deflection correction terms. Because of a standardised 'ring' approach in each of these computations it was possible to use the same basic versions of CONTRL and of the sub-routines in each computation with only slight modifications to suit the particular variables of computation, memory requirement etc.

The subroutine SORT3 was used to find the mid-compartment values for Δg out to about 10 km. Thence the subroutine SORT7 (Appendix I) and PLNFIT (Appendix J) were used for this purpose. If the

mid-compartment point is within an area covered by both GRAVBNK and HTBIN, then the height points as well as the gravity stations are used in the prediction of the height of the prediction point.

The effect of this predicted value on the deflection at P is computed, split into the two components and accumulated throughout the whole pattern of rings. If at any stage the value of the deflection contribution appears excessive (taken as $\Delta\varepsilon > 0''.3$ i.e. the magnitude of the desired accuracy for the purpose of this investigation) the compartment unit is subdivided into the basic 10^{o} and the sum total of each small compartment summed into the accumulator of the contribution to the deflection.

All predicted quantities were printed out together with the values which were used in the prediction itself. This facilitated graphical checking for abnormal values as it made for easy and direct comparisons of the computation against 'true' values from the medium scale maps. The values at each of the stations are listed in row 5, table 6. The expected accuracy of this computation is not listed here, but will be given in section 7.3.2, where an error analysis of the approach is undertaken.

Even a superficial analysis of table 6 shows that the final value of the deflection of the vertical can be largely dependent upon an accurate evaluation of the inner zone contribution. This is illustrated clearly by analysing this contribution to the deflection at Kaputar. In table 7 the contributions per ring to each component ($d\xi$, $d\eta$) are tabulated. The squares of these parameters are also tabulated and accumulated through the rings to give an indication of the strength of the 'signal' being received at the computation point at each step in the evaluation.

The accumulation of the contribution from $d\xi$ is rapid, and reaches $0''.8$ only 400 m from the computation point. By contrast $d\eta$ has reached only $0''.2$ in this distance. This difference reflects the asymmetry of the free-air anomaly field about Kaputar. The reverse situation exists in the outer rings. The prime vertical component receives a large contribution in the rings beyond ring 16 ($r > 24$ km) whilst the meridian component is affected relatively slightly by the contributions from these rings.

The above comments are illustrated more graphically when one analyses the signals received per ring ($d\xi^2$, $d\eta^2$). In this regard it is important to note that, by analysis of table 6, the INNER zone contributes over 60% of the total signal in the ξ component and almost 90% in the η component. This latter percentage is an overestimate in view of the findings in section 8.2.1 which shows that the outer zone contribution is systematically under-estimated by about $1''.5$. If this amount is included in the total signal the INNER xone is found to contribute about 80% of the total signal and is obviously still highly significant.

The ξ value accumulates at a steady rate ($\simeq 0''.4$ per ring) and by ring 12(r = 4.3 km) 75% of the whole inner zone signal has been received. This is approximately 50% of the *total* signal in this component. On the other hand the η component has received about 25% of the whole inner zone signal. In fact 50% of the signal for this component comes from the rings beyond ring number 17 ($r > 24$ km), compared with the 6% contribution toward the ξ component from these rings. This region is therefore of significance for the η component as approximately 40% of the total signal comes from this area.

The above comments emphasize the importance the inner zone can have in the evaluation of the deflection of the vertical. In some cases the bulk of the signal comes from this zone and significant contributions can be missed if a detailed survey and computation of this zone is not carried out.

NAME / ZONE	1. Culgoora		2. Beelera		3. Willalla		4.Binalong		5. Goonbri		6. Byar		7. Kaputar		8.Blue Nobby		9.Gulf Creek		10. Newry		11. Baldwin		12.Somerton	
	ξ	η	ξ	η	ξ	η	ξ	η	ξ	η	ξ	η	ξ	η	ξ	η	ξ	η	ξ	η	ξ	η	ξ	η
1. UT $\psi > 15^{o}$	-0.31	-0.94	-0.31	-0.94	-0.29	-0.92	-0.37	-0.75	-0.38	-0.74	-0.38	-0.73	-0.40	-0.77	-0.40	-0.75	-0.40	-0.75	-0.43	-0.80	-0.42	-0.80	-0.40	-0.81
2. MD $15^{o} > \psi > 7.5$	-1.92	-1.28	-1.93	-1.27	-1.83	-1.25	-1.63	-1.31	-1.67	-1.30	-1.70	-1.30	-1.73	-1.32	-1.76	-1.30	-1.76	-1.30	-1.68	-1.13	-1.63	-1.12	-1.59	-1.12
Σ to here	-2.23	-2.22	-2.24	-2.21	-2.12	-2.17	-2.00	-2.06	-2.05	-2.04	-2.08	-2.03	-2.13	-2.09	-2.16	-2.05	-2.16	-2.04	-2.11	-1.93	-2.05	-1.92	-1.99	-1.93
3. NE $7^{o}.5 > \psi > 1^{o}.5$	+1.76	-2.50	+1.81	-2.87	+1.96	-2.93	+1.75	-1.68	+1.48	-1.83	+1.31	-1.92	+1.13	-1.91	+1.16	-2.03	0.90	-2.31	1.20	-2.18	1.48	-2.10	1.79	-1.97
Σ to here	-0.47	-4.72	-0.43	-5.08	-0.16	-5.10	-0.25	-3.74	-0.57	-3.87	-0.77	-3.95	-1.00	-4.00	-1.00	-4.08	-1.24	-4.39	-0.91	-4.11	-0.57	-4.02	-0.20	-3.90
4. MELD	+0.33	-0.62	+0.37	-0.63	+0.35	-0.54	+0.20	-0.82	+0.31	-1.09	+0.59	-1.23	+0.70	-0.90	+0.74	-1.16	+0.60	-1.04	+0.54	-1.13	+0.10	-0.94	-0.07	-0.92
TOTAL OUTER $\psi > 128$ km	-0.14	-5.34	-0.06	-5.71	+0.19	-5.64	-0.05	-4.56	-0.26	-4.96	-0.18	-5.18	-0.30	-4.90	-0.26	-5.24	-0.64	-5.43	-0.37	-5.24	-0.47	-4.96	-0.27	-4.82
5. INNER	+1.28	-4.50	-0.07	-3.70	+1.17	-1.98	+1.58	-0.77	-1.66	-3.73	-5.47	-6.73	+2.89	-7.38	+5.34	+1.14	+2.18	-1.38	-0.68	+0.26	-5.06	-2.31	-1.55	-3.98
6. INNERMOST	-	-	-	-	-	-	-0.02	-0.05	+0.42	-0.24	+0.05	+0.06	+0.56	+0.01	+0.17	+0.14	0.00	-0.20	-0.15	-0.21	-0.04	+0.07	-	-
TOTAL ε	+1.14	-9.84	-0.13	-9.41	+1.36	-7.62	+1.51	-5.38	-1.50	-8.93	-5.60	-11.85	3.15	-12.27	5.25	-3.96	+1.54	-6.93	-1.20	-5.19	-5.57	-7.20	-1.82	-8.80

TABLE 6 CONTRIBUTION OF VARIOUS ZONES TO THE DEFLECTION OF THE VERTICAL

Ring No.	Outer Radius (km)	CONTRIBUTION Per Ring $d\xi$	CONTRIBUTION Accumul $[d\xi]$	$[d\xi^2]$	SIGNAL Per Ring $\frac{d\xi^2}{\Sigma d\xi^2}$	SIGNAL Accum. $\frac{[d\xi^2]}{\Sigma d\xi^2}$	$d\eta$	$[d\eta]$	$[d\eta^2]$	SIGNAL Per Ring $\frac{d\eta^2}{\Sigma d\eta^2}$	SIGNAL Accum. $\frac{[d\eta^2]}{\Sigma d\eta^2}$
2	0.14	+0.06	0.06	0.004	-	-	0.02	0.02	-	-	-
3	0.2	+0.23	0.29	0.06	0.03	0.03	-0.01	0.01	-	-	-
4	0.3	+0.21	0.50	0.10	0.02	0.05	-0.04	-0.03	-	-	-
5	0.4	+0.34	0.84	0.22	0.06	0.11	-0.14	-0.17	.02	.01	0.01
6	0.6	+0.39	1.23	0.37	0.07	0.18	-0.18	-0.35	.05	.01	0.02
7	0.8	+0.49	1.72	0.61	0.12	0.30	-0.26	-0.61	.12	.02	0.04
8	1.1	+0.50	2.22	0.86	0.12	0.42	-0.44	-1.05	.32	.06	0.10
9	1.5	+0.44	2.66	1.05	0.09	0.51	-0.48	-1.53	.56	.07	0.17
10	2.2	+0.39	3.07	1.20	0.07	0.58	-0.49	-2.04	.79	.07	0.24
11	3.1	+0.47	3.54	1.42	0.11	0.69	-0.28	-2.32	.86	.02	0.26
12	4.3	+0.29	3.83	1.51	0.04	0.73	-0.13	-2.45	.88	.01	0.27
13	6.1	+0.18	4.01	1.54	0.02	0.75	-0.46	-2.91	1.09	.06	0.33
14	8.6	-0.12	3.89	1.56	0.01	0.76	-0.44	-3.35	1.29	.06	0.39
15	12.0	-0.46	3.37	1.77	0.10	0.86	-0.31	-3.66	1.38	.03	0.43
16	16.9	-0.17	3.20	1.80	0.01	0.87	-0.36	-4.02	1.51	.04	0.47
17	23.8	-0.39	2.81	1.95	0.07	0.94	-0.43	-4.45	1.70	.06	0.53
18	33.5	-0.15	2.66	1.97	0.01	0.95	-0.55	-5.00	2.00	.09	0.62
19	46.9	-0.17	2.49	2.00	0.01	0.96	-0.70	-5.70	2.49	.14	0.76
20	65.8	+0.09	2.58	2.01	-	0.96	-0.56	-6.26	2.80	.09	0.85
21	92.1	+0.14	2.72	2.03	0.01	0.97	-0.52	-6.78	3.07	.08	0.93
22	128.6	+0.17	2.89	2.06	0.01	1.00	-0.60	-7.38	3.43	.10	1.00

Legend:

$d\xi$, $d\eta$: Contribution to ξ , η for a ring

$[d\xi]$, $[d\eta]$: Accumulated contribution to ξ , η up to and including the subject ring.

$[d\xi^2]$, $[d\eta^2]$: Accumulation of $d\xi^2$, $d\eta^2$ up to and including the subject ring.

$\frac{d\xi^2}{\Sigma d\xi^2}$, $\frac{d\eta^2}{\Sigma d\eta^2}$: Proportion which the subject ring contributes to the total $d\xi^2$, $d\eta^2$ of the whole inner zone.

$\frac{[d\xi^2]}{\Sigma d\xi^2}$, $\frac{[d\eta^2]}{\Sigma d\eta^2}$: Accumulation of the above proportion up to and including that subject ring.

NOTE: For this station the inner zone contributes about 60% of the total signal in the ξ component, and about 80% of the total signal in the η component.

TABLE 7 ANALYSIS OF INNER ZONE CONTRIBUTION TO THE DEFLECTION COMPONENTS AT KAPUTAR

6.2.3 Outer Zones Contribution

The contribution of the outer zones (ie. the area beyond the radius of the outer-most ring used to compute the INNER contribution were determined, in the main, by MATHER (1970) in the 1970 geoid solution of Australia. As described in section 4.2 the inner zone in this solution was the 1.5° x 1.5° area centred on the 1° square containing the computation point. The bulk of the contribution now sought will come from the outer zones exterior to the above regions. The values were computed for the twelve test stations, with the contribution for the transition from the outermost ring (approximately 128 km radius from the computation point) to the inner boundary of the 1970 geoid outer zone being evaluated as a separate unit.

This "transition" zone was computed using data held in GRAVBNK and HTBIN by a program denoted MELD, the results of which are listed in row 4 of table 6. As can be seen from the values, this zone makes a significant contribution to the deflection both in terms of the absolute quantity (of the order of 0".5 in ξ and 1" in η) and in terms of the relative difference in the contributions to each station. The contribution to ξ ranges from +0".74 for Blue Nobby in the north to -0".20 for Somerton in the south-east, and to η from -1".6 for Blue Nobby to -0".54 Willalla in the south-west. These ranges, of approximately 1" and 0".6 respectively are considerable when viewed against an expected accuracy of ±0".3, and reflect the asymmetry of the gravity field at angular distances from the 1.0° to 1.5° radius from the region.

The approach adopted in evaluating all outer zone contributions was described in section 4.2, the data sets used in this evaluation being compiled as follows (see MATHER 1970a, p 73). The 0.5° x 0.5°, and 1° x 1° area means were based on gravity surveys carried out throughout the Australian region by the BMR, with extra information (particularly in the ocean areas) being obtained from such bodies as private researchers or geophysical exploration companies, or the gravity holdings of the Aeronautical Chart and Information Center, St. Louis, Mo. (now the Defence Mapping Agency Aerospace Center) for regions within 25 degrees of the continental margins. The 5° x 5° area means were compiled from both surface and satellite gravimetry such that, where necessary, these mean values were consistent with the smaller area means derived above. A summary of the techniques used to achieve consistency can be found in (MATHER 1970a, pp 83-84).

The contributions of the outer zone was computed as that due to three regions NE, MD and UT. These results are shown respectively in rows 1, 2 and 3 of table 6. As can be seen, the contribution of the field 15° distance from the region changes slowly from station to station, contribution approximately -2".0 to the values of ξ and η , and varying only by the expected order of accuracy of the computed result. The NE zone ($1.5^{\circ} < \psi < 7.5^{\circ}$) varies considerably, whilst adding something of the order of 1".5 to 2".0 in ξ , and -1".7 to -2".9 in η. This difference in η is a further reflection of the asymmetry of the field at the $\psi = 1^{\circ}.5$ level remembering in particular that the starting data used for stations west of 150°E will differ from that used for stations east of 150°E as a result of the method of square selection used.

6.3 Astro-Geodetic Deflections

6.3.1 Evaluation Techniques

As mentioned above in section 1.4 the computation stations were chosen because they were part of the astro-geodetic levelling network of Australia, and as such were fixed both by astronomical observation and by geodetic survey on the Australian Geodetic Datum.

a) Astronomical Position

The astronomical positions were fixed by observers from the Division of National Mapping, Australia using in the main Kern DKM 3A theodolites (the only exception being at Somerton where a Wild T4 was used). Latitude was usually fixed by observing circum-meridian altitudes on σ octantis, whilst longitude was fixed by means of a 35^{o} impersonal almucantar, transits being recorded on a FAVAG chronograph, with time signals originating from the radio station Lyndhurst VNG time service. The values obtained, along with their estimated accuracies (LEPPERT 1976) are listed in columns 2 and 3 of table 8. It should be noted that these accuracies are based on the analysis of the observations alone, and must be considered as estimates of the internal accuracy of the observation rather than as a statement of absolute accuracy. In fact absolute positional accuracy as estimated from an overall analysis of the Australian network (FRYER 1970, p 50) appears to be more of the order of ±0".25 in latitude and ±0".45 in longitude.

b) Geodetic Position

The geodetic positions at these stations are based on the geodetic control network in the region, observed to 1st order specifications and computed on the Australian Geodetic Datum (see equations 6.5, 6.6 in section 6.3.2 for details). The values obtained are listed in column 4 of table 8 and can, for the purposes of this investigation, be assumed error free. This means that the deflections obtained astro-geodetically should be of the same accuracy as the astronomical position fixes ie. ±0".25 in ξ and ±0".45 in η.

6.3.2 Corrections for Model Differences

(a) Correction for elevation of ground point above the ellipsoid

The gravimetric values of the deflection are being computed at the point P on the surface. The astronomical position is determined at this same point, but its geodetic position is computed on the ellipsoid. It will be necessary to correct for the curvature of the normal in the meridian plane through P in order to achieve a proper A/G deflection at the surface.

The derivation for this correction is well-known (eg. BROVAR ET AL 1964, p 228; HEISKANEN AND MORITZ 1967, p 196; MATHER 1968, p 216-221) and will not be repeated here.

The correction is found from the expression

$$C_{\xi} = -0.17 \; h \sin 2\phi$$

where h = height of the P in km

and $C_{\xi} = \xi_{surface} - \xi_{A-G}$.

In other words,

$$\xi_{surface} = \xi_{A-G} - 0.17 \; h \sin 2\phi \qquad (6.4)$$

$$\eta_{surface} = \eta_{A-G}$$ (because the rotational symmetry of the ellipsoid of revolution introduces no differential curvature into the prime vertical component of the normal).

1 STATION	2 ϕ_A λ_A	3 S_{MEAN} "	4 ϕ_G λ_G	5 HEIGHT(m)	6 ξ_{AGD} η_{AGD}	7 c_ξ	8 $\Delta\xi'$	9 $\Delta\xi''$ $\Delta\eta''$	10 Σ correction	11 $\xi_{cor.}$ $\eta_{cor.}$
1. Culgoora	- 30 18 52.45 149 33 32.39	0.17 0.22 (0.45)	- 30 18 55.73 149 33 39.51	207.9	+3.28 -4.99 (-6.15)	-0.03	+2.53	-4.51 -3.41	-2.01 -3.41	+1.27 -8.40 (-9.56)
2. Beelera	- 30 18 37.33 149 48 44.31	0.22 0.21	- 30 18 39.17 149 48 51.22	246.0	+1.84 -5.97	-0.04	+2.53	-4.52 -3.41	-2.03 -3.41	-0.19 -9.38
3. Willalla	- 30 49 58.19 149 45 46.30	0.12 0.22	- 30 49 60.43 149 45 47.90	495.9	+2.24 -1.37	-0.07	+2.56	-4.53 -3.39	-2.04 -3.39	+0.20 -4.76
4. Binalong	- 30 47 32.10 150 00 55.06	0.14 0.20	- 30 47 35.93 150 00 55.81	520.9	+3.83 -0.64	-0.08	+2.56	-4.54 -3.38	-2.06 -3.38	+1.77 -4.02
5. Goonbri	- 30 37 11.06 150 13 02.76	0.17 0.19	- 30 37 11.51 150 13 07.63	545.9	+0.45 -4.19	-0.08	+2.55	-4.54 -3.37	-2.07 -3.37	-1.62 -7.56
6. Byar	- 30 29 19.75 150 17 20.37	0.15 0.23	- 30 29 16.21 150 17 29.16	852.5	-3.54 -7.57	-0.13	+2.54	-4.54 -3.37	-2.13 -3.37	-5.67 -10.94
7. Kaputar	- 30 16 25.58 150 09 40.05	0.18 0.45	- 30 16 30.12 150 09 48.03	1508.5	4.54 -6.89	-0.22	+2.53	-4.53 -3.37	-2.22 -3.37	+2.32 -10.26
8. Blue Nobby	- 30 13 16.21 150 29 31.86	0.21 0.20	- 30 13 23.09 150 29 33.15	928.4	6.88 -1.11	-0.14	+2.53	-4.54 -3.36	-2.15 -3.36	+4.73 -4.47
9. Gulf Creek	- 30 11 53.73 150 40 03.46	0.15 (0.32) 0.19	- 30 11 57.42 150 40 05.99	933.6	3.69 (-0.95) -2.19	-0.14	+2.53	-4.54 -3.35	-2.15 -3.35	+1.54 (-4.30) -5.54
10.Newry	- 30 29 20.13 150 38 22.71	0.13 0.15	- 30 29 20.95 150 38 22.18	722.4	0.82 0.46	-0.11	+2.54	-4.55 -3.35	-2.22 -3.35	-1.30 -2.89
11.Baldwin	- 30 43 59.18 150 38 47.40	0.14 0.10	- 30 43 55.83 150 38 50.28	890.0	-3.35 -2.48	-0.13	+2.56	-4.55 -3.35	-2.12 -3.35	-5.47 -5.83
12.Somerton (Sth.Base)	- 30 56 13.97 150 35 09.59	0.17 0.12	- 30 56 14.26 150 35 09.59	332.5	+0.29 -4.01	-0.05	+2.56	-4.55 -3.35	-2.06 -3.35	-1.75 -7.36

TABLE 8 ASTRO GEODETIC DEFLECTIONS CORRECTED TO GROUND LEVEL WITH RESPECT TO THE INTERNATIONAL ELLIPSOID

This correction is tabulated in column 7 of table 8. (It is assumed that the geoidal height is equivalent to the ellipsoidal elevation for this purpose as the difference ($\simeq$ 40 m) will have insignificant effect). It can be seen that the maximum correction of -0".22 for Kaputar is not insignificant and that for stations of 2500 ft ($\simeq$ 750 m) and higher in this latitude this correction should be applied.

(b) Correction for changes in model dimensions

The values for the gravity anomalies computed from equation (2.5) are based on the normal gravity computed from the International Ellipsoid whose parameters are stated in equation (2.1). The geodetic values of the control stations are computed on the Australian Geodetic Datum (AGD), details of which are as follows (see LAMBERT 1968, p 95).

The model used is known as the Australian National Spheroid (ANS), with

$$a = 6\ 378\ 160 \text{ m}$$

$$f = 1/298.25 \qquad (6.5),$$

whose orientation is determined by adopting geodetic coordinates and ellipsoidal elevation at the Johnston Origin of

$$\phi_{GO} = -25^{o}\ 56'\ 54".5515$$

$$\lambda_{GO} = 133^{o}\ 12'\ 30".0771$$

$$h_{so} = 571.2 \text{ m} \qquad (6.6)$$

It can be seen on comparing (6.5) with (2.1) that the changes in the model parameters are

$$da = -228 \text{ m}$$

$$df = -1.41 \times 10^{-5} \quad (\simeq 2.5 \text{ arcsec})$$

to correct from the ANS to the International Ellipsoid.

The expression which gives the effect of these changes on the meridional deflection (as again the value of η is unaffected) to a significant order of accuracy is derived in (HEISKANEN AND MORITZ 1967, pp 206-208; MATHER 1968, pp 281-285). It can be stated as

$$\Delta\xi' = -df \sin 2\phi - f \frac{da}{a} \sin 2\phi + df \frac{h}{a} \sin 2\phi -$$

$$- 2 f\, df \sin 2\phi \cos^2 \phi \qquad (6.7)$$

The first term in this expression is the predominating one (the remaining three being of the order of f^3), and this changes slowly throughout the extremes of the test area, ranging from $\Delta\xi' = +2".52$ for $\phi = -30^{o}$ to $\Delta\xi' = +2".57$ for $\phi = -31^{o}$.

The values as computed are shown in column 8 of table 8.

(c) Change in orientation of ellipsoidal model

The effect on the deflections of the vertical due to a change in the orientation of the reference ellipsoid, as derived in (MATHER 1968a, pp 281-285, and FRYER 1970, pp 30-34) are given as

$$\begin{aligned} -\Delta\xi''(\rho + h) &= -\Delta\xi_o(\rho_o + h_o)[\cos\phi_o\cos\phi + \sin\phi_o\sin\phi\cos\Delta\lambda] \\ &\quad + \Delta\eta_o(\nu + h_o)\sin\phi\sin\Delta\lambda \\ &\quad + \Delta N_o[\sin\phi_o\cos\phi - \cos\phi_o\sin\phi\cos\Delta\lambda] \end{aligned} \tag{6.8}$$

and

$$\begin{aligned} -\Delta\eta''(\nu + h) &= -\Delta\xi_o(\rho_o + h_o)\sin\phi_o\sin\Delta\lambda \\ &\quad - \Delta\eta_o(\nu_o + h_o)\cos\Delta\lambda - \Delta N_o\cos\phi_o\sin\Delta\lambda \end{aligned} \tag{6.9},$$

where $\Delta\lambda = \lambda - \lambda_o$,

ρ, ν = radius of curvature in the meridian, prime vertical respectively and the subscript $_o$ refers to values at the origin (see equation 6.6).

The values for $\Delta\xi_o$, $\Delta\eta_o$ and ΔN_o were found in 1970 as part of the 1970 geoid solution of Australia. These values were computed from a least squares fit of 38 well-distributed A-G stations onto a geocentric ellipsoid, and were found to be (MATHER 1970, p 117)

$$\begin{aligned} \Delta\xi_o &= -4.2 \pm 0.2 \text{ sec} \\ \Delta\eta_o &= -4.5 \pm 0.2 \text{ sec} \\ \Delta N_o &= 10.0 \pm 0.2 \text{ m} \end{aligned} \tag{6.10}$$

These values are substituted into (6.8) and (6.9) for each of the 12 control stations and the results listed in column 9 of table 8.

Consideration of the expressions used to compute each of these three corrections shows that the values resulting can be assumed error-free. For the same reasons the order in which the computations are carried out will have no significant effect on the results.

6.4 Correction Terms

6.4.1 The Effect of G' on ξ and η

The method adopted to compute G' was discussed in section 4.3.2 wherein it was decided to use a ring technique similar to Rice's Rings, to evaluate G' at every gravity station in GRAVBNK (see section 4.1.1) and store this value with all other information for the point in GRAVBNK. It was then possible to interpolate G' in exactly the same manner as Δg is interpolated in order to extend the G' field beyond the discrete points. In this way maximum advantage could be taken of the subroutine and systems set up to compute the deflections of the vertical.

It is neither practicable nor desirable to present the results of the G' evaluation at each station in this context. It is worth pointing out that the computer technique was tested against a hand computation at three of the test stations (Kaputar, Baldwin and Newry). These stations provided a range of terrain types and showed the computer system to have very good agreement with the hand computation (0 {± 1-2 mGal}) for Kaputar, whose total G' correction is ≃ 34 mGal and free-air anomaly ≃ 112 mGal). This afforded confidence in not only the ring system used to evaluate G' but also in the prediction technique.

The G' values as computed are shown, together with the free-air anomalies and heights, for the gravity stations in the immediate vicinity of the relevant test stations in figures 13 to 20. It should be noted that the greater the distance of the gravity station from the computation station (P) the weaker will be the evaluation of G' because of the lower density of auxiliary height points away from the test station. This is not considered serious, however, because the influence of errors in G' at such distances from P will be much less, and in general in this region the value of G' will also be lower because of the less rugged nature of the topography as one moves away from the computation point. As will be shown in section 7.3.2, the error is further diminished if the over- or under- estimation of G' is symmetrical about the computation point. It is reasonable to assume that this will in fact happen, as the density of the height points is a function of distance from the computation point, and the choice of height point and the method of interpolation should ensure that the errors in G' are symmetrically located about P.

The effect of the correction G' on the deflections of the vertical was computed as a separate stage of the computation in CONTRL2 (Appendix H). In this way, the Vening Meinesz effect and the terrain correction effects could be easily compared at each stage of the computation. Because of the flatness of the terrain around Culgoora, Beelera, Willalla and Somerton it was not necessary to compute this correction at these stations. The corrections to ξ and η for the remaining stations are listed in columns 1 and 2 of table 9.

Further comments will be made on the significance of these corrections in chapter 8.

6.4.2 Correction Terms for Green's Third Identity

The computational techniques for finding the ground slopes are described in section 4.3.4 and are needed to evaluate the terrain correction term as expressed in equations (2.72), (2.73). Other necessary parameters are the geoidal components ξ, η and N at each mid-compartment point (Q) in the Rice Rings solution. These are obtained by applying a special version of SORT3 (Appendix F) to the geoidal data described in section 4.1.3. The values of h and ψ are found as a matter of course during the Rice Rings solution of the Vening Meinesz expression, and thus equipped, it is a simple matter to evaluate the $\bar{\psi}$ needed, keeping in mind the comments made at the end of section 2.3.4 on the necessity to use $\bar{\psi}$ rather than ψ in this term.

It is now possible to evaluate (2.72) and (2.73) as modified in section (3.3.3), viz.

$$\xi_i' = \frac{1}{2\pi} \iint \left[\frac{-\cos \alpha_i}{\bar{\psi}^2} \left(\xi \tan \beta_1 + \eta \tan \beta_2 \right) + (N_q - N_p) \left\{ \left(2\frac{dh}{dr_o} + 3\,\frac{h_p - h}{r_o}\right) \cos \alpha_i - \frac{\partial}{\partial \alpha} \frac{dh}{dr_o} \sin \alpha_i \right\} \right] d\sigma \qquad i = 1, 2 \qquad (6.11)$$

where $\xi_1 = \xi$, $\xi_2 = \eta$

$\alpha_1 = \alpha$, $\alpha_2 = 90 - \alpha$.

Because of the slow-changing nature of the N value in the test region (see figure 23) the terms in $(N_q - N_p)$ were very small, making negligible contributions to the correction. The values of the corrections, which are in effect the evaluation of the first term, are listed for all relevant stations in columns 3 and 4 of table 9.

It is interesting to compare these values with the values which result had not the datum shift in N been adopted in the second term, ie, if the full geoid-ellipsoid separation had been used as the coefficient in this term. The values of the corrections evaluated thus are listed in columns 5 and 6 of table 9.

It is also of interest to note the effect of using the value for ψ (as opposed to $\bar{\psi}$) in the above expression using $(N_q - N_p)$ as the coefficient for the second term. These values for the relevant computation points are listed in columns 7 and 8 of table 9.

For further discussion of these results refer to chapter 8.

NAME	MOLODESKY'S CORRECTION		USING ARNOLD-TYPE EXPRESSIONS(equation 6.11)							
			$\bar{\psi}$				ψ			
	Contribution From G'		Using $N_Q - N_p$		Using N_Q		Using $N_Q - N_p$		Using N_Q	
	ξ' 1	η' 2	$\delta\xi$ 3	$\delta\eta$ 4	$\delta\xi$ 5	$\delta\eta$ 6	$\delta\xi$ 7	$\delta\eta$ 8	$\delta\xi$ 9	$\delta\eta$ 10
5. Goonbri	-0.20	-0.16	-0.31	+0.04	-4.59	-1.46	+0.01	-0.70	-8.44	-1.00
6. Byar (Cont.n to Ring 5)	-0.38	-0.06	-1.06 (-0.80)	-1.04 (-0.53)	-6.48	-5.34	-3.16	-2.00	-12.76	-11.05
7. Kaputar (Cont.n to Ring 5)	-0.64	+0.19	-0.05 (-0.84)	-1.03 (-0.14)	-14.00	-4.30	-1.40	-1.01	-20.05	- 3.62
8. Blue Nobby (Cont.n to Ring 5)	-0.53	+0.25	-1.86 (-1.72)	+2.16 (+1.91)	-18.49	-5.58	-2.17	-0.65	-30.52	7.36
9. Gulf Creek (Cont.n to Ring 5)	+0.13	+0.13	+0.45 (+0.39)	-0.41 (-0.26)	-3.32	-3.55	+0.11	+0.13	-1.22	-2.19
10. Newry (Cont.n to Ring 5)	.00	+0.14	+0.12 (+0.20)	.00 (+ .23)	-0.66	-1.80	-0.01	-0.01	-0.66	-0.82
11. Baldwin (Cont.n to Ring 5)	- .20	+ .10	-1.88 (-1.74)	+1.90 (+1.60)	+5.14	+7.11	+0.64	-0.82	-3.16	-6.05

TABLE 9 TERRAIN CORRECTIONS TO ξ , η

7. ERROR ANALYSIS

7.1 Introduction

It is a common and a valuable practice to make a theoretical estimate of the accuracy of derived quantities based on the expected accuracy of the data and the method of evaluation adopted. This assists in comparing values derived in a similar fashion at different stations, or in placing the method of solution in perspective when comparing that particular technique against a different means of obtaining the same quantity. For example, in the present study it is of interest to compare the gravimetrically derived deflections at different stations throughout the region and also to compare the expected accuracies of the gravimetric deflections with those of the astro-geodetically derived values.

There are two problems which must be considered in the present analysis. The first is the problem of estimating the faithfulness with which the data value used in the solution represents the mean value for the compartment (referred to as the 'error of representation' by de Graaff-Hunter (see MOLODENSKII ET AL 1962, p 172)). This itself will be a function of both the accuracy of the original data used in the estimation and the technique adopted to predict the mean compartment value. The second problem is to estimate the error introduced by the evaluation technique itself ie. by the fact that that the integral is approximated by a summation of mean values throughout the computational surface. This error is known as the 'numerical process error' by HENRICKSON AND NASH (1970, p 4017) and applies mainly to methods which use a grid approach in the evaluation. It will vary in the present study according to which zone is being treated (see section 6.2), but because a Rice Rings approach is used to evaluate the critical zone of the computation it need not be considered in this analysis.

Because of a general lack of observational data and the problems mentioned above, error analyses have been concentrated on different approaches to the method of analysis, the numerical error of evaluation on adopting the grid approach, or the evaluation of the error in deflections due to failure to account for the gravity field in the middle to outer zones. For example, KAULA 1957 (in what is basically a covariance analysis of the accuracy of gravimetrically computed deflections) used rms values of the mean anomalies of certain sized areas and the cross-correlation between these areas which were derived from analyses of two long gravity profiles in south-central United States. To assume that such an analysis is applicable in all other regions has already been shown to be doubtful, particularly for localised regions (see section 5.3.3), but nevertheless the paper gives important insight into the errors resulting in deflections due to either the stated uncertainties or the neglect of the gravity field beyond certain radii. HENRICKSON AND NASH (1970), in a similar approach to the analysis based their theoretical estimate of the error in the gravity anomaly on the drift pattern of the gravimeter and the pattern of the gravity survey (the work is mainly applicable to gravimetric surveys at sea) and a particular discrete sum algorithm for the Vening Meinesz integral based on a grid subdivision of the surface. OBENSON (1970; 1973) uses estimates of accuracy based on covariance functions for the gravity anomalies, and finds the induced error in the deflection using a rectangular grid in the evaluation of the Vening Meinesz integral similar to that developed by Fischer (section 4.2.2). WROBEL (1967) is more concerned at finding the errors in the differences of deflections in order to improve on astro-gravimetric interpolations of these deflections. NAGY AND PAUL(1973) experiment with different combinations of errors for surveyed and unsurveyed regions to find the resultant error in the geoid height at various locations on the Earth's surface. Thus it can be seen that the bulk of the papers written on this subject whilst giving insight into the techniques which can be used in error analysis, are not directly related to this particular study because of the differences in computational and prediction techniques.

The effects of errors in data and of the interpolation method on the mean compartmental value are

considered in section 7.2, whilst the actual effect these errors have on the computed deflection are evaluated in section 7.3. An estimate of the accuracies in the correction terms is presented in section 7.4.

7.2 Errors in the Data

7.2.1 Point Free-Air Anomalies

The usual method of gauging the accuracy of an observation, ie. by repetition and subsequent analysis of the discrepancies of the individual observations from some superior estimate of the observation such as the mean value, is not available in this case as repeated and independent determinations of gravity and height for each gravity station was not practicable. It is therefore necessary to rely on experience, *a priori* determinations and check readings to provide this estimate of accuracy.

As described in section 4.1.1 the techniques adopted for fixing the height of a gravity station varied from precise EDM trig. levelling for some stations close to the computation point to the less rigid method of barometric levelling for more distant points. This means that errors in the differences in the free air anomalies as a result of uncertainties in height will vary from negligible amounts to about ±0.3 mGal, depending on, in general, the situation of the gravity station. The errors in the observed gravity itself may be larger than this, although because of the organisation of the gravity traverses (see table 1, section 4.1.1) it seems reasonable to assume a standard error in the gravity reading of less than ±0.3 mGal. (Certainly this figure is borne out from the checks taken on stations from different field trips. Values are also in general agreement with the Bouguer anomalies interpolated from the BMR gravity maps). It appears justified therefore (as the gravity model can be taken as error-free) to assume a standard error in the free-air anomaly to range from about ±0.2 mGal to about ±0.4 mGal. As stated in section 4.1.1, the accuracy quoted for the BMR Bouguer anomalies is $\frac{1}{2}$ ±1 mGal, and this data was used in the more distant compartments of the inner zone computation, with extra observations to intensify the field where necessary.

Correlation will exist between errors in the anomaly values at some gravity stations, eg. stations fixed in gravity on the same gravity traverse or in height on the same barometric levelling run. In the critical area, however, the heights of the gravity stations will have been independently fixed (the only connection being the height of the computation point which is, in any case, assumed error free). Although correlation will exist in the gravity values, it can be shown that the relative accuracies of anomaly values at successive stations is in fact higher than the values for the standard error quoted above. Zero correlation is assumed in the absence of any definitive estimate of correlation. It is felt unwarranted in view of the comments in section 5.3.4 to invoke covariance methods for this purpose.

7.2.2 Mean Compartmental Anomaly

In the computational technique adopted the predicted value for the mid-point of a compartment was used as an estimate of the mean anomaly of that compartment. The accuracy of this estimate depends on two main factors; (i) the interpolation procedure and the relationship of the circumscribing triangle (see section 5.2.3) to the compartment, (ii) the nature of the topographic and the anomaly surface and the size of the compartment. These aspects will now be treated in turn.

(i) The accuracy of the interpolated point will be dependent on 2 factors, firstly the errors in the data discussed in 7.2.1 above and secondly the nature of the interpolation. This latter effect

is known as the 'pure interpolation error' and is considered in detail in (MOLODENSKII ET AL 1962, p 171) and (BROVAR ET AL 1964, pp 280-282). For a survey of normal density (ie. about 1 point per 1000 km^2) the pure error of interpolation of free air anomalies for plain areas amounts to ±7.0 mGal, whilst in mountain areas this error reaches ±28 mGal for free-air anomalies and ±11 mGal for Bouguer anomalies (IBID, p 281). In the present study point density is higher than this, particularly in the closer compartments. In fact for these close compartments the interpolation error must be almost negligible and the error in the interpolated value(s) must approach that of the standard error of the closest gravity stations.

It is, of course, possible to find the error in the interpolated station by means of an error analysis of the interpolation formula (equation 5.3).

If

$$\alpha_i = \frac{(x_i - x)(y_k - y_j) - (y_j - y)(x_k - x_j)}{(x_i - x_k)(y_k - y_j) - (y_j - y_i)(x_k - x_j)} \qquad i = 1, 3$$

where $\begin{matrix} j \\ k \end{matrix} = \begin{matrix} i+1 \\ i+2 \end{matrix}$, unless $\begin{matrix} j \\ k \end{matrix} > 3$, where $\begin{matrix} j \\ k \end{matrix} = \begin{matrix} i+1-3 \\ i+2-3 \end{matrix}$

then $$z_q = \sum_i \alpha_i z_i \qquad , \qquad i = 1, 3 \qquad (7.1) .$$

By the law of the combination of variances,

$$\sigma_d^2 = \alpha_1^2 \sigma_z^2 + \alpha_2^2 \sigma_{z2}^2 + \alpha_3^2 \sigma_{z3}^2 \qquad (7.2) .$$

Now this expression can be used to estimate the error in the Bouguer anomaly and the height at the interpolated station, where the coefficients α_i will differ for the anomaly and height prediction in areas with height augmentation. In areas defined only by the anomaly points, the z_i in equation 7.1 are the free-air anomalies.

(ii) It is also necessary to gauge the accuracy of the value interpolated as a representative value for the compartment. This 'pure' error of representation will obviously be a function of the anomaly or terrain smoothness in the region of representation. For example, investigations reported in (BROVAR ET AL 1964, pp 278-279) show that for fairly flat regions and 'normal' survey density (1 point per 1000 km^2) the error of representation of the free air anomaly is ±7 mGal, whilst in mountainous regions the same error is ±25 mGal and about ±13 mGal for the Bouguer anomaly.

In fact, if the pure error of representation of the anomaly ($\delta g'$) is assumed to be a function of the dimensions x and y of the rectangle the anomaly is meant to represent, it has been found by empirical means that

$$\sigma_p = c' (x^{\frac{1}{2}} + y^{\frac{1}{2}}) \qquad (7.3)$$

where x , y are the dimensions of the rectangle being represented in km, and in regions of average disturbance, $c' = \pm 0.54$ mGal $km^{-\frac{1}{2}}$. When the density of the gravity stations is increased the pure error of representation may be expressed by

$$\sigma_p = \pm 0.24x \text{ mGal} \qquad (7.4)$$

where x is the distance between gravity stations in km.

The magnitudes of the errors of representation for flat areas, with a single station every 3 to 4 km^2 is found to be (IBID, p 280)

Square side (km)	σ_p (mGal)
5	1.5 ± 0.1
10	2.8 ± 0.2
20	4.4 ± 0.4
30	7.0 ± 0.6

By combining the measurement error with the pure error of representation it is possible to estimate the total representation error of each predicted point. It is found, on an actual comparison of the predicted values against mean values obtained graphically, that this error is of the order of 0.5 to 3.0 mGal (depending on terrain) for compartments predicted by means of a plane triangle fit. Good agreement is obtained partly because the gravity stations (and, where applicable, the height points) were chosen points of change of grade on the surface so that the mid point value will indeed give a good estimate of the mean value if the circumscribing triangle used in the interpolation process contain the compartment. This was achieved by varying the compartment sizes at different stages of the computation. In fact, in the outer rings where a least squares plane was fitted to seven points (see section 5.2.2) the compartmental contribution dropped to a third that of the earlier stages of the computation, helping to control the pure errors of representation in these rings.

It is impossible to obtain an exact estimate of the error of representation without a fully digitised terrain or anomaly model. In fact, even the comparisons above contain the errors in the graphical interpretation estimated by Rice to vary from of the order ±0.2 mGal for distances up to 500 m, to ±5 mGal for the outermost rings (RICE 1962, p 293). In the circumstances it is obvious that the graphical analysis must achieve a higher order of accuracy than the computerised approach, and one could use the error of representation quoted above as the figure for the subsequent error analysis. However, this would not reflect the different pattern of gravity and height points used in the deflection computation for each computation point. It seems more realistic to use an expression combining the error in the value of the midpoint as found from the geometry of the interpolating triangle with the pure error of representation (see equation 7.7).

7.3 Errors in the Gravimetrically Determined Deflections of the Vertical

7.3.1 The Innermost Zone

From expressions (6.3a), (6.3b) the error relationships for the innermost zone can be derived, namely

$$\partial\xi = 0''.105\ r_o\ \partial\left(\frac{\delta\Delta g}{\delta x}\right) \qquad (7.5)\ ,$$

with an analogous expression for $\partial\eta$.

As a consequence of the manner in which the gravity gradient is determined, it is seen that

$$\partial\xi = \frac{c}{2}\left(\frac{\delta\Delta g'_1}{2} + \delta\Delta g'_2 + \frac{\delta\Delta g'_3}{2}\right),$$

where $\delta\Delta g'_i$ = the error in the gravity gradient determined for the i th N-S gradient line in this zone,

and $c = 0.105\ r_o/\delta x$ arcsec.

On assuming zero correlation between successive gradient lines,

$$\sigma^2_\xi = \frac{c^2}{4}\left(0.25\ \sigma^2_{\Delta g'_1} + \sigma^2_{\Delta g'_2} + 0.25\ \sigma^2_{\Delta g'_3}\right) \qquad (7.6)$$

Since in the present evaluation the r_o value is small (100 m), the Bouguer anomaly can be assumed constant and the free air anomalies will be a reflection of the terrain heights. If the heights at the cardinal points were taken from the 1:31 680 maps with 25 ft (≃ 6.5 m) contours they will be accurate to about 10 ft (≃ 3.0 m) (≃ 1 mGal) and the $\sigma^2_{\Delta g'}$ will be of the order of 2 $mGal^2$. Substitution of these values in equation (7.6) produces a error in the deflection of about 0.1 arcsec. This is not insignificant and shows the potentially critical nature of the computation in this innermost zone.

The following comments should be made concerning this phase of the computation,

(i) The effect of the error of representation on the gravity gradient will be very small because of the local nature of the computation (see equation 7.4). However, for central zones extending up to 4 km from the computation point this will increase the standard error in the gravity gradient markedly, particularly in broken terrain.

(ii) If reliable large to medium scale maps are not available, the uncertainty of the gravity gradient will increase and the innermost zone should be fixed by field survey. In the absence of a proper survey it would be of value to obtain an estimate of the gravity gradient in the field by using the gravimeter as an altimeter. Over such small distance it is feasible to assume the Bouguer anomaly constant and hence any changes in gravity will be due mainly to changes in height.

(iii) RICE (1962, p 293) estimates the effect of the innermost zone for station computed to about 0.01 arcsecs over a radius of about 280 m. This estimate is apparently based on a comparison of the values obtained from the three cardinal lines used in the evaluation and reflects the relatively smooth nature of the anomaly field in this area particularly when compared to the more difficult stations in the present test.

7.3.2 The Inner Zone

One advantage of the rings approach to the computation of the deflection is the relative simplicity of the error analysis of values evaluated by this method. For example Rice (IBID, p 293) adopted a value for the probable error for the mean anomaly of each compartment which was a function of the radius of that compartment. Using the average value of $\cos^2\alpha$ and $\sin^2\alpha$ for all sectors in one ring as 0.5, the expression for the expected error in the deflection (E_t) is given as

$$E_t^2 = 18\ \Sigma(E_r \times 0.001)^2\ \text{arcsec}^2\ ,$$

where E_r = expected error of the mean anomaly per compartment.

Rice deduces that the 'precision' (apparently the probable error) for the contribution of gravimentric deflection up to $\psi \simeq 5^{o}$ as determined in this manner is of the order of 0.1 arcsec.

Molodensky (MOLODENSKII ET AL 1962, pp 174-177) in a formal development assuming a uniformly accurate gravity map for the entire Earth shows that the resultant error in the deflection is

$$\delta\xi'_j = \pm \frac{1}{\sqrt{2}\gamma} \delta g' = \pm 0''.15 \quad \delta g' \qquad j = 1, 2$$

where $\delta g'$ is the error of representation in mGal.

Using a mean distance between gravity stations of $2X$ and a template of rings whose radii are $(2n \pm 1)\ X$, n being the number of the ring, the error in the deflection owing to the n-th ring may be written as

$$\delta\xi' = \frac{1}{2\pi\gamma} \ell n \left(\frac{2n+1}{2n-1}\right) \Sigma \cos^2 \alpha (\Delta\alpha)^2 \quad \delta g'$$

where $\Delta\alpha$ is the step in the azimuth or apex angle for a compartment. This expression leads to the conclusion that, for this particular array of points the standard error in the deflection introduced by errors in the gravity field beyond the radius X is $\pm 0''.063\ \delta g'$. If the data field in the present study is idealised to give an X and $\delta g'$ (as averaged for the inner zone region) of 5 km and ±2 mGal the error in the deflection due to the contribution of this region would still only be $0\ \{\pm 0''.15\}$.

For the technique adopted in the present study it is possible to compute the expected error of representation (σ_r). The error in measurement (σ_d) is derived from equation (7.2), where $\sigma_{\Delta g} = \pm 0.3$ mGal if a surveyed point, $\sigma_{\Delta g} = \pm 1$ mGal if a height from the map (the $\sigma_{\Delta g}$ of the Bouguer anomaly is assumed to be swamped by the errors in the height). The pure error of representation (σ_p) is based on equation (7.3) where the compartment is approximated as a trapezium, x being the base and y its height.

Hence

$$\sigma_r^2 = \sigma_d^2 + \sigma_p^2 \qquad (7.7)$$

This error is then split into its two components and standard deviations obtained for both components of the deflection.

The results of the initial analysis, using a value of $0''.54$ for c' in equation (7.3) for all predicted points, are listed in columns 1 and 2 of table 10. It can be seen that

(i) the error is very small ($\simeq .06$); and
(ii) there is little change at different computation stations.

In an attempt to make the analysis reflect more accurately the influence of terrain types on the σ_p^2, a value for c' of 3.0 mGal $km^{-\frac{1}{2}}$ was used in hilly to mountainous areas as opposed to the value of 0.54 for the flatter regions. The resultant estimate is felt to be too high, but relative accuracies do now reflect the type of terrain in the computation region (see columns 3 and 4 table 10). (It is interesting that the values in the flatter areas approximate the $0''.15$ estimated from Molodensky's approach mentioned above). The exception to this comment is Willalla where neither the accuracy of the gravity nor the density of the station are properly reflected by the estimates obtained.

	ANALYSIS 1		ANALYSIS 2		ANALYSIS 3	
	1 σ_ξ	2 σ_η	3 σ_ξ	4 σ_η	5 σ_ξ	6 σ_η
1. Culgoora	0.06	0.06	0.10	0.19	0.10	0.19
2. Beelera	0.06	0.06	0.13	0.24	0.14	0.24
3. Willalla	0.06	0.06	0.14	0.19	0.14	0.19
4. Binalong	0.06	0.06	0.17	0.21	0.18	0.22
5. Goonbri	0.08	0.08	0.31	0.30	0.31	0.30
6. Byar	0.08	0.08	0.32	0.33	0.32	0.33
7. Kaputar	0.07	0.07	0.29	0.31	0.29	0.31
8. Blue Nobby	0.08	0.08	0.31	0.32	0.32	0.33
9. Gulf Creek	0.07	0.07	0.30	0.29	0.30	0.29
10. Newry	0.07	0.07	0.33	0.32	0.34	0.33
11. Baldwin	0.09	0.08	0.32	0.31	0.33	0.31
12. Somerton	0.06	0.06	0.31	0.27	0.31	0.28

TABLE 10 EXPECTED ERROR FOR INNER ZONE COMPUTATIONS

Analysis 1: $\sigma_r^2 = \sigma_d^2 + \sigma_p^2$ where $c' = 0.54$ throughout

Analysis 2: As above ; $c' = 0.54$ in plains) in equation (7.3)
$c' = 3.00$ in hilly country)

Analysis 3: As for 2, except $\sigma_p^2 = c'^2(x^{\frac{1}{2}} + y^{\frac{1}{2}})^2 + (0.24)^2 \ m^2$; m = minimum distance in equation (7.4).

In an attempt to make the estimates more sensitive to the differences in gravity density, a third analysis was performed which included a factor for the distance of the prediction point from the nearest known point in σ_p. Equation 7.4 was used for this, x being the minimum distance in km in this case. However, as can be seen from columns 5 and 6 of table 10, this new factor had little impact on the results.

For a proper analysis each height and gravity point should have an independent estimate of accuracy based on the factors mentioned in section 7.2.1. However, the data error is only effective out to about ring 12 (4.5 km), the σ_p adding little to the total error thus far. Beyond this the pure error of representation dominates because of the larger compartmental sizes. Because of this it is felt reasonable to adopt a general value for errors in data for these closer points, noting that, because of the survey methods used, they are likely to be overestimates of the real values.

It is a feature of computation of the deflections that systematic error will cancel provided, of course, it is symmetrical about the computation point. As symmetry is likely to be present in the systematic errors (eg. in the heights of points extracted from maps based on the same control system, in gravity data based upon a common datum point and even in the interpolation technique adopted for prediction) it is reasonable to assume for the inner zone computations that systematic errors have little effect on the precision of the computation.

7.3.3 The Outer Zone

The values for the outer zone contribution to the deflection had, as explained in section 6.2.3, been computed as part of the 1970 geoid solution for Australia by MATHER (1970a) and it is interesting to consider the estimates of accuracy for this contribution. As the outset the following points should be made.

(i) The random errors in data must be large to have any great impact on the accuracy of the computed values of the deflections.

(ii) Because of the asymmetry of the test area with respect to the Australian continent and hence the distribution of observed gravity data, similar asymmetry is expected in the accuracy of the data. It should be noted that the field to the west which is based on land survey extends for about 36°, whilst to the east the relatively sparse ocean gravity surveys as supplemented by predictions for completion of representation start at about $\psi = 3^{\circ}$. Accuracy of data in the north-south direction is roughly symmetrical, the coast being about 5 to 6 degrees away in both cases.

(iii) Whilst it is possible to obtain realistic assessments of accuracy when data is plentiful, such assessments become more formal in sparsely populated areas such as ocean regions, and accuracy assessment becomes far less meaningful due to the inability to realistically estimate the correlated components of the error of prediction.

MATHER (1968, pp 173-198) shows in full the method he used to estimate the accuracies of representation for various square sizes, and this is not repeated in the present development.

It is interesting to note that an expression similar to that in equation (7.7) is used to get the final statement of accuracy, viz.

$$e_p^2 = e_{rep}^2 + e_{ext}^2$$

where e_p^2 = the error in the prediction
e_{ext}^2 = the error due to the 'extension' of the field and

e^2_{rep} = the error of representation (equivalent to the 'pure' error of representation above).

e^2_{ext} depends on the method used to interpolate/extrapolate from the known field to the 'predicted' field and the accuracy of the known data and is determined by experiment (IBID, pp 194-196). The e^2_{rep} is estimated by analysis of the amount of known data in the represented area (IBID, p 192). This method of estimating errors fails because

$$e_p = \pm(e^2_{ext} + e^2_{rep})^{\frac{1}{2}} + e_{sys}$$

where e_{sys} is the systematic component in e_p whose magnitude cannot be estimated.

The final computations included a statement of the expected standard error and these proved, at least by formal analysis to be negligible for each of the outer, middle and near zones, being of the order of .002 arcsec in each case.

7.4 Errors in Terrain Correction Terms

Because of the similarity in the technique developed to evaluate G' with that used in the inner zone computations, the error analysis developed for the deflection evaluation were adapted to obtain estimates of errors in G'.

From section (4.3.2),

$$G' = \sum_i c_i \, \Delta h_i \, \Delta g_i \quad , \quad \text{where} \quad i = \text{compartment number}$$

so that

$$\sigma^2_G = \sum_i c_i^2 \, (\Delta h_i^2 \, \sigma^2_{\Delta g_i} + \Delta g_i \, \sigma^2_{\Delta h_i}) \tag{7.8}$$

An expression similar to equation (7.7) is used to find σ^2_r, except that the error in gravity and height are analysed separately. The error in the gravity value is taken as ±0.3 mGal, and the error in the height data is taken to be either ±1 m (for a gravity station) or ±3.3 m (for a height value from a map). This means that separate errors of interpolation and 'pure' representation are found for both gravity and height (assuming no error in either parameter at the computation station). Variances in each predicted value of G' can be estimated according to (7.8) and summed through the whole G' computation.

It is not feasible to quote the estimates of errors for all values of G' computed for they are very small. For example the values around Kaputar (where the error would be largest) is only 4×10^{-4} mGal. Differences between manual and computer determined values were certainly larger than this (≃1-2 mGal), but this theoretical estimate does demonstrate the stability of the approach.

Because of the difficulties encountered in accurately evaluating the 'Arnold' type correction terms it was considered impracticable to carry out an analysis on this computation. It would be possible to do this by using the errors in the heights as determined above to find the errors in the ground slopes and then the effect these have on the correction term, but the discrepancies apparent in this technique rendered the effort of such an exercise to be of limited value.

8. ANALYSIS OF RESULTS

8.1 Introduction

In a comparative analysis which follows the parameters which are of interest are

$$\begin{aligned} \Delta\xi &= \xi_{A/G} - \xi_G \\ \Delta\eta &= \eta_{A/G} - \xi_G \end{aligned} \qquad (8.1)$$

ie. the difference in each component between the astro-geodetic and the gravimetric deflections of the vertical (ξ_G , η_G). These differences are listed for each station in column 6 of table 11, and are found by subtraction of the column 2 values (of this table) (transferred from row 7 of table 6) from the column 5 values (transferred from column 11 of table 3).

The quantities which result from a statistical analysis of $\Delta\xi$, $\Delta\eta$ are

(i) their mean values $(\mu_{\Delta\xi} , \mu_{\Delta\eta})$, which will show any systematic errors in the differences, and

(ii) the standard errors $(\sigma_{\Delta\xi} , \sigma_{\Delta\eta})$ which will enable an estimation of the accuracy of the gravimetrically determined deflections.

As a first step the astro-geodetic deflections will be assumed error-free (sections 8.2 & 8.3). Estimates of the errors in these parameters will be included in the subsequent analysis in section 8.4.

A superficial review of the discrepancies shows that it is reasonable to separate the analysis of the ξ component from that of the η component. The ξ components are generally in good agreement whereas the η components are more discrepant and a detailed review of these values must be undertaken. It is also valuable to separate those stations only marginally affected by terrain effects from those which are apparently subject to these corrections. For this purpose the stations were divided into two categories as follows:-

Category	Description	Stations
1	Stations marginally effected by terrain effects.	Culgoora, Beelera, Binalong, Somerton.
2	Stations apparently subject to terrain effects	Goonbri, Byar, Kaputar, Blue Nobby Gulf Creek, Newry, Baldwin

As will be demonstrated, Willalla, with large discrepancies in both ξ and η which fail the 3σ test for acceptance, will be deleted from consideration. It will be remembered that the survey at this station was never completed satisfactorily and no confidence was placed in the gravimetric value at this station (see section 4.1).

1	2	3	4	5	6 Δξ / Δη 7 (A/G - GRAV.)		8 Δξ / Δη w/o systematic	9 (0.06 / 1.47
NAME (Category)	GRAVIMETRIC ξ_G η_G	CORRECTION FOR TERRAIN ξ' η'	CORRECTED G. GRAVIMETRIC ξ_G η_G	A/G $\xi_{A/G}$ $\eta_{A/G}$	W/O CORRECTION	WITH CORRECTION	W/O CORRECTION	WITH CORRECTION
1. Culgoora	+1.14	-	+1.14	+1.27	+0.13	+0.13	+0.07	+0.07
(1) (i)	-9.84	-	-9.84	(-9.56)	(+0.28)	(+0.28)		
(ii)	"	-	"	-8.40	+1.44	+1.44	-0.03	-0.03
2. Beelera	-0.13	-	-0.13	-0.19	- .06	- .06	-0.12	-0.12
(1)	-9.41	-	-9.41	-9.38	(+ .03)	(+ .03)(?)	-	-
3. Willalla	+1.36	-	+1.36	+0.20	(-1.16)	(-1.16)(?)	-	-
-	-7.62	-	-7.62	-4.76	(+2.86)	(+2.86)(?)	-	-
4. Binalong	+1.51	-	+1.51	+1.77	+0.26	+0.26	+0.20	+0.20
(1)	-5.38	-	-5.38	-4.02	+1.36	+1.36	-0.11	-0.11
5. Goonbri	-1.50	-0.20	-1.70	-1.62	-0.12	+0.08	-0.18	+0.02
(2)	-8.93	-0.16	-9.09	-7.56	+1.37	+1.53	-0.10	+0.06
6. Byar	-5.60	-0.38	-5.98	-5.67	-0.07	+0.31	-0.13	+0.25
(2)	-11.85	-0.06	-11.91	-10.94	+0.91	+0.97	-0.56	-0.50
7. Kaputar	+3.15	-0.64	+2.51	+2.32	-0.83	-0.19	-0.77	-0.13
(2)	-12.27	+0.19	-12.08	-10.26	+2.01	+1.82	+0.54	+0.35
8. Blue Nobby	+5.25	-0.53	4.72	+4.73	-0.52	+0.01	-0.58	-0.07
(2)	-3.96	+0.25	-3.71	-4.47	(-0.51)	(-0.76)(?)	-	-
9. Gulf Creek	1.54	+0.13	1.67	+1.54	0.00	-0.13	-0.06	-0.19
(2) (i)	-6.93	+0.13	-6.80	-5.54	+1.39	+1.26	-0.08	-0.21
(ii)	"	"	"	(-4.30)	(+2.50)	(+2.37)(?)		
10.Newry	-1.20	0.00	-1.20	-1.30	-0.10	-0.10	-0.16	-0.16
(2)	-5.19	+0.14	-5.05	+2.89	+2.30	+2.16	+0.83	+0.69
11.Baldwin	-5.57	-0.20	-5.77	-5.47	+0.10	+0.30	+0.04	+0.24
(2)	-7.20	+0.10	-7.10	-5.83	+1.37	+1.27	-0.10	-0.20
12.Somerton	-1.82	-	-1.82	-1.75	+0.07	+0.07	+0.01	+0.01
(1)	-8.80	-	-8.80	-7.36	+1.44	+1.44	-0.03	-0.03

TABLE 11 COMPARISON OF GRAVIMETRIC AND ASTRO-GEODETIC DEFLECTIONS OF THE VERTICAL

		1	2	3	4	5	6	7
ξ	No. in Sample	12	12	11	4	7	11	7
	$E(\mu_{\Delta\xi})$	-0.11	-0.19	-0.10	+0.10	-0.22	+0.06	0.04
	$E(\sigma_{\Delta\xi}) \pm$	2.5	0.43	0.31	0.13	0.33	0.18	0.20
	$\overline{\sigma}_{\xi A/G} \pm$	N.A.	N.A.	0.17	0.18	0.16	0.17	0.16
	$E(\sigma_{\xi G}) \pm$			0.26	0	0.29	-	0.12
η	No. in Sample	12	12	9	3	6	9	6
	$E(\mu_{\Delta\eta})$	1.20	1.33	1.51	1.41	1.56	1.47	1.50
	$E(\sigma_{\Delta\eta}) \pm$	1.44	0.91	0.41	0.05	0.50	0.34	0.43
	$\overline{\sigma}_{\eta A/G} \pm$	N.A.	N.A.	0.21	0.19	0.22	0.24	0.22
	$E(\sigma_{\eta G}) \pm$			0.35	0	0.45	0.26	0.37

Legend

Column 1: Comparison A/G with 1970 Gravimetric Geoid Solution Values
2: " " " All Stations included
3: " " " Stations Failing 3σ test rejected
4: " " " Category One Stations
5: " " " Category Two Stations without Terrain Corrections
6: " " " All accepted stations - after applying terrain corrections
7: " " " Category Two stations - after applying terrain corrections

TABLE 12 COMPARISON OF DIFFERENCES - MEANS AND STANDARD ERRORS

8.2 Comparison of Gravimetric and Astro-Geodetic Deflections before Applying Terrain Correction

8.2.1 All Stations included in the Analysis

In the first instance all stations will be considered without reference to their categories. A statistical analysis of $\Delta\xi$, shows the following:-

		$E(\mu_{\Delta\xi})$	$E(\sigma_{\Delta\xi})$
(i)	with Willalla	-0".19	±0".43
(ii)	without Willalla	-0".10	±0".31

The $\Delta\xi$ for Willalla differs from $E(\mu_{\Delta\xi})$ above by $0\ \{\pm1".0\}$. This difference increases to 1".26 when the better estimate for $E(\mu_{\Delta\xi})$ of +0".1, found in section 8.2.2(a), is used. This shows the $\Delta\xi$ for this station to be unreliable as its difference equals the 3σ limit which is set by the above analysis. A similar analysis of the η component is not possible at this stage due to the larger discrepancies which exist in $\Delta\eta$. A study of these elements now follows for the problem values.

(i) It will be noted that there are two values for $\Delta\eta$ at Culgoora resulting from two determinations of $\lambda_{A/G}$ at this station. The first value (-9".56) which results from 7 pairs on one night's determination of λ gives good apparent agreement with the η_G whilst the second value (-8".40), the product of 3 nights' observations (26 pairs) for λ, produces a discrepancy of +1".44. Because this $\lambda_{A/G}$ is more precise and because the general disagreement ($\Delta\eta$) in the region appears to be of the order of +1".5 it was felt from all viewpoints that the second value was the most reasonable one to choose.

(ii) The η_G at Beelera, whilst in apparent good agreement with the $\eta_{A/G}$, does not reflect the general systematic difference of +1.5 in this component. There is no apparent reason for this (eg. terrain effects will be negligible) and the $\Delta\eta$ will be treated with caution.

(iii) On the basis of earlier remarks Willalla will be dropped from the analysis.

(iv) The value of $\Delta\eta$ at Blue Nobby is also greatly discrepant, being about 2".0 less than the mean difference in η. There is no apparent reason for this, the corrections for terrain to the η_G not being expected to exceed ±0".5 and the internal precision of the $\eta_{A/G}$ being quoted as ±0".2. The value easily fails the 3σ test and it is reasonable to delete it from the consideration.

(v) There are two values given fro the $\eta_{A/G}$ on Gulf Creek which, as for Culgoora, are the result of different determinations of $\lambda_{A/G}$ for this station. The -4".30 value which was determined in 1969 from 18 pairs has an internal precision of ±0".32, whilst the -5".54 value determined in 1968 from 28 pairs has an internal precision of ±0".19. Whilst this second value is apparently more precise it is not significantly so, but since the difference of the earlier value (+1".39) compares much more favourably with the average than the later it appears reasonable to accept this earlier determination as the $\eta_{A/G}$ for this station. Otherwise the station would have to be dropped altogether from the analysis.

In the cases above where two values have been listed for $\eta_{A/G}$ the value rejected has been bracketed in the table. Using the values accepted, an analysis of the 9 stations remaining gives an $E(\mu_{\Delta\eta})$ of 1".51 and an $E(\sigma_{\Delta\eta})$ = ±0".41 (see column 3 of table 12).

It should be noted at this stage that whereas the $E(\mu_{\Delta\xi})$ is small and all well-surveyed stations

are in reasonably good agreement. On allowing that the gravimetric deflections may receive corrections for terrain effects of up to 0".5, the $E(\mu_{\Delta\eta})$ is large (≈1".5). Analysis of the gravity field suggests that this is probably due to the weakness of the gravity field about 3° east of the test area (see section 7.3) which is introducing a systematic effect into the η_G. A similar effect was found by FRYER (1970, p 82) where computation of the orientation parameters for the AGD onto the geocentric ellipsoid using only stations in or near NSW revealed a value for $\Delta\eta_o$ of -5".52 instead of the -3".97 value obtained on the basis of comparisons for the whole of Australia. Use of the NSW-derived parameters in fact produces agreement of η_G with $\eta_{A/G}$. On the other hand this does not explain the large discrepancies existing at some of the stations in this prime vertical component. The astro-geodetic values for η must be treated with caution, particularly when differences such as those cited at Culgoora and Gulf Creek occur. This argument is strengthened when it is remembered that the gravimetric determinations for η uses exactly the same inner zone data and computational technique as the determinations for ξ. However, the determinations for $\phi_{A/G}$ and $\lambda_{A/G}$ (and hence $\xi_{A/G}$ and $\eta_{A/G}$) involve distinctly different observational techniques, it being widely recognised that the $\phi_{A/G}$ determination is of higher accuracy than that of $\lambda_{A/G}$ (BOMFORD ET AL 1970, p 1). Since agreement in ξ is good this tends to confirm the accuracy of the gravimetric approach. It appears likely therefore that discrepancies in $\Delta\eta$ from the mean are due to errors in the values of $\eta_{A/G}$.

Whether or not this is the case, it is certainly feasible and desirable to continue the analysis for ξ and η separately. This will allow a proper estimate of the systematic error in the two components to be made. Finally, because of the different variances for the astro-geodetic ξ and η, two separate estimates of the precision of the gravimetric calculation can be made.

It is also of interest to compare these values with equivalent values taken from the 1970 geoid solution (listed in column 1 of table 12). They are found to be $E(\mu_{\Delta\xi})$ = -0".17 ±2".5 and $E(\mu_{\Delta\eta})$ = +1".57 ±1".44. It appears from these values that without an accurate definition of the inner zone gravity field, an accuracy of only ±1".5 to ±2".5 for the gravimetric computation can be expected. This accords generally with the value quoted by Fryer for the continent-wide comparisons of ±2".0 and ±2".5 for $\Delta\xi$ and $\Delta\eta$ (FRYER 1970, p 79). On the other hand, these 'errors' do appear to be random, producing quite good agreement in the $E(\mu_{\Delta\xi})$, $E(\mu_{\Delta\eta})$ values which differ from those computed from the more precise determination by approximately ±0".2 to ±0".3.

It can be tentatively concluded that proper field definition and computational techniques introduces significant improvement in the accuracy of the deflections computed gravimetrically (from say ±2".0 to ±0".5), and that the discrepancies in the less accurate determination appear to be random, producing reasonable agreement in the mean differences.

8.2.2 Comparisons according to category

(a) The $\Delta\xi$, $\Delta\eta$ for stations in category 1 (ie. those unaffected by terrain) can be anlysed using only those values accepted in section 8.2.1 above. These are listed in column 4 of table 12 and show values of +0".10 and ±0".13 for $E(\mu_{\Delta\xi})$ $E(\sigma_{\Delta\xi})$ respectively for the 4 stations involved, whilst $E(\mu_{\Delta\eta})$, $E(\sigma_{\Delta\eta})$ for the 3 stations used are +1".41 and ±0".05. Although the sample is small this provides an estimate of the accuracy attainable for computation stations located in well-surveyed areas of low topographic relief. These values also provide an unbiased estimate for the systematic differences. It appears as if the mean difference should be +0".1 in ξ and +1".4 in η, compared with the values obtained in 8.2.1 above of -0".1 and 1".5 respectively.

(b) An analysis for stations in category 2 is shown in column 5 table 12. For a population of 7 in

$\Delta\xi$ the expected mean with standard error is -0".22 ±0".33, whilst in $\Delta\eta$ (population 6), these parameters are +1".56 ±0".50. A number of points should be noted with these figures.

(i) It appears that in areas of hilly to mountainous terrain, provided the free-air gravity field is well defined, an accuracy of about 0".5 can be achieved without applying terrain corrections.

(ii) This comment must be qualified by the remark that many of the stations in this category eg. Goonbri, Gulf Creek, Newry and Baldwin are located on hills which are both symmetrical and isolated (see figs. 14, 18, 19, 20) giving values of -0".03 ±0".10 and 1".61 ±0".46 for $\Delta\xi$ and $\Delta\eta$ respectively. On the other hand the stations which are located in more mountainous and complex terrains, ie. Byar, Kaputar and Blue Nobby (see figs. 15, 16 and 17) produce values of -0".47 ±0".33 and 1".46 ±0".78 respectively. The populations are small in both cases, so definite conclusions cannot be drawn. However it is obvious that the accuracy of the second set of stations is inferior. Furthermore, whilst the standard error of the ξ component is quite good, the mean difference of $\simeq$ -0".5 differs significantly from the expected value of +0".1, suggesting that the terrain effects for these three stations have acted in the same direction. This contrasts with the η component which implies the terrain corrections are more random, although the sample here (2) is too small to allow meaningful deduction.

(iii) This systematic difference in the mean of $\Delta\xi$ is reflected in the analysis of all category 2 stations, where $E(\mu_{\Delta\xi})$ = -0".22 (see (b) above), and the same comments apply. It should be realised therefore that the improvements sought in applying the terrain correction will result in $E(\mu)$ tending toward 0".10, ie. the value obtained from category 1, and a decrease in the $E(\mu_{\Delta\xi})$.

8.3 Comparisons After Application of Terrain Corrections Computed from G'

The effects on ξ, η resulting from G' computed throughout the inner zone field were computed in section 6.4.1, and the results are transferred from columns 1 and 2 of table 9 to column 3 of table 11 for convenience. The $\Delta\xi$, $\Delta\eta$ resulting from subtracting the corrected ξ_G, η_G from the $\xi_{A/G}$, $\eta_{A/G}$ are listed in column 7 of table 11.

8.3.1 All Stations Analysed

Analysis of all stations acceptable for analysis shows that the values for $E(\mu_{\Delta\xi})$, $E(\sigma_{\Delta\xi})$ are +0".06 ±0".18 and for $E(\mu_{\Delta\eta})$, $E(\sigma_{\Delta\eta})$ are 1".47 ±0".34 as shown in column 6 of table 12. Comparing this with the equivalent analysis *before* applying terrain corrections (column 3, table 12) the following observations are made.

(i) The standard error in $\Delta\xi$ has decreased from ±0.3 to ±0.2 and the mean difference has increased from -0".10 to +0".06. The mean difference has thus moved closer to the expected value of +0".10 and at the same time the discrepancies have decreased. The improvement in the standard error can be tested by means of an F test, wherein the expected ratio of variances $F_{0.95,10,10} = 2.98$, and the actual ratio is 2.97. In other words the null hypothesis that the samples before and after correction belong to the same population is sorely tested at the 95% confidence level.

(ii) The $\Delta\eta$ exhibits a less striking improvement from 1".51 to ±0.41 to 1".47 ±0.34. There is a slight shift in the mean difference toward the estimate of this parameter from the unaffected values, ie. toward 1".41, but this is hardly significant. There is also an improvement in the standard error,

but this, in itself, would not have any statistical significance. It is felt that the small change in $E(\mu_{\Delta\eta})$ reflects the random effect of the terrain corrections on this component, whilst the comparatively small improvement in the $E(\sigma_{\Delta\eta})$ may reflect the errors present in the $\eta_{A/G}$ which have been ignored to date.

8.3.2 The Analysis of Stations in Category 2

The stations in category 2, after correction produce an $E(\mu_{\Delta\xi})$, $E(\sigma_{\Delta\xi})$ of +0.04 ±0.20 and $E(\mu_{\Delta\eta})$, $E(\sigma_{\Delta\eta})$ of 1.50 ±0.43 (see column 7 of table 12). These should be compared with the same parameters obtained before the terrain correction was applied (column 5, table 12).

(i) In the case of $\Delta\xi$ it will be seen that the move toward the estimate of the mean difference (-0".22 to 0.04) is even more striking than in 8.3.1 whereas the improvement in the standard error is roughly the same (±0.33 to ±0.20) as in that comparison. Again the F-test only just succeeds, which again casts doubt on the validity of the null hypothesis mentioned in 8.3.1(i) above. The fact that the absolute value of $E(\sigma_{\Delta\xi})$ and of $E(\sigma_{\Delta\eta})$ is smaller when all stations are included for analysis reflects the damping effect of the category 1 stations.

(ii) The comparison in $\Delta\eta$ reveals a shift toward the estimated mean difference, but it is fairly small (0".06). Again there is an improvement in the standard error, but the value after correction is still quite large (±0".43), possibly reflecting the uncertainty in the $\eta_{A/G}$ which has yet to be accounted for.

(iii) It is also of interest to consider separately the two classes of stations in category 2, viz. those on regular isolated hills and those in more rugged mountain areas. The first-mentioned class produce statistical parameters of 0".04 ±0.20 for $\Delta\xi$, 1".54 ±0.44 for $\Delta\eta$ (cf. -0".03 ± ".10 and 1.61 ± .46 respectively), (see 8.2.2(ii)), whilst the second group give 0".04 ±0.25 for $\Delta\xi$, 1.40 ±0.60 for $\Delta\eta$ (cf. -0".47 ±0".33, 1.46 ±0".78 respectively). The most striking improvement appears in the $\Delta\xi$ components of the second class, whilst the standard errors in the $\Delta\eta$ components of both classes are barely affected by the correction. The standard error in $\Delta\xi$ of the first group actually deteriorates slightly after correction. This suggests that the errors in the gravimetric deflections have attained such low proportions that the errors in the astro-geodetic deflections are now dominating the analysis. It is necessary, therefore, to extend the analysis to include the estimate of errors in the astrogeodetic deflections.

8.4 Standard Errors in Astrogeodetic Deflections included in the Analysis

8.4.1 Estimates of Accuracies of Gravimetric Deflections

The parameter which has been the basis of the analysis to date is $\Delta\xi_i$, where

$$\Delta\xi_i = \xi_{iA/G} - \xi_{iG} \qquad i = 1, 2$$

and $\xi_1 = \xi$, $\xi_2 = \eta$.

By applying the law of combination of variances to this equation, remembering that the covariance between astrogeodetic and gravimetric deflection is zero,

$$\sigma^2_{\Delta\xi_i} = \sigma^2_{\xi_iA/G} + \sigma^2_{\xi_iG} \qquad i = 1, 2 .$$

In the analysis so far $\sigma^2_{\xi iA/G}$ has been assumed zero and thus $\sigma^2_{\xi iG}$ put equal to $\sigma^2_{\Delta\xi i}$. However the basic assumption is known to be wrong and it is valuable to include the $\sigma^2_{\xi iA/G}$ in further analysis.

Estimates of $\sigma_{\xi A/G}$ and $\sigma_{\eta A/G}$ have been made in earlier studies. For example, Fryer, after consultation with A.G. Bomford of the Division of National Mapping and G.G. Bennett of the School of Surveying, UNSW, used values of $\sigma_{\xi A/G} = \pm 0''.25$ and $\sigma_{\eta A/G} = \pm 0''.45$ for observations made on an Kern DKM 3A with impersonal micrometer (FRYER 1970, pp 49-50). The estimates in the standard errors of the means resulting from analysis of the *actual observations* for ϕ and λ in the test area are quoted in column 3 of table 8. Taking the mean of these quoted errors it is found that

$$\bar{\sigma}_{\xi A/G} = \pm 0''.17 \qquad \text{and} \qquad \bar{\sigma}_{\eta A/G} = \pm 0''.21$$

using all stations in obtaining the mean. The values for these parameters used in the subsequent analysis will be the mean of the $\sigma_{\xi A/G}$, $\sigma_{\eta A/G}$ quoted for the stations used in the various analyses. These are listed in table 12 in the rows containing $E(\sigma_{\xi A/G})$, $E(\sigma_{\eta A/G})$ respectively.

It is of interest to review all the comparisons above, and obtain new estimates of the standard errors for the gravimetric deflections.

(i) Taking all stations taken without reference to category and without terrain corrections a $E(\sigma_{\xi G})$, $E(\sigma_{\eta G})$ of $\pm 0''.26$, $\pm 0''.35$ respectively, (column 3, table 12) is obtained.

(ii) Stations in category 1 (column 4), give zero (in fact, negative!) variances, implying the errors in the gravimetric deflections at these stations are relatively small or perhaps even that the $\sigma_{\xi A/G}$, $\sigma_{\eta A/G}$ are too high for these stations. However the sample is small, and little weight can be placed on this comparison.

(iii) The category 2 stations before correction (column 5) show poorer accuracy as would be expected ($E(\sigma_{\xi G}) = \pm 0''.29$, $E(\sigma_{\eta G}) = \pm 0''.45$).

(iv) After terrain corrections are applied, an analysis of all stations in the test region shows that the $\sigma_{\Delta\xi} = \sigma_{\xi A/G}$, implying that the ξ_G are subject to much smaller error whilst $E(\sigma_{\eta G})$ appears to be $\pm 0''.26$. It is tempting to suggest that, because $E(\sigma_{\xi G})$ appears to be very small and because of the probable under-estimation of the $\sigma_{\eta A/G}$, that the $E(\sigma_{\eta G})$ should in fact also approach zero (there being no apparent reason why $\sigma_{\xi G}$ should be more accurate than $\sigma_{\eta G}$) and that the $\sigma_{\eta A/G}$ should be increased slightly.

(v) Some damping occurs in column 6 to the terrain corrected terms, because when only category 2 stations are used the $\sigma_{\xi G}$ now appears to be $\pm 0''.12$ and the $\sigma_{\eta G}$ $\pm 0''.37$ (see column 7). Again, however, for no apparent reason the η_G calculates to be less accurate than the ξ_G, and again attention should be given to the value of $\bar{\sigma}_{\eta A/G}$ adopted. In fact, if a value of $\bar{\sigma}_{\eta A/G}$ is adopted to make the $\sigma_{\eta G} = \sigma_{\xi G}$, then this value would be $\pm 0''.41$, which approaches the value quoted by Fryer (IBID) for this quantity.

(vi) It is interesting to note that if the values arrived at by Fryer had been used, it would have been necessary to conclude the correct gravimetric deflections were comparatively error-free because in each case the $\sigma_{\Delta\xi}$, $\sigma_{\Delta\eta}$ is less than the ± 0.25, ± 0.45 quoted for the $\sigma_{\xi A/G}$, $\sigma_{\eta A/G}$ by him.

(vii) The estimates of $\sigma_{\xi G}$, $\sigma_{\eta G}$ above appear to be smaller than those obtained by error analysis in section 7.3. This is to be expected because, owing to the difficulty in obtaining good estimates of the errors of representation, this analysis was performed to provide the relative accuracies of the gravimetric evaluations rather than their absolute estimates. It does now appear certain however that the values used in the error analysis for the errors of representation are overstated and would need to be reviewed in future analyses.

8.4.2 ANALYSIS OF INDIVIDUAL STATIONS

It is also of interest to look at values of $\Delta\xi$, $\Delta\eta$ of those stations which receive large corrections from the G' term. For this analysis the systematic effects, as evaluated in column 6 of table 12, are removed and the resultant discrepancies listed in columns 8 and 9 of table 11.

a) Kaputar

This station is situated on a sharp drop which falls 500 m in about 600 m to the North, with a high ridge running west from the station and a high plateau extending some 3 km south (see figure 16). As a result the greatest correction is to be expected in the ξ component and this is in fact the case on evaluation, where application of the correction reduced the discrepancy from -0".77 to -0".13. The discrepancy in η is large (0".5) and is not explained in the same way, the terrain correction apparently accounting for about 0".2 of this. The $\sigma_{A/G}$ for this station is large (±0".45) and this could well be causing the large $\Delta\eta$.

Second-order effects could also be present. Pick has calculated these effects (PICK 1973) in terrain similar to that around Kaputar (except that the axis of the ridge now runs north-south), and found corrections of about 0".2 in ξ and -0".4 in η. These corrections could also be present in the opposite components at Kaputar except, judging from the map of the topography, they would attain smaller absolute values at Kaputar. Without the direct measurement of $\frac{d^2T}{dh^2}$ it is not possible to estimate this effect precisely. According to Pick an accuracy of 20 to 50 E (.02 to .05 mGal/m) is needed in this parameter, and it is felt that the equipment used in the present survey could not produce this desired accuracy.

b) Byar

Byar is situated on a mountain which exhibits symmetry along the north-south axis, but the ground drops away fairly steeply to the west (≈ 1:3) (see figure 15). Surprisingly, the terrain correction in ξ is larger in absolute terms than that in η , brought about partly by the steepness of the terrain to the north and south of the computation point and the comparatively small slope to the east. The terrain correction in ξ in fact increases the $\Delta\xi$ from -0".13 to +0".25 which in terms of the $\sigma_{\xi A/G}$ is hardly significant. The absolute value of $\Delta\eta$ is large and is only slightly improved after terrain correction (-0".56 to -0".50). There are three possible reasons for this:

(i) The η_G is poor. This is apparently supported by the fact that the $\Delta\eta$ of Newry appears too large by +0".8, suggesting an error in the gravity field between these two stations. Checks of the predicted field against the map do not show any significant discrepancy. Also, if this field is poor it should also be reflected in the ξ_G at Blue Nobby but the $\Delta\xi$ at this station is small. It is concluded that this is not the reason.

(ii) The terrain correction may be too small. Judging from the magnitudes of the corrections at

Kaputar it appears most unlikely that the correction would account for this discrepancy.

(iii) The astro-geodetic η may be in error. The stated precision for this station is ±0".2. However this value may not be a realistic estimate of absolute accuracy and it could conceivably reach a magnitude which could explain much of the discrepancy.

c) Blue Nobby

The ground at this station drops away sharply (1:2) to the north-east with a plateau to the west (see figure 17) producing surprisingly large corrections in both ξ and η . The correction in ξ appears to account for the discrepancy in this component. However, because $\Delta\eta$ has been rejected from the analysis for the reasons given in section 8.2.1(iv), it is not possible to judge the quality of the correction in this component.

d) Newry

The large discrepancy in the η at this station(and a possible reason for it) was mentioned in the discussion on Byar. It certainly could not be due to the terrain correction as the station is situated on a relatively low hill which is almost symmetrical along the east-west axis. Newry is the one station whose geodetic coordinates were not obtained by observation ie. it was not included in the recent re-observation of the network. It was in fact obtained by Lauf transformation (LAUF 1961) from original geodetic coordinates and these must be open to suspicion. As a result, although the $\Delta\xi$ is small, which apparently confirms the geodetic latitude, it is difficult to place much confidence in the $\eta_{A/G}$ at this station.

It appears that, for the rest of the stations in category 2, the terrain corrections are at the level of the expected error in the astro-geodetic deflections. The full analysis does appear to show that these corrections do improve agreement significantly. This is particularly the case in the values of ξ which are the more reliable of the two indicators of accuracy.

8.5 Arnold-Type Corrections

The correction values computed from the Arnold-type expressions (equation 6.11) show large discrepancies from the expected corrections (see columns 3 and 4 in table 9). These discrepancies cannot be explained in terms of errors in the astro-geodetic or gravimetric deflections. As has already been stated, the indirect connection between this form of the correction and the G' form (see section 3.2.1(d)) shows that the theory is sound. Therefore the discrepancies must be due mainly to the inaccuracies in the evaluation of the parameters in this correction term, particularly in the ground slope in the northerly and easterly directions.

It will be remembered from section 6.4.2 that the ground slope is estimated from the three points in the circumscribing triangle used to predict the height of the midcompartment point. Whilst this technique is successful in the height prediction it is apparently inaccurate in finding the ground slope from the same data. Inspection of table 13 shows that, for the stations most affected the corrections attain very large values (>1") within only 0.5 km of the computation point. Beyond this radius the changes are relatively small (0".2), the exception being Kaputar which continues to reflect the steep drop to the north from the ridge which bears west from this station. The obvious reason for these large corrections so close to the station is that the errors in the estimate of the slope are greatly magnified when multiplied by the $\bar{\psi}^{-2}$ factor. Such errors are not compensating as the computation proceeds around the ring.

Further investigation into the evaluation of these terms should concentrate on either better representation of the ground slope or in reorganising the terms such that some damping effect is introduced (eg. in a way similar to the devise used in the development of ξ_i at ground level in section 2.3.4, where the $\frac{\Delta g}{\gamma}$ tan β term cancels before evaluation).

An advantage of the Arnold approach is that it avoids the two distinct stages in the computation which are inherent in the G' approach. On the other hand, estimates of ξ and η must be obtained, which suggests that a Vening Meinesz solution is a prerequisite to determining terrain corrections. However it is apparent that for most stations the deflections will change slowly in the critical region of computation and it would be quite adequate to assume ξ and η to be constant in this region.

It will be recalled that the terrain correction was evaluated for each compartment and the effects accumulated through the ring. This is in contrast to the evaluation of the correction from the G' term, wherein G' was computed at each gravity station and the G' value for the compartment found by interpolation between the gravity stations. This method is theoretically more correct in that the correction is only found at points at which terrain-affected gravity has been measured. To apply corrections to gravity values which were themselves obtained only by interpolation is to correct for an effect which is strictly speaking not there. The computation was repeated at Kaputar using the proper technique but without improvement. Again the difficulty in estimating ground slope and the magnification of this problem at stations near the computation station appeared to be the source of error.

In an attempt to dampen the corrections the ground slopes were computed using only the height data at the gravity points (ie. HTBIN was ignored). This completely oversmoothened the terrain and produced nil results for all computation points.

This approach is simpler to evaluate and is not subject to the theoretical limitations as $\beta \to 45^{\circ}$ which hampers the G' correction. Disappointingly, however, it is oversensitive to ground slope errors in the critical area close to the computation station. By contrast G' requires much more computation and must be cautiously applied in steep country, but evaluation of the correction from this parameter though tedious, is fairly straightforward and accurate.

Ring No.	Outer Radius(m)	GOONBRI		BYAR		KAPUTAR		BLUE NOBBY		GULF CREEK		NEWRY		BALDWIN	
		ξ	η	ξ	η	ξ	η	ξ	η	ξ	η	ξ	η	ξ	η
2	141	+0.10	+0.15	-0.31	-0.13	-0.32	-0.27	-0.91	+0.65	+0.06	-0.09	-0.01	-0.08	-0.50	+0.02
3	200	-0.01	+0.09	-0.37	-0.50	-0.82	+0.24	-1.58	+1.66	+0.17	-0.12	0.00	-0.11	-0.59	+0.15
4	280	-0.05	0.00	-0.45	-0.71	-0.83	+0.26	-1.67	+1.70	+0.32	-0.23	+0.01	-0.12	-1.07	+0.62
5	390	-0.06	-0.05	-0.80	-0.53	-0.84	-0.14	-1.72	+1.91	+0.39	-0.26	+0.01	-0.11	-1.74	+1.60
6	550	-0.08	-0.09	-1.14	-0.63	-0.76	+0.22	-1.91	+2.09	+0.38	-0.31	+0.06	-0.10	-1.90	+1.75
7	780	-0.20	-0.15	-1.41	-0.66	-0.57	-1.26	-2.03	+2.16	+0.38	-0.31	+0.12	-0.11	-2.00	+1.71
8	1100	-0.26	-0.12	-1.25	-0.84	-0.79	-1.56	-1.88	+2.13	+0.39	-0.32	+0.15	-0.10	-1.95	+1.74
9	1550	-0.22	+0.05	-1.35	-0.96	-0.32	-1.14	-1.92	+2.08	+0.43	-0.40	+0.18	-0.09	-1.93	+1.87
10	2180	-0.28	+0.05	-1.18	-1.00	-0.15	-0.78	-1.83	+2.23	+0.44	-0.41	+0.15	-0.05	-2.04	+1.94
11	3070	-0.29	+0.05	-1.16	-0.98	-0.09	-0.85	-1.85	+2.25	+0.45	-0.41	+0.12	-0.02	-1.95	+1.88
12	4320	-0.29	+0.06	-1.13	-1.04	-0.10	-1.10	-1.83	+2.19	+0.45	-0.41	+0.12	0.00	-1.93	+1.91
13	6080	-0.31	+0.04	-1.06	-1.04	-0.05	-1.03	-1.86	+2.16	+0.45	-0.41	+0.12	0.00	-1.88	+1.90

TABLE 13 ARNOLD TYPE CORRECTIONS - CUMULATIVE CONTRIBUTIONS

9. CONCLUSIONS

9.1 Introduction

The primary purpose of this investigation is to test the practicality of determining the deflection of the vertical using gravimetry. To this end field expeditions were undertaken to define the anomalous gravity field in the area immediately surrounding the test stations. The various theories concerning this approach have been analysed for their feasibility and strength in solution. Computational techniques have been developed and tested for the realistic extension of the gravity field and the accurate evaluation of the parameters and of their expected errors. The end products are the gravimetric deflections of the vertical which are compared against deflection values found independently by astro-geodetic means. The analysis of the differences of the two values gives insight into the strengths and weaknesses of the gravimetric approach, this fulfilling the purpose outlined above.

The stations chosen for the investigation adequately filled their chosen role. The twelve stations are situated in a variety of topographic environments ranging from featureless plains to rugged mountain regions. The departure of the topography around the computation point from a level surface can introduce significant corrections to the gravimetric deflection. Thus having the test stations situated in different types of terrain enabled some control to be placed on this factor in the gravimetric computation. The effects of the corrections for the topographic effects on the comparison between gravimetric and astro-geodetic deflection values are summarised in section 9.2. Also in this section estimates of the precision and of the systematic error of the gravimetric evaluation of the systematic error derived by the comparisons with the astro-geodetic value are discussed.

As a result of the investigation some comments can be made about the problems associated with the evaluation process. In particular, difficulties associated with the extension of the gravity field and also with the evaluation of the parameters describing the terrain will be reviewed. This is the subject matter of section 9.3.

It is valuable to examine the role which the deflection of the vertical could play in contemporary geodesy. The relevance of this parameter and a comparison of the various techniques available for its determination are discussed in section 9.4.

Finally recommendations based on the findings of this investigation are made in section 9.5.

9.2 The Precision and Systematic Error of the Deflection of the Vertical determined Gravimetrically

9.2.1 The Importance of the Inner Zone in the Evaluation

It is apparent that the inner zone gravity field ($0 < \psi < 1^{\circ}.5$) has a large influence on the gravimetrically determined value of the deflection of the vertical. This is to be expected from consideration of equations 2.26 and 2.27, but it is graphically illustrated by an analysis of the 'signal' received at the computation point from various parts of the entire gravity field. For example it is found that for stations situated in a disturbed free-air gravity anomaly region, as much as 50% of the total 'signal' (ie. the signal from all zones where 'signal' is defined in section 6.2.2) can be received from the anomaly field within 4.3 km of the computation point. (See table 6 and section 6.2.2). This is of interest because in some investigations (eg. SZABO 1962)

this distance is the radius of the innermost zone. The assumptions of planarity usually made in the evaluation of this zone will not be adequate in mountain areas and the precision of such a computation will suffer. The results of the present study also show that for a station sited as above as much as 80% of the total signal can come from the INNER zone (see section 6.2.2). By contrast, a point located on the plains in this general area receives only about 20% of the total signal for the ξ component from this zone, reflecting the relatively similar and undisturbed nature of the field to the north and south of this point. However about 70% of the signal in the η component at such a point is received from the INNER zone, contrasting with the ξ component and reflecting the differences in the outer reaches of the INNER zone in the field to the east and that to the west of the point.

The above comments emphasize the need for a full and accurate representation of the gravity field within the INNER zone. Particularly is this so for stations situated in broken terrain, where the immediate vicinity $(0 < \psi < 0^{\circ}.1)$ of the computation point needs full description. This may take the form of a fairly dense gravity survey (eg. 1 point per 1 km^2)but of more importance is an adequate description of the terrain. This may be gained from large to medium scale map of the area (eg. 1:50 000), or even more conveniently from data banks of the terrain data stored on magnetic tape if such are available. It appears that a representation with an accuracy of about ±10 m to ±20 m is adequate for the task. Obviously for rugged terrain this would only be feasible in areas which have already been mapped. To obtain this data by field survey in such areas would be costly and prohibitive if it was only for the purpose of the gravimetric data. However for computation points situated on plains or on isolated hills the height data from the gravity stations gives an adequate description of the terrain.

It is possible to estimate the improvement in the gravimetric evaluation brought about by the densification of the gravity data at the test stations. This can be done by comparing the results of this investigation with those obtained by MATHER (1970a) for the same points in the 1970 geoid solution of Australia (see columns 2 and 3 of table 12 and column 1 of the same table). This comparison shows that whilst the mean of the differences between gravimetric and A/G values of the 1970 solution are within 0".3 of the mean value obtained in the present study, the standard errors of the mean of the 1970 study are ±2".5 in the ξ component and ±1".4 in the η component. The evaluation technique used in this study was fairly insensitive to short wave-length signals, relying on $0^{\circ}.1$ square means throughout the INNER zone. The values for these means were obtained from the BMR gravity coverage and did not include any special data surveyed around the computation points. Also planar conditions for an 'innermost' zone were assumed over a 3 km radius from the computation point. Two points of interest emerge from this comparison

(i) The limitation of the accuracy of a gravimetrically determined deflection of the vertical is about ±2" if the inner zone computation is performed as described above.

(ii) The errors in individual stations compensate to produce a reasonable mean of differences in this region. This effect is not necessarily accidental. The deficiency in the value at one station due to a poorly represented area will show as an excess in the value at a station on the opposite side of this field. This phenomenon has already been mentioned as a possible reason for discrepancies in the η components of two stations which lie in the same latitude (see section 8.4.2(d)). It could be used for precision computations of deflections for (say) datum orientations and this suggestion is enlarged in section 9.4.

9.2.2 Systematic Differences in the Gravimetric Deflection Values

The comparison of the gravimetric deflection values after terrain corrections are applied with the A/G values gives the best estimate of the means of the differences in both ξ and η. These are found to be +0".06 and 1".47 respectively (see column 6, table 12). Whilst the mean of the differences in the ξ component approaches zero, this value in the η component is surprisingly large. The most probable reason for this is that the gravity field off the east coast of Australia in the latitude of the test area is inadequately surveyed and the inaccuracy in the predicted values used in the evaluation introduces a systematic error in the η value. This problem demonstrates the danger of trying to determine absolute values of the deflections from gravimetry if a poorly represented area lies within the $3^{\circ} < \psi < 6^{\circ}$ region. On the other hand good estimates of this systematic error can be obtained if precise gravimetric evaluations are made at suitably corrected astro-geodetic stations (see section 6.3.2) along the edge of the poorly surveyed region. These differences found at a network of points thus located can be used to correct gravimetric determinations made subsequently in the affected region by a simple linear interpolation of the correction. Such a scheme is recommended as a possibility for Australian use in section 9.5.

It is also of interest to consider the systematic errors which may result from the omission of different parts of the outer zone data in the evaluation process. For example if the contribution from the UT zone (ie. the field beyond $\psi = 15^{\circ}$) is neglected, a systematic error of about 0".3 in ξ and 0".8 in η will result (see table 6, row 1). However, because of the long wavelength of the signal from this region relative changes of only 0".1 in ξ and 0".2 in η will occur at the test stations. If the region $\psi > 7^{\circ}.5$ is excluded (ie. both zones UT and MD, in table 6, rows 1 and 2), the magnitudes of the relative changes are still of this order whilst the systematic error increases to about -2".1 in both components. However exclusion of the field beyond $\psi = 1^{\circ}.5$ introduces relative errors of about 1".0 in both ξ and η (see table 6, row 3). Thus for precise relative determinations this zone must be included although in view of the discovery of the systematic error in η above it may be possible to exclude the region beyond 3° without introducing significant relative differences.

Another source of systematic errors in the differences between the gravimetric and A/G deflection values is the non-coincidence of the two models (ie. the gravimetric ellipsoid and the geodetic ellipsoid; see section 6.3.2). As can be seen from column 10 of table 8 the difference in the models used in this investigation introduces a systematic error of about -2".0 in ξ and -3".4 in η. However the range of the corrections through the test area is insignificant and this effect could be applied as a systematic correction to deflection differences over a region such as the test area. Conversely this shows that providing all other systematic effects are corrected for, precise gravimetric comparisons at a small number of well fixed astro-geodetic stations can provide valuable information about the orientation of one datum with respect to the other.

9.2.3 The Precision of the Gravimetrically Determined Deflection of the Vertical

The combined effect of the improvement in the inner zone data and the strengthening of the evaluation procedure appears to improve the precision of the gravimetric value of the deflection from the ±2" obtained in the 1970 geoid solution to about +0".5 (see table 12, column 3). The sample used to obtain this value includes both stations minimally affected by terrain effects (category 1 stations) and those significantly affected by these effects (category 2 stations). Comparison of the values according to category shows a greater improvement for the precision of stations in category 1 ie. to about ±0".1 (table 12, column 4), whilst the precision of the category 2 stations appears to be

±0".3 in ξ and ±0".5 in η. This value is probably too low because in this sample there are a number of stations at which the terrain effects are small. Nevertheless it appears that the improved data and evaluation techniques increases the precision of the gravimetric deflection from about ±2".0 to at least ±0".5.

The above analysis was performed using the differences in the gravimetric from the A/G deflection values. These differences are due to errors in the A/G as well as the gravimetric values, and in order to get a realistic picture of the precision of the gravimetric evaluation it is necessary to include an estimate of the error in the A/G values of the deflections in the analysis. This error is difficult to estimate with confidence. If the standard errors obtained from the actual astronomical observations at the test stations are used, the error in the gravimetric values become quite small at the category 1 stations (see section 8.4.1 and column 4, table 12). For category 2 stations after applying the terrain corrections this error is about ±0".1 in the ξ component and ±0".4 in the η component (see column 7 table 12). A few comments should be made concerning these values.

(i) The precision of the gravimetric value of ξ is apparently inferior than that of η. The most reasonable explanation for this is that the value of ±0".2 used as the standard error for the A/G values of η was too low (see section 8.4.1). If the more realistic value of ±0".4 is used for this parameter the precision of the gravimetric value for η approaches that for ξ ie. ±0".1.

(ii) It is apparent that even after correction the category 2 stations do not reach the precision of the category 2 stations suggesting that the terrain effects have not been fully removed or even that second-order effects such as those mentioned in section 8.4.2(a) may be present. Nevertheless the application of the corrections does significantly improve the precision of the gravimetric deflection (see section 8.3.2).

(iii) It does appear possible to obtain a precision of ±0".1 to ±0".2 for a value of the deflection of the vertical computed gravimetrically. In rugged, mountainous regions a good representation of both the gravity field and the topography will be needed. Terrain effects are best computed using Molodensky's G' correction term (see equation 3.3) providing ground slopes in the vicinity of the computation point do not exceed 45° (see section 2.4.2).

(iv) These estimates of precision are quite similar to those resulting from a theoretical error analysis of the evaluation (see section 7.3.2 and table 10, solumns 1 to 4). This fact lends credence to the analysis itself although it must be remembered that such an analysis can never correctly estimate the systematic errors in the evaluation. However, because of the higher precision of category 1 stations over category 2 stations mentioned in (ii) above, the analysis which differentiates between plain and hilly country (see results in columns 3 and 4, table 10) seems to reflect the actual results more accurately than the analysis which assumes a constant error of representation regardless of terrain (columns 1 and 2, table 10).

9.3 Review of Evaluation Techniques

9.3.1 Computer Methods used in the Evaluation of the Deflection of the Vertical

The apparent success of the gravimetric evaluation justifies the decision to use a Rice Rings technique in the evaluation procedure (see section 4.3.1). This technique showed itself to be

completely adaptable to programming (see Appendix A) and lent the computer evaluation strength and flexibility not readily achievable from the usual routines adopted for such evaluations.

A real advantage of the method used in this investigation was that the data did not have to be pre-processed in order to obtain area means. Such processing would have seriously dampened the signal in the vicinity of the computation point unless very small squares were used for the areas. The problems associated with the manipulation of the data from station to station and with the augmentation of the data would also have been increased. The rings approach using discrete data was used in the computation of the G' term and the Arnold-type corrections, the original technique for deflection computation being easily adapted for these purposes (see sections 4.3.2 and 4.3.3 respectively).

9.3.2 Field Extension and Prediction

The problem of field extension is inherent in any approach which uses discrete data for the representation of a continuous field. This is a standard problem in topographic surveying where it is necessary to derive contour diagrams of the topography from discrete points which have been fixed in three dimensions. Experimentation proved that suitably modified computer techniques developed for contouring were best suited to the problem of gravity and height field extension (see section 5.2.3). Techniques which fitted second order or plane surfaces to a sampling of points in the area of extension proved to be too coarse for the purpose of this study (see sections 5.2.1 and 5.2.2). Similarly the technique of covariance analysis which is widely used for gravity field prediction in largely unsurveyed regions of the Earth was found to be unreliable for the purposes of this study. In fact, at the risk of including erroneous data it seemed preferable to limit the data points used for the interpolation process to those immediately surrounding the point of interpolation. This ensured that maximum sensitivity to the actual data field was maintained in the process of interpolation. This technique was applied within a radius of $\simeq$ 10 km from the test station which meant that the gravity field in the critical region near the computation point was reflected accurately in the evaluation process.

The density requirements for the gravity stations as stated in section 4.1.1 were not always fulfilled (see figures 10-21). The results of the computations are nevertheless quite satisfactory and it is felt that these requirements may be unnecessarily demanding for most of the test stations. On the other hand it was found that the original density of height points chosen at major changes of grade (see section 4.1.2) was inadequate in the immediate area of the test station and that this needed further augmentation. The final density reflected the pattern of the modified Rice Rings (section 4.3.1) generated at the computation point with heights taken at the mid-point of the compartments of every third ring out to about 5 km. Altogether the data requirements indicate a shift in effort away from the field survey toward an office task. This is beneficial from a cost-benefit viewpoint as the compilation of the height data requires little skill. In some areas where topographic information has been stored on tape as part of the mapping process the compilation process in unnecessary and height data extraction could be made a routine part of the whole computation.

9.3.3 Evaluation of Terrain Effects

(a) The G' Correction Term.

A 'rings' system was devised to compute G' which meant that with a minimum of modification it was

possible to adapt the system developed for the deflection computation for the evaluation of this term (see Appendix C and section 4.3.2). The expected error in this term is found to be very small by formal analysis (see section 7.4). Although this does not seem to be matched in practice, there do not appear to be significant errors in these values. Consideration of equation 3.3 indicates that the contribution to G' falls away according to the third power of r (the distance between computation point and elemental area). For the magnitudes of height and gravity anomaly likely to occur, this evaluation does not have to continue beyond a radius of 40 km from the computation point.

The G' value was found at about 600 gravity stations with the region affected by the terrain. This value is then stored in the data bank with the other information about the gravity station. This enables the effect on the deflection of the vertical from this terrain correction to be evaluated separately (see table 9, columns 1 and 2).

It is found that the correction to the deflection for the terrain effects significantly improves the precision of the gravimetric deflection from about ±0".5 to ±0".2. However the workload to bring about this improvement is quite high. For example a total of 1 hour's computing time on a CYBER 70/72 were needed to evaluate G' at all relevant gravity stations. This time excludes the time taken for development and testing of the programmes (see Appendix C), and the recomputations at some critical stations when extra height data was added to this data file. On the other hand the computation time was minimised by terminating evaluation once the contribution per ring dropped below a certain value (0.3 mGal in this study). Also once computed, there should be no need to change this value so it can be stored with other data for the gravity station in the data file and used in all subsequent evaluations.

(b) Computation of 'Arnold'-type Correction Terms

It is of interest to recall that the correction term developed from the application of Green's Third Identity to the Earth's surface (section 2.3, section 3.3 and section 6.4.2) does not suffer the same theoretical disadvantage that is noted for the G' term (compare the comments in section 3.3(ii) with those made at the end of section 2.4.2). Nonetheless the evaluation of the Arnold-type terms proved quite unstable, due mainly to the oversensitivity of this term to errors in the ground slope (see equation 6.11). This was particularly so in the evaluation of these terms within a radius of 500 m of the computation point (see table 13, particularly the columns for Byar, Kaputar, Blue Nobby and Baldwin). The corrections computed at stations sited in less broken terrain were more acceptable (see columns for Goonbri and Newry in table 13 and listings for Goonbri and Newry in table 9). Overall the evaluation was unreliable (see table 9) and the following comments should be made.

(i) The computer technique used successfully for the interpolation of heights proved unreliable when modified to compute ground slopes. It is thought that an estimate of β should be submitted as separate data for this computation. This may involve the user in laborious graphical interpretation from maps or require survey parties to obtain estimates of ground slope as part of the necessary field observation at a gravity station.

(ii) It is possible that the computation could be improved by introducing some damping into the evaluation procedure. It is felt that the modified Rice Rings (see section 4.3.1) may be too fine a subdivision for the slope computation. It could even be that the data is too dense and gives too discrete a description of the topography for this purpose.

(iii) It should be remembered that some knowledge of ξ and η is needed. This infers that a first estimate of these two parameters must be obtained, possibly from a solution of the Vening Meinesz integral. This increases the work load of the evaluation by a factor of about 3. Obviously the computation of the terrain effect by this method must be improved if the extra effort involved in its evaluation is to be justified. The need for a value of ξ and η also means that a special file of deflection values needs to be created, further increasing the work load. In regions where the values of these parameters change little it is possible to assume a constant value throughout the computation. Even in disturbed regions, this assumption can be made within a radius of 500 to 1000 m from the computation point, but beyond this it is necessary to draw on the data bank and find the value for ξ and η by some method of interpolation.

9.4 The Deflection of the Vertical in Contemporary Geodesy

9.4.1 The Role of the Deflection of the Vertical

The advent of position fixing techniques which use the doppler effect from artificial satellites is being a profound impact on modern geodesy. 'Translocation' techniques are claimed to be capable of producing a positional accuracy of better than ±2 m in each of the 3 principal directions (see KOUBA 1974, p 484). Geodetic networks have traditionally been based on a reference system which uses precise positional astronomy to assist in its definition. The superior accuracy of doppler will inevitably mean that this technique will displace positional astronomy from its traditional role. It is against this background that the role of the deflection of the vertical must be analysed.

(a) Datum Orientation

Probably the greatest difference in approach which results from the use of doppler for planimetric control arises from the fact that the control will now be based on a geometric rather than a geopotential reference frame. The coordinates of the position are fixed with respect a three dimensional axis system with origin at the geocentre whilst astronomical positions are related to the local vertical. This latter fact has influenced some geodetic networks (eg the AGD) to be computed on an ellipsoid chosen to 'fit' the local geoid (see section 1.2). In order to transform this geodetic network onto a geocentric system one must establish the geocentric orientation vector of the local system with respect to the geocentric system. This can be done either by fitting the existing geodetic network onto the doppler-based control (eg. see PETERSON 1974) or by comparing the geoid-ellipsoid separation and deflections of the vertical derived astro-geodetically with these same parameters derived gravimetrically using for the gravimetric model a geocentric ellipsoid (eg. MATHER 1970b). It has been shown that systematic errors in scale can significantly affect a wide area of the geodetic network, placing constraints on the use of the former approach (ROELSE 1976). Judicious choice of stations for comparison makes the second approach quite feasible, particularly if the gravimetric deflections are evaluated using the techniques as adopted in this study. This decreases the need to control accidental errors by taking comparisons at a large number of stations (MATHER 1970b, p 69). Conversely, use of the same number of stations evaluated as suggested would increase the accuracy of the value of the geocentric orientation vector.

If the former approach is used it is necessary in any case to ensure that the existing geodetic coordinates are reduced to the ellipsoid. Failure to do this could introduce inconsistencies into the geodetic coordinates which would show as large systematic errors when comparing them with the

geocentric (doppler) coordinates. For this reason it is necessary to know the geoid-ellipsoid separation to at least ±6 m. This accuracy is for the most part available from existing geoid maps of the Earth. It may be that in some particularly disturbed regions (eg. high mountainous regions) these geoid solutions do not include the high frequency fluctuations of the geoid and in these areas available global determinations will have to be supplemented by local geoid studies. Again the techniques presented in this study will prove useful in so far as they are particularly sensitive to local variations of the geoid.

(b) Azimuth Control

Although, through its superior positional accuracy, doppler techniques will supersede positional astronomy in the provision of a reference frame for present-day geodetic networks, the state-of-the-art of this approach does not improve astronomical techniques in the determination of azimuth. This is particularly so if lines of sight (< 120 km) are used for azimuth control in the geodetic networks. For such lines the present achievable directional accuracy is 0 {±7''} from doppler if one assumes the ±2 m positional accuracy quoted above. This must be compared with the precision obtainable by astronomical azimuths of 0 {±0''.5} (BOMFORD ET AL 1970). The positional accuracy in the two primary directions at both ends of the line for a 120 km line must be 0 {0.3 m} to equal this precision. There will obviously need to be a great improvement in the positional accuracy of doppler before it can achieve such precision and supersede astronomy in the provision of azimuth control.

This means that the meridian defined by the vertical at a point on the Earth's surface must be related to the meridian defined by the normal by means of Laplace equation. This immediately involves the prime vertical component of the deflection of the vertical, η (eg. see HEISKANEN AND MORITZ 1967, p 197). The error in η enters into the correction to the astronomical azimuth as the tan of the latitude. It is therefore important in mid- and high latitudes to minimise such errors. It is conceivable in countries such as Australia which have good gravity coverage and little topographic relief that this parameter could be determined gravimetrically to increase the accuracy of η. Thus it is possible in the near future for geodetic networks to be an amalgam of doppler, astronomic, geodetic and gravimetric surveys with each method giving strength where the others are weak to provide a superior control system.

(c) Civil Engineering Purposes

Hydrographers, hydraulic engineers and construction engineers are concerned with relating their designs which are based on energy calculations to the geopotential surface. To them a survey network defined purely in terms of a geometric framework has limited use and it is necessary to show the relationship which exists between this framework and the 'natural' or geopotential system. This is provided by means of the deflection of the vertical which is effectively transforming the geocentric coordinates from an artificially induced horizontal onto a truly horizontal or level surface. In fact the majority of map users require contours to relate to a dynamic level rather than to some level surface generated by geometrical considerations. For this reason it will always be necessary to map with respect to the geoid rather than the ellipsoid and thus deflections of the vertical or geoid-ellipsoid separations will need to be evaluated. For most purposes existing geoid maps will be adequate but for precise local determinations particularly in mountainous areas it is apparent that deflections will provide a more sensitive register of this relationship than will the separation.

9.4.2 Comparison of Methods of Evaluating the Deflection of the Vertical

A number of different methods can be used to determine the deflection of the vertical. These are now reviewed and analysed from a cost-benefit viewpoint.

(a) Astro-geodetic Methods

The astro-geodetic method has traditionally been the technique used to provide horizontal and azimuth control in geodetic surveys. The deflections of the vertical resulting from comparisons of astronomic and geodetic positions throughout a network enabled the computation of geoid - ellipsoid profiles. As mentioned in section 9.4.1(b) above,positional astronomy will be superseded by doppler techniques in the provision of reference frame for geodetic purposes. It could still be used in order to obtain deflections of the vertical to provide information needed in the items mentioned above (section 9.4.1). The deflection values will be relative to a local ellipsoid unless a datum orientation has been performed (see section 9.4.1(a)). The precision of the deflection determined in this way is about ±0".2 in ξ and about ±0".5 in η (see section 8.4.1), the dominant contribution towards the error being due to inaccuracies in the astronomical data.

The cost of establishing an astro-geodetic station (in 1976 Australian dollars) is quite high, being between $900 - $1100 (LEPPERT 1976). This is because the observations require a skilled observer and a well-trained party of two assistants. The station is usually occupied for at least three nights, the observations being subject to favourable weather conditions. (The figure quoted above includes 2 nights lost due to poor weather conditions). The estimated cost of computing and documenting the data is $250 - $300 giving a total cost of between $1150 and $1400.

As the astronomical observations must be made at a station whose geodetic coordinates are known this often means that the deflection is determined at trig stations on the tops of mountains. The level surfaces in these situations are subject to strong local effects and the deflection evaluated here is likely to give a poor estimate of the slopes of the geops in the general vicinity.

It is apparent that the astro-geodetic values for the deflection components may contain large systematic effects. Whilst any systematic error in the meridian component appears small and in fact seems to be masked out by the accidental errors in the observations used in this particular study, this is not the case with the prime vertical component. It has been noted in section 8.2.1 that the $\eta_{A/G}$ can contain large systematic errors, of the order of 2", even though the precision of the $\lambda_{A/G}$ is estimated to be ±0".2. That such errors may be present in the prime vertical component is of particular significance as it is this component which is used in the Laplace equation (see section 9.4.1(b)) to provide azimuth control. Errors of such magnitude would seriously weaken the confidence which could be placed in azimuth misclosures derived using the Laplace equation particularly in countries in middle to high latitudes.

(b) 'Approximate' Gravimetric Determinations

It appears from section 9.2.1 that a gravimetric solution for the deflection which does not include data from special surveys around the computation point and which uses mean anomalies for (say) $0^{\circ}.1$

squares is capable of producing a value which is accurate to about ±1".5 to ±2".0. If a number of such values are computed at properly situated stations within an area the mean value may be improved to about ±0".5. This computation will be quite cheap provided that the data files are already compiled, the programmes for this computation having already been developed and tested.

(c) Collocation Techniques

Recent studies (eg. TSCHERNING 1973, p 13; LACHAPELLE 1975, p 106) indicate that collocation techniques are capable of producing results with an accuracy of about ±1".5 to ±2".0. This is to be expected as in this technique much of the high frequency signal in the critical region near the computation point is likely to be filtered out. In this sense it is similar to the technique in (b) above and for this reason it gives a comparable accuracy. No cost has been found by the author for this technique, but it is expected to be quite inexpensive providing the data is compiled and presented in a suitable form.

(d) Inertial Surveying Systems

The Inertial Surveying System (ISS) is a highly sophisticated inertial navigation system with an extremely high accuracy, developed especially for surveying. It is basically a precise inertial platform with gyroscopes keeping its three orthogonal axes oriented in space. Each axis contains a very sensitive accelerometer which defines the acceleration in the direction of each axis. These, when integrated over short periods of time enable changes in the latitude, longitude elevation and deflection of the vertical to be determined (GREGERSON ET AL 1975, pp 1-3). The method of evaluating the deflection which is needed to correct the 'astronomic' to a geodetic azimuth is of particular interest here. "The system keeps track of the amount of torque needed to relevel the platform to the local vertical whenever it is stopped. The levelment occurs by driving the standing platform into a position where the two horizontal accelerometers do not sense the gravity components any more. This can only occur when the sensitive axes of the accelerometer are exactly perpendicular to the direction of gravity. Thus the system describes the change in the deviation of the vertical with respect to the origin" (IBID, p 4).

The ISS can be mounted in a truck or a helicopter which is of advantage in areas inaccesible by road. The results of test runs to data suggest that the precision of the deflection is about ±1".5 in mountainous terrain with a slight improvement in flat country (IBID, pp 43-45). The cost of the equipment is high (0 {$100,000}) being still in the experimental stage. In addition to this capital cost the operators must be skilled, with training in electronics, inertial navigation systems and computer science. Consequently the ISS is not yet a feasible proposition for general production purposes. On the other hand it promises to be of great benefit in the future particularly for countries with difficult terrain which are as yet unmapped.

(e) Precise Gravimetric Determination

As mentioned above (section 9.2) it appears that a precision in the two components of the deflection of the vertical ±0".1 to ±0".2 is attainable. This is provided there is adequate representation of the gravity field and the topography within a radius of about 1°.0 from the computation point and that the remaining field is well represented to a radius of about 6°. If a good gravity coverage (say 1 point per 20 km^2) already exists it is likely that this gravity field need only be supplemented

by a further 10 to 15 gravity stations in the vicinity of the computation point to provide sufficient coverage. Medium scale maps (1:25 000 to 1:100 000) should be available for areas of broken terrain to provide the topographic information.

The cost of the extra gravity stations is a function of the terrain in which the computation point is located. If road access is available and heights are already provided or can be determined by altimetry the current cost per station is $25. If the gravimeters are helicopter-borne this cost increases to $35 per station. In the case where heights have to be obtained by actual field survey the cost per station increases to about $60 per station (BARLOW 1976). These costs cover all normal losses of time including time lost due to unsuitable weather which is practically negligible. The computations needed to obtain the principal facts for the data bank adds about $1.20 to the cost of a station. It can be seen therefore that the cost of the total survey may range from $260 to $900 depending on the terrain access and the number of gravity stations needed. To these costs should be added the cost of abstracting the height information from the topographic maps and of computing the actual deflection value. However these will not be high and in any case each of these processes can be easily automated.

It should be noted that the location of the computation point is not restricted as it is in the case of an astro-geodetic station (see 9.4.2(a) above). This will not only have the advantage of siting stations in locations likely to give a more representative value for the tilt of the geopotential but will assist in cutting costs. The gravity survey will only take 1 to 2 days field work in contrast to a minimum of 3 nights needed for the astronomical observations. Also the gravity survey is only slightly inconvenienced by poor weather whereas the astronomical work requires clear skies for the observations. Obviously the gravimetric approach will benefit countries which suffer from less temperate climatic conditions. To this comparison must be added the factor of the relative precisions of the two methods. As has been mentioned above it appears that the gravimetric technique is capable of producing a higher precision than can be obtained by astro-geodetic means, particularly in the prime vertical component. This may be dependent on good gravity and map coverage, but most developed countries of the world are adequately provided with these two requirements. It therefore appears that for about $\frac{1}{4}$ the cost the gravimetric method is capable of obtaining a value of the deflection of the vertical which is about twice as accurate as its astro-geodetic counterpart.

9.5 RECOMMENDATIONS

It appears that the future role of the deflection of the vertical lies in its ability to relate dynamical and geometrical elements of a geodetic network. In particular it is essential to relate astronomically determined azimuths to the geodetic meridian and thus provide precise azimuth control for first-order geodetic systems. From the foregoing study it is apparent that gravimetric methods can produce superior results for this parameter.

For computation points located on plains or isolated hills gravity should be measured at the point itself and at about 6 stations within a radius of 1 km of the point. Additional measurements are required at 6 or more points within a radius of 5 to 10 km. For computation points located in rugged country this density of stations may need to be increased and it will be necessary to have medium scale topographic maps or their equivalent (eg. height data banks) of the area. It is felt that the heights of the cardinal points of the innermost zone at a radius of (say) 100 m should be determined in the field. The location for these points is not critical and can be fixed by approximate survey methods (eg. pace and compass) but their heights need to be known more accurately (to ±1 m). There is a problem with systematic errors in the gravimetric determination. To

establish the magnitude of this error it is necessary to establish a network of stations, about 1^{o} apart and within about 1^{o} of the poorly defined gravity field, at which comparisons of gravimetric and astro-geodetic deflections can be made. Systematic errors at points between these stations can be obtained by linear interpolation due to the slow changing nature of this effect. Gravimetric determinations can then be corrected and absolute values of the deflections obtained. The corrected values will also eliminate any residual errors due to an inadequate orientation of the geodetic datum.

Because of the possibility of errors it is wise to take these comparisons at more than one station. Ideally three or four stations should be positioned in a triangular or cross pattern (about areas of poorer gravity definition if such exist) and roughly 30 km apart. This helps to control small local systematic effects and greatly strengthens the value of the comparison derived.

This study also shows the benefit which would accrue if data banks of height information stored in a computer compatible form were available. Such data would benefit many scientific users of maps, as it would save the expense and effort which each individual user currently expends in extracting the topographic information needed for their purpose for the available maps. Much of this information is already available, as such data is gathered and stored on magnetic tape by mapping authorities as part of the mapping process (FRYER 1976). The existence of such tapes is not widely publicised, and there is a need for some policy on the collation and distribution of such data both on a national and international level.

ACKNOWLEDGEMENTS

I would like to thank the many people who, through lending me their time, advice and support have helped me in various aspects of this study.

In particular I am most grateful to Professor R.S. Mather for his guidance and assistance in both the theoretical and practical aspects of the work. I am also grateful to Professor P.V. Angus-Leppan for his encouragement and for providing the financial assistance without which the field work could not have been undertaken.

I would like to thank Mr. L. Berlin, Professor R.S. Mather, Dr. A.J. Robinson, Dr. G. Hoar, Dr. E.G. Anderson, Mr. R. Beeston and Mr. M. Legge for lending their time and expertise in the field work associated with the gravity surveys. I acknowledge with thanks the loan of the Worden Gravimeters from the BMR through Mr. B.C. Barlow, and from the School of Applied Geology, UNSW through Dr. I.R. Qureshi.

For advice on various technical matters thanks go to Mr. Klaus Leppert and Mr. Adrian Roelse of the Division of National Mapping, Canberra, to Mr. B.C. Barlow, BMR, Canberra, to Mr. Alec Teoh of the NSW Department of Lands, Sydney and to Mr. C.B. Kirkpatrick of the School of Mathematics, UNSW.

I am grateful to Mr. W. Kent and Mr. B. Hirsch, UNSW for their help in the programming and data handling aspects of the programmes. I would also like to thank my wife Rosalinde for typing the first draft of the thesis and Mrs. Sue Kiriazis for such a professional job in the typing of the final draft and the tables. Also my thanks goes to Mr. Malcolm Legge for assistance at such late notice in the preparation of the figures.

BIBLIOGRAPHY

ARNOLD, K. 1975. Proof of the Uniqueness of the Free Boundary-Value Problem of Physical Geodesy. *Gerlands Beitr. Geophysik, Leipzig* 84, 381-388.

BARLOW, B.C. 1967. National Report of Gravity in Australia, January 1963-December 1966. *Bureau of Mineral Resources Rep.*, No. 1968/21. Canberra, Australia.

BARLOW, B.C. 1976. Private Communication. *Bureau of Mineral Resources, Geology and Geophysics.* Canberra, Australia.

BJERHAMMAR, A. 1964. *A New Theory of Geodetic Gravity.* Stockholm, Trans. Roy.Inst.Technol., No. 243.

BJERHAMMAR, A. 1969. Theory of a New Geoid. *Bull.Géod.*, 92, 173-203.

BJERHAMMAR, A. 1973. On the Discrete Boundary Value Problem. *Proc. Symposium on Earth's Gravitational Field and its Variations in Position,* 475-488.

BOMFORD, A.G. 1967. The Geodetic Adjustment of Australia, 1963-1966. *Survey Review,* 144, 52-71.

BOMFORD, A.G. ET AL, 1970. Astronomic Observations in the Division of National Mapping 1966-1970. *Technical Report No.* 10, Division of National Mapping, Canberra, Australia.

BOTT, M.H.P. 1959. The Use of Electronic Digital Computers for the Evaluation of Gravity Terrain Corrections. *Geophysical Prospecting,* 7, 45-54.

BRIGGS, I.C. 1974. Machine Contouring using Minimum Curvature. *Geophysics,* 39, 1, 39-48.

BROVAR, Y.V. 1964. On the Solutions of Molodensky's Boundary Value Problem. *Bull. Géod.*, 72, 167-173.

BROVAR, V.V. ET AL, 1964. The Theory of the Figure of the Earth (Translation). *Clearing House* #AD 608975.

BUCK, R.J. & TANNER, J.G. 1972. Storage and Retrieval of Data. *Bull. Géod.*, 103, 63-84.

BURSA, M. 1965a. Determination of the Interpolation Error of the Astro-Geodetic Deflections of the Plumb-line in Czechoslovakia (in Russian). *Travaux Inst. Geoph. Acad. Tchéckosl. Sci.*, No. 216, Geophysikálni Sbornik, 1965.

BURSA, M. 1965b. On the Practical Application of the Solution of Molodensky's Integral Equation in 1st Approximation. *Stud. Geoph. et Geod.*, 9, 144-149.

BURSA, M. 1967. On the Determination of Gravimetric Deflections of the Vertical for the Centre Area. *Travaux Inst. Géophys. Acad. Tchéchosl.Sci.* No. 263, Geofysikálni Sbornik (1967).

BURSA, M. 1968. The Interpolation Error of Quasigeoidal Heights on the Territory of Czechoslovakia. *Travaux Inst. Géophys.Acad.Tchéchosl.Sci.*, No. 288; Geopysikálni Sbornik, 1968.

BURSA, M. 1969. Effect of Removed Topography and Condensation on Deflections of the Vertical on the Territory of Czechoslovakia. *Travaux Inst.Géophys.Acad.Tchéchosl.Sci.* No. 303; Geofysikálni

Sbornik, 1969.

BURSA, M. 1970. Accuracy of Differences of Astrogeodetic and Gravimetric Deflections of the Vertical on the Territory of Czechoslovakia. *Travaux Inst. Géophys, Acad.Tchéchosl.Sci.* No. 319; Geofysikálni Sbornik, 1970. Praha, 1972.

CAMPBELL, A.C. 1963. Rigorous Solution for the Determination of the Deflection of the Vertical for the Centre Area. *Bull. Géod.*, 69, 281-291.

COLOMBO, O. 1976. Private Communication. *Dept. of Geodesy, UNSW, Kensington, Australia.*

DE GRAAFF-HUNTER, J. 1960. The Shape of the Earth's Surface in terms of Gravity at Ground Level. *Bull. Géod.*, 56, 191-200.

DIMITRIJEVICH, INEZ J. 1972. The Use of Terrain Corrections in Computing Gravimetric Deflections of the Vertical and Geoid Heights. *Presented at 53rd Annual Meeting of the American Geophysical Union.*

DOBRIN, M.B. 1960. *Introduction to Geophysical Prospecting.* 2nd edition, McGraw Hill, New York.

EMRICK, H.W. 1973. *Computation Techniques for Various Gravity Anomaly Correction Terms and their Effect upon Deflection of the Vertical Computation in Mountainous Areas.* Ph.D. Dissertation, Ohio State University, 1973.

FISCHER, I. 1966a. Slopes and Curvatures from Δg by Electronic Computer. *Journal of Geophysical Research,* No. 20, 4909-4916.

FISCHER, I. 1966b. Gravimetric Interpolation of Deflections by Electronic Computer. *Bull. Géod.* No. 81.

FRYER, J.G. 1970. The Effect of the Geoid on the Australian Geodetic Network. *UNISURV Report* No. 20, School of Surveying, UNSW.

FRYER, J.G. 1971. The Geoid in Australia - 1971. Division of National Mapping, *Technical Report No.* 13.

FRYER, J.G. 1976. Private Communication. *School of Civil Engineering, University of Newcastle,* Newcastle, NSW, Australia.

GAPOSHKIN, E.M.(ed) 1973. Standard Earth Model III - 1973. *Special Report* 353, Smithsonian Astrophysical Observatory, Cambridge, Mass.

GREGERSON, L.F. & CARRIERE, R.J. 1975. Inertial Surveying System Experiments in Canada. *Publication No.* 13414, Geodetic Survey of Canada.

GROTEN, E. 1974. Problems Related to Absolute Orientation of Geodetic Systems. *Canadian Surveyor,* 28, 5, 616-625.

HAGIWARA, Y. 1973. G_1 Distribution over Models of Topographic Relief. *J.Phys.Earth,* 21, 305-311.

HAGIWARA, Y. 1974. Numerical Calculation Method of Molodensky's G_1, with Specific Application to the Gravity Data of the Tanzawa Mountain Area. *J.Phys.Earth*, 22, 441-453.

HEISKANEN, W.A. & MORITZ, H. 1967. *Physical Geodesy*. W.H. Freeman & Co., San Francisco.

HENRICKSON, P. & NASH, R.A. 1970. A Statistical Analysis of Errors in Gravimetrically Computed Deflections of the Vertical. *J.Geophys.Res.*, 75, 20, 4017-4028.

HIRVONEN, R.A. 1960. A New Theory of Gravimetric Geodesy. *Ann.Acad.Scient.Fenn.*, AIII 56.

HIRVONEN, R.A. 1962. On the Statistical Analysis of Gravity Anomalies. *Pub.Isost.Inst.Int.Assoc.Geod.* No. 37. Helsinki.

HONKASALO, T. 1974. Detailed Gravimetric Geoid of Finland. *International Gravity Commission, Paris*.

HÖRMANDER, L. 1975. *The Boundary Problems of Physical Geodesy*. The Royal Institute of Technology, Division of Geodesy, Stockholm.

HOTINE, M. 1969. Mathematical Geodesy. *ESSA Monograph #2*.

KANE, M.F. 1962. A Computational System of Terrain Corrections using a Digital Computer. *Geophysics*, 27, 455-462.

KAULA, W.M. 1957. Accuracy of Gravimetrically Computed Deflections of the Vertical. *Trans.Am, Geophys., Union*, 38, 297-305.

KAULA, W.M. 1959. Statistical and Harmonic Analysis of Gravity. *Journal of Geophysical Research*, 64, 2401-2421.

KEARSLEY, A.H.W. 1973. Deflections of the Vertical from Gravimetry in the Narrabri Region of N.S.W. *Proc. Symposium on Earth's Gravitational Field and Secular Variations in Position*, Sydney, Australia, 189-201.

KELLOGG, O.D. 1929. *Foundations of Potential Theory*. Dover Publications, New York, 1953.

KIRKPATRICK, C.B. 1975. Private Communication. *School of Mathematics, University of N.S.W.* Sydney, Australia.

KOUBA, J. 1974. Reduction of Doppler Satellite Data Observed in Canada. *Canadian Surveyor* 28, 5, 480-486.

LAMBERT, B.P. 1968. The Johnston Geodetic Survey Station. *The Australian Surveyor*, 22, 93-96.

LAUF, G.B. 1961. Conformal Transformations from one Map Projection to another, using Divided Difference Interpolation. *Bull.Géod.*, 61, pp 191-207.

LEPPERT, K. 1976. Private Communication. *Division of National Mapping*, Queanbeyan, Australia.

MATHER, R.S. 1967. The Extension of the Gravity Field in South Australia. *UNISURV Report* No. R19, School of Civil Engineering, UNSW.

MATHER, R.S. 1968a. The Free Air Geoid in South Australia and its relation to the Equipotential Surfaces of the Earths Gravitational Field. *UNISURV Report* No. 6, School of Surveying, U.N.S.W.

MATHER, R.S. 1969. The Free Air Geoid for Australia. *Geophys. J.R.astr.Soc.* 18, 499-516.

MATHER, R.S. 1970a. The Australian Geodetic Datum in Earth Space. *UNISURV Report* No. 19, School of Surveying, UNSW.

MATHER, R.S. 1970b. The Geocentric Orientation Vector for the Australian Geodetic Datum. *Geophys. J.R.Ast.Soc*, 22, 22-81.

MATHER, R.S. 1973. A Solution of the Geodetic Boundary Value Problem to the order e^3. *Goddard Space Flight Centre*, X-592-73-11.

MATHER, R.S. 1975. Gravimetric Investigations on the North American Datum 1972-73. *Goddard Space Flight Centre*, X921-75-244.

MATHER, R.S. BARLOW, B.C. & FRYER, J.G. 1971. A Study of the Earth's Gravitational Field in the Australian Region. *Paper presented at XV General Assembly, IAG*, Moscow.

MAUGHAN, M. 1975. Survey Computations. *Monograph No.* 5, School of Surveying, UNSW.

MEISSL, P. 1975. Elements of Functional Analysis. *Methoden und Verfahren der Mathematischen Physik/Band* 112. Mathematical Geodesy, Part 1, pp 19-78.

MOLODENSKY, M.S., EREMEEV, V.F. & YURKINA,M.I. 1962. Methods for Study of the External Gravitational Field and Figure of the Earth. *Israel Program for Scientific Translations*, Jerusalem.

MORITZ, H. 1965. The Boundary Value Problem of Physical Geodesy. *Ann.Acad.Scient.Fenn.* A-III-83.

MORITZ, H. 1966. Linear Solutions of the Geodetic Boundary Value Problem. *Dept. of Geodetic Science, Report No.* 79, Ohio State Univ., Columbus Ohio.

MORITZ, H. 1968a. On the Use of the Terrain Correction in Solving Molodensky's Problem. *Department of Geodetic Science, Report No.* 108, Ohio State University, Columbus Ohio.

MORITZ, H. 1968b. On the Computation of the Deflection of the Vertical. *Bolletino di Geofisica Teorica ed Applicata*, X, 40.

MORITZ, H. 1969. Non-linear Solutions of the Geodetic Boundary Value Problem. *Department of Geodetic Science, Report No.* 126, Ohio State University, Columbus Ohio.

MORITZ, H. 1971. Series Solution of Molodensky's Problem. *Deutsche Geodätische Kommission, Reihe A. Höhere Geodäsie - Heft Nr.* 70.

MORITZ, H.(Chairman) 1975a. Report of Special Study Group 5.39. *Bull.Geod.* 118, p 405.

MORITZ, H. 1975b. Integral Formulae and Collocation. *Department of Geodetic Science, Report No.* 234, Ohio State University, Columbus Ohio.

LACHAPELLE, Gérard. 1976. Prediction of Deviations of the Vertical using Heterogeneous Data. *Canadian Surveyor*, 30, 2, 97-108.

MUELLER, Ivan I. 1974. Review of Problems Associated with Conventional Geodetic Problems. *Canadian Surveyor*, 28, 514-523.

NAGY, D. & PAUL, M.F. 1973. Gravimetric Geoid of Canada. *IAG Symposium on the Earth's Gravitational Field and its Variations in Position*, Sydney, 1973, 188-202.

NEDOMA, J. 1973. Contribution to the Variational Formulation of the Boundary Value Problem of the Gravity Field and the Discrete Gravity Field. *Proc. Symposium on Earth's Gravitational Field and Secular Variations in Position*, pp 222-226.

NEWTON, Isaac. 1686. *Mathematical Principles of National Philosophy*. Great Books of the Western World, Vol. 34; Encyclopaedia Britannica, Inc; 1952.

OBENSEN, G.F.T. 1970. The Covariance Matrix for Deflections and Undulations based on Actual Gravity Data. *Report No.* 136, Dept. of Geodetic Sci, Ohio State Uni., Columbus Ohio.

OBENSEN, G.F.T. 1973. Error Analysis of Deflections of the Vertical and Undulations from the Accuracy of Δg. *Bull.Géod.* 108, 141-155.

ORLIN, H. (Ed) 1966. Gravity Anomalies: Unsurveyed Areas. *Geophysical Monograph No.* 9.

PAUL, M.K. 1973. On the Computation of Equal Area Blocks. *Bull.Géod.* No. 107, 73-84.

PAUL, M.K. & NAGY, D. 1973. The Accuracy of Geoidal Height obtainable from Gravity Data Alone. *Canadian Surveyor*, 27, 2, 149-156.

PELLINEN, L.P. 1962. Accounting for Topography in the Calculation of Quasi-Geoidal Heights and Plumbline Deflections from Gravity Anomalies. *Bull.Géod.* 63, 57-62.

PELLINEN, L.P. 1964. Expedient Formulae for Computation of Earth's Gravitational Field Characteristics from Gravity Anomalies. *Bull.Géod.* 74, 327-333.

PELLINEN, L.P. 1968. Comparison of Different Methods of Computing the Plumbline Deflection in Mountainous Areas. *Bull.Géod.*, 89, 345-354.

PETERSON, A.E. 1974. Merging Canadian Triangulation Network with 1973 Doppler Satellite Data. *Canadian Surveyor*, 28, 5, 487-494.

PICK, M. 1970. Determination of the Deflections of the Vertical for a Mathematical Model with Slopes over 45°. *Stud. Geoph.et Geod.*, 14, 180-182.

PICK, M. 1973. On the Boundary Condition of the Gravity Disturbing Potential. *Stud.Geoph. et Geod.*, 17, 173-177.

PICK, M. PICHA, J. & VYSKOVIL, V. 1962. A Contribution to the Methods of Calculating Gravity Terrain Corrections. *Bull.Géod.* 63.

PICK, M. & JAKUBCOVÁ, I. 1973. Artificial Models for Checking Different Methods of Determining the Figure of the Earth. *Studia Geoph.et Geod.* 17, 245-252.

RAPP, R.H. 1964. The Prediction of Point and Mean Gravity Anomalies through the Use of a Digital Computer. *Department of Geodetic Science, Report No.* 43, Ohio State University, Columbus, Ohio.

RICE, D.A. 1952. Deflections of the Vertical from Gravity Anomalies. *Bull. Géod.*, 25, 285-308.

ROELSE, A. 1976. Private Communication. *Department of National Mapping, Canberra,* Australia.

SOLLINS, A.D. 1947. Tables for the Computation of Deflections of the Vertical. *Bull.Géod.* 6, 279-309.

STOKES, G.G. 1849. On the Variation of Gravity at the Surface of the Earth. *Trans.Camb.Phil.Soc.*, 8, 672-695.

SZABO, B. 1962. Comparisons of the Deflection of the Vertical Components computed by Astro Geodetic, Gravimetric and Topographic Isostatic Techniques. *Bull.Géod.* 65, 227-242.

TEOH, A. 1975. Private Communication. *Computing Section, NSW Department of Lands,* Sydney, Australia.

TSCHERNING, C.C. 1973. Problems and Results in Least Squares Collocation. *Paper presented at the Annual Fall Meeting of the American Geophysical Union.*

VANICEK, P. & MERRY, C.L. 1973. Determination of the Geoid from Deflections using a Least Squares Fitting Technique. *Bull.Géod.* 109, 261-279.

VELKOBORSKY, P. 1970. On the 2nd Approximations of the Deflections of the Vertical and the Quasi Geoid Height. *Studia Geoph.et Geod.*, 14, 135-145.

VENING MEINESZ, F.A. 1928. A Formula Expressing the Deflection of the Plumb-line in the Gravity Anomolies and some Formulae for the Gravity Field and Potential Outside the Geoid. *Proc. Koninkl.Ned.Akad.Wetenschap.*, 31(3), 315-331.

VYSKOČIL, V. 1970. On the Covariance and Structure Functions of the Anomalous Gravity Field. *Studia Geoph.et Geod.*, V 14, No. 2, 174-177.

WROBEL, B. 1967. On the Numerical Calculation of Gravimetric Differences of Deviations of the Vertical and the Accuracy. *Dissertation for the Degree of Dr.Ing.*, Friedrich-Wilhelms Univ., Bonn.

YEREMEEV, V.F. 1970. An Investigation of some Methods of Calculating Deflections of an Earth Model. *Studia Geoph.et Geod.*, 14, 2.

NOTES ON APPENDICES

The appendices A to I contain flow charts for some of the main programs and subroutines developed for this investigation. These flow charts illustrate the main concepts involved in the programs. Many of the details and devices (eg. for saving computer time and space) have been omitted as they unnecessarily confuse the general picture being presented.

Data files for gravity (GRAVBNK) and height (HTBIN) were stored on permanent files in the manner described in sections 4.1.1(c) and 4.1.2.

APPENDIX A. FLOW CHART FOR SUBROUTINE RICERNG

Description: Computes Mid-points of Compartments generated to give a nominated radial deflection of the vertical at the computation point for a nominated gravity anomaly.

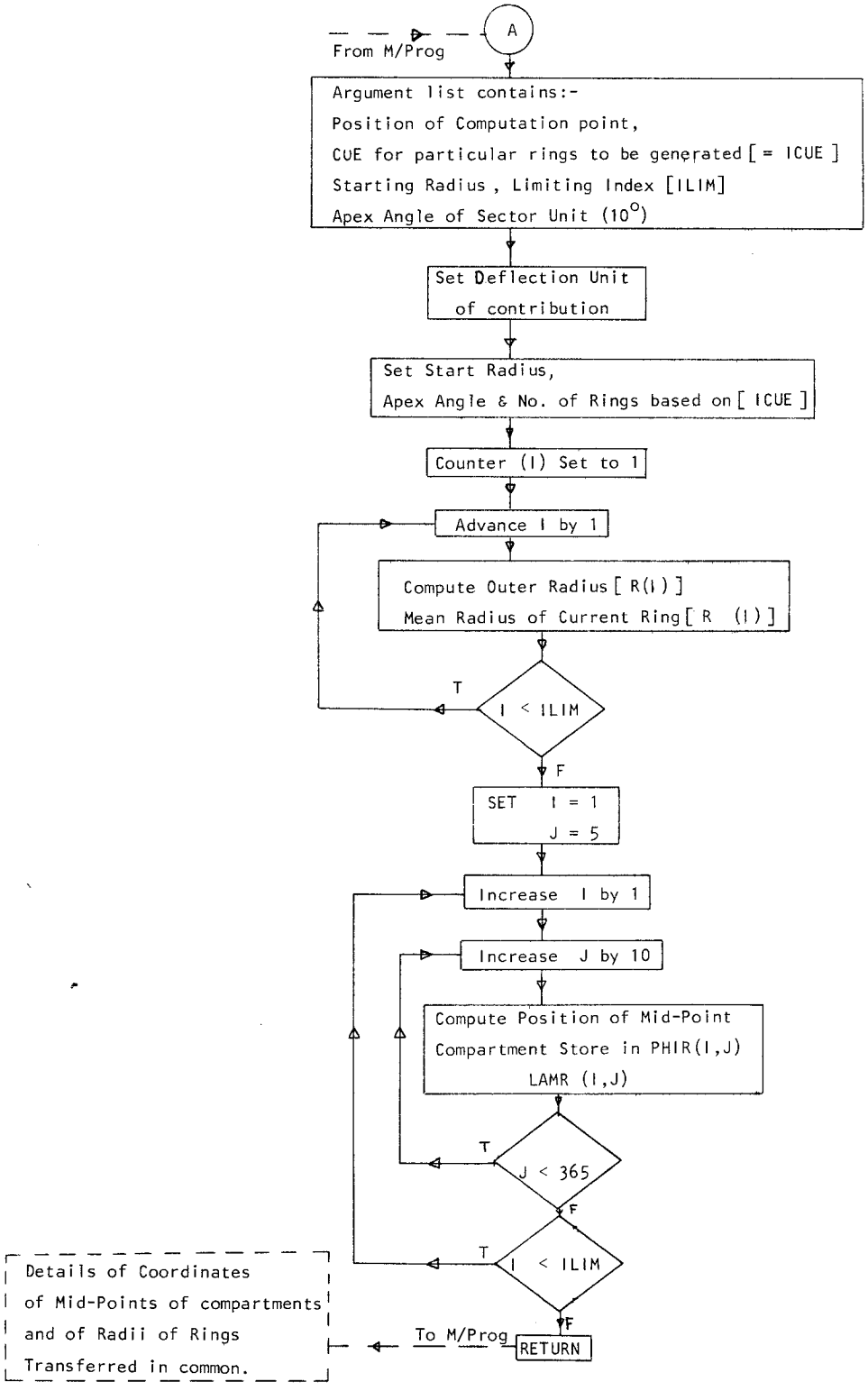

APPENDIX B - FLOWCHART FOR SUBROUTINE KSRINGS

Description: Computes Mid-points of compartments giving predetermined contributions of G' at the computation point for nominated difference in gravity anomaly and height (see also Table 4).

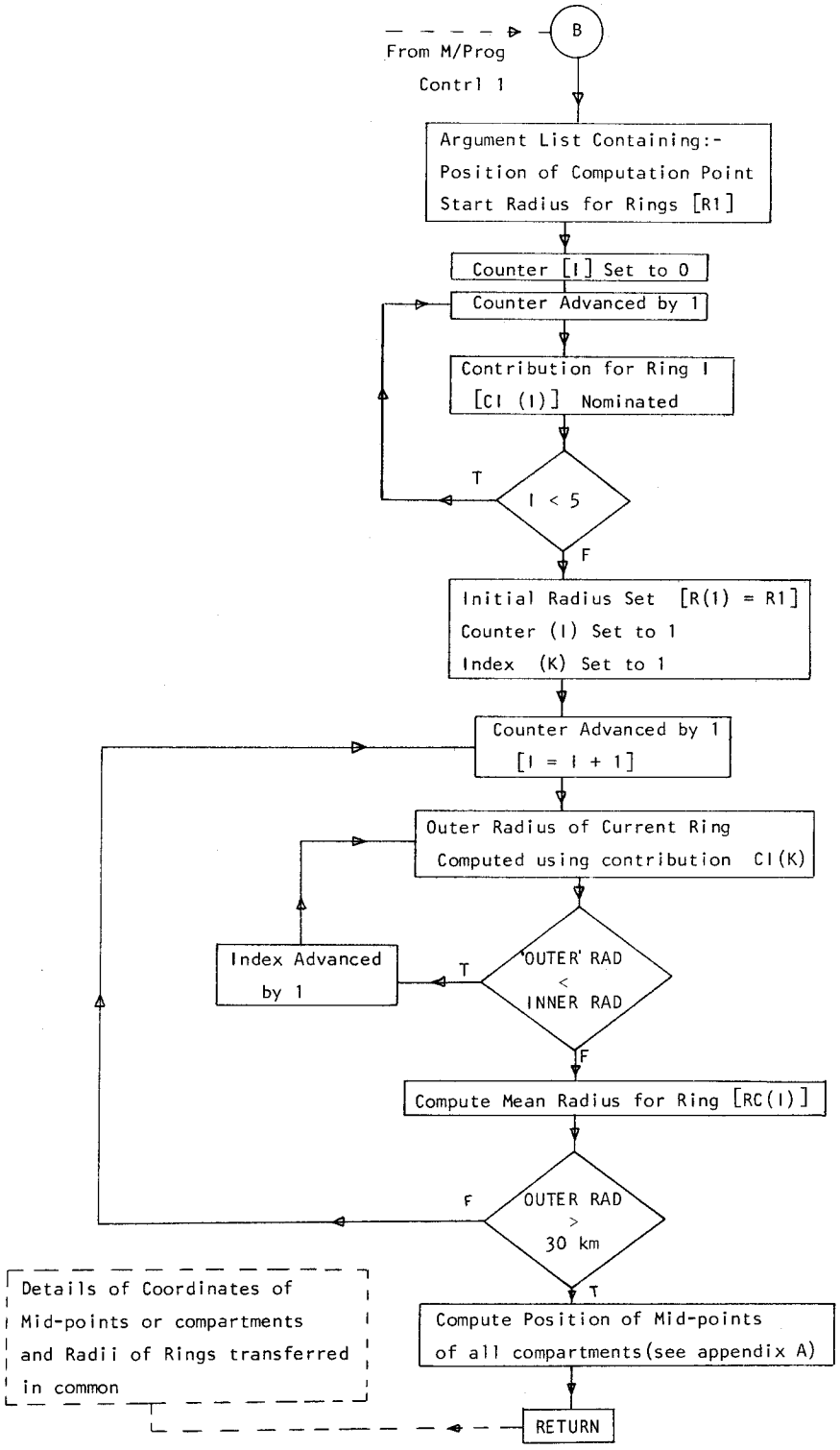

APPENDIX C - FLOW CHART FOR PROGRAM CONTRL1

Description: Computes the terrain correction G' at all gravity stations within certain predefined limits. See also Section 4.3.2.

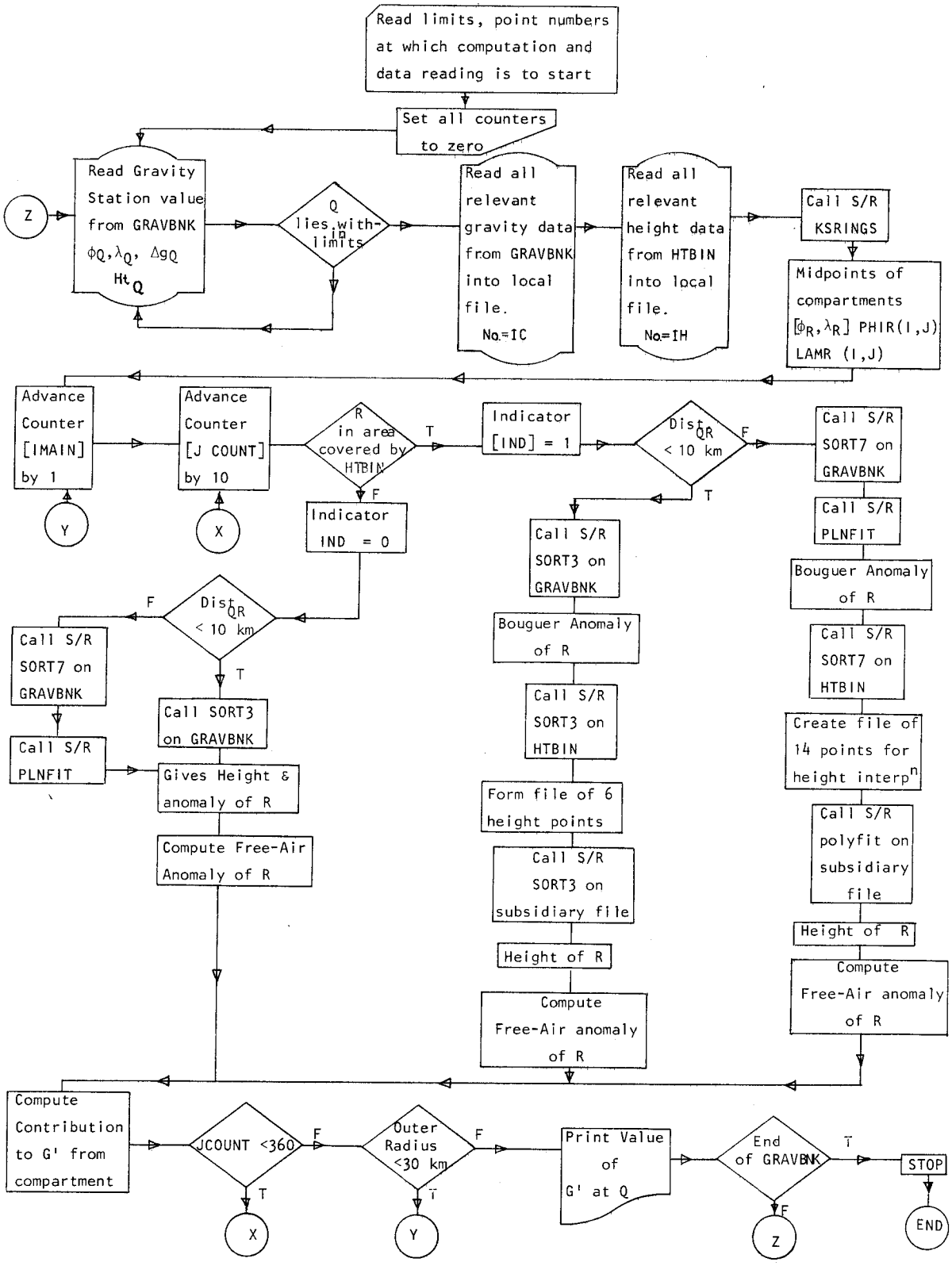

APPENDIX D - FLOW CHART FOR SUBROUTINE GRSLP

Description: Computes maximum slope (β_{max}) and azimuth (α_{max}) of line of maximum slope from plane defined by three points

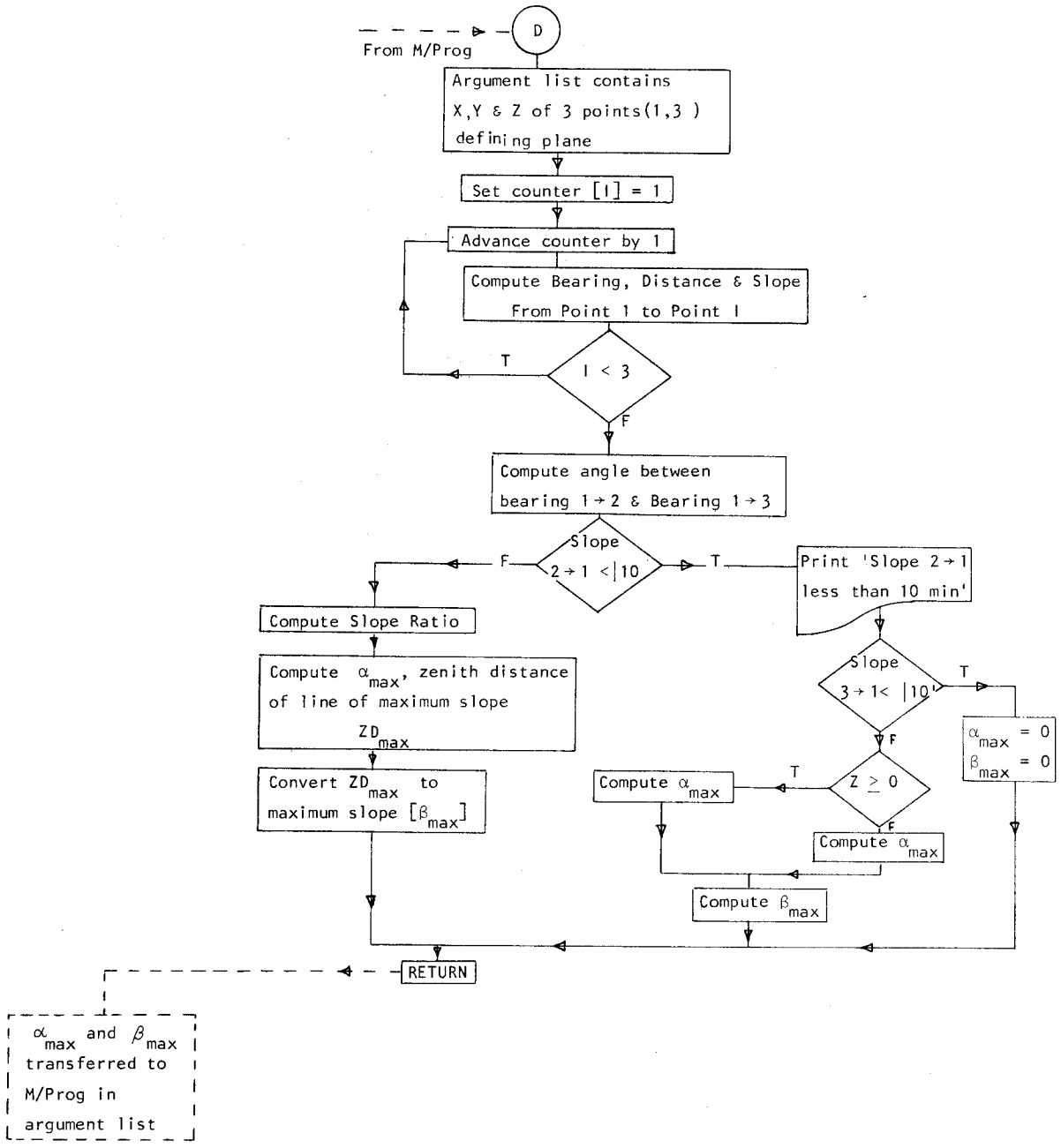

APPENDIX E - FLOW CHART FOR SUBROUTINE POLYFIT

Description: Fits by least-squares a second-order surface to a maximum of 14 points, and interpolates the height of a nominated point on this surface (see equation 5.1)

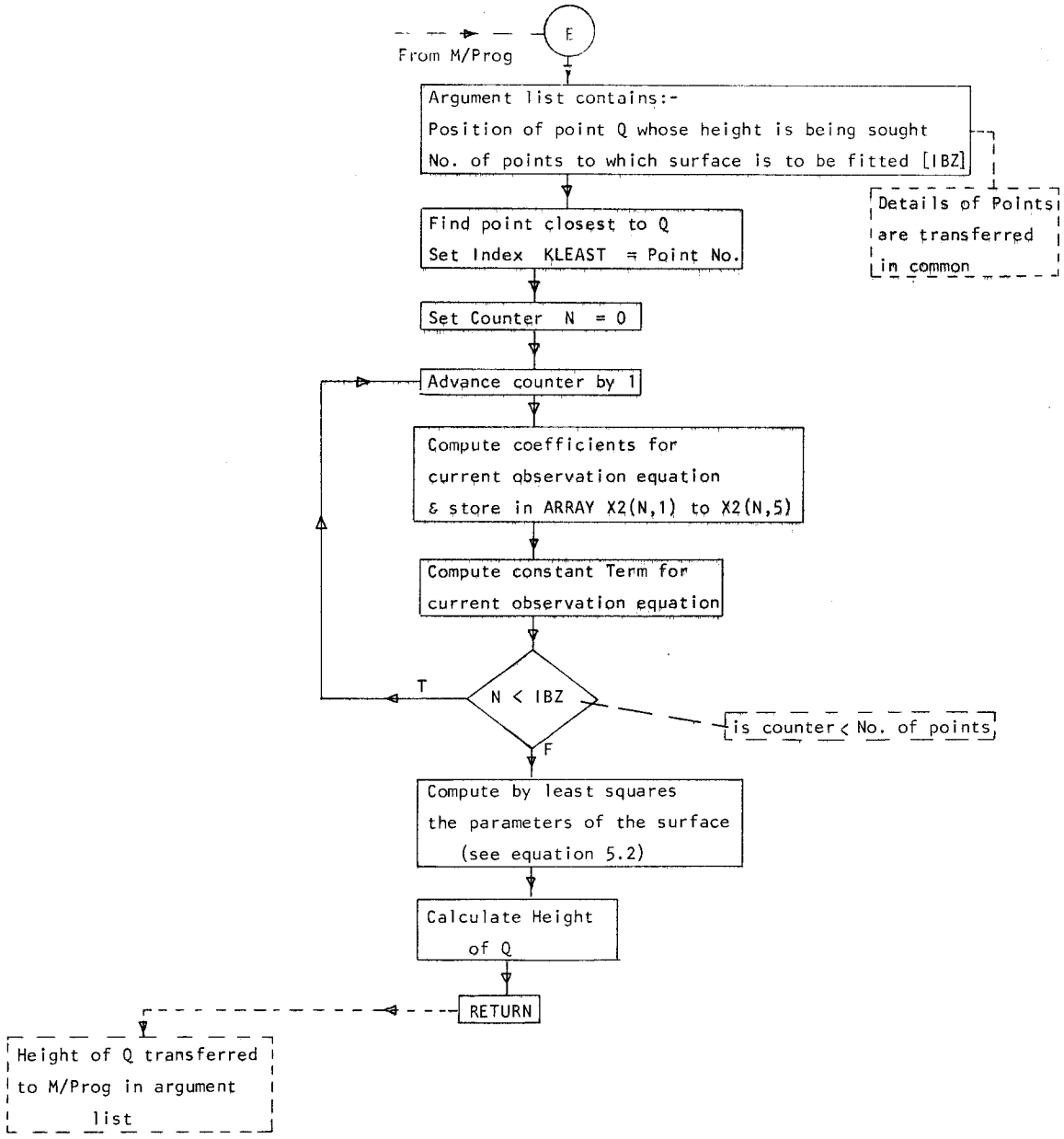

APPENDIX F - FLOW CHART FOR SUBROUTINE SORT3

Description: From an unordered array of points whose positions are known, finds the 3 points which form the smallest triangle about a nominated point Q, then uses this triangle to interpolate value of height/gravity for Q.

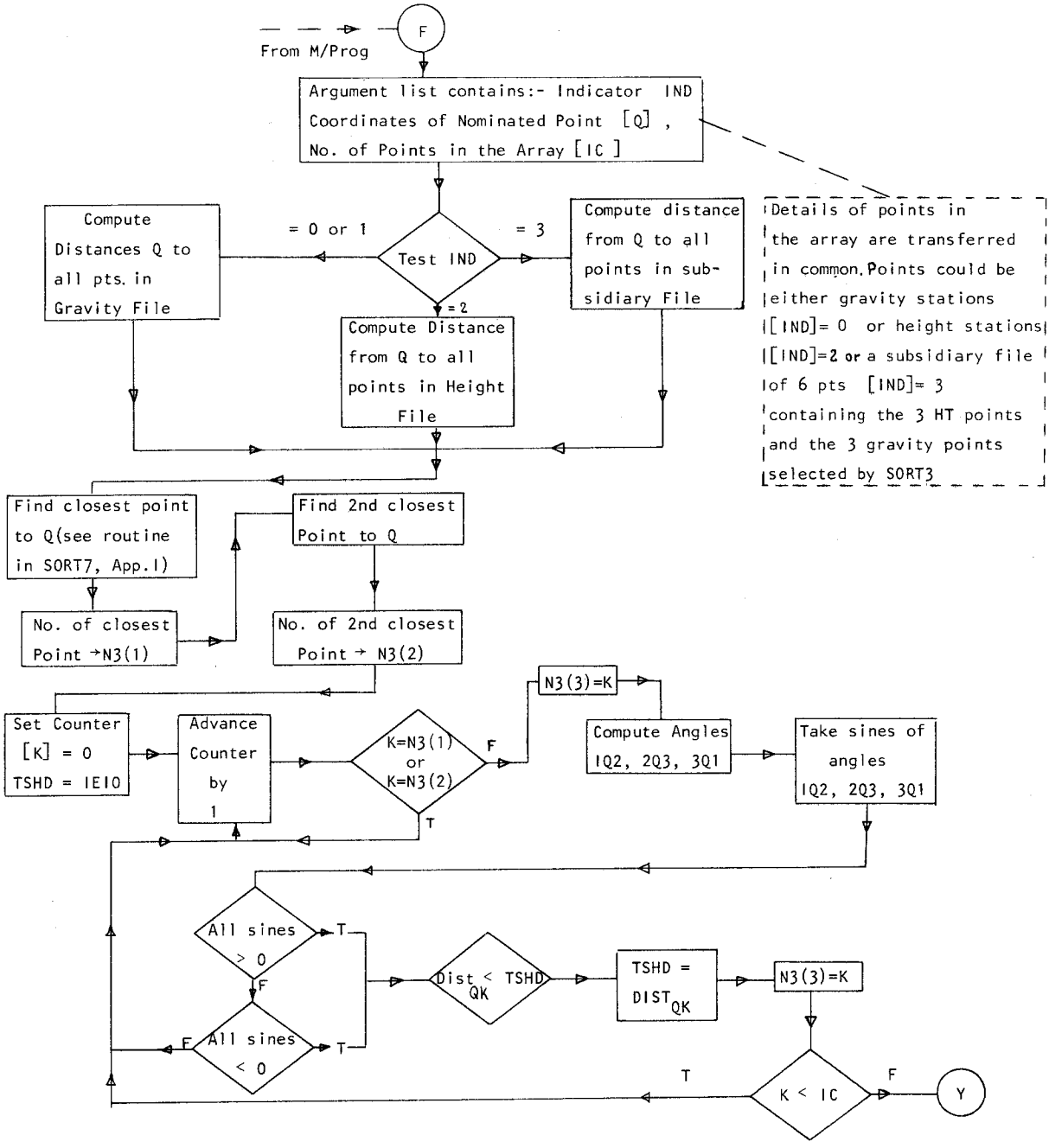

SUBROUTINE SORT3 (cont)

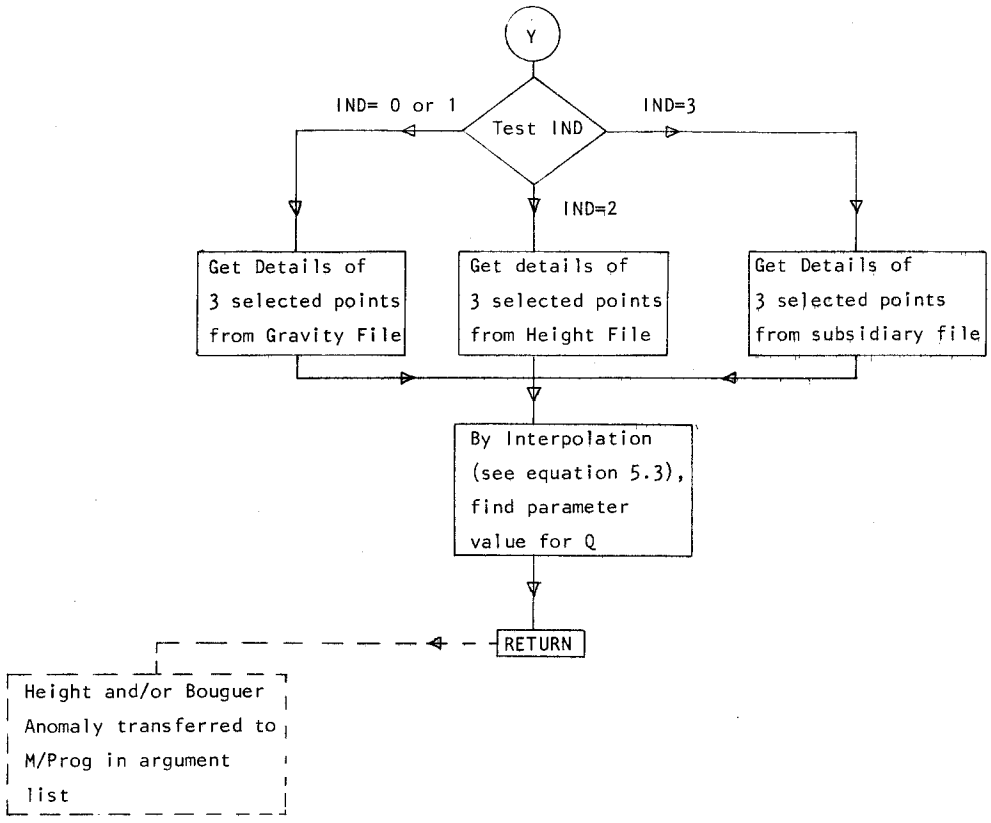

APPENDIX G - FLOW CHART FOR PROGRAM COVFN

Description: From an unordered array of points whose positions and gravity anomalies are known computes the covariance relationships for all points in the field, and separates the cross-products according to separation and takes a simple statistical analysis of data in each cell so produced.

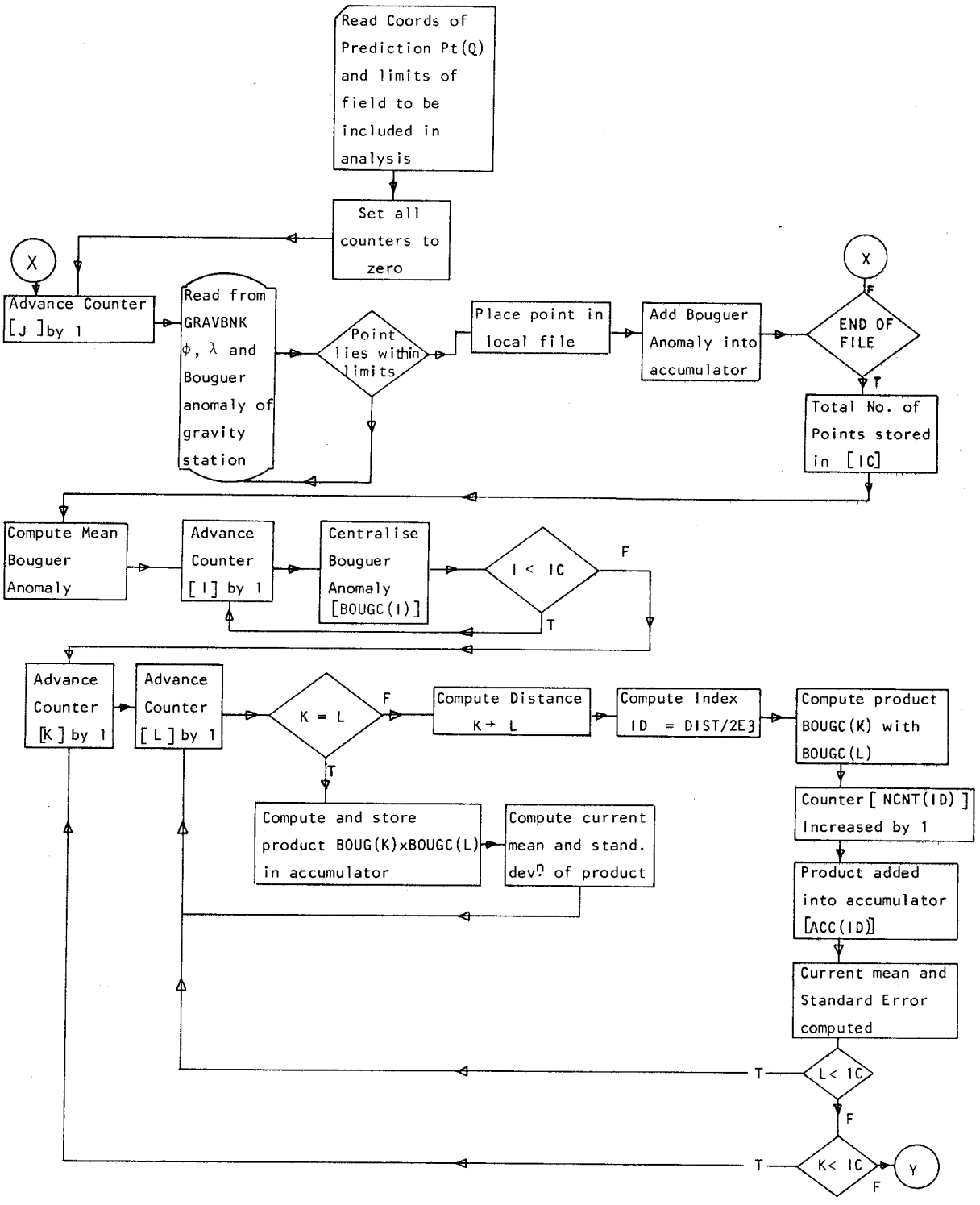

FLOW CHART FOR PROGRAM COVFN (contd)

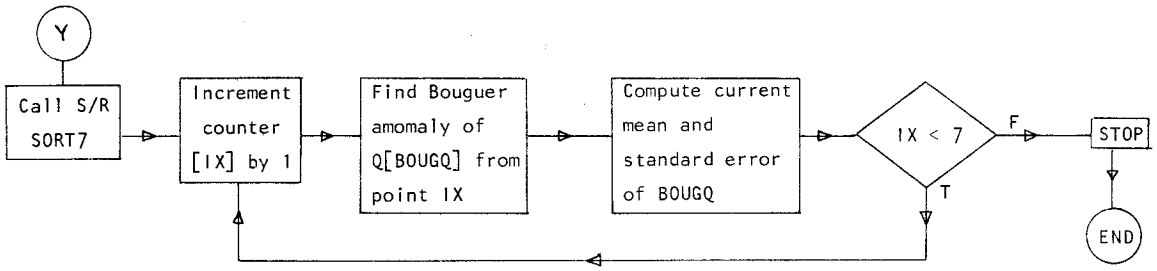

APPENDIX H - FLOW CHART FOR PROGRAM CONTRL2

Description: Computes the components of the deflection of the vertical (ξ , η) at a point whose position is specified. See also section 6.2.2

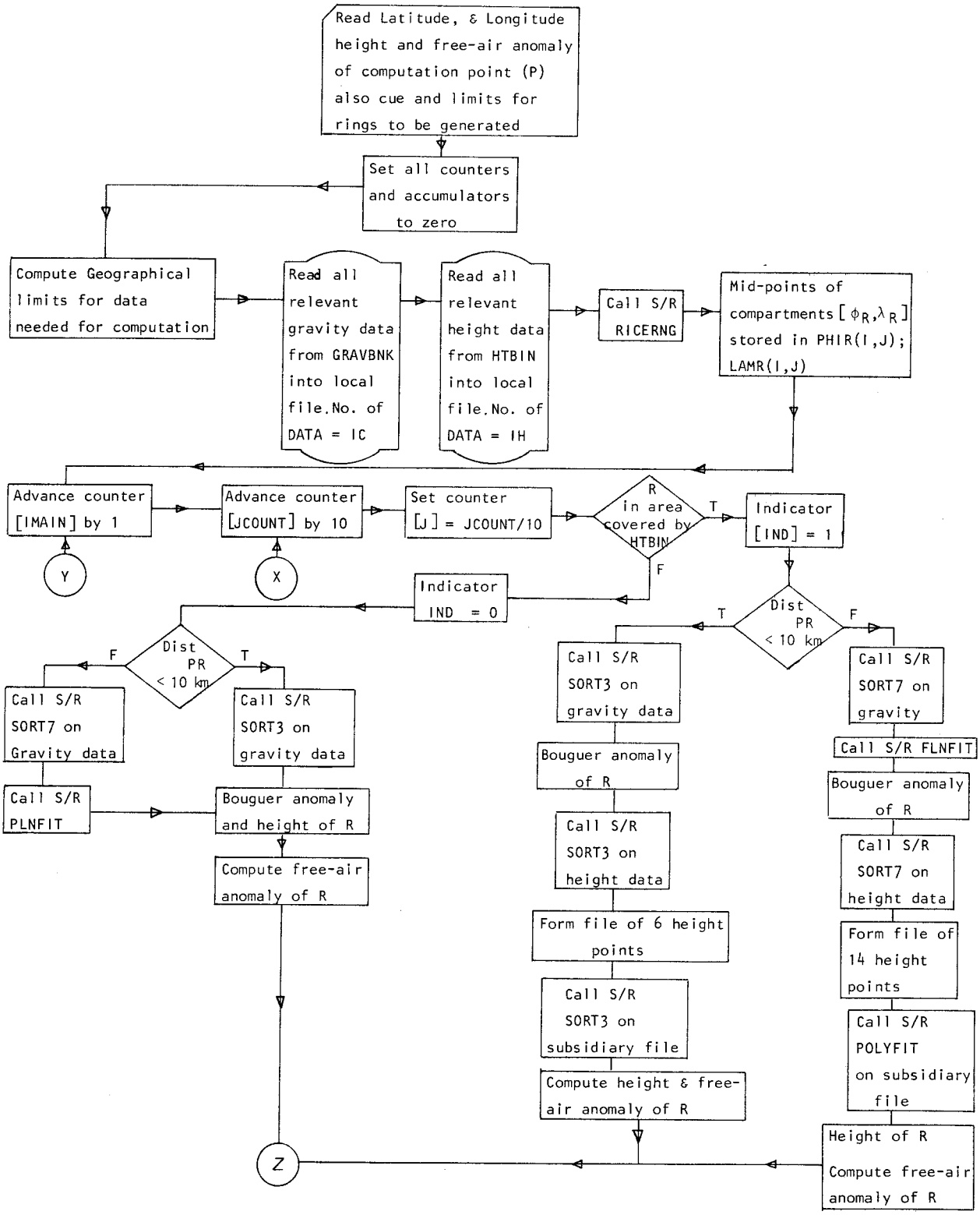

FLOW CHART FOR PROGRAM CONTRL2 (contd)

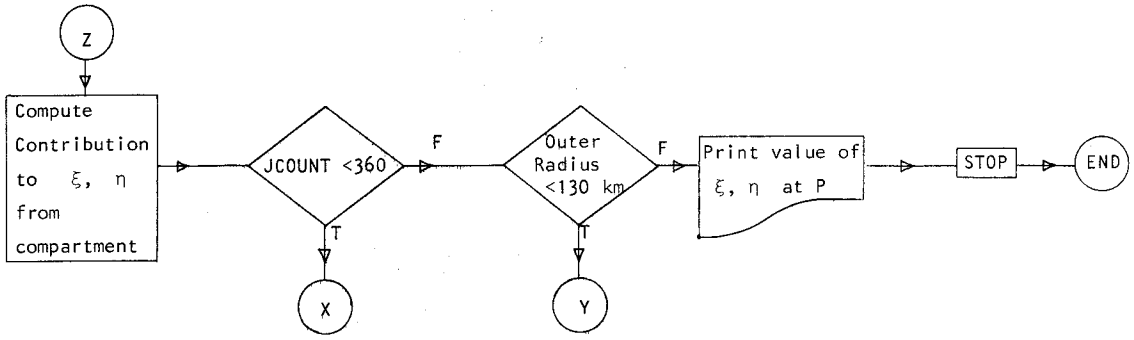

APPENDIX I - FLOW CHART FOR SUBROUTINE SORT7

Description: From an unordered array of points whose positions are known finds the seven points close to a nominated point Q. The 7 points are made up of the three closest points without regard to direction thence the next closest point in each of the four quadrants from Q.

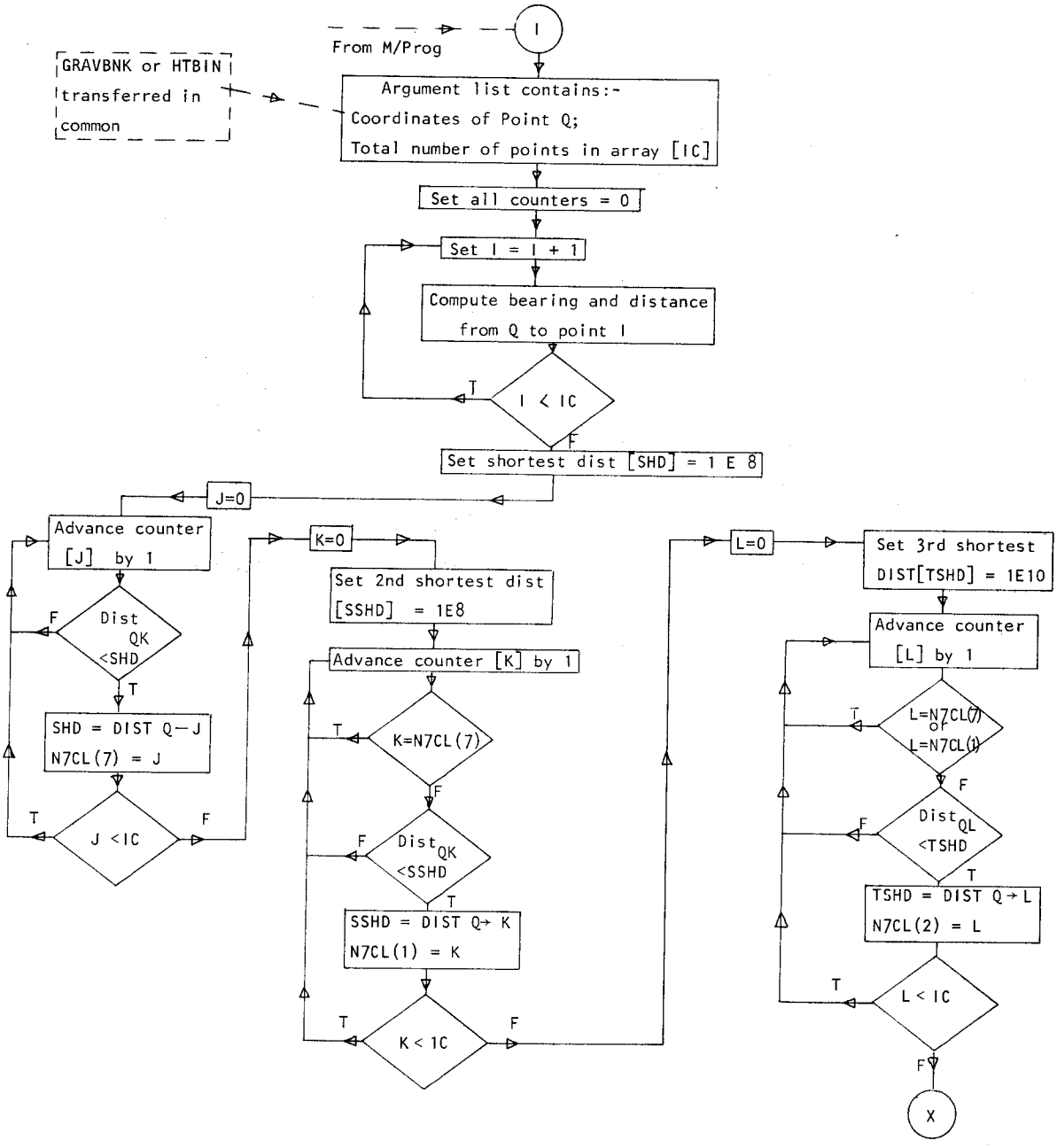

SUBROUTINE SORT7 (contd)

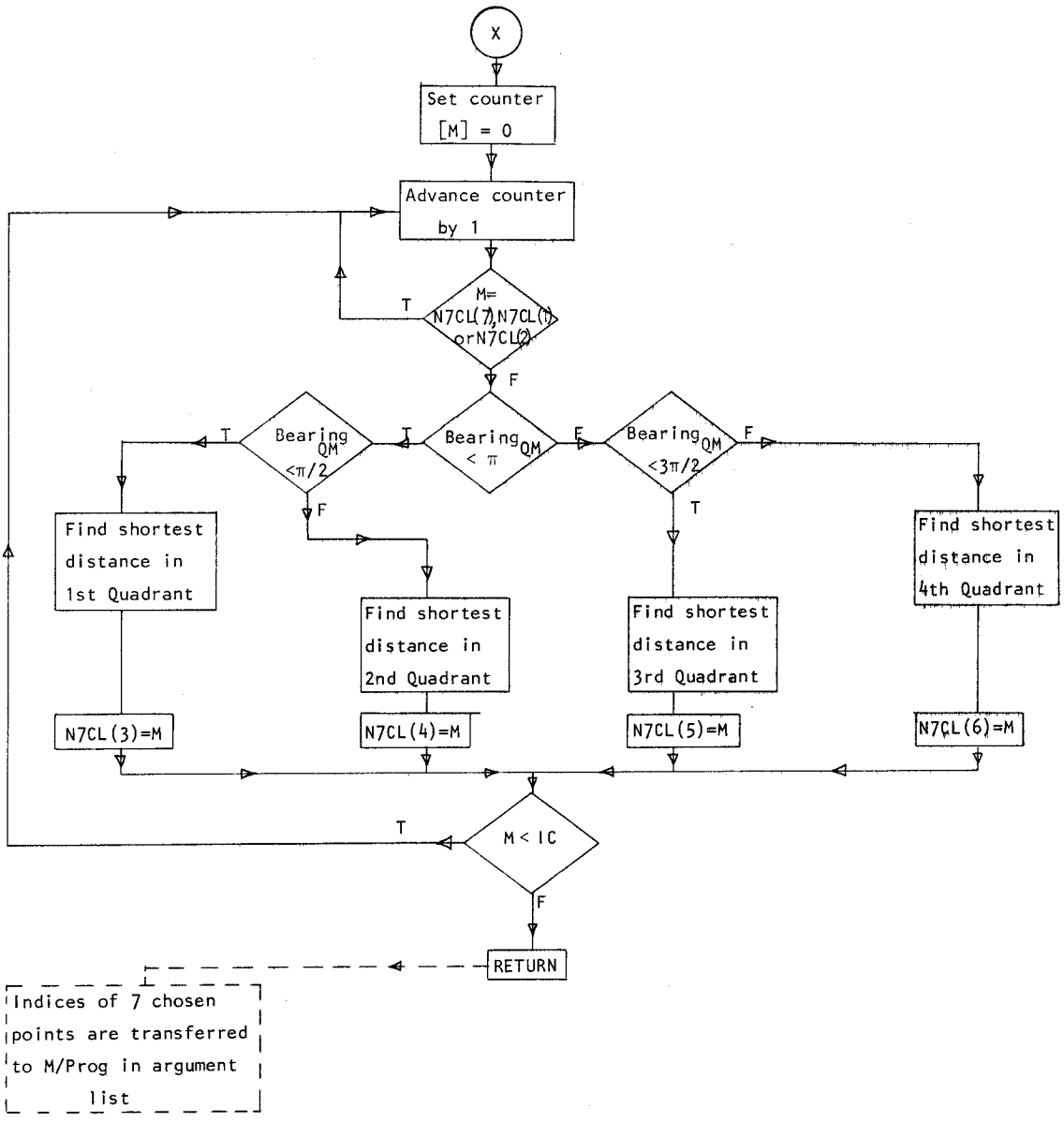

APPENDIX J - FLOW CHART FOR SUBROUTINE PLNFIT

Description: Fits by Least-Squares a plane surface to 7 points, and finds the Bouguer anomaly or height of a nominated point on this plane.

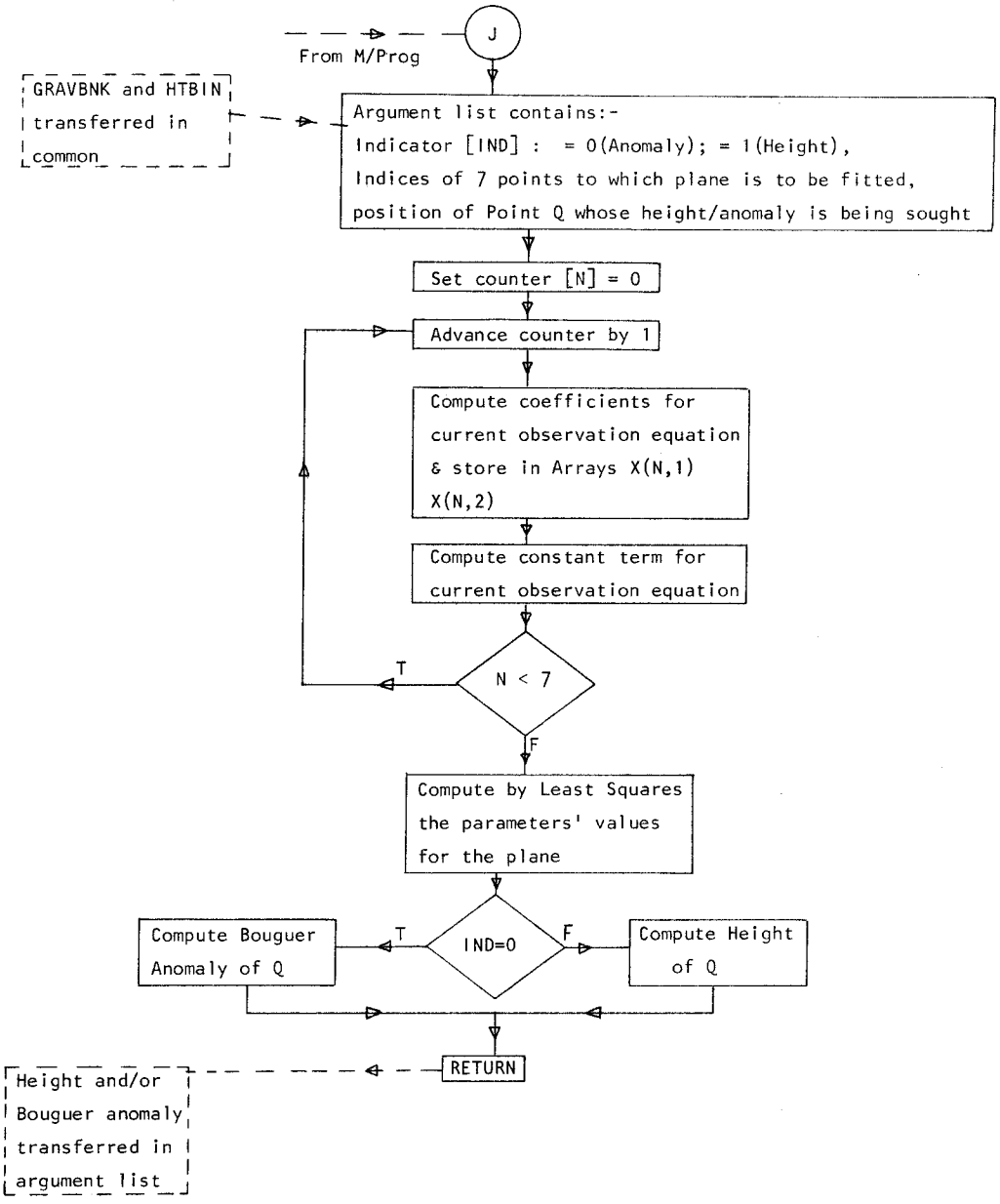

Publications from

THE SCHOOL OF SURVEYING, THE UNIVERSITY OF NEW SOUTH WALES

P.O. Box I, Kensington, N.S.W. 2033

AUSTRALIA

Reports

1.*	The discrimination of radio time signals in Australia *G.G. Bennett*		*Uniciv Rep.* D-1	(G 1)
2.*	A comparator for the accurate measurement of differential barometric pressure *J.S. Allman*	9pp	*Uniciv Rep.* D-3	(G 2)
3.	The establishment of geodetic gravity networks in South Australia *R.S. Mather*	26pp	*Uniciv Rep.* R-17	(G 3)
4.	The extension of the gravity field in South Australia *R.S. Mather*	26pp	*Uniciv Rep.* R-19	(G 4)
5.*	An analysis of the reliability of barometric elevations *J.S. Allman*	335pp	*Unisurv Rep.* 5	(S 1)
6.*	The free air geoid for South Australia and its relation to the equipotential surfaces of the earth's gravitational field *R.S. Mather*	491pp	*Unisurv Rep.* 6	(S 2)
7.*	Control for mapping (Proceedings of Conference, May 1967) *P.V. Angus-Leppan (Editor)*	329pp	*Unisurv Rep.* 7	(G 5)
8.*	The teaching of field astronomy *G.G. Bennett & J.G. Freislich*	30pp	*Unisurv Rep.* 8	(G 6)
9.*	Photogrammetric pointing accuracy as a function of properties of the visual image *J.C. Trinder*	64pp	*Unisurv Rep.* 9	(G 7)
10.*	An experimental determination of refraction over an icefield *P.V. Angus-Leppan*	23pp	*Unisurv Rep.* 10	(G 8)
11.*	The non-regularised geoid and its relation to the telluroid and regularised geoids *R.S. Mather*	49pp	*Unisurv Rep.* 11	(G 9)
12.*	The least squares adjustment of gyro-theodolite observations *G.G. Bennett*	53pp	*Unisurv Rep.* 12	(G 10)
13.*	The free air geoid for Australia from gravity data available in 1968 *R.S. Mather*	38pp	*Unisurv Rep.* 13	(G 11)
14.*	Verification of geoidal solutions by the adjustment of control networks using geocentric Cartesian co-ordinate systems *R.S. Mather*	42pp	*Unisurv Rep.* 14	(G 12)
15.*	New methods of observation with the Wild GAKI gyro-theodolite *G.G. Bennett*	68pp	*Unisurv Rep.* 15	(G 13)
16.*	Theoretical and practical study of a gyroscopic attachment for a theodolite *G.G. Bennett*	343pp	*Unisurv Rep.* 16	(S 3)
17.	Accuracy of monocular pointing to blurred photogrammetric singals *J.C. Trinder*	231pp	*Unisurv Rep.* 17	(S 4)
18.	The computation of three dimensional Cartesian co-ordinates of terrestrial networks by the use of local astronomic vector systems *A. Stolz*	47pp	*Unisurv Rep.* 18	(G 14)
19.	The Australian geodetic datum in earth space *R.S. Mather*	130pp	*Unisurv Rep.* 19	(G 15)
20.*	The effect of the geoid on the Australian geodetic network *J.G. Fryer*	221pp	*Unisurv Rep.* 20	(S 5)
21.*	The registration and cadastral survey of native-held rural land in the Territory of Papua and New Guinea *G.F. Toft*	441pp	*Unisurv Rep.* 21	(S 6)
22.	Communications from Australia to Section V, International Association of Geodesy, XV General Assembly, International Union of Geodesy & Geophysics, Moscow 1971 *R.S. Mather et al*	72pp	*Unisurv Rep.* 22	(G 16)
23.	The dynamics of temperature in surveying steel and invar measuring bands *A.H. Campbell*	195pp	*Unisurv Rep.* S 7	

* Out of print

Publications from the School of Surveying
(contd.)

Reports (contd)

24. Three-D Cartesian co-ordinates of part of the Australian geodetic network by the use of local astronomic vector systems
A. Stolz 182pp *Unisurv Rep.* S 8

25. Papers on Four-dimensional Geodesy, Network Adjustments and Sea Surface Topography
R.S. Mather, H.L. Mitchell, A. Stolz 73pp *Unisurv* G 17

26. Papers on photogrammetry, co-ordinate systems for survey integration, geopotential networks and linear measurement
L. Berlin, G.J.F. Holden, P.V. Angus-Leppan, H.L. Mitchell and A. Campbell 80pp *Unisurv* G 18

27. Aspects of Four-dimensional Geodesy
R.S. Mather, P.V. Angus-Leppan, A. Stolz and I. Lloyd 100pp *Unisurv* G 19

28. Relations between MSL & Geodetic Levelling in Australia
H.L. Mitchell 264pp *Unisurv Rep.* S 9

29. Study of Zero Error & Ground Swing of the Model MRA101 Tellurometer
A.J. Robinson 200pp *Unisurv Rep.* S 10

30. Papers on Network Adjustments, Photogrammetry and 4-Dimensional Geodesy
J.S. Allman, R.D. Lister, J.C. Trinder and R.S. Mather 133pp *Unisurv* G 20

31. An Evaluation of Orthophotography in an integrated Mapping System
G.J.F. Holden 232pp *Unisurv Rep.* S 12

32. The Analysis Precision and Optimization of Control Surveys
G.J. Hoar 200pp *Unisurv Rep.* S 13

33. Papers on Mathematical Geodesy, Coastal Geodesy and Refraction
E. Grafarend, R.S. Mather and P.V. Angus-Leppan 100pp *Unisurv* G 21

34. Papers on Gravity, Levelling, Refraction, ERTS Imagery, Tidal Effects on Satellite Orbits & Photogrammetry
R.S. Mather, J.R. Gilliland, F.K. Brunner, J.C. Trinder, K. Bretreger and G. Halsey 96pp *Unisurv* G 22

35. Papers on Earth Tides, Sea Surface Topography, Atmospheric effects in physical geodesy, Mean sea level, Systematic errors in levelling
R.S. Mather, E.G. Anderson, C. Rizos, K. Bretreger, K. Leppert, B.V. Hamon, P.V. Angus-Leppan 96pp *Unisurv* G 23

36. Papers on Adjustment theory, Sea surface topography determinations, applications of Landsat imagery, Ocean loading of Earth tides, physical geodesy, photogrammetry and oceanographic applications of satellites
R. Patterson, R.S. Mather, R.C. Coleman, O.L. Colombo, J.C. Trinder, S.U. Nasca, T.L. Duyet, K. Bretreger *Unisurv* G 24

37. The Effect of Topography on Solutions of Stokes' Problem
E.G. Anderson 252pp *Unisurv Rep.* S 14

38. The Computation of Deflections of the Vertical from Gravity Anomalies
A.H.W. Kearsley 161 pp *Unisurv Rep.* S 15

39. Papers on Hydrostatic Equilibrium Figures of the Earth, Earth Tides, Gravity Anomaly Data Banks for Australia, Recovery of Tidal Signals from Satellite Altimetry, Meteorological Parameters for Modelling Terrestrial Refraction, Crustal Motion Studies in Australia
S.M. Nakiboglu, B. Ducarme, P. Melchior, R.S. Mather, B.C. Barlow, C. Rizos, B. Hirsch, K. Bretreger, F.K. Brunner, P.V. Angus-Leppan *Unisurv* G 25

Prices

G. General Series

Subscription for 1976 Postfree
To Libraries $11.00
To Individuals $8.00

S. Special Series (Limited Printing)

Postfree
To Libraries $11.00 each copy.
To Individuals $8.00 each copy.

Publications from the School of Surveying (contd.)

Proceedings

Proceedings of conferences on refraction effects in geodesy & electronic distance measurement
P.V. Angus-Leppan (Editor) 264pp Price: $10.00**

Australian Academy of Science/International Association of Geodesy Symposium on Earth's Gravitational Field & Secular Variations in Position
R.S. Mather & P.V. Angus-Leppan (eds) 764pp Price: (A)

(A) Price to Libraries, etc. $25.00**
or, to individuals $20.00**

Monographs

1. The theory and geodetic use of some common projections (2nd edition)
R.S. Mather 125pp Price: $ 4.50**
2. The analysis of the earth's gravity field
R.S. Mather 172pp Price: $ 4.50**
3. Tables for Prediction of Daylight Stars
G.G. Bennett 24pp Price: $ 2.00**
4. Star Prediction Tables for the fixing of position
G.G. Bennett; J.G. Freislich & M. Maughan 200pp Price: $ 7.50**
5. Survey Computations
M. Maughan 98pp Price: $ 3.00**
6. Adjustment of Observations by Least Squares
M. Maughan 57pp Price: $ 3.00**

** Including postage